A Tracer Study on the Penetration of a Sample Solution into Carbon Electrode of Spectrographic Analysis

By Kenjiro KIMURA and Kazuo SAITO

(Received August 28, 1956)

Quantitative spectrographic analysis of non-ferrous metals is carried out by means of spark spectra. This method is normally satisfactory to obtain accurate results, but is less desirable when applied to samples of a high purity, since its sensitivity is rather low. Non-ferrous metals of a high purity are analysed through the solution-arc method, which consists in dissolving the sample in acid, making the solution up to a definite volume, impregnating it into a porous carbon electrode and using this in an arc discharge. This method is certainly very sensitive; it requires however, a very careful procedure in accordance with precise directions.

The present authors are of the opinion that the need for precision could be, at least partly, ascribed to the different nature of the carbon electrode. They intended therefore to examine the penetration process into a carbon electrode with the aid of tracer technique[1].

Radioactive Isotope. — Radioactive zinc-65 was used as indicator. Its β-activity (electron capture 97.5%, β^+ 2.5%) of a half life of 245 days is satisfactory for the present purpose; since its decay product is not radioactive, the measurement of activity directly indicates the relative amount of zinc. A solution was prepared from a solution of radioactive zinc chloride and pure lead nitrate, which contained 0.24 g. of lead nitrate and 0.11 mg. of zinc (carrier) in one cc., corresponding to 0.07% of zinc in lead. This content is slightly greater than the practical content of zinc in lead ingot, but a less concentrated solution could not maintain radioactivity strong enough to be measured. This solution was used throughout this work.

Procedure.—Several sorts of carbon electrode were examined as shown in Table I. Each capital letter A, B etc. corresponds to a product of a different manufacturer. The preliminary treatment of an electrode may affect the penetration of the sample solution; the various treatments are also shown in Table I. After the preliminary discharge, carbon electrodes were cooled to about 60°C and the sample solution was dripped from a measuring pipette so slowly that the second drop was not added until the first one had already been absorbed. Then they were dried in an air-bath and sections cut with a saw so that several fractions of carbon powder containing salt were obtained corresponding to the definite distance from the top of the elctrode. They were weighed in a steel dish and their radioactivity measured with a counter. Some of the electrodes are of so close a texture that it takes a long time for the solution to penetrate into them, whilst that of others is less so. About 30 mg. of the powder were used for each activity measurement. The influence of geometrical distribution of the sample powder in the dish was examined and not found to be significant.

Table I shows the results. Each frame corresponds to a fraction of the carbon powder, each figure showing the average count per 10 mg. of the powder. The count should be directly proportional for any one elctrode to the amount of zinc in the sample. The error of measurement was of the order of 10%.

Autoradiograph. — A carbon electrode, after being submitted to impregnation of the solution, is vertically divided into two pieces and put on to a piece of photographic film. Non-screen Eastman Kodak X-ray film was used, since it is quite sensitive, though coarse grained. They were set aside for six days and developed. The results coincide well with those in Table I.

Measurement of Density.—The apparent density (d) of the carbon electrodes was found from their size and weight. The real density (d_0) was measured with a pyknometer and benzene. The porosity (p) can be calculated from the following formula. $p=(d_0-d)/d_0$. They were measured at 15 ± 0.02°C and the results are tabulated in Table II. When an electrode is heated at a high temperature for a long time, the apparent density decreases and the real density increases, resulting in a higher porosity. (Electrodes of maker B do not do this, but the quality is not uniform even in one packet so that no account was taken of these results.)

Discussion

From Table I it can be seen that the zinc ion penetrates farther into a carbon electrode than expected, showing a marked maximum at a distance several millimeters from the top. The apparent hardness of carbon appears to bear little relation to the extent of penetration, presumably because the apparent hardness depends

1) The authors could not find any reference about such a consideration nor any such kind of application of radioactive tracers.

CHEMISTRY HALL LIBRARY

TABLE I

Carbon	A	B	B	C	C	A	B	C	D	A	A
Diameter	5.2	5.4	5.4	8.1	8.1	5.3	5.7	8.3	7.9	5.3	5.3
Preliminary Discharge (sec.)	55V 6A 40	55V 5A 30	55V 8A 60	55V 6A 50	55V 6A 50	none	none	none	none	55V 6A 30	55V 6A 30
Solution Added, ml.	0.2	0.2	0.2	0.5	0.2	ca. 0.02	ca. 0.02	ca. 0.01	ca. 0.01	0.15	0.15
Distance from the top of the electrode, mm. 2	377	277	252	620	357	168	125	276	120	58	68
				190	314	118		0	8		
4	205	172	243	152				0	0	70	113
				166	220	52	74				
6	187	153	231	231					0		
				558	167	6					127
8	505		184	405	200		14			69	
				148							
10	228	185	118	90							220
				132	128					123	
12	87	201	128								172
				290	6					138	
14		175	187								198
16		211								89	
18				125							120
20		143								44	
22			156								
24		5									
26											
Note						Without preliminary discharge, the solution soaks very slowly and with difficulty.				Kerosene, 0.07 ml.	

mainly on the nature of the binding material and not on the nature of carbon itself. The penetration should, on the contrary, be dependent on the nature of carbon, the conditions of preliminary discharge and the way the solution is put on to the electrode. Since the zinc ion extends in front of the lead ion in a chromatographic series, the formation of a maximum point of zinc content can be correlated to the chromatographic effect of capillary texture of the carbon, although the way of addition of the solution is certainly too complicated for the comparison to be made. As a matter of fact, the heterogeneous distribution of the zinc ion should be considered in connection with the relative ratio of zinc to lead, nevertheless this fact ought to be taken into account in the practice of spectrographic analysis.

Another line of argument may be introduced from the data of porosity. It should be noticed that the values of d, d_0 and p are independent of the apparent hardness

TABLE II

MEASUREMENT OF DENSITY AND POROSITY

Manufacturer	Preliminary Discharge	d	d_0	p
A	Without	1.65	2.20	0.25
A	6A, 40 sec.	1.47	2.26	0.35
B	Without	1.43	1.89	0.24
B	5A, 30 sec.	1.51	1.65	0.08
B	6A, 40 sec.	1.42	1.70	0.16
B	8A, 60 sec.	1.40	1.84	0.24
C	Without	1.28	1.55	0.17
C	6A, 50 sec.	1.27	2.01	0.37
D	Without	1.38	1.64	0.16
D	6A, 50 sec.	1.29	1.89	0.32

of the carbon, and so is the extent of penetration. This fact can be easily seen from the comparison of Tables I and II. The depth of penetration appears to increase with porosity, at least for the electrode of the same manufacturer, whilst the time taken for penetration depends on the apparent hardness of the carbon.

The authors also examined the effects of some liquids on the penetration, including liquid paraffine and other organic solvents, which may affect the surface state of carbon, only to find that these have very little effect. These liquids were dripped on to the electrode prior to the addition of the sample solution.

The authors wish to express their thanks to Chairman Professor Hidehiro Goto of Tohoku University and other members of "JIS Committee for Spectroscopic Analysis of Zinc and Lead Metal" for their interest and valuable discussion.

Department of Chemistry
Faculty of Science
The University of Tokyo
Hongo, Tokyo

Synthetic Studies on the Benzofuran Derivatives. II. Reactions of Aromatic o-Hydroxyaldehyde Derivatives and Ethyl Bromomalonate

By Takashi MATSUMOTO and Kenji FUKUI

(Received June 18, 1956)

Since the discovery of the new synthetical method of coumarones by Tanaka[1] this process has been widely utilized for obtaining many sorts of benzofuran derivatives, for instance, 6-nitro- and 6-aminocoumarones[2]; 5,6-dimethoxycoumarone[3]; karanjin[4]; 3-methylcoumarilic acid[5]; coumarones[6].

It was already noticed by Tanaka[7] that his intermediate product I of benzofuran (or its derivatives) synthesis starting from salicylic aldehyde (or its derivatives) and bromomalonic ester, was not obtained in some cases but II was procured instead. The reason for this exceptional appearance of II in the course of benzofuran synthesis was fully interpreted by the oral presentation of S. Akagi[8] who insisted that the essential point lies in the previous dehydration of the solvent (methyl ethyl ketone) applied in this reaction. When the solvent had been completely dried the reaction product was I, while II was obtained in place of I when the solvent there applied had been carelessly dried previously.

In an earlier paper[4], we and Kawase reported that 3-methoxyflavone-7,8-furan-

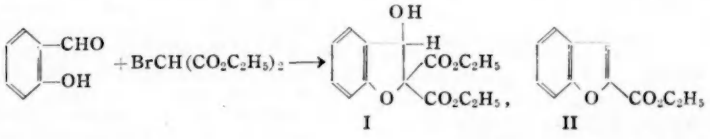

1) S. Tanaka, *J. Am. Chem. Soc.*, **73**, 872 (1951).
2) P. Rumpf, Ch. Gansser, *Helv. Chim. Acta.*, **37**, 435 (1954).
3) F. E. King, J. R. Housley and T. J. King, *J. Chem. Soc.* 1392 (1954).
4) Y. Kawase, T. Matsumoto and K. Fukui, This Bulletin, **28**, 273 (1955).
5) T. A. Geissmann and A. Armen, *J. Am. Chem. Soc.*, **77**, 1623 (1955).
6) Y. Odaira, This Bulletin, **29**, 470 (1956).
7) S. Tanaka, *J. Chem. Soc. Japan (Pure Chem. Sect.)* **73**, 282 (1953)
8) Presented at the Annual Meeting of Pharmaceutical Society of Japan, April 10, 1955.

α-carboxylic acid ethyl ester (III) was obtained directly as an intermediate product from 7-hydroxy-3-methoxyflavone-8-aldehyde and ethyl bromomalonate by the method of Tanaka[1] for benzofuran synthesis. This compound III corresponds to the intermediate product II.

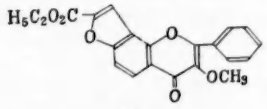

III

We examined the condensation products between some another aromatic o-hydroxyaldehyde derivatives and ethyl bromomalonate.

2, 6-Dihydroxy-3-carbomethoxybenzaldehyde (IV)[9,10] and ethyl bromomalonate were refluxed in methyl ethyl ketone or acetone in the presence of potassium carbonate, and 2-carbethoxy-4-hydroxy-5-carbomethoxycoumarone (V) was obtained as colorless needles of m.p. 133–4°C.

This condensation product V was hydrolysed to 4-hydroxycoumarone-2,5-dicarboxylic acid (VI), m.p. 287–9°C (decomp.) or a mixture of VI and 2-carbethoxy-4-hydroxycoumarone-5-carboxylic acid (VII), m.p. 192–3°C by the reaction condition. Then, this dibasic acid VI was decarboxylated at 155–165°C (bath temperature) in quinoline in a stream of nitrogen gas with copper powder into karanjol (VIII), m.p. 55–6°C and karanjic acid (IX), m.p. 219–220°C (decomp.), which was identical with an authentic sample[4,11].

When the same condensation reaction was carried out with 4-benzyloxy-2-hydroxybenzaldehyde (X)[12,13], 2, 2-dicarbethoxy-3-hydroxy-6-benzyloxycoumaran (XII) was obtained as colorless crystals of m.p. 105–6°C, but ethyl 6-benzyloxycoumarone-2-carboxylate (XIV)[14] was not obtained.

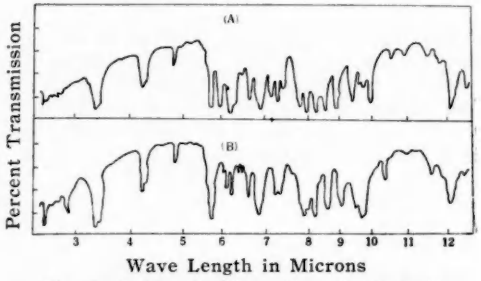

Fig. 1. Infrared Absorption Spectra (in Nujol).
A: Ethyl 5-benzyloxy-2-formylphenoxyacetate (XI)[14].
B: 2, 2-Dicarbethoxy-3-hydroxy-6-benzyloxycoumaran (XII).

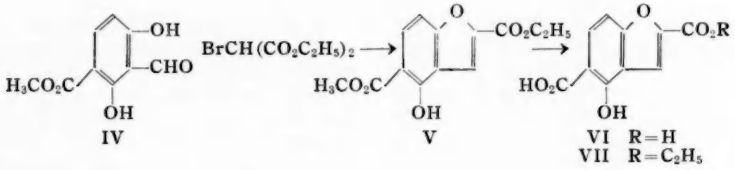

IV V VI R=H VII R=C_2H_5

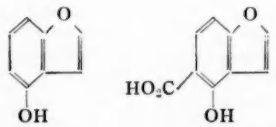

VIII IX

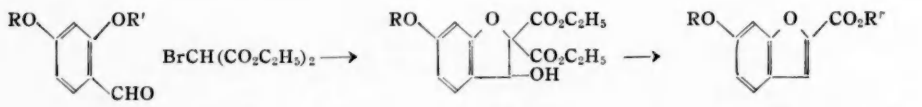

X R=$CH_2C_6H_5$ R'=H
XI R=$CH_2C_6H_5$ R'=$CH_2CO_2C_2H_5$
XII R=$CH_2C_6H_5$
XIII R=$CH_2C_6H_5$ R'=H
XIV R=$CH_2C_6H_5$ R'=C_2H_5

9) K. Nakazawa, *J. Pharm. Soc. Japan*, **59**, 169(1939).
10) R. C. Shah and M. C. Laiwalla, *J. Chem. Soc.*, 1828 (1938).
11) R. T. Foster and A. Robertson, ibid., 115 (1948).
12) J. S. H. Davis, P. A. McCrea, W. L. Norris and G R. Ramage, ibid. 3206 (1950).
13) T. Reichstein, R. Oppenauer, A. Grussner, H. Hirt, L. Rhymer and C. Glatthaar, *Helv. Chim. Acta*, **18**, 816 (1935).
14) R. T. Foster, Alexander Robertson and Anis Bushura, *J. Chem. Soc.*, 2254 (1948).

The structure of XII was characterized by microanalytical data and infrared spectra which proved to have a hydroxyl group, as shown in the Fig. 1. This condensation product XII was hydrolysed to 6-benzyloxycoumarone-2-carboxylic acid (XIII), m.p. 199–200°C* (c.f. Reichstein et al.[13], who gave m.p. 208–9°C**) with alkaline solution or a mixture of XIII and XIV, m.p. 94°C with potassium carbonate solution.

As the result of the present investigation, 2-carbethoxy-coumarone (V) or 2,2-dicarbethoxy-3-hydroxycoumaran derivative (XII) was obtained by the condensation reaction of *o*-hydroxybenzaldehyde derivatives and ethyl bromomalonate, and it may be due to the structure of starting *o*-hydroxybenzaldehyde derivatives.

More detailed studies of this reaction are in progress.

Experimental*

2,6-Dihydroxy-3-carbomethoxybenzaldehyde (IV).—This aldehyde was prepared from methyl β-resorcylate by the method of Nakazawa[9].

2-Carbethoxy-4-hydroxy-5-carbomethoxycoumarone (V).—A mixture of 4.7 g. of 2,6-dihydroxy-3-carbomethoxybenzaldehyde (IV), 6.0 g. of ethyl bromomalonate, 12 g. of anhydrous potassium carbonate in 200 cc. of absolute methyl ethyl ketone was refluxed eight hours in a steam bath. The precipitates were filtered off immediately and washed with methyl ethyl ketone. After distilling off the solvent, water and the excess of dilute sulfuric acid were added. The precipitates were collected, washed with water and recrystallised from aqueous acetone in colorless needles of m.p. 133–4°C, which gave a dark violet ferric reaction in alcohol and gave no 2,4-dinitrophenylhydrazone; yield 1.7 g.

Anal. Found: C, 58.88; H, 4.57. Calcd. for $C_{13}H_{12}O_6$: C, 59.09; H, 4.58%.

The potassium carbonate salts were dissolved in water and the solution was acidified with dilute sulfuric acid. The precipitates were collected and recrystallised from alcohol. 0.6 g. of unchanged 2,6-dihydroxy-3-carbomethoxybenzaldehyde (IV) was recovered.

The same result was obtained also with acetone.

4-Hydroxycoumarone-2,5-dicarboxylic Acid (VI) and 2-Carbethoxy-4-hydroxycoumarone-5-carboxylic Acid (VII).—a) A mixture of 5.1 g. of 2-carbethoxy-4-hydroxy-5-carbomethoxycoumarone (V) and 50 cc. of aqueous potassium hydroxide solution (10%) was heated in a steam bath with occasional shaking for thirty minutes. After cooling, the solution was acidified with dilute sulfuric acid and the precipitates thus formed were collected, washed with water and yielded obtained 4.2 g. of crude 4-hydroxycoumarone-2,5-dicarboxylic acid (VI), m.p. 278–280°C (decomp.). This crude substance was recrystallised from aqueous methanol in colorless crystals of m.p. 287–9°C (decomp.), which gave a blue ferric reaction in alcohol.

Anal. Found: C, 53.98; H, 3.12. Calcd. for $C_{10}H_6O_6$: C, 54.06; H, 2.72%.

b) A mixture of 1.7 g. of 2-carbethoxy-4-hydroxy-5-carbomethoxycoumarone (V) and 1.7 g. of potassium hydroxide in 100 cc. of methanol was refluxed for twenty minutes on a steam bath. After the solvent was acidified with dilute sulfuric acid and distilled off, the precipitates were collected, washed with water and recrystallised from methanol in colorless needles of 2-carbethoxy-4-hydroxycoumarone-5-carboxylic acid (VII), m.p. 192–3°C, having a dark violet ferric reaction in alcohol; yield 0.4 g.

Anal. Found: C, 57.90; H, 4.35. Calcd. for $C_{12}H_{10}O_6$: C, 57.60; H, 4.03%.

From the mother liquor of recrystallisation, 4-hydroxycoumarone-2,5-dicarboxylic acid (VI) was obtained.

Karanjol (VIII) and Karanjic Acid (IX).—A mixture of 3.5 g. of 4-hydroxycoumarone-2,5-dicarboxylic acid (VI), 3.5 g. of copper powder in 110 cc. of quinoline was heated under stirring in an atomosphere of nitrogen gas for about 2.5 hr. at 155–165°C (bath temperature) until evolution of carbon dioxide ceased. After being cooled and filtered from copper powder, the solution was acidified with dilute sulfuric acid and extracted with ether. The ethereal layer was extracted with an aqueous sodium bicarbonate solution and then with an aqueous sodium hydroxide solution (5%). Aqueous sodium bicarbonate extract (acid fraction) was acidified with dilute sulfuric acid and extracted with ether.

The crystals obtained on solvent removal from the dried ethereal extract were recrystallised from aqueous alcohol with the aid of charcoal in colorless needles, m.p. 219–220°C (decomp.), having a blue ferric reaction in alcohol; yield 0.43 g.

Anal. Found; C, 60.84; H, 3.66. Calcd. for $C_9H_6O_4$: C, 60.68; H, 3.40%.

These crystals were identical with an authentic karanjic acid prepared by the alkaline decomposition of karanjin[4] or by the method of Robertson et al.[11] Then, aqueous sodium hydroxide extract (phenol fraction) was acidified with dilute sulfuric acid and extracted with ether. The oil obtained on solvent removal from the dried ethereal extract was recrystallised from petroleum ether in colorless needles of karanjol (VIII), m.p. 55–6°C; yield 0.6 g.

Anal. Found: C, 71.70; H, 4.71. Calcd. for $C_9H_6O_2$; C, 71.63; H, 4.51%.

4-Benzyloxy-2-hydroxybenzaldehyde (X).—This aldehyde was prepared from resorcylaldehyde by the method of Davis et al.[12]

Ethyl 5-Benzyloxy-2-formylphenoxyacetate (XI).—This aldehyde was prepared from 4-benzyloxy-2-hydroxybenzaldehyde (X) by the method of Foster et al.[14] for the comparison of infrared spectra.

* No melting points were corrected.
** The melting point was corrected.

2,2-Dicarbethoxy-3-hydroxy-6-benzyloxycoumaran (XII).—A mixture of 11.4 g. of 4-benzyloxy-2-hydroxybenzaldehyde (X), 18 g. of ethyl bromomalonate, 25 g. of anhydrous potassium carbonate in 150 cc. of absolute acetone was refluxed for 7.5 hr. on a steam bath. The reaction mixture was filtered, distilled off the acetone and was mixed with water. The precipitates were collected, washed with water and recrystallised from dilute alcohol in colorless plates, m.p. 105–6°C, which gave a negative ferric reaction in alcohol and gave no 2,4-dinitrophenylhydrazone. Yield 11.7 g.

Anal. Found: C, 65.36; H, 5.85. Calcd. for $C_{21}H_{22}O_7$: C, 65.27; H, 5.74%.

6-Benzyloxycoumarone-2-carboxylic Acid (XIII) and Ethyl 6-Benzyloxycoumarone-2-carboxylate (XIV).—a) A mixture of 2.0 g. of 2,2-dicarbethoxy-3-hydroxy-6-benzyloxycoumaran (XII) and 50 cc. of aqueous sodium hydroxide (1 N) was heated in a steam bath with occasional shaking for twenty minutes. The cooled mixture was filtered and the filtrate was acidified with dilute sulfuric acid. The precipitates were collected, washed with water and then recrystallised from dilute alcohol. 6-Benzyloxycoumarone-2-carboxylic acid (XIII) was obtained in colorless plates, m.p. 199–200°C; yield 1.2 g.

Anal. Found: C, 71.92; H, 4.55. Calcd. for $C_{16}H_{12}O_4$: C, 71.63; H, 4.51%.

b) A mixture of 3.8 g. of 2,2-dicarbethoxy-3-hydroxy-6-benzyloxycoumaran (XII), 2.0 g. of potassium carbonate, 50 cc. of alcohol and 15 cc. of water was refluxed for 1.5 hr. on a steam bath. After distilling off the alcohol, the residue was cooled and acidified with dilute sulfuric acid. The precipitates were collected, washed with water and separated by the trituration with dilute sodium bicarbonate solution. Crystallisation of the residual solid from alcohol gave the ethyl 6-benzyloxycoumarone-2-carboxylate (XIV) in colorless plates, m.p. 94°C; yield 0.5 g. The melting point of this substance was not depressed by admixture with the sample prepared by the method of Foster et al.[10] Sodium bicarbonate solution was acidified with dilute sulfuric acid. The precipitates were collected, washed with water and recrystallised from alcohol in colorless plates, m.p. 199–200°C, yield 0.7 g., identical with the above (a).

Summary

2-Carbethoxy-4-hydroxy-5-carbomethoxycoumarone (V) and 2,2-dicarbethoxy-3-hydroxy-6-benzyloxycoumaran (XII) were synthesized respectively from 2,6-dihydroxy-3-carbomethoxybenzaldehyde (IV) or 4-benzyloxy-2-hydroxybenzaldehyde (X) and ethyl bromomalonate by the method of Tanaka for benzofuran synthesis. 2-Carbethoxy-4-hydroxy-5-carbomethoxycoumarone (V) was hydrolysed to 4-hydroxycoumarone-2,5-dicarboxylic acid (VI).

This dibasic acid VI was decarboxylated in quinoline with copper powder into a mixture of karanjol (VIII) and karanjic acid (IX).

2,2-Dicarbethoxy-3-hydroxy-6-benzyloxycoumaran (XII) was hydrolysed to 6-benzyloxycoumarone-2-carboxylic acid (XIII).

The authors are grateful to the Institute of Organic Chemistry, Osaka City University for the measurement of infrared spectra and to the Institute of Agricultural Chemistry, Faculty of Agriculture, Kyoto University for carring out microanalyses.

Faculty of Literature and Science
Toyama University, Toyama

Photo-dichroism of Printed-out Silver. I. Some Experimental Evidences in Favor of the View that the Photo-dichroism of Printed-out Silver is an Anisotropic Herschel Effect

By Isao KAMIYA

(Received June 20, 1956)

Introduction

A film of a partially printed-out emulsion which has been isotropic becomes anisotropic in its optical nature when exposed to linear polarized red light for a considerable period. This phenomenon which was discovered by Weigert[1] in 1919, is called either the "Weigert effect" or photo-dichroism.

Many discussions on this subject have been carried out by many authors[2].

1) F. Weigert, *Ver. Phys. Ges.*, **21**, 479 (1919).

2) For example, F. Weigert, *Ann. Phys.*, **63**, 681(1920); F. Weigert and J. Shidei, *Z. Phys. Chem.*, **B9**, 344(1930); S. V. Chrdynlsev, *J. Phys. Chem.(USSR)*, **15**, 441(1941); J. Shidei, D. Yamamoto and I. Kamiya, *J. Chem. Soc. Japan*, **72**, 171 (1951); A. Narath and K. Warserroth, *Science et inds. phot.*, **23A**, 38 (1952); I. Kamiya, *J. Chem. Soc. Japan*, **76**, 576 (1955).

Weigert and Stiebel[3] postulated a theory that the colloidal particles of metallic silver in photographic emulsion (such as printed-out silver or latent image) would undergo a change to a vibrating of their structure, as they termed it "*Form-faktor*", in planes parallel to the electric vector of the light when exposed to polarized red light.

Cameron and Taylor advanced[4] the above theory and proposed a mechanism in a somewhat concrete way as follows.

Pointing out the fac* that the colloidal particles such as printed-out silver are unlikely spherical but will have their long axes along planes of weakness in crystal of silver halide, they assumed that the particles which resonate to any particular wave-length would be destroyed by prolonged exposure, and that if the long axis of a particle is parallel to the electric vector of the exposed light, the destruction of this resonator would be the greatest.

These discussions are said to be unsatisfactory because of being based on such a metaphysical interpretation as *Form-faktor* or *destruction of resonator*. Moreover, it will be perhaps questionable as to whether such particles can operate in this manner.

The work reported here was undertaken in the hope that a more satisfactory theory of the phenomenon might be formulated.

The present author would prefer to propose the following explanation.

The phenomenon might be some specific effect related to Herschel effect; that is; this might be an anisotropic Herschel effect.

In the next paper, the author will discuss the mechanism, based on Herschel effect, by which the anisotropic nature is formed.

In the present paper, some experimental evidences in favor of this view are reported.

Experimental Evidences

The first part of the work consisted in search for necessary and sufficient conditions for the production of the phenomenon.

The colloidal silver and selenium were prepared by the following method.

Adding the dilute solution of ammonium hydroxide to one per cent of a solution of silver nitrate until the white precipitation became soluble, and adding 5-6 drops of tannin solution; dark reddish colloidal silver was produced. Pouring 2 l. of warm water to 1 g. of selenium oxide, 15-16 drops of the solution of hydrazin hydrate, were added; it was then heated; dark reddish colloidal selenium was produced.

Each colloidal solution was added to gelatin emulsion to prepare the films. The absorption spectra of these films were analogous to that of the film of printed-out silver (printed-out Valenta's emulsion[5]).

These films were exposed to linear polarized red light, so that they could be examined to see if the phenomenon would be produced in them. There was found no phenomenon in the films, which means that silver chloride will be necessary to the phenomenon.

To decide this, another experiment was undertaken.

In the first place, a film of printed-out silver which had been previously fixed in the solution of alkaline hypo to avoid the dissolving silver chloride was exposed to polarized red light. In the second place, the film which had been exposed to the light for a short time was fixed, and then it was exposed again. In the third, it was never fixed. The values of dichroism observed in the three cases are shown in Table I, where, for simplicity, the angle of maximum rotation (2α)* is directly taken to express the degree, as proposed by Weigert.

TABLE I

PHOTO-DICHROISM IN FIXED AND IN UNFIXED FILMS

	Time of Exposure (min.)				
	1	5	10	20	30
No. I	0.00	0.00	0.01	0.02	0.03
No. II	1.52	4.78	5.88	5.90	5.90
No. III	1.00	2.72	3.12	4.44	6.76

It can be seen as the results of these experiments that silver chloride would be necessary to produce the phenomenon.

On the other hand, Zocher and Coper[6] have found the phenomenon in a silver mirror treated with chlorine gas to produce silver chloride on its surface (Chlorierten Silber Spiegeln) when exposed to polarized light, and Cameron and Taylor[4] have also observed it in a single crystal of blue silver chloride (containing printed-out silver).

From this point of view, it can be said that the phenomenon is to be observed in the systems in which the solid medium (such as gelatin or collodion) is absent.

Next, the author has examined the reversible effect in the partially printed-out Valenta's emulsion.

After exposure to the polarized red light for about forty minutes, the plane of polarization of the light was turned by 90°, so that the degree of dichroism began to diminish and soon had

3) F. Weigert and F. Stiebel, *Z. Phys. Chem.*, **B13**, 279 (1931).

4) A. E. Cameron and A. M. Taylor, *J. Opti. Soc. Am.*, **24**, 316 (1934).

5) Valenta in Eder, *Jahrb. Photogr.*, **76**, 960 (1898).

* $D=2\log\tan(45\pm\alpha)$, D : dichroism

6) H. Zocher and M. Coper, *Z. Phys. Chem.*, **132**, 303 (1928).

entirely disappeared. Now, if the exposure was still continued, the phenomenon appeared again in the reversed direction as at first. This has beed termed *reversible effect*[7]. The experimental results are shown in Fig. 1, where it can clearly be seen that the degree of dichroism tends to diminish as repeating the reversed exposure. This tendency depends on the time of pre-illumination to print out the film, i.e. when the film is pre-illuminated for a long time, it is not so remarkable even though the degree is comparatively small, while it is remarkable for a short-time pre-illumination.

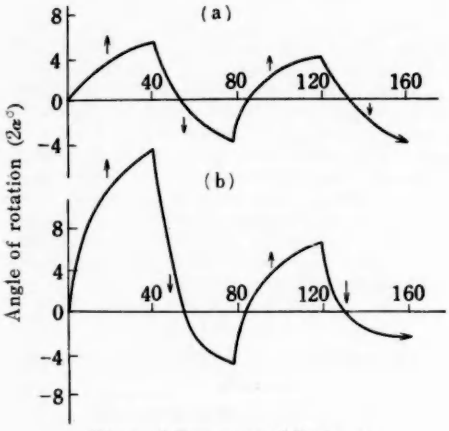

Fig. 1. Reversible effect of Photo-dichroism.
(a) and (b) show the results after 30 and 10 minutes' pre-illumination.

As the result of this, it is found that the production of photo-dichroism would be due to the partial bleaching of colloidal silver.

Finally, it is concluded that silver and silver chloride are the necessary and sufficient conditions to produce the phenomenon.

The phenomenon of photo-dichroism has been observed in the films of some gelatin-dye system as well as in the film of printed-out silver.

According to Ungar, Nikitine, and Yamamoto[8], the phenomenon observed in the films of gelatin-dye is due to an anisotropic bleaching of dye molecule; in other words, the molecules of dye-stuff of which the absorption axes orientate to the direction parallel to the electric vector of the light would be bleached, so that there remain unbleached molecules being arranged in the film after exposure to polarized light.

From this point of view, it will be emphasized that the degree of dichroism of gelatin-dye systems will decrease with increasing temperature owing to disturbance in such an arrangement.

The experimental evidence in favor of the conclusion has not been reported.

For this reason, the author has studied the temperature dependence of the phenomenon in gelatin-dye systems in just the same manner as reported by J. Shidei, M. Hosohara and D. Yamamoto[9].

The experimental results obtained in several kinds of dye-stuff are shown in Table II, where the degree of dichroism was measured with white light using 100 watt tungsten lamp, and is denoted as 2α as before. It can be seen that the degree decreases with increasing temperature as has been expected.

TABLE II

TEMPERATURE DEPENDENCE OF DEGREE OF PHOTO-DICHROISM IN GELATIN-DYE FILMS

(a) Pinacyanol-gelatin Film (observed in white light)

	Time of Exposure (min.)						
	0	1	2	5	10	20	40
6°C	0.00	0.03	0.05	0.08	0.13	0.24	0.41
Temp. 15°C	0.00	0.00	0.02	0.03	0.04	0.07	0.15
40°C	0.00	0.00	0.00	0.00	0.00	0.03	0.03

(b) Pinachrome-gelatin Film. (Observed in white light)

	Time of Exposure (min.)						
	0	1	2	5	10	20	40
6°C	0.00	0.01	0.02	0.04	0.05	0.11	0.16
Temp. 15°C	0.00	0.00	0.01	0.03	0.04	0.07	0.11
40°C	0.00	0.00	0.00	0.00	0.01	0.01	0.02

On the contrary, it has been reported[9] that the degree of dichroism of printed-out silver is increased with increasing temperature. To make this sure, the decisive test was undertaken using partially printed-out Valenta's emulsion in more detail in the same manner as with the method reported by above authors[9]. These results are shown in Table III. From these evidences, it would be concluded that the mechanism of the phenomenon in printed-out silver is different essentially from that of in gelatin-dye systems.

TABLE III

TEMPERATURE DEPENDENCE OF THE DEGREE OF PHOTO-DICHROISM IN VALENTA'S FILM (OBSERVED IN RED LIGHT OF 630 mμ)

	Time of Exposure (min.)			
	5	10	20	40
10°C	1.32	1.54	1.95	2.74
Temp. 30°C	2.72	3.12	4.04	5.86
45°C	4.34	5.88	7.30	9.92
60°C	5.36	6.02	7.06	8.90

7) S. Horiba and R. Kondo, "The Sexagint (Osaka-Fest.)" Kyoto Univ, p. 61.
8) G. Ungar, *Z. phys. Chem.*, **B38**, 427 (1938); S. Nikitine, *Ann. Phys.*, **15**, 284 (1941); D. Yamamoto, *J Chem. Soc. Japan*, **72**, 948 (1951).
9) J. Shidei, M. Hosohara and D. Yamamoto, *J. Chem. Soc. Japan*, **73**, 184 (1952).

Now, if D_T is the value of dichroism at T°K of temperature, and $\log D_T$ is plotted against $1/T$, then an almost approximate line is to be obtained as is shown in Fig. 2. This means that the relation between D_T and T must be given as,

$$\log D_T = a + b/T \qquad (1)$$

where, a and b are constant.

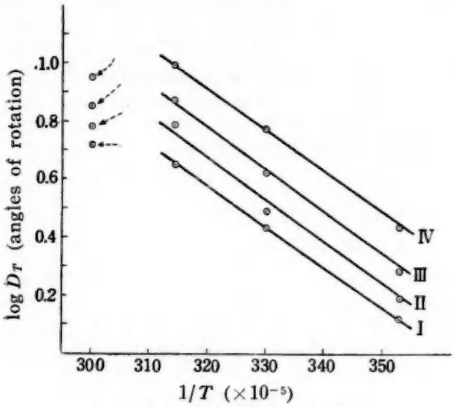

Fig. 2. Log D_T vs. $1/T$.
I, II, III and IV show the results after 5, 10, 20 and 40 minutes excitation.

These esults support the author's theory, which will be reported in the next paper, that the D_T is to be shown as,

$$\log D_T = \log D_0 - U/2.3RT \qquad (2)$$

where, R is gas constant, D_0 is a constant and U is activation energy.

The probable value of U obtained from (1), are shown in Table IV.

TABLE IV
ACTIVATION ENERGY OF PHOTO-DICHROIC CHANGE IN VALENTA'S FILM

Time of Exposure (min.)	5	10	20	40
Activation energy (cal./mol.)	6941	7066	7091	7120

Note: On this caluclation, the values observed at 60°C were neglected, probably because of deviation on account of distortion of gelatin molecules.

In the course of these experiments, the source of pre-illuminating light was a Hg-lamp, filtrated with a UVD_1 filter glass, (Matsuda), and that of exposing polarized red light was a five ampare carbon arc filtrated with a filter consisting of a glass tank filled with the scarlet solution transmitting the spectrum region between 630–650 mμ, and a Nicol's prism. These values were measured with the 100 watt tungsten lamp, filtrated with S-63 glass filter (Shimazu).

Discussion

It was shown in the first part of the experimental results that silver and silver chloride are the necessary and sufficient conditions to produce the phenomenon.

It has already been known that the wave length of exposed light which is the most effective is in the region between 600 mμ and 650 mμ, and that the exposing for a long period is necessary to produce the phenomenon. All these facts are very similar to that in Herschel effect. Cameron and Taylor[4] have reported that the phenomenon is not produced in the film, which has been previously printed out, at the temperature of liquid nitrogen. The same behavior has also been observed by Evans and Webb[10] in the experiment on Herschel effect.

Moreover, we have just seen that the activation energy for dichroic change is obtained as about 7000 cal./mol., which is almost the same value as that of diffusion of interstitial silver ions in silver chlroride. According to the mechanism proposed by Mott and Gurney[10] the activation energy to produce the Herschel effect will be explained by the same mechanism (i.e. be diffusion energy of interstitial ions).

There is a suggestion, in opposition to the author's conclusion, that the phenomenon would be due to a solarisation. This suggestion, however, would seem not to be permissible by the following evidences.

If the solarization is, as explained by Eder[11] and Mott[10], due to the formation of a layer of silver chloride covering the metallic silver which has been attacked by the chlorine liberated in the photochemical reaction, it is not possible to explain the following fact that there is no change in the total amount of photo-silver during exposure to polarised light, which has been reported by Cameron and Taylor[4] and Weigert. Moreover, if the mechanism based on such solarization were true, the chlorine atom liberated by exposing light would be able to attack the particle of metallic silver, so that there could be found the phenomenon at liquid air temperature.

The author wishes to express his thanks to the late Prof. J. Sidei and to Dr. Yamamoto for their kind advice.

Department of General Education
Nagoya University, Nagoya

10) N. F. Mott, R. W. Gurney, "Electronic Processes in Ionic Crystals," Oxford Press(1950), p. 243; J. H. Webb and C. H. Evans, *J. Opti. Soc. Am.*, **28**, 294 (1938).
11) J. M. Eder, *Z. Phys. Chem.*, **117**, 293 (1925).

A Thermistor Method for the Determination of Velocity Coefficients of Vinyl Polymerization. IV

By Hajime MIYAMA

(Received July 5, 1956)

Introduction

In the Previous paper[1] the variation of the ratio of velocity constants of propagation and termination, k_p/k_t, was studied with use of a thermistor method against the conversion in vinyl acetate polymerization. In that study, however, each value of k_p and k_t could not be obtained. The author wishes to report, in this paper, the determination of the values of k_p and k_t through the study of the decomposition velocity of the sensitizer 1,1'-azo-biscyclohexanecarbonitrile, under the same conditions.

Theoretical

Polymerization velocity $-dM/dt$ of vinyl acetate, as is well known, can be given as follows[2], provided that the concentration of activated molecule is constant and that the chain is long enough for the initiation velocity against the propagation to be ignored.

$$-dM/dt=k_p(V_{init.}/k_t)^{1/2}M \qquad (1)$$

where $V_{init.}$ represents the velocity of initiation and M the concentration of the monomer. Therefore, fractional velocity V can be given by

$$V=-(1/M)dM/dt=k_p(V_{init.}/k_t)^{1/2} \qquad (2)$$

V and k_p/k_t are known, as reported in the previous paper, hence k_p can be calculated by the following equation when $V_{init.}$ is determined.

$$k_p=V^2\times(k_t/k_p)\times(1/V_{init.}) \qquad (3)$$

As to the mechanism of photosensitized polymerization by 1,1'-azo-biscyclohexanecarbonitrile, it is considered probable that sensitizer S is decomposed by photon $h\nu$ and two activated products or radicals R^* are formed from a molecule of the sensitizer,

$$S+h\nu\rightarrow 2R^* \qquad (4)$$

and this radical further activates the monomer M

$$R^*+M\rightarrow R+M^* \qquad (5)$$

If the following equation is taken in this mechanism, as Matheson et al.[3] assumed in the styrene polymerization with use of 2,2'-azo-bisisobutyronitrile,

$$V_{init.}=2V_s \qquad (6)$$

then equation (3) can be written as follows

$$k_p=V^2\times[2(k_p/k_t)V_s]^{-1} \qquad (7)$$

When V and k_p/k_t values obtained in the previous paper and V_s which can be measured, are applied to the above equation (7), k_p and k_t values can be obtained.

Results

Experimental apparatus and purification of samples were the same as described before[1] and the measurement was carried out at 20°C. As mentioned in the previous paper, 1,1'-azo-biscyclohexanecarbonitrile shows a big absorption band at ca. 3500 Å. Beer's law could be applied for the optical density at certain wave lengths and concentrations of the sensitizer and this relation at 3660 Å is shown in Fig. 1. D was

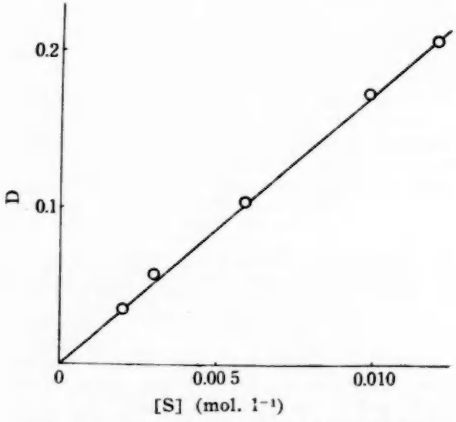

Fig. 1. Variation of the optical density with concentration of 1,1'-azo-biscyclohexanecarbonitrile.

1) H. Miyama, This Bulletin, **29**, 711, 715, 720 (1956).
2) C. E. H. Bawn, "Chemistry of High Polymers," London (1948), p. 68.
3) M. S. Matheson, E. E. Auer, E. B. Bevilacquer and E. J. Hart, *J. Am. Chem. Soc.*, **73**, 1700 (1951).

measured by use of Hitachi Spectrophotometer EPB-U in vinyl acetate and the thickness of the cell was 1 cm. Thus the decomposition velocity of the sensitizer could be determined from the optical density which, in turn, showed the concentration during the polymerization. A relation between decomposition velocity of sensitizer in vinyl acetate and initial concentration when intensity of illumination is constant, is shown in Fig. 2 and

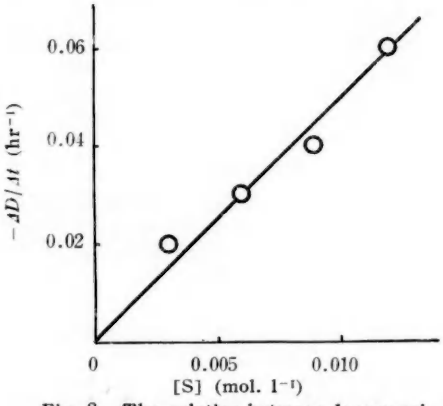

Fig. 2. The relation between decomposition velocity and concentration of 1, 1'-azo-biscyclohexanecarbonitrile.

that between intensity of light and decomposition velocity when concentration of sensitizer is constant (0.012 mol./l.), in Fig. 3. In Figs. 2 and 3, decomposition

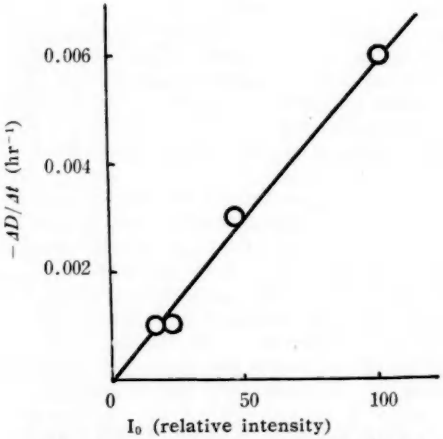

Fig. 3. The relation betweeen decomposition velocity of 1, 1'-azo-biscyclohexanecarbonitrile and intensity of illumination.

velocity $-\Delta D/\Delta t$ is a decrease of the optical density of sensitizer after one hour irradiation.

The author obtained the results shown in Fig. 4 on determination of variation of

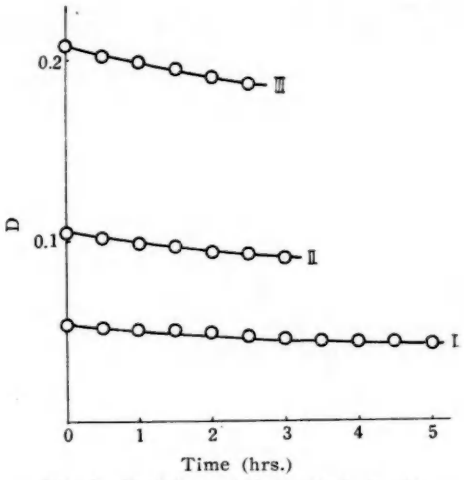

Fig. 4. Variation of the optical density of 1, 1'-azo-biscyclohexanecarbonitrile with time.
I, 0.003 mol. l^{-1}; II, 0.006 mol. l^{-1}; III, 0.012 mol. l^{-1}.

the optical density of sensitizer with time when continuous irradiation was applied under the same conditions as described for the vinyl acetate polymerization, which was photosensitized, in the third paper of this series. The initial concentration of the sensitizer was 0.003 mol./l., 0.006 mol./l. or 0.012 mol./l.

From the results shown in Figs. 2 and 3, it is clear that the decomposition velocity of sensitizer V_s is proportional to the concentration of sensitizer $[S]$ and the intensity of light I_0. Absorbed light $I_{abs.}$ is shown by the next formula

$$I_{abs.}=I_0(1-e^{-\alpha[S]l}) \qquad (8)$$

where α is molar absorption coefficient of sensitizer (40.1) and l is the thickness of the reaction vessel (8 mm.). The value of $\alpha[S]l$ is 0.096 at the concentration of sensitizer 0.003 mol./l., hence the next approximation is materialized within the error

$$I_{abs.}\fallingdotseq I_0\alpha l[S] \qquad (9)$$

thus V_s is obtainable from the next equation

$$V_s=-\mathrm{d}[S]/\mathrm{d}t=kI_{abs.}=kI_0\alpha l[S] \qquad (10)$$

Since $K=kI_0\alpha l$ can be considered constant

during the measurement in Fig. 4, next equation is obtained by integrating equation (10)

$$2.303 \log [S]_0/[S] = Kt \qquad (11)$$

thus there should be a linear relation between $\log [S]_0/[S]$ and time t, where $[S]_0$ is the initial concentration of sensitizer. This relation can be shown in Fig. 5, in

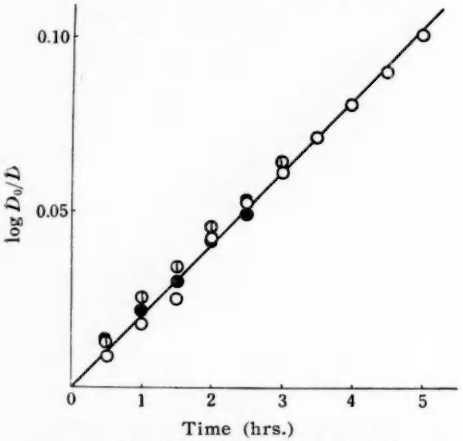

Fig. 5. Variation of $\log D_0/D$ with time. ○, 0.003 mol. l^{-1}; ⓘ, 0.006 mol. l^{-1}; ●, 0.012 mol. l^{-1}.

which $\log D_0/D$ is used instead of $\log [S]_0/[S]$ the former being obtained from the result of Fig. 4. The equation (11) is apparently materialized. The constant K obtained from the tangent of this line is 4.66×10^{-2}hr^{-1}. The concentration of sensitizer in the case of determining k_p/k_t of vinyl acetate polymerization was 0.003 mol./l. in the third paper of this series and thus V_s at arbitrary time can be calculated by the next equation when the above value of K is used.

$$V_s = K[S]_0 e^{-Kt} \qquad (12)$$

The above equation is obtained by eliminating $[S]$ from equations (10) and (11).

TABLE I

VALUES OF CONVERSION, V_s, V AND k_p/k_t AT VARIOUS IRRADIATION PERIODS

Time (hr.)	Conversion (%)	V_s (mol. l^{-1}. s^{-1})	V (s^{-1})	k_p/k_t
0	0	3.87×10^{-9}	2.16×10^{-5}	1.08×10^{-5}
3	28.15	3.36×10^{-8}	2.98×10^{-5}	2.82×10^{-5}
4	39	3.21×10^{-8}	3.06×10^{-5}	4.13×10^{-5}
5	49.80	3.06×10^{-8}	2.95×10^{-5}	9.55×10^{-5}
6	59.30	2.92×10^{-8}	2.34×10^{-5}	32.3×10^{-5}
7	66.40	2.79×10^{-8}	1.61×10^{-5}	48.6×10^{-5}
8	71.10	2.66×10^{-8}	1.00×10^{-5}	64.2×10^{-5}

The values of V_s, V and k_p/k_t, the latter two of which were obtained in the previous paper, at various times are shown in Table I. The values of k_p and k_t, which were calculated by using equation (7) and the above values in Table I, were tabulated in Table II.

TABLE II

VALUES OF k_p AND k_t AT VAROUS CONVERSIONS

Conversion (%)	k_p	$k_t\times10^{-5}$
0	559	518
28.15	484	172
39	354	85.8
49.80	149	15.6
59.30	29.0	0.90
66.40	9.52	0.20
71.10	2.93	0.05

Discussion

Since k_p and k_t values at the early stage of polymerization were obtained by many other workers, the results are shown in Table III for comparison.

TABLE III

THE VALUES OF k_p AND k_t OF VINYL ACETATE POLYMERIZATION AT 15°C[4]

Reference	k_p	k_t
This work	505	5.15×10^{7}
Bengough and Melville (1955)	574	2.4×10^{7}
Bartlett et al. (1950)	800	5.7×10^{7}
Dixon-Lewis (1949)	4180	2.2×10^{8}
Matheson et al. (1949)	630	4.5×10^{7}
Burnett and Melville (1947)	720	4.5×10^{8}

The value of k_p obtained by the author is a little lower than the others and the k_t is about the same. The methods of determination and calculation, however, are different, therefore this amount of deviation seems to be reasonable. It is doubtful whether the theory which is used for the explanation of the results at the early stage of polymerization is applicable for the later stage, but, from the results of Table II, it can be qualitatively said that k_p is considered to be constant up to 40% conversion while k_t gradually decreases and thus the polymerization velocity increases up to 40% conversion. As the conversion exceeds 40%, k_p decreases to lower the velocity of polymerization. It is possible to consider that the velocity probably depends on the reactivity of

4) The author corrected the values at 15°C assuming that E_p=3.7 kcal./mole and E_t=0. The other values have been summarized in a literature (W. I. Bengough & H. W. Melville, *Proc. Roy. Soc.*, **230**, 429 (1955)) and corrected assuming that E_p=4.2 kcal./mole and E_t=0.

radicals or radical and monomer at the early stage of polymerization and on diffusion at the later stage, because, in the latter, viscosity increases to make diffusion very slow. From Table II, the effect of diffusion first appears in the termination process

$$M_n^* + M_m^* \rightarrow M_{n+m} \qquad (13)$$

On the other hand the propagation process shown by the next formulas is not so greatly affected by viscosity and only in conversion of more than 40% diffusion comes to have some effect on the velocity.

$$\left.\begin{aligned} &M_1^* + M \rightarrow M_2^* \\ &M_2^* + M \rightarrow M_3^* \\ &\cdots\cdots\cdots\cdots\cdots \\ &M^*_{n-1} + M \rightarrow M_n^* \end{aligned}\right\} \qquad (14)$$

This difference may be explained by the difference of mobility of monomer M and radical M_n^* in viscous solution.

Summary

Concentration change of sensitizer during vinyl acetate polymerization photosensitized by 1, 1'-azo-biscyclohexanecarbonitrile was measured with use of a spectrophotometer and the initiation velocity of polymerization was determined. Values of k_p and k_t at various degree of conversion were calculated from this value and the results of the previous paper. From this experiment, it was concluded that k_p was nearly constant up to 40% conversion and as the conversion exceeded 40%, it decreased, while k_t gradually decresed with the increase of the conversion.

The author wishes to express his hearty thanks to Dr. Momotaro Suzuki of this Academy for his helpful advice and to Mr. Shinichi Taira of Tokyo Metropolitan University for preparation of 1,1'-azo-biscyclohexanecarbonitrile.

Department of Chemistry Defense Academy Yokosuka

Structures of the Erdmann's Salt, $NH_4[Co(NH_3)_2(NO_2)_4]$ and Some Other Related Nitro-ammine-cobalt (III) Complexes

By Yoshimichi KOMIYAMA

(Received July 14, 1956)

Introduction

Since the pioneer work of Shibata and Maruki[1], many attempts have been made to determine the configuration of tetranitro-diammine-cobaltiate ion, $[Co(NH_3)_2(NO_2)_4]^-$. As disubstituted octahedral complex has two stereoisomers, the *cis*- and the *trans*-form, there exist two possibilities in the configuration of the complex ion $[Co(NH_3)_2(NO_2)_4]^-$; i.e. the forms (A) and (A') shown in Fig. 1.

Shibata and Maruki[1] converted ammonium tetranitro-diammine-cobaltiate, $NH_4[Co(NH_3)_2(NO_2)_4]$, (Erdmann's salt) into an oxalato compound, $NH_4[Co(NH_3)_2(NO_2)_2(C_2O_4)]$. If this is derived directly from the *trans*-tetranitro-diammine (A), it can not show optical isomerism; if from the *cis*-compound (A'), two oxalato compounds should be formed, one of which, (C), has a plane of symmetry while the other (D) has no plane of symmetry so that it should be resolvable. They reported that the oxalato compound from Erdmann's salt was resolved into optical isomers ($[\alpha]_D = \pm 115°$) in the form of a potassium salt, by using brucine, strychnine and cinchonine as resolving agents and concluded that the Erdmann's salt has the *cis*-structure.

Riesenfeld and Klement[2] reported that the same attempt to resolve the oxalato compound into optical isomers was unsuccessful. Taking its chemical properties into account, they came to the conclusion that the Erdmann's salt has the *trans*-structure.

On the other hand, Thomas[3] repeated fractional crystallization of the barium

1) Y. Shibata and T. Maruki, *J. Chem. Soc. Japan*, **37**, 1142 (1916).

2) F. H. Riesenfeld and R. Klement, *Z. anorg. Chem.*, **124**, 1 (1922).

3) W. Thomas, *J. Chem. Soc.*, **123**, 617 (1923).

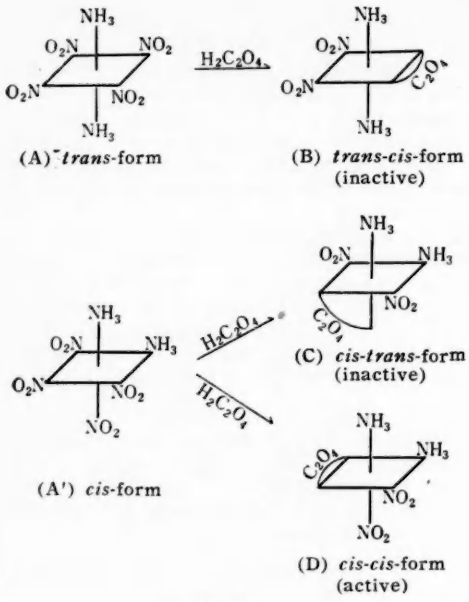

Fig. 1.

salt of the oxalato compound and obtained two different fractions; one was rhombohedral and the other was monoclinic. The rhombohedral fraction was found to be resolvable by means of strychnine and α-phenylethylamine. The specific rotations of the optically active potassium salts measured by Na-D line were $\pm 154°$ respectively. Therefore, Thomas concluded that the two fractions had the structure (C) and (D) respectively, and assigned the *cis*-structure (A') to the Erdmann's salt.

However, the result obtained by Ray[4] was quite contradictory. He reported that it was impossible to resolve the oxalato compound by means of salts of strychnine and *l*-$[Co\ en_3]^{3+}$. This result combined with the absorption spectrum and chemical behaviour of the compound led him to conclude that Erdmann's salt had the *trans* structure and the two fractions obtained by Thomas had been nothing but two different modifications of one compound (C).

In 1949, Kuroya and Yamasaki[5] repeated fractional crystallizations of ammonium and barium salts of the oxalato compound very carefully and concluded that the *cis*- and the *trans*-isomers of $[Co(NH_3)_2(NO_2)_4]^-$ should coexist in solution at room temperature as an equilibrium mixture.

In determining the configuration of a complex ion by various indirect means, as mentioned above, it has to be assumed that the mechanism of substitution reaction is such that they do not bring about any change of the configuration at any stage. This assumption, however, does not always seem to be valid in the case of Erdmann's salt.

Wells[6] was the first who determined the configuration of the complex anion by direct means; the crystal structure of a silver salt, $Ag[Co(NH_3)_2(NO_2)_4]$, was determined by the use of X-rays and it was shown that the complex ion possessed the *trans*-configuration. Recently, the same result was reported by E. A. Gilinskaya[7], too.

In view of the confusing results obtained by many authors, it would be of interest to determine the configuration of the complex anion in crystals of Erdmann's salt itself. As a first step, the author determined the crystal structure of a potassium salt, $K[Co(NH_3)_2(NO_2)_4]$, which was isotype to the Erdmann's salt, and the details of the work were published already in the previous report[8]. In this paper, the crystal structure of Erdmann's salt will be described, and some discussions will be given concerning the structures of various nitro-ammine-cobalt (III) complex salts, whose crystal structures[8-11] have been analyzed mainly by the author for these several years. Furthermore, the results of absorption measurements on their aqueous solutions will be reported. Since many investigators[12-14] have found interesting and important relations between the absorption spectra and the stereochemical configurations of cobalt (III) co-ordination compounds, it may be worth while to re-examine their absorption spectra.

Experimental

Erdmann's salt, $NH_4[Co(NH_3)_2(NO_2)_4]$, has been prepared according to the method described by Jörgensen[15]. The crystals belong to the orthorhombic bipyramidal class with the axial ratio;

4) B. C. Ray, *J. Indian Chem. Soc.*, 440 (1937).
5) Read at the meeting of Chem. Soc. Japan, (1949).
6) A. F Wells, *Z. Krist.*, (A)., **95**, 74 (1936).
7) E. A. Gilinskaya, *Ser. Fiz-Mat. i Estestven. Nauk*, **3**, 133 (1953).
8) Y. Komiyama, This Bulletin, **29**, 300 (1956).
9) Y. Tanito, Y. Saito and H. Kuroya, This Bulletin, **25**, 188 (1952).
10) Y. Tanito, Y. Saito and H. Kuroya, ibid., **25**, 328 (1952).
11) Y. Tanito, Y. Saito and H. Kuroya, ibid., **26**, 420 (1953).
12) H. Sueda, *J. Chem. Soc. Japan*, **57**, 406 (1936).
13) H. Kuroya, *J. Inst. Polytech*, Osaka City Univ., Vol. 1, Ser. C, 1 (1950).
14) M. Linhard and M. Weigel, *Z. anorg. Allgem. Chem.*, **267**, 113 (1951).
15) S. M. Jörgensen, *Z. anorg. Chem.*, **17**, 477 (1898).

TABLE I

ABSORPTION MAXIMA OF NITRO-AMMINE-COBALT(III) COMPLEXES

	$\lambda_1(m\mu)$	$\log \varepsilon_1$	$\lambda_2(m\mu)$	$\log \varepsilon_2$	$\lambda_3(m\mu)$	$\log \varepsilon_3$
Cis$[Co(NH_3)_4(NO_2)_2]NO_3$	442.0	2.21	325.0	3.62	233.5	4.27
Trans$[Co(NH_3)_4(NO_2)_2]Cl$	429.0	2.49	341.5	3.83	251.5	4.37
$[Co(NH_3)_3(NO_2)_3]$	432.0	2.46	340.0	3.81	251.0	4.35
$[Co(NH_3)_3(NO_2)_2Cl]$	452.0	2.18	334.0	3.62	236.0	4.15
$K[Co(NH_3)_2(NO_2)_4]$	421.0	2.71	348.0	4.05	253.5	4.43

$a:b:c=0.8837:1:0.5226$ and are dark reddish brown in colour. They are well-formed and elongated along the *c*-crystal axis. In these respects they resemble the corresponding potassium salt.

The ammonium salt has $a=11.39\pm0.02$ Å, $b=12.97\pm0.02$ Å, and $c=6.74\pm0.01$ Å, $Z=4$. These values give the axial ratio $a:b:c=0.878:1:0.520$, which are in good agreement with those obtained by crystal measurement.

From the systematic absences; $(h00)$, $(0k0)$ and $(00l)$ for h, k and l odd, the space group was found to be $P2_12_12_1$. The calculated density 1.966 g./cc. is in agreement with that observed, 1.954 g./cc. at 25.5°C.

All the equatorial reflections around the three principal axes were recorded by using Fe K_α radiation on a pack of three films and the intensity of the reflections were visually estimated. The usual correction factors were applied by means of Cochran's chart[16]. Observed structure amplitudes were then placed on the absolute scale by Wilson's method[17].

The measurements of absorption spectra of these nitro-ammine-complexes and two others for reference, were made over the range from 220 to 500 mμ with Beckman Model DU spectrophotometer. Concentrations of aqueous solution used for measuring absorption was ranging from 10^{-3} to 10^{-5} mol./*l*.. The absorption maxima are tabulated in Table I.

Determination of the Structure

By comparing the general features of structure amplitudes and Patterson projections along the three principal axes of Erdmann's salt with those of the potassium salt, it was seen that they are isotype. As the first step, therefore, F values were calculated by using the parameter values of the potassium salt. The agreement between the observed and calculated F values was good enough to enable the usual Fourier refinement to be started. Then all the parameter values were refined successfully and the final parameters listed in Table II were obtained. A final electron density projection on a plane perpendicular to the *c*-axis is shown in Fig. 2.

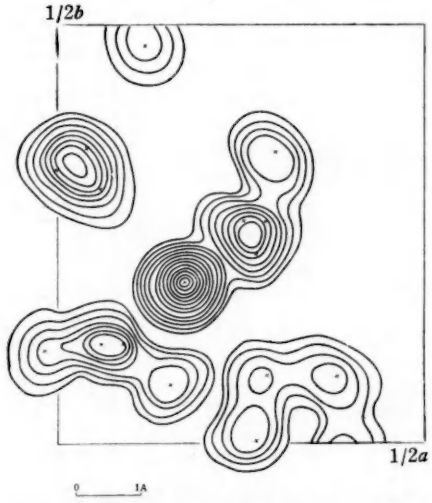

Fig. 2. Electron densities along *c*-axis of $NH_4[Co(NH_3)_2(NO_2)_4]$. Contours are at intervals of 2 e.Å^{-2}.

The atomic scattering factors used for the calculation of the structure factors were those listed in the International Tables. A temperature factor of the form $\exp-B(\sin\theta/\lambda)^2$ was used, where B was given the value 2.5 Å^2. The value of B and the scale factor were estimated by plotting the values of $\log F_c/F_o$ versus $(\sin\theta)^2$ at the final stage. The reliability factors $R=\Sigma||F_o|-|F_c||/\Sigma|F_o|$ are 0.160, 0.243 and 0.208 for $(hk0)$, $(0kl)$ and $(h0l)$ respectively. The weighted mean value of R is 0.188, for which only the observed reflections up to $\sin\theta/\lambda=0.501$ have been used.

Description of the Structure

The structure projected upon a plane normal to the *c*-crystal axis is shown in Fig. 3. The structure is built of ammonium ions and complex anions $[Co(NH_3)_2(NO_2)_4]^-$, thus being essentially ionic.

Interatomic distances and bond angles

16) W. Cochran, *J. Sci., Inst.*, **25**, 253 (1949).
17) A. J. C. Wilson, *Acta Cryst.*, **2**, 318 (1949).

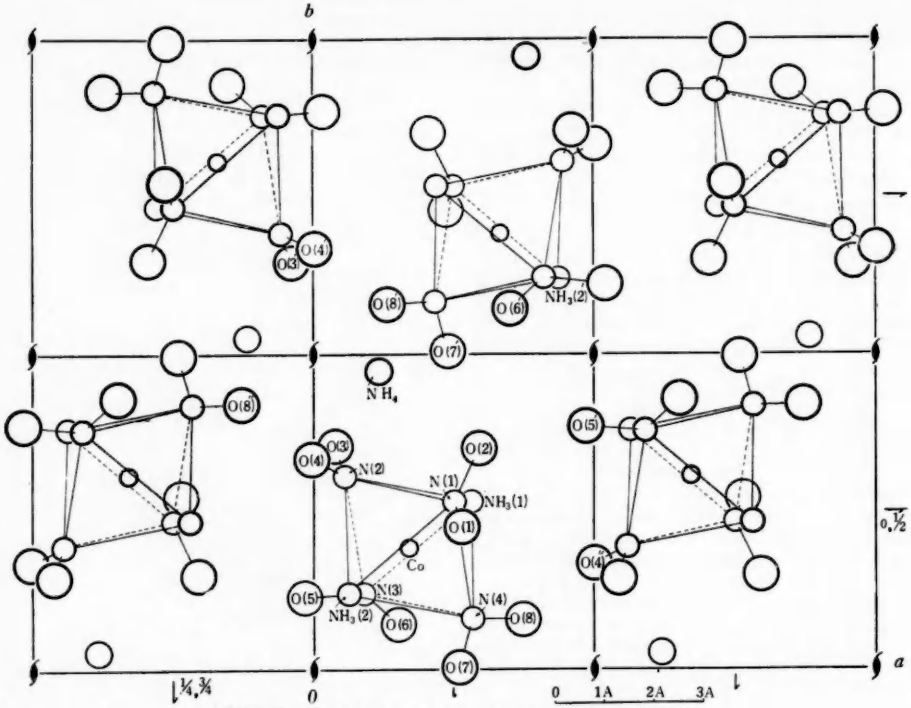

Fig. 3. Projection of the structure upon (001).

calculated on the basis of the atomic parameters in Table II are given in Table III. Two ammonia molecules are found to be co-ordinated to a cobalt atom in the *trans*-positions at the distance of 2.01 Å. Within the errors of the experiments this structure is exactly isotype to the corresponding potassium salt, and hence the detailed description of the structure will be discussed in the next section together with

TABLE II

FINAL PARAMETERS

	x/a	*y/b*	*z/c*
Co	0.1690	0.1915	0.2500
NH_4	0.117	0.473	0.695
$NH_3(1)$	0.279	0.265	0.064
$NH_3(2)$	0.059	0.118	0.436
N(1)	0.250	0.264	0.466
N(2)	0.056	0.305	0.234
N(3)	0.088	0.119	0.034
N(4)	0.281	0.078	0.266
O(1)	0.264	0.226	0.632
O(2)	0.293	0.350	0.442
O(3)	0.040	0.353	0.077
O(4)	−0.003	0.332	0.383
O(5)	−0.018	0.112	0.017
O(6)	0.150	0.070	−0.074
O(7)	0.260	0.005	0.376
O(8)	0.370	0.076	0.171

TABLE III

INTERATOMIC DISTANCES AND INTERBOND ANGLES

Co−$NH_3(1)$	2.01 Å	NH_4	···O(2)	3.08 Å
−$NH_3(2)$	2.01		···O(3)	3.15
−N(1)	1.96		···O(4)	3.10
−N(2)	1.96		···O(3′)	2.99
−N(3)	1.96		···O(4′)	3.11
−N(4)	1.96		···O(7′)	3.24
			···O(8′)	2.81
N(1)−O(1)	1.23		···O(8″)	3.02
−O(2)	1.23			
∠ONO	116°	$NH_3(1)$	···O(5′)	2.86
		$NH_3(1)$	···O(1)	2.96
N(2)−O(3)	1.24	$NH_3(2')$	···O(5′)	3.07
−O(4)	1.26			
∠ONO	118°	O(1)	···O(4″)	2.76
		O(2)	···O(6′)	3.06
N(3)−O(5)	1.22	O(2)	···O(7′)	3.00
−O(6)	1.20	O(3)	···O(7′)	3.03
∠ONO	119°	O(3)	···O(8″)	2.72
N(4)−O(7)	1.23			
−O(8)	1.20			
∠ONO	118°			

those of other nitro-ammine-cobalt (III) complexes.

Discussions on the Structure of Nitro-ammine-cobalt (III) Complexes

General Features of Crystal Structure. —The crystal data of various nitro-ammine-cobalt(III) complexes are listed in Table IV.

It is worth while to point out that in all these structures the cobalt atoms always occupy the sets of positions having higher symmetry than the corresponding space group. The symmetries of the arrangement of cobalt atoms, are shown in Table V.

Crystals of trinitro-triammine-cobalt(III) $[Co(NH_3)_3(NO_2)_3]$[9] and chlorodinitro-triammine-cobalt(III) $[Co(NH_3)_3(NO_2)_2Cl]$[11] are molecular, while those of potassium and ammonium tetranitro-triammine-cobaltiate(III) $K[Co(NH_3)_2(NO_2)_4]$[8], $NH_4[Co(NH_3)_2(NO_2)_4]$ are essentially ionic.

Characteristics of this structure seem to be the presence of spatial network consisting of the complex radicals. The binding force between the complex radicals is mainly due to the NH···O bonds between NH_3 and NO_2 groups.

Fig. 4 illustrates a network of complex radicals found in the structure of $[Co(NH_3)_3(NO_2)_3]$. It is perpendicular to the *a*-crystal axis. Each complex ion forms four hydrogen bonds with four neighboring complex radicals.

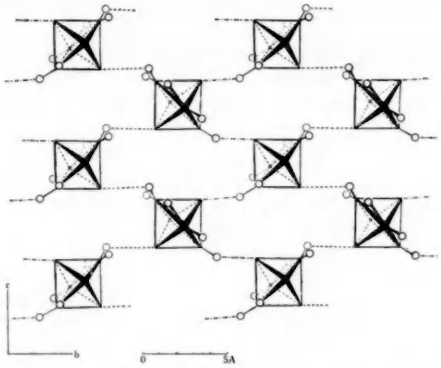

Fig. 4. Two dimensional network of complex radicals found in crystal of $[Co(NH_3)_3(NO_2)_3]$.
----: linkages of 2.74 Å.
-·-·-: linkages of 2.78 Å.

Only one of the two oxygen atoms of NO_2 groups which are in the *trans*-positions with respect to each other is used to form a NH···O bond of 2.74 Å and 2.78 Å with NH_3 of the adjacent complex radicals, and the other oxygen atom is farther from its nearest NH_3 groups, (3.10 Å and 3.29 Å apart).

A similar type of network was found in the structure of $[Co(NH_3)_3(NO_2)_2Cl]$, which

TABLE IV

CRYSTAL DATA OF NITRO-AMMINE-COBALT(III) COMPLEXES

	Crystal System	Space Group	Lattice Constants			β	Z
			a	b	c		
$[Co(NH_3)_3(NO_2)_3]$	Orthorhombic	$D_2^4-P2_12_12_1$	10.20 Å	11.77 Å	6.99 Å		4
$[Co(NH_3)_3(NO_2)_2Cl]$	Tetragonal	$C_{4h}^6-I4_1/a$	9.87		16.51		8
$[Co(NH_3)_3(NO_2)_2Br]$	Monoclinic	$C_{2h}^5-P2_1/n$	12.24	10.31	6.85	103.5°	4
$K[Co(NH_3)_2(NO_2)_4]$	Orthorhombic	$D_2^4-P2_12_12_1$	11.38	12.95	6.76		4
$NH_4[Co(NH_3)_2(NO_2)_4]$	Orthorhombic	$D_2^4-P2_12_12_1$	11.38	12.97	6.74		4

TABLE V

PSEUDO-SYMMETRIES OF THE ARRANGEMENT OF COBALT ATOMS

	x/a	y/b	z/c	
$[Co(NH_3)_3(NO_2)_3]$	0.0686	1/4	1/4	$D_{2h}^{17}-Bbmm$
$[Co(NH_3)_3(NO_2)_2Cl]$	0	0	0.267	$D_{4h}^{19}-I4_1/amd$
$[Co(NH_3)_3(NO_2)_2Br]$	1/4	y	0	C_{2h}^6-A2/n
$K[Co(NH_3)_2(NO_2)_4]$	0.1690	0.1915	1/4	$D_{2h}^{16}-Pbnm$
$NH_4[Co(NH_3)_2(NO_2)_4]$	〃	〃	〃	〃

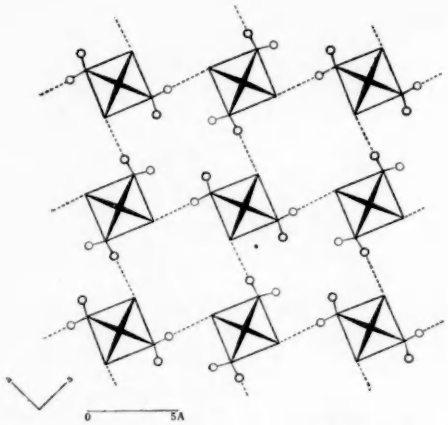

Fig. 5. Two dimensional network of complex radicals found in crystal of $[Co(NH_3)_3(NO_2)_2Cl]$.
----: linkages of 2.84 Å.

is shown in Fig. 5. The network is perpendicular to the *c*-crystal axis. Each complex ion is held together by a hydrogen bond of 2.84 Å, the mode of binding being essentially similar to that illustrated in Fig. 4. However, in the structure of $[Co(NH_3)_3(NO_2)_2Cl]$ these networks are held together by another NH···O bond between NO_2 and NH_3 of complex radical belonging to the adjacent layers, forming a three-dimensional network.

Thus, both of the oxygen atoms in the nitro-group are used to form NH···O bonds as follows:

N $\begin{cases} O\cdots NH_3 \text{ (within a layer)} \\ O\cdots NH_3 \text{ (within an adjacent layer).} \end{cases}$

In Fig. 6 is shown a network which is found in crystals of $K[Co(NH_3)_2(NO_2)_4]$ and $NH_4[Co(NH_3)_2(NO_2)_4]$. The plane of the network is perpendicular to the *b*-crystal axis. NH···O hydrogen bonds which are responsible for binding the complex anions with each other in a single layer are 2.87 Å and 2.97 Å.

It is interesting that the arrangement of cobalt atoms only in the network is remarkably similar to that found in the structures of $[Co(NH_3)_3(NO_2)_3]$, except that the orientation of octahedra consisting of

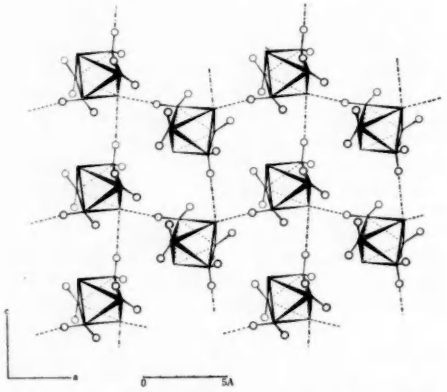

Fig. 6. Two dimensional network of complex radicals found in crystals of $K[Co(NH_3)_2(NO_2)_4]$ and $NH_4[Co(NH_3)_2(NO_2)_4]$.
----: linkages of 2.87 Å.
-·-·-: linkages of 2.97 Å.

TABLE VI

THE INTERATOMIC DISTANCES BETWEEN COBALT AND ITS LIGAND ATOMS

	Co—NH_3	In *trans*-co-ordination with respect to	Co—NO_2	In *trans*-co-ordination with respect to	Co—Cl	In *trans*-co-ordination with respect to
$[Co(NH_3)_3(NO_2)_3]$	1.98 Å	NH_3	1.96 Å	NH_3		
	1.99	〃	1.97	NO_2		
	1.97	NO_2	1.97	〃		
$[Co(NH_3)_3H_2OCl_2]$	1.96	NH_3			2.33 Å	Cl
$[Co(NH_3)_3(NO_2)_2Cl]$	1.99	NH_3	1.99	NO_2	2.30	NH_3
	1.90	Cl				
$K[Co(NH_3)_2(NO_2)_4]$	2.00	NH_3	1.96	NO_2		
	2.00	〃	1.96	〃		
			1.96	〃		
			1.96	〃		
$NH_4[Co(NH_3)_2(NO_2)_4]$	2.01	NH_3	1.96	NO_2		
	2.01	〃	1.96	〃		
			1.96	〃		
			1.96	〃		

six nitrogen atoms around each cobalt atom is slightly different from that of $[Co(NH_3)_3(NO_2)_3]$, and that the mode of binding is different. In case of $[Co(NH_3)_3(NO_2)_3]$ one ammonia group is used to form NH···O hydrogen bond with only one nitro-group, but in Erdmann's salt one ammonia group is bound to the two oxygen atoms of NO_2 groups belonging to different complex anions.

Potassium and ammonium ions are distributed between these networks. Hence the distances between the layers, 6.48 Å and 6.49 Å, are longer than the corresponding one, 5.10 Å, found in the crystals of $[Co(NH_3)_3(NO_2)_3]$.

Two nitro-groups which are in the *trans*-co-ordination seem to be more likely to form NH···O bonds than the case in which a nitro-group and other ligand are co-ordinated to the central cobalt atom in the *trans*-positions with respect to each other.

The interatomic distances between cobalt and its ligand atoms found in these four nitro-ammine-cobalt (III) complexes as well as dichrochloride $[Co(NH_3)_3H_2OCl_2]Cl$[10] are tabulated in Table VI.

The Shape of Nitro-groups in Nitro-ammine-cobalt (III) Complexes.—There have been no accurate data available for the shape and size of nitro-groups in nitro-ammine-cobalt(III) complexes. The present investigation provides the results shown in Table VII. The average of these values are: N—O=1.23Å, ∠ONO=119.3°. Such a shape and size are not very different from those found in various inorganic[6,7,19] and organic[20] compounds.

TABLE VII

THE SHAPE OF NITRO-GROUPS IN NITRO-AMMINE-COBALT(III) COMPLEXES

	N—O		∠ONO
$[Co(NH_3)_3(NO_2)_3]$	1.24 Å	1.25 Å	127°
	1.25	1.27	119°
	1.25	1.27	121°
$[Co(NH_3)_3(NO_2)_2Cl]$	1.22	1.24	119°
$K[Co(NH_3)_2(NO_2)_4]$	1.23	1.24	115°
	1.21	1.26	116°
	1.20	1.22	118°
	1.20	1.23	124°
$NH_4[Co(NH_3)_2(NO_2)_4]$	1.23	1.23	116°
	1.24	1.26	118°
	1.20	1.22	119°
	1.20	1.23	118°

18) To be published shortly.

19) Van Driel, M. and Vermeel, H. J., *Z. Krist.*, **A. 95**, 308 (1936); Gene B. Carpenter, *Acta Cryst.*, **5**, 132 (1952); Mary R. Truter, ibid., **7**, 73 (1954).

20) S. C Abrahams and J. Monteath Robertson, ibid., **1**, 252 (1948); D. June Sutor, F. J. Llewellyn and H. S. Maslen, ibid., **7**, 145 (1954); D. June Sutor, L. D. Calvert and F. J. Llewellyn, ibid., **7**, 767 (1954).

Relation between Absorption Spectra of Aqueous Solution and Configuration of the Complex Radicals

A number of studies have been made on the relation between the structures of nitro-ammine-complexes of cobalt(III) and their absorption spectra in solution. These results are summarized as follows:

1) The special absorption band of nitro-radical appears in the region from 350 to 330 mμ ($\nu=86\sim90\times10^{13}$ sec.$^{-1}$). Since this band is extremely bathochromic, the second absorption band found in ordinary cobalt (III) complexes is strongly masked. Thus the absorption curves are usually observed which are quite different from those obtained in case of $[Co(NH_3)_6]^{+3}$, $[Co\,en_3]^{3+}$ and $[Co(NH_3)_5Cl]^{++}$.

2) When two nitro-groups enter into combination to the central cobalt atom in *trans*-positions, the third absorption band appears at approximately 250 mμ ($\nu\simeq120\times10^{13}$ sec.$^{-1}$)[21–23]. For instance see Figs.

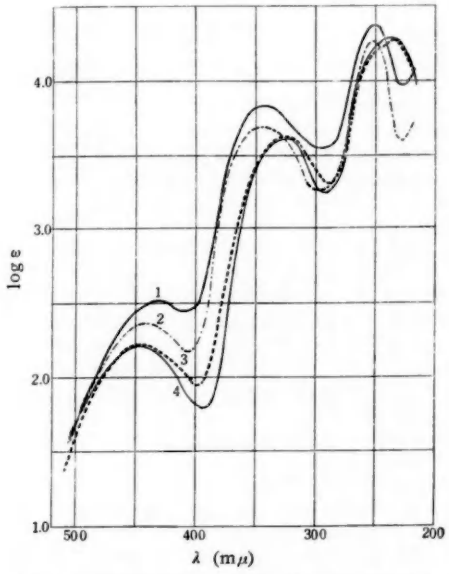

Fig. 7. Absorption spectra of *trans*- and *cis*-$[Co(NH_3)_4(NO_2)_2]^+$ in aqueous solutions.
1 and 2: *trans*-isomor, 3 and 4: *cis*-isomer,
2 and 4: obtained by M. Linhard.

21) R. Tsuchida, "Colours and Structures of the Metallic Compounds" (1944), p 96-113.

22) H. Kuroya and R. Tsuchida, This Bulletin, **15**, 427 (1940).

23) M. Linhard and M. Weigel, *Z. anorg. allgem. Chem.*, **267**, 113 (1950).

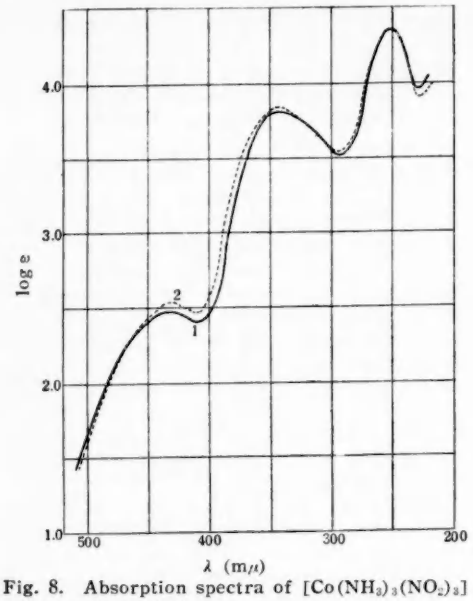

Fig. 8. Absorption spectra of $[Co(NH_3)_3(NO_2)_3]$ in aqueous solution.
2: obtained by M. Linhard.

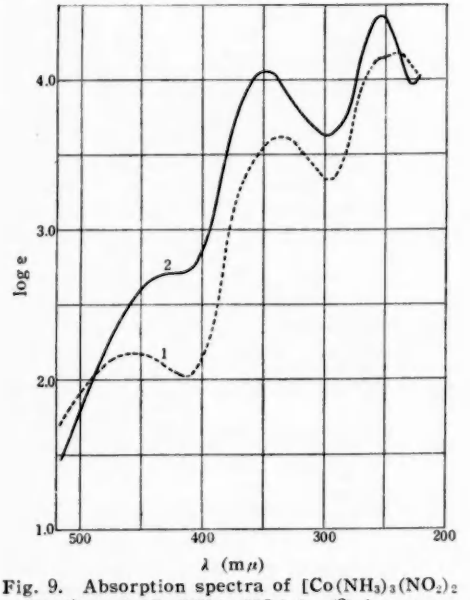

Fig. 9. Absorption spectra of $[Co(NH_3)_3(NO_2)_2Cl]$ (1) and $[Co(NH_3)_2(NO_2)_4]^-$ (2) in aqueous solutions.

7, 8 and 9. This fact has been a part of the basis of "*trans*-negative radical hypothesis". This hypothesis states that the third band appears when two negative ligands are in the *trans*-co-ordination with respect to each other. It turned out later that even when two nitro-groups or some other negative radicals are co-ordinated even in the *cis*-positions, similar third band can still be observed, but in this case the absorption maximum is very much shifted towards shorter wave lengths[24]. Therefore the "*trans*-negative radical hypothesis" should be stated as follows: the third band appears in the region near 250 mμ when two negative radicals are co-ordinated in the *trans*-positions.

The author has measured the absorption spectra of the following complex compounds: (A) $[Co(NH_3)_3(NO_2)_3]$, (B) $[Co(NH_3)_3(NO_2)_2Cl]$, (C) $K[Co(NH_3)_2(NO_2)_4]$, (D) *cis*$[Co(NH_3)_4(NO_2)_2]NO_3$ and (E) *trans* $[Co(NH_3)_4(NO_2)_2]Cl$.

Among these the crystal structures of (A), (B) and (C) have been determined by the present author. The absorption spectra of (D) and (E) were measured merely for reference. The results obtained are shown in Figs. 7, 8 and 9. All these curves were in good accord with those observed by other investigators. For comparison, the corresponding curves obtained by Linhard[23] are inserted in Figs. 7 and 8.

The X-ray evidence revealed that in (A) three nitro-groups are in the *trans-cis*-positions, and in (B) and (C) two nitro-groups are found to be in the *trans*-co-ordination. Corresponding to these configurations, the third bands appear at about 250 mμ in the absorption spectra of these compounds, as in the case of (E).

On the other hand, in (D), where two nitro-groups are in the *cis*-positions, the third band appears in the region of far shorter wave-lengths. Thus the "*trans*-negative radical hypothesis" was indeed confirmed, since the configurations of these nitro-complexes was established by the present investigation.

In view of this result a different configuration would be assigned to $[Co(NH_3)_3(NO_2)_3]$ prepared by Sueda[25], as the absorption curve is different from the one shown in Fig. 6. $[Co(NH_3)_3(NO_2)_2Br]$[26] shows similar absorption spectra to $[Co(NH_3)_3(NO_2)_2Cl]$. Since the configuration of the latter has been established, the configuration of the former is expected to be a *trans*-form with respect to two nitro-groups. The crystal structure analysis is

24) F. Basolo, *J. Am. Chem. Soc.*, **72**, 4393 (1950).
25) H. Sueda, *J. Chem. Soc. Japan*, **59**, 47 (1938).
26) M. Kobayashi, A. Hagitani and I. Mita, ibid., **58**, 391 (1937).

now being continued by the present author. The result will be published soon.

Summary

$NH_4[Co(NH_3)_2(NO_2)_4]$ belongs to the space group $P2_12_12_1$, with four formula units per unit cell. All the atomic coordinates were determined by the method of two-dimensional Fourier series. The structure is found to be isotype to $K[Co(NH_3)_2(NO_2)_4]$. Two ammonia groups are co-ordinated to the central cobalt atom in the *trans*-positions.

General features of the structures of various nitro-ammine-cobalt(III) complexes were discussed. The absorption spectra of these complexes were reexamined in their aqueous solutions. Results are briefly discussed in relation to their steric configurations.

The author wishes to express his sincere thanks to Professor H. Kuroya, Dr. Y. Saito and Professor Y. Morino, who have shown keen interest during the course of this study, have critically read the manuscript, and have given the author much invaluable advice. Part of the cost of this study has been defrayed from the Grant in Aid for Fundamental Scientific Research from the Ministry of Education.

Institute of Polytechnics
Osaka City University, Osaka

---

*The Separation of α-Glycerophosphoric Acid from its β-Isomer by Paper Chromatography**

By Chieko URAKAMI and Yoshiko KAKUTANI

(Received June 24, 1956)

Introduction

Chemical configurations of naturally occurring phosphatides or phosphatidic acids have been questioned for a long time, the difficulty being due to the reversible migration or hydrolysis of the phosphoryl group during the course of isolation or hydrolytic decomposition in the determination of the structures. Recently, Baer and co-workers have shown for a number of naturally occurring phosphatides that they possess the α-structure and L-configuration[1]. The L-α-configuration of lecithins was confirmed later by Long and Maguire[2]. In addition to the reversible migration of the phosphoryl group, difficulty arises because there has been developed no simple and adequate method of direct determination or identification of β-glycerophosphoric acid (β-GPA), which is less stable than α-GPA.

For either identification or quantitative determination of the α and β-isomers, the following methods have been used: the determination of their rates of hydrolysis by enzymes[3], the isolation of barium α-glycerophosphate (GP) and the barium nitrate complex of barium β-GP[4], the periodate oxidation method[5,6], and the determination of inorganic phosphoric acid derived from oxidative and hydrolytic decomposition[7]. All of these methods are time consuming and do not afford direct identification or determination of the β-isomer. Therefore, simple methods which would give this information would have useful applications.

Although a number of papers dealing

* This work was prescnted, in part, before the Eighth Annual Meeting of The Chemical Society of Japan, April, 1955.

1) E. Baer and M. Kates, *J. Am. Chem. Soc.*, **70**, 1394 (1948); *J. Biol. Chem.*, **175**, 79 (1948); *J. Am. Chem. Soc.*, **72**, 942 (1950); *J. Biol. Chem.*, **185**, 615 (1950); E. Baer, H. C. Stancer and I. A. Korman, ibid., **200**, 251 (1952); E. Baer, J. Maurukas and M. Russell, *J. Am. Chem. Soc.*, **74**, 152 (1952); E. Baer and H. C. Stancer, ibid., **75**, 4510 (1953); E. Baer and J. Maurukas, *J. Biol. Chem.*, **212**, 25 (1954); ibid., **212**, 39 (1954); E. Baer, D. Buchnea and A. G. Newcombe, *J. Am. Chem. Soc.*, **78**, 232 (1956).

2) C. Long and M. F. Maguire, *Biochem. J.*, **57**, 223 (1954).

3) H. D. Kay and E. R. Lee, *J. Biol. Chem.*, **91**, 135 (1931).

4) P. Karrer and B. P. Benz, *Helv. Chim. Acta*, **10**, 87 (1927).

5) F. Rapoport, I. Reifer and H. Weinmann, *Mikrochim. Acta*, **1**, 290 (1937).

6) P. Fleury and J. Courtois, *Bull. soc. chim.*, **8**, 397 (1941).

7) C. F. Burmaster, *J. Biol. Chem.*, **164**, 233 (1946).

with the chromatographic separation of organic esters of phosphoric acid of chemical and biological interest have appeared elsewhere, none of these have applied specifically to the problem of separating the glycerophosphates. Khym[8] attained a certain degree of separation of the isomers on an anion exchanger column, but it was not quite complete.

Conditions to be used for chromatography should be selected to eliminate hydrolysis and isomerization reactions. It has been shown that alkaline rather than acidic conditions are preferable[9,10] in order to avoid the occurrence of these two reactions in the case of the glycerophosphates.

We have studied the behaviors of α-GPA and β-GPA, and their alkaline metal and ammonium salts on alumina impregnated paper and achieved a complete separation of the two isomers as sodium salts, by using methanol-ammonia (60 : 5) as a developing solvent. Since it is known that alumina gives rise to secondary reactions in the presence of alkali during the course of chromatography[11], it would be necessary to examine if the compounds under consideration have undergone any chemical changes such as hydrolysis or migration of the phosphoryl group. It has been demonstrated that no hydrolysis or migration of the phosphoryl group takes place during the course of the chromatography. The system presented utilizes the ion exchange property of alumina and exploits differences of the ionic attractive forces which might be exhibited between a cation and anions of different acidities[12].

Experimental

Alumina Impregnated Paper.—Toyo filter paper No. 50 (2×40 cm.) was used. The paper was prepared according to Bush's method[13], except that a twenty-four hour washing time and a forty-eight hour exposure time to ammonia vapor were maintained. The paper prepared in this manner showed pH 8 and had adsorbed an average of 8 per cent by weight of alumina. These conditions should be maintained in order to obtain compact spots of the glycerophosphoric acids. The paper remained sensitive for four to five days when kept in an air-tight container.

Sample Solutions.—The solutions of sodium α-*, sodium β-**, barium α-*, and barium β-glycerophosphates*** were prepared by dissolving a weighed amount of the respective salt in distilled water so that each 10 μl. of the solution contained 250 μg. of the free acid. For the preparation of a solution of a mixture of the sodium salts of the α- and β-isomers, 104 mg. each of the salts were dissolved in 1 cc. of distilled water so that each 30 μl. of the solution contained 250 μg. of the free acids. Barium α-GP was converted to the ammonium salt by interacting with ammonium sulfate, and sodium β-GP to the free acid by adding 1N hydrochloric acid. The solutions of these two compounds were prepared so that each 30 μl. of the solution contained 250 μg. of the free acid.

Chromatographic Technique.—The sample solution was applied at 3 mm. from one end of the paper (after removing 1.5 cm. from both ends of the air-dried paper) with a number of applications under air-drying at 25-30° so that the dried spot was 0.6-0.8 mm. in diameter. The temperature specified here is an important factor, and must be adhered to since the solute is strongly adsorbed at a higher temperature and the spot will not move at all. The paper was equilibrated in a closed tower containing a mixture of methanol and ammonia (60 : 5) for four hours and developed for 2.5 hr. at 11-14°C by the descending method. After airdrying, the paper was sprayed with bromothymol blue indicator, whereupon the acidic spot appeared in a distinct yellow color and a cation, when present, in a blue against a grass-green backgound. This method of identification is much easier than the one commonly used[14] for the organic phosphates. The chromatogram so obtained remained unchanged for a considerable length of time, more than a year, if kept in an air-tight container.

Although we used a sample size of 250 μg. for each spot in order to make a distinct observation of the color, the method was found to be sensitive to an amount less than 60 μg. The Rf values are not affected by varying the time of pre-exposure to the solvent vapor but are somewhat affected by varying temperature.

Tests for Hydrolysis and Migration of the Phosphoryl Group.—The alumina impregnated paper was cut in a length a few mm. longer than

8) Private communication.
9) M. C. Bailly, *Compt. rend.*, **206**, 1902 (1938).
10) M. C. Bailly, *Bull. soc. chim.*, **9**, 314, 340 (1942).
11) E. Lederer and M. Lederer, "Chromatography", Elsevier Publishing Co., New York, N. Y. (1954), pp. 276-9.
12) W. Kiessling, *Biochem. Z.*, **273**, 103 (1934).
13) I. E. Bush, *Nature*, **166**, 445 (1950).

* The sample was prepared from the corresponding barium salt (C. Urakami and Y. Kakutani, Repts. Sci. Living, Osaka City Univ., Series D, No. 1, 3 (1953)) by removing the barium ion as the sulfate, by adding 1N sodium hydroxide to the ammonium salt formed, by precipitating the salt with alcohol, and finally by removing any excess of alkali present by repeated washing with alcohol.

** The sample was obtained from Delta Chemical Works and was reported to be 98 per cent pure.

*** The sample was prepared from the corresponding sodium salt by converting first to the ammonium salt with ammonium oxalate and then to the barium salt with barium chloride, and by precipitating the latter salt from its concentrated aqueous solution by adding a mixture of alcohol and ether. It was purified by preparing its barium nitrate complex.

14) F. A. Isherwood and C. S. Hanes, *Nature*, **164**, 1107 (1949).

the length corresponding to the Rf value of the glycerophosphoric acids and one end was cut in a zigzag manner. Five hundred μg. each of the α and β-isomers in the free acid forms were chromatographed on a separate sheet of paper under the conditions employed previously and the solvent allowed to drip from the irregularly cut end into a small collector. Several similar runs were made with each acid so that at least 10mg. of the sample were collected. The removal of the acid from the paper took a little over 2.5 hr.; thereafter the paper showed no acid spot remaining when sprayed with the indicator. The liquid collected was concentrated at room temperature under reduced pressure and the residue converted to the barium salt in both cases. In these samples no inorganic phosphorous was detected. The barium salt of the α-compound did not give any insoluble precipitate with barium nitrate, but barium β-GP did give an insoluble precipitate. Both samples were chromatographed on fresh papers and their Rf values were found to be identical with those previously found. The sodium salt prepared from the liquid collected from the chromatogram of barium β-GP was applied on a fresh paper and developed as described above. The acid spot was detected only at the position of the application.

To test whether or not the unmoved spot of sodium β-GP had undergone any chemical changes, the salt was applied on a small piece of the paper cut in a length of about 7 mm. from the starting line and eluted for four hours to collect the sodium ion and a further three hours to collect ammonium β-GP. Within the respective time, any alkaline or acid spot disappeared from the paper. The second fraction collected was applied on a fresh paper and chromatographed. The Rf value found for this sample was identical with that observed for either its free acid or barium salt, 0.46.

Behavior of Inorganic Phosphate, Sulfate and Chloride Ions.—Since an inorganic phosphate ion might be formed as a product of hydrolysis during the course of the chromatography and a small amount of $(NH_4)_2SO_4$ or HCl might be present in the sample solutions prepared, it would be necessary to examine the behavior of these ions on the paper. The dilute solutions of NaH_2PO_4, $(NH_4)_2SO_4$, and HCl were subjected to chromatography under the conditions specified above. The phosphate and sulfate ions were found to remain unmoved (B and D in Fig. 2), whereas the chloride ion showed a strong yellow spot at the position of application and a faint one at the Rf value corresponding to that of the α-isomer (C Fig. 2). The yellow spot found at Rf 0.45 with the β-isomer was not, however, due

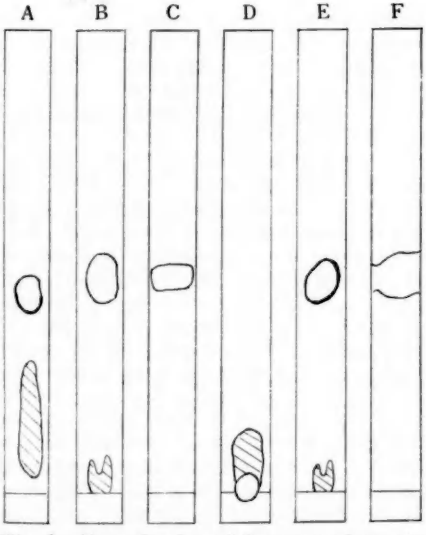

Fig. 1. Reproduction of the paper chromatograms of the glycerophosphates by the descending method. Solvent, methanol-ammonia (60 : 5); 4 hours pre-exposing to the solvent vapor; 2.5 hours developing. The shaded spots represents cations and the unshaded spots anions. A, sodium α-GP; B, barium α-GP; C, ammonium α-GP; D, sodium β-GP; E, barium β-GP; F, β-GP.

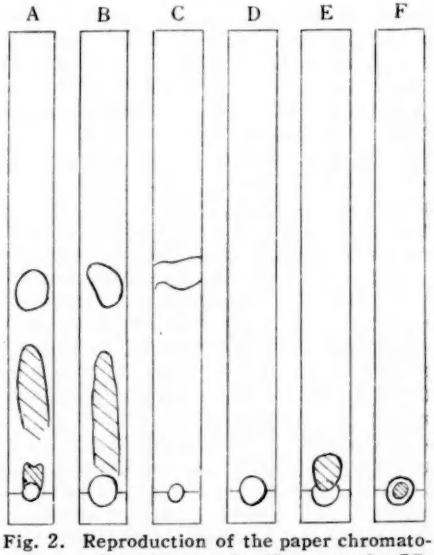

Fig. 2. Reproduction of the paper chromatograms of a mixture of sodium α- and β-GP, inorganic anions and glucose phosphates. The conditions employed are identical with those given for Fig. 1. A, a mixture of sodium α- and β-GP; B, a mixture of sodium α-GP and monosodium phosphate; C, HCl; D, ammonium sulfate; E, potassium glucose 1-phosphate*; F, barium glucose 6-phosphate*.

* We are indebted to Professor Jiro Nikuni of the Osaka University for these samples.

to this chloride ion alone since organic phosphorous was detected in the eluate.

Results

As shown in Table 1, ammonium, barium and sodium salts of α-GPA, barium β-GP and β-GPA showed almost the same Rf value, 0.45–0.46. The Rf value of sodium α-GP was found, however, to be always somewhat lower than that of barium α-GP. Sodium β-GP, on the other hand, remained unmoved, the blue spot of the sodium ion being found just above or covering the upper half of the yellow spot of the acid (D in Fig. 1). A complete separation of α-GPA from β-GPA and from inorganic phosphoric acid was attained (A and B in Fig. 2). No hydrolysis or migration of the Phosphoryl group was found to occur during the course of the chromatography. Results of Burmaster's method on the sample collected by the column method[15] support our present observation.

The compounds which are more acidic than the glycerophosphoric acids, such as glucose 1- and 6-phosphoric acids were examined under the identical conditions. They were found to remain unmoved from the initial position of application.

Discussion

When the behavior of the anions and cations of the sodium glycerophosphates and the glucose phosphates on the paper are examined, it is seen that dissociation of the salts becomes difficult with increase in acidity of the acid residues (A and D in Fig. 1; E and F in Fig. 2): pKa_1 of α-GPA, β-GPA, glucose 1- and 6-phosphoric acids are 1.40, 1.37[12], 1.10[16] and 0.94[17], respectively. This does not, however, apply to the case of the barium glycerophosphates (B and E in Fig. 1), where the Rf values of both isomers are identical (Table I). The significant difference in Rf value is observed with the sodium salts. In affording the resolution of the isomers, the effect of the sodium ion appears, therefore, to be more pronounced than that of the difference in acidity of the two isomers[18]. Analogous effects have been observed with inorganic salts[19~21]. Of course, further study on this point is indicated, but we consider that there probably exists a stronger ionic attractive force between a strongly basic cation and an anion of a salt, under the conditions specified here, than between a less basic cation and the same anion.

TABLE I

Rf VALUES OF α- AND β-GLYCEROPHOSPHATES

Temp. °C	α			β		
	Ba	Na	NH_4	Ba	Na	Free
12	0.46	0.44	0.46	0.46	0.00	0.45
14		0.42				0.46
		0.45[a]				
15		0.43[b]				

Each of these Rf values represents an average of those obtained from 4 or 5 chromatograms. [a] Four hours of developing time. [b] Obtained from the chromatogram of a mixture of sodium α- and β-glycerophosphates.

The movement of these acid spots is primarily facilitated by the cellulose present, since it has been observed that the acid residue of the glycerophosphates advances with wide zone formation on a plane filter paper strip at a much faster rate than on the alumina impregnated paper; and, furthermore, that it does not move at all when the concentration of alumina is increased by more than 20 per cent by weight on the paper. Thus, with respect to the apparent movement of the ions, the capillary movement through the cellulose fibers is considered to be more effective than the ion exchange mechanisms of alumina.

The compactness of the acid and base spots is perhaps brought about by such ion exchange mechanisms, exerted by the alumina adsorbed on the filter paper, since the spreading of the anions observed on the plane filter paper can be brought under control to a certain extent on the alumina impregnated paper. In the presence of a strong acid, alumina ionizes in the following manner and behaves as a base[22]:

$$Al(OH)_3 \rightarrow Al(OH)_2^+ + OH^-$$

The anion of an organic acid salt is then attracted by the cation of the alumina ionized as indicated. On the other hand, in the presence of a strong base, the alumina ionizes into the following ionic species and behaves as an acid:

$$Al(OH)_3 \rightarrow H^+ + AlO_3H_2$$
$$\rightarrow H^+ + AlO_2^- + H_2O$$

15) Presented before the 9th Annual Meeting of The Chemical Society of Japan, April, 1956.
16) C. F. Cori, S. P. Colowick and G. T. Cori, *J. Biol. Chem.*, **121**, 465 (1937).
17) O. Meyerhof and K. Lohmann, *Biochem. Z.*, **185**, 113 (1927).
18) W. D. Kumler and J. J. Eiler, *J. Am. Chem. Soc.*, **65**, 2355 (1943).
19) L. Sacconi, *Discuss. Faraday Soc.*, **7**, 173 (1949).
20) M. Shibata, Science (Japan), **19**, 570 (1949).
21) M. Tanaka and M. Shibata, *J. Chem. Soc. Japan*, **71**, 312 (1950).
22) F. P. Treadwell and W. T. Hall, "Analytical Chemistry", Vol. I, John Wiley and Sons, Inc., New York (1937), Ed. 9, pp. 189-192.

The cation dissociated from an organic phosphate is then attracted by the anion derived from the alumina as shown above.

There is, however, another factor to be taken into consideration, the solvent system. If a solvent system is of such a nature that it helps in dissociating salts into their respective ionic species, and also increases the solubilities of the anions formed, their movement may be facilitated. Such may be the case with the glucose phosphates.

When separation by electrophoretic or ion exchange methods alone fails, it may be possible to achieve a better resolution of homologoues or isomeric organic acids with somewhat different acid strengths by selecting an appropriate cation and by chromatographing on this type of adsorbent system.

Summary

The behaviors of α- and β-glycerophosphoric acids, their alkaline metal and ammonium salts on alumina impregnated paper, developed with a mixed solvent of methanol and ammonia (60 : 5), have been described. It has been demonstrated that a mixture of the sodium salts of the two acids may be completely separated in this way without hydrolysis or migration of the phosphoryl group. The method also affords a distinct separation of α-glycerophosphoric acid from a mixture of the inorganic phosphates, the β-glycerophosphates, and the glucose 1- and 6-phosphates; and also of the β-glycerophosphates from a mixture of the inorganic phosphates, the glucose 1- and 6-phosphates. The mechanisms possibly involved have been discussed.

Faculty of The Science of Living
Osaka City University, Osaka

Studies on the Dipole Moments of Acenaphthene and its Derivatives

By Tetsuro Ishiguro, Takehiko Chiba and Nobuyuki Gotoh

(Received August 1, 1956)

The dipole moment of acenaphthene was determined in 1949 by Lumbroso[1] as 0.97D, and then in 1950 by Bergmann et al.[2] as 0.85D, both measurements being made in benzene solution. Recently, Chau and Le Fèvre[3] gave the value 0.81D for this substance first determined in the gaseous phase and 0.80D in carbon tetrachloride solution.

Since there is divergence of moment values, it was thought worth while to make an exact measurement on this polar hydrocarbon using the gas-optical method at several temperatures. Measurements were carried out also in benzene solution for the sake of comparison.

Two chlorine derivatives of acenaphthene were prepared for the present work and their dipole moments were also measured in benzene solution at 25°C.

A discussion is given on the polarity of acenaphthene and on related problems.

Experimental Procedure

1. Materials.—(I) *Acenaphthene.*—M.p. 95-96°C. This substance (supplied from Yawata Ironworks) was recrystallized from benzene.

(II) 5-*Chloroacenaphthene.*—M. p. 69.5-70.5°C. Acenaphthene was dissolved in chloroform, and chlorinated by sulfuryl chloride. Then the chlorinated product was distilled twice in vacuo (5 mmHg). The fraction boiling at 145-155°C was recrystallized from ethanol, and then from carbon tetrachloride.

(III) 5,6-*Dichloroacenaphthene.*—M. p. 166-168 °C. 5-Chloroacenaphthene was dissolved in 1,2-dichloroethane and chlorinated by sulfuryl chloride in the presence of PCl_5. The product was recrystallized from benzene.

Solvent Benzene.—The solvent benzene was made free from thiophene by anhydrous $AlCl_3$. It was then dried over metallic sodium and distilled.

2. Measurement.—The dielectric constants were measured by the heterodyne double-beat method in the gaseous state[4], and by the resonance method in solution[5].

1) H. Lumbroso, *Compt. rend.*, **228**, 1425 (1949).
2) E. D. Bergmann et al., *J. chim. phys.*, **48**, 356(1951).
3) J. Y. H. Chau and R. J. W. Le Fèvre, *Australian J. Chem.*, **8**, 562 (1955).
4) T. Chiba, This Bulletin (to be published).
5) R. J. W. Le Fèvre and P. Russel, *Trans. Faraday Soc.*, **43**, 374 (1947).

The density d was measured by a pycnometer. The molar polarization of the solute extrapolated to the infinite dilution ($P_{2\infty}$) was calculated by means of the equation proposed by Halverstadt and Kumler[6].

The sum of atomic and electronic polarization (P_E+P_A) was assumed to be equal to MR_D, where MR_D is the molar refraction at D-line.

MR_D of (I) was calculated from refractive index and density obtained for the melted state. MR_D of chlorine derivatives were taken as the sum of MR_D (I) and the atomic refraction of Cl, i. e., $MR_D(\mathrm{II})=MR_D(\mathrm{I})+AR_D(\mathrm{Cl})-AR_D(\mathrm{H})$.

Results

TABLE I

(I) Acenaphthene $MR_D=52.0$ cc.

Gaseous State

T(°K)	p(mmHg)	n	P(cc.)	ΔP(cc.)	μ(D)
464.2	45—63	13	63.8	2.0	0.95
466.3	42—70	11	63.4	1.0	0.93
476.5	57—90	9	63.1	0.8	0.93

Mean value: 0.93D

p: Pressure of the observations
n: Number of the observations
P: Molecular polarization
ΔP: Mean deviation of P

(I) Acenaphthene $MR_D=52.0$ cc.

In benzene at 25°C

w(%)	ε	d	v	
0	2.2720	0.8722	1.1465	
1.2096	2.2868	0.8744	1.1436	$A=0.866$
2.036	2.2898	0.8759	1.1417	$B=-0.232$
3.578	2.3034	0.8787	1.1380	$P_{2\infty}=66.9$ cc.
5.496	2.3187	0.8820	1.1338	$\mu=0.85$D
8.162	2.3421	0.8869	1.1275	

(II) 5-Chloroacenaphthene $MR_D=56.9$ cc.

In benzene at 25°C

w(%)	ε	d	v	
0.6078	2.2920	0.8743	1.14.8	$A=4.006$
1.3654	2.3246	0.8763	1.1412	$B=-0.3605$
2.229	2.3607	0.8782	1.1387	$P_{2\infty}=186.4$ cc.
3.098	2.3914	0.8810	1.1351	$\mu=2.50$D

(III) 5,6-Dichloroacenaphthene $MR_D=61.7$ cc.

In benzene at 25°C

w(%)	ε	d	v	
0.492	2.3118	0.8741	1.1440	$A=7.649$
0.996	2.3488	0.8757	1.1419	$B=-0.429$
1.395	2.3812	0.8769	1.1404	$P_{2\infty}=369$ cc.
1.929	2.4243	0.8786	1.1382	$\mu=3.85$D

w: Concentration
ε: Dielectric constant
d: Density
v: Specific volume
A, B: Rates of change of the dielectric constant ε and specific volume v with weight fraction $w/100$.

Discussion of Results

In agreement with the results of the preceding workers, a dipole moment of acenaphthene 0.93D as vapor was found in the present measurement.

This marks high polarity as a hydrocarbon. It is to be noted in this connection that the moment of acenaphthene is approximately equal to, or slightly larger than, twice of that of toluene, that is, $0.37\mathrm{D}\times2=0.74$D.

Further, the existence of an abnormal solvent effect as suspected from the previous data*[1,2] can be definitely ruled out both from the work of Chau and Le Fèvre[3] and from the present research.

The dipole moments of acenaphthene, 5-chloroacenaphthene and 5,6-dichloroacenaphthene are compared with those of naphthalene, 1-chloronaphthalene and 1,8-dichloronaphthalene[8] (see Fig. 1). Almost equal increases in moment upon the successive substitution of Cl atoms are found both in acenaphthene and naphthalene. The increase 1.31–1.35D on the introduction of the second Cl atom is lower than the increase on the first substitution 1.51–1.65D. The apparent reduction is due to the mutual induction of the two C–Cl dipoles.

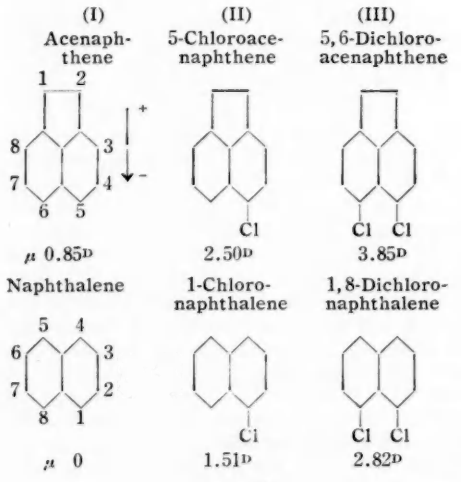

Fig. 1

From the above comparison, it will be seen that the electron displacement in an acenaphthene molecule caused by the substitution of Cl atoms is essentially not

6) I. F. Halverstadt and W. D. Kumler, *J. Am. Chem. Soc.*, **64**, 2988 (1942).
7) v. Auers and Frühling, *Ann.* **422**, 200 (1921).

* Lumbroso's value in 1947 was 1.57D.
8) G. C. Hampson and A. Weissberger, *J. Chem. Soc.*, **1936**, 393.

much different from that in naphthalene. In other words, no special change occurs which might be expected from the existence of the linkage C_1–C_2. Therefore, the dipole moments of Cl-derivatives of acenaphthene can be calculated by the simple rule of vector addition.

The moment of 5-chloroacenaphthene is larger by 0.99D than that of 1-chloronaphthalene while 5,6-dichloroacenaphthene is larger by 1.03D than 1,8-dichloronaphthalene. It can be concluded, therefore, that the dipole moment of acenaphthene of about 0.9D has the direction shown by the arrow head in Fig. 1.

This fact may deserve special attention, since it has been reported[9] that the most reactive positions of acenaphthene in the substitution reactions are its 5 and 6 positions.

Summary

The dipole moment of acenaphthene (I) was measured in the gaseous phase as 0.93D. Measurement in benzene solution at 25°C gave the following moment values: acenaphthene (I) 0.85D; 5-chloroacenaphthene (II) 2.50D; and 5,6-dichloroacenaphthene (III) 3.85D. By the comparison with the moments of naphthalene derivatives it was shown that the moments of (II) and (III) are approximately equal to the sums of the moment of (I) and the moments arising from one and two C–Cl bonds, respectively.

The authors wish to express their sincere thanks to Prof. K. Higasi for the helpful suggestion and discussion on this subject, and to Prof. Y. Nagai, to Prof. Y. Morino, and to Dr. I. Miyagawa for the kind guidance and valuable advice through this study.

Department of Industrial Chemistry
Faculty of Engineering, Chūō University
Department of Chemistry, Faculty of Science, The University of Tokyo
The Institute of Industrial Science
The University of Tōykō

9) H. E. Nürsten and A. T. Peters, *J. Chem. Soc.*, **1950**, 729; N. Gotoh and Y. Nagai, *J. Chem. Soc. Japan*, (Ind. Chem. Sec.) **58**, 50 (1955).

Studies on the Organic Phosphorescence. II. A Revision of Lewis' Mechanism for the Phosphorescence

By Shunji KATO and Masao KOIZUMI

(Received August 18, 1956)

Introduction

In the previous paper[1] the decay curves (i. e. the plots of the logarithms of the phosphorescence intensities against time) of the phosphorescence of trypaflavine-filter paper were measured and found to be approximately of the first order. The concentration effect of dye was particularly studied and the conclusion was reached, on the basis of Lewis' triplet theory, that the neighboring dye molecules chiefly affect S′ state and not T state.

Since then the apparatus has been much improved and it has now become possible to catch the features of the decay curves in the initial stage of the phosphorescence as well as to prolong the observation towards a much later stage. With this apparatus, similar experiments as reported in the previous paper were repeated, and the decay curves were found to deviate a little from a straight line, although the deviations were not so great in magnitude and moreover, only limited at the initial stage. The deviation from linearity was also observed when polyvinyl alcohol, cellophane and other substances were used as carriers, in agreement with the results reported in the literature[2], of the subject but it was most prominent in the case of trypaflavine-silica gel phosphor.

The object of the present paper is to report some experiments undertaken to

1) S. Kato and M. Koizumi, This Bulletin, **27**, 189 (1954).

2) G. N. Lewis, D. Lipkin and T. T. Magel, *J. Am. Chem. Soc.*, **63**, 3005 (1941).

elucidate the cause for this deviation, chiefly using trypaflavine-silica gel phosphor, and the conclusion obtained therefrom.

It will be found that the results obtained are interpreted by an introduction of another metastable state coupled directly with T state, the emission taking place only in S'→S transition. Furthermore, the decay curves will successfully be analysed quantitatively on the ground of the above mechanism.

Experimental Procedures

Materials.—Silica gel was boiled in concentrated hydrochloric acid and was washed by hot water repeatedly until no chloride ion was detected by silver nitrate. Then the purified gel was dyed in the aqueous solution of trypaflavine in vacuum, and after decantation it was evacuated at 200°C.

To remove any trace of oxygen as completely as possible, the sample was further treated twice with water vapor, adsorption and desorption being done at room temperature and at 200°C respectively.

Apparatus.—The block diagram is shown in Fig. 1. At the beginning, the intensity of the

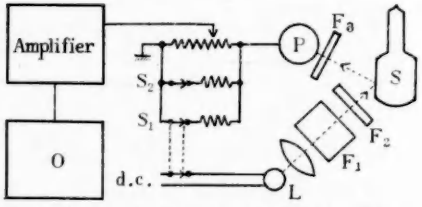

Fig. 1. Block diagram of the apparatus.
S: sample;
F_1: $CuSO_4$ solution;
F_2: Mazda V-VI filter which transmits 330–450 mμ;
F_3: a yellow filter which cuts off shorter than 450 mμ;
L: high pressure d. c. mercury lamp;
P: photomultiplier RCA 1P21;
O: electromagnetic oscillograph (Yokogawa, N-3).

luminescence under steady excitation (fluorescence plus phosphorescence) is recorded with switch S_1 and S_2 being closed. At the instant when the lamp is turned off, the switch S_1 is opened automatically, increasing the gain of the amplifier to some extent. When the photocurrent decreases under a certain value, the switch S_2 is opened also by an automatic device and the gain is once more increased so much that the later stage of a decay curve is accurately recorded.

In flash experiments, photoflash valves (the duration time is about 6 millisec.) are used as an exciting light. A shutter is inserted close to the window of a photomultiplier, which is opened immediately after the flashing of a valve.

Experimental Results and Discussion

In this paper the following notations are employed.

I_L: The intensity of luminescence during excitation.
I_P: The intensity of phosphorescence.
I_{P0}: The intensity of phosphorescence extrapolated to $t=0$.
$I_F=I_L-I_{P0}$: The intensity of pure fluorescence.

a) The Main Features of the Decay Curves.—All the decay curves were found to be practically linear in the later stage but they markedly deviate upwards in the initial stage. When measurements were extended as long as ca. five minutes*, however, the later stage was also found not to be exactly linear. An example is shown in Fig. 2. The latter deviation, which may plausibly be due to non-uniformity in the state of adsorbed dye or to

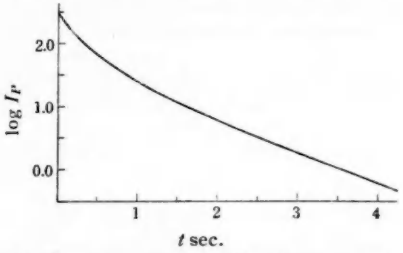

Fig. 2. An example of the decay curve.

reabsorption of phosphorescence, is so small in magnitude compared with the initial deviation, that the main points in the phosphorescence phenomenon will surely be elucidated by analysing the decay curves on the assumtion of the linearity in a later stage.

Now in order to interpret the above result, it is evidently necessary to modify more or less the scheme proposed by Lewis[2], according to which the decay is to be expressed by

$$I_P=A\exp(-\alpha t).$$

A formal amendment which occurs at once is to express I_P as the sum of several exponential terms. In practice, however, it was found that the introduction of another exponential term (equation (1)) is enough to represent the experimental results satisfactorily.

* The measurements were not usually extended so long.

3) D. Yamamoto, *J. Chem. Soc. Japan*, **74**, 173 (1953).

$$I_P = A \exp(-\alpha t) + B \exp(-\beta t) \quad (1)$$

Two other mathematical formulas were also tested in view of the mechanism proposed by Yamamoto[3] (for the phosphorescence in solid solution), who assumed the existence of a conduction band and took into consideration a bimolecular process between electrons in the conduction band and dye ions, simultaneously occurring with a main unimolecular process.

One formula here attempted corresponds to the scheme in which the phosphorescent state declines as a simultaneous process consisting of unimolecular and bimolecular emitting processes, and the other refers to the case in which the unimolecular emitting process and the radiationless bimolecular process take place. Putting N_T as a number of dye molecules in the phosphorescent state, the above two schemes are expressed analytically as follows:
for the former

$$I_P \propto -dN_T/dt = \alpha N_T + \beta N_T^2 \quad (2)$$

while for the latter

$$I \propto_P \alpha N_T, \quad -dN_T/dt = \alpha N_T + \beta N_T^2 \quad (3)$$

and the integrated forms for (2) and (3) are respectively

$$I_P = \frac{\alpha^2 C \exp(-\alpha t)}{\{1+\beta C \exp(-\alpha t)\}^2} \quad (4)$$

$$I_P = \frac{\alpha^2 C \exp(-\alpha t)}{1-\beta C \exp(-\alpha t)}\ ; \quad (5)$$

(4) and (5) can represent the experimental results equally well and as satisfactorily as (1), hence it is not possible to decide which of (1), (4) and (5) is suitable from the analysis of decay curves.

b) Effect of Exciting Light Intensity. —The superiority of (1) against (4) and (5) was established by the examination of the effect of exciting light intensity, the results of which will be described below.

The intensity was varied with neutral filters and several decay curves were taken at various intensities down to 6 per cent of the full intensity. The result was that the shape of decay curves do not change; in other words, the curves under different intensities can be put upon one another by parallel displacement along the intensity axis, and the values of I_L and I_{P0} are proportional to the intensity of exciting light (Fig. 3).

The above result requires that the inclination of the curve or $d/dt \log I_P$ is a function only depending upon t and is not affected by the intensity of exciting light. This requirement is consistent with (1), since according to (1)

$$\frac{d \ln I_P}{dt} = -\frac{A\alpha \exp(-\alpha t) + B\beta \exp(-\beta t)}{A \exp(-\alpha t) + B \exp(-\beta t)}$$

which is a function of only t, if both A and B are proportional to the exciting light intensity.

On the contrary, for the case (2)

$$-d \ln I_P/d t = \alpha + 2\beta N_T \quad (6)$$

and for the case (3)

$$-d \ln I_P/dt = \alpha + \beta N_T \quad (7)$$

and according to these relations, $-d \ln I_P/dt$ must depend on N_T, the number of dyes in the phosphorescent state, which depends on the intensity of light source. Thus the schemes (2) and (3) which involve the bimolecular process can be discarded definitely.

Constants α, β, A and B in (1) can easily be obtained in the following way. If β is larger than α, then the second term will vanish at larger t values and the straight part of the decay curve corresponds to the first term. Extrapolating this straight part to the ordinate, α and A can be decided from the inclination and the intersection respectively. Then the second term is obtained by substracting $A \exp(-\alpha t)$ from I_P and putting logarithms of these values against t, a straight line results from which B and β can be determined. In Fig. 3, the values of

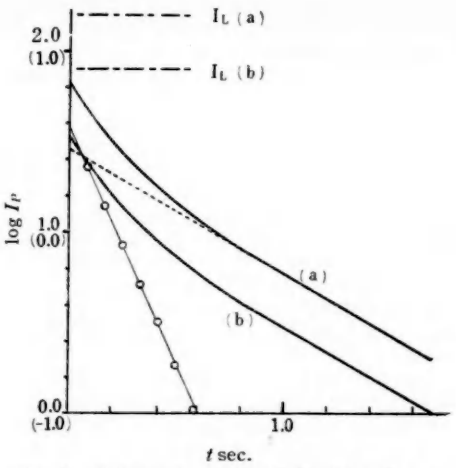

Fig. 3. Effect of exciting light intensity on the decay curve. (a) : 100, (b) : 6.0. In (b), the intensity scale takes the values in brackets.

TABLE I

AT 25°C; THE TIME UNIT IS ONE SECOND

Dye Concentration 10^{-6} mol./g. silica gel	α	β	A/B	I_L/I_{P0}	π_1	π_2	$n_1 n_2$	$n_u n_u'/\pi$
0.039	1.98	6.7	0.83	3.13	5.5	3.1	3.9	2.0
0.077	1.95	6.3	0.82	2.94	5.4	2.8	3.1	2.2
0.21	1.89	6.3	0.99	2.90	5.3	2.9	3.5	2.2
0.44	1.83	5.8	0.98	2.87	4.9	2.8	2.9	2.1

$\log\{I_P - A\exp(-\alpha t)\}$ are plotted against t as small circles, which lie satisfactorily on a single straight line.

Some examples of the analysis are shown in Table I, which contains the results for samples of different dye concentrations. It is seen from this table that A, B, α and β are almost constant, the concentration quenching being negligible in the region of dye concentration lower than 0.5 μmol./g. A slight decrease in α and β with the increase of dye concentration may perhaps be due to the reabsorption of phosphorescence[4]. The last four columns will be refered to later.

From the fact that formula (1) fits the experimental results there is no doubt that another metastable state other than Lewis' T state participates in the phenomenon of phosphorescence, the life of the former being of the same order as that of the latter.

This metastable state will be denoted conventionally as "M" state in distinction from Lewis' T state.

Thus it has now become another interesting problem to characterize this M state and further to elucidate the interrelation between M and T states.

The remainder of this paper will chiefly be devoted to this problem.

c) Absorption and Emission Spectra. —Supposedly if M and T state were completely independent, it might happen that the emission of two different types would be observed. Hence the spectra of phosphorescence (corresponding to I_P) and fluorescence (plus phosphorescence in a rigorous sense—corresponding to I_L) were at first examined and were compared with the absorption spectra.

Absorption spectra of trypaflavine adsorbed on silica gel were measured by use of the following technique. First, the sample was ground into powder and was mixed with silica gel powder to make its optical density suitable for measurement. Then the mixture of benzene and petroleum benzine with the same refractive index as that of the sample was poured into the cell. The sample now became transparent and the absorption spectra could easily be measured by a Beckman D. U. spectrophotometer. The result was that the maximum of the extinction displaced about 10 mμ to longer wave length compared with that in an aqueous solution.

The fluorescence and phosphorescence spectra were taken by a spectrograph at 25°C using a high pressure mercury lamp as a light source. A phosphoroscope with a rotatory disc was employed for taking the phosphorescence spectrum. Both spectra were almost identical and were approximately a mirror image of the absorption spectrum as shown in Fig. 4.

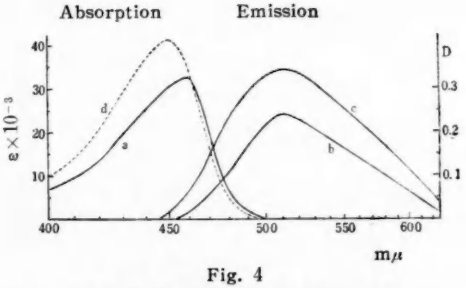

Fig. 4

a) Trypaflavine-silica gel 0.25 μmol./g.;
b) Fluorescence spectrum of the same sample;
c) Phosphorescence spectrum;
d) Trypaflavine in aqueous solution 12 μmol./l.;
ε: Extinction coefficient 1000 cm²/mol.;
D: Density of plate darkening.

Next, the decay curve for the limited wave-length region of phosphorescence was taken and compared with the result in (a); thus an orange filter cutting off shorter than 540 mμ was used in place of a yellow one, but the decay curve was exactly the same in shape.

Lastly, it was cheked by the following experiments that Lewis' β phosphorescence is negligible for such an adsorbed phosphor at room temperature. When a film of polyvinyl alcohol dyed with trypaflavine

4) J. B. Birks and W. A. Little, Proc. Phys. Soc. (London), **66A**, 921 (1953).

(4.88×10^{-7} mol./g. P. V. A.) was stretched, it showed a distinct dichroism. The extinction was about seven times larger when the electric vector of the light was perpendicular to the stretched direction than parallel. (The decay curve showed a slight deviation from linearity at the initial stage, though the order of magnitude was much smaller than in the case of trypaflavine-silica gel phosphor.) Now it was found that the green phosphorescence (and fluorescence) at room temperature had a polarization perpendicular to the stretched direction, while at liquid air temperature, the yellow phosphorescence that is Lewis' β phosphorescence, was polarized parallel, and at dry ice temperature, the phosphorescence consisted of α- and β-components, the former being observed only in a perpendicular direction, while the latter in a parallel direction.

At room temperature there was no β phosphorescence observed in a parallel direction, hence β phosphorescence can be ignored in the case of polyvinyl alcohol trypaflavine phosphor at room temperature. The situation may be the same for the case of silica gel phosphor.

From the results mentioned in this section, it is almost certain that there is only one type of emission and that it corresponds to Lewis' α phosphorescence.

A Plausible Scheme for the Phosphorescence

In order to make the quantitative investigation about the decay curve, it may be desirable to put forward, at this stage, a plausible scheme which will enable us to carry out the mathematical analysis.

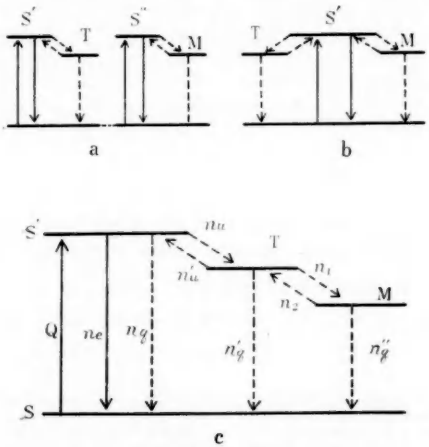

Fig. 5. Possible schemes for the phosphorescence.

Now, for the interrelation between T and M states, there are three possible schemes conceivable, which are shown in Fig. 5. In this figure, the full lines are transitions connected with radiation, while the dotted ones are radiationless transitions. The most suitable scheme will be selected by examining which of these three will fit best the following experimental results.

1) The variation of dye concentration does not affect the decay curve (at least in the small concentration range). (Table I)

2) Deviations from linearity in decay curves depend upon the nature of a carrier (the fact mentioned in introduction).

3) There is only one emitting state at ordinary temperature (the result demonstrated in (c)).

4) Even at liquid air temperature, deviations from linearity are still observed, though the magnitude becomes much smaller (preliminary observation).

Now the scheme (a) which consists of two independent processes is not compatible with the result (3), unless one supposes that the two processes are not the ones in isolated molecules but are closely related with the state of adsorption. But even if one adopts the view that there are statistically two different states of adsorption (which cause different lifetimes but do not affect the spectral behaviors), this scheme is not compatible with the result (1), since the participation of M and T states should vary in magnitude with the dye concentration.

Scheme (b) in which M and T states are separately coupled with S' state does not fit the fact (4). Because if one assumes scheme (b) the result (4) must be interpreted to be due to the fact that M state as well as T state must emit phosphorescence at low temperature and this seems very improbable from the general view about the emission phenomena. Moreover, it seems quite strange that T and M states which have a long life don't interrelate with each other and yet they are separately coupled with an extremely short-lived S' state.

The remaining scheme (c) in which T and M are directly coupled, is not only plausible from the general view point, but also fits the above facts well, if one assumes that M state is closely connected with the state of adsorption. Thus the result (1)

can be comprehended as due to the fact that the state of adsorption is uniform at least approximately.

There is no question about the results (2) and (3) on the basis of this scheme.

The result (4) can be comprehended if the transition between T and M takes place partially by virtue of tunneling effect.

Thus although the above discussions are not quite conclusive, the scheme (c) seems to be most suitable; hence the quantitative treatment will be given below on the basis of this scheme. One may expect that the plausibility of this scheme will be further supported by the results obtained from such an analysis. (See the following two papers)

Quantitative Interpretation of the Decay Curve

The mathematical treatment will be given on the basis of scheme c) as shown schematically in Fig. 5c.

In this figure, S, S′ and T are ground state, excited singlet state and triplet state respectively; M is a metastable state with a life time of the same order as that of T state.

Since the spectra of phosphorescence are identical with those of fluorescence and the yellow phosphorescence is never observed at room temperature, the direct emitting transition from T or M to S can be ignored.

Furthermore

n_e: The rate constant of S′→S emitting transition.

n_q, n_q', n_q'': The rate constant of S′→S, T→S, M→T transition respectively (without emission).

Q: The number of molecules excited per second by irradiation.

From the above scheme, the phosphorescence intensity I_P (in number of photons), the rate of the decrease in the number of the molecules in T state and that in M state are represented respectively by the following equations

$$I_P=n_e n_u' N_T/\pi \tag{8}$$

$$-\mathrm{d}N_T/\mathrm{d}t=\pi_1 N_T-n_2 N_M \tag{9}$$

$$-\mathrm{d}N_M/\mathrm{d}t=\pi_2 N_M-n_1 N_T \tag{10}$$

where

$$\pi_1=n_u'(1-n_u/\pi)+n_q'+n_1{}^{*}$$

$$\pi_2=n_2+n_q''$$

$$\pi=n_e+n_q+n_u.$$

Integrating (9) and (10) one gets

$$N_T=a_1\exp(-\alpha t)+b_1\exp(-\beta t) \tag{11}$$

$$N_M=a_2\exp(-\alpha t)+b_2\exp(-\beta t) \tag{12}$$

where

$$\alpha,\beta=\frac{1}{2}\{\pi_1+\pi_2\mp\sqrt{(\pi_1-\pi_2)^2+4n_1n_2}\} \tag{13}$$

and from (9), (11) and (12)

$$a_2/a_1=(\pi_1-\alpha)/n_2,\quad b_2/b_1=(\pi_1-\beta)/n_2. \tag{14}$$

The values of a_1, a_2, b_1 and b_2 are determined by the initial condition, which corresponds to a stationary state (during the illumination) established between the exciting light and all the states involved.

The stationary state in question can be represented by the following equations,

$$-\mathrm{d}N_S/\mathrm{d}t=\pi N_{S0}-Q-n_u'N_{T0}=0 \tag{15}$$

$$-\mathrm{d}N_T/\mathrm{d}t=(\pi_1+n_u n_u'/\pi)N_{T0}-n_u N_{S0}-n_2 N_{M0}=0 \tag{16}$$

$$-\mathrm{d}N_M/\mathrm{d}t=\pi_2 N_{M0}-n_1 N_{T0}=0 \tag{17}$$

where N_{S0}, N_{T0} and N_{M0} are the values of N_S, N_T and N_M in the stationary state. From (11) and (12) on the other hand

$$N_{T0}=a_1+b_1,\quad N_{M0}=a_2+b_2 \tag{18}$$

From (14), (15), (16), (17) and (18) one gets

$$a_1=\frac{\pi_2-\alpha}{\alpha(\beta-\alpha)}\frac{n_u Q}{\pi},\quad b_1=\frac{\beta-\pi_2}{\beta(\beta-\alpha)}\frac{n_u Q}{\pi} \tag{19}$$

Substituting (11) and (19) into (8), an ultimate expression for the phosphorescence intensities is obtained as follows:

$$I_P=A\exp(-\alpha t)+B\exp(-\beta t) \tag{20}$$

where

$$A=\frac{n_e n_u n_u'(\pi_2-\alpha)Q}{\pi^2\alpha(\beta-\alpha)}$$

$$B=\frac{n_e n_u n_u'(\beta-\pi_2)Q}{\pi^2\beta(\beta-\alpha)}$$

(20) is identical with (1) and the following relations hold, as are easily verified.

$$A/B=(\pi_2-\alpha)/(\beta-\pi_2)\times\beta/\alpha \quad \text{(i)}$$

$$\alpha+\beta=\pi_1+\pi_2,\quad \alpha\beta=\pi_1\pi_2-n_1n_2 \quad \text{(ii)} \tag{21}$$

$$I_L/I_{P0}=\pi\alpha\beta/n_u n_u'\pi_2+1 \quad \text{(iii)}$$

* Since the life time of S′ is 10^7~10^8 times shorter than that of T and M, it is possible to apply a stationary state method to S′ state. Hence it is easily proved that, the fraction n_u/π of the molecules transferred from T to S′ returns to T state, leading the net decrease of the molecules in T via S′ as $n_u'(1-n_u/\pi)$.

Since A/B, α, β and I_f/I_{P0} are determined experimentally, π_1, π_2, n_1n_2 and n_un_u'/π can be calculated from (21). Some of the results are shown in Table I.

Flash Excitation.—Now it will be interesting to examine how the decay curve will change in shape when a sample is excited by a flash lamp. In this case, since the duration of a flash (several milliseconds) is much shorter than the life time of T and M state, the stationary state cannot be established except for S'. Thus the initial condition for the decay curve will approximately be such that there are no molecules in M state.

Assuming such an initial condition, (16) and (17) must be replaced by the following relations.

$$N_{M0}=0 \quad \text{hence} \quad a_2+b_2=0 \qquad (22)$$

$N_{T0}=Qn_u/\pi$ (Q is a total number of photons absorbed)

From (22) and (14) one gets

$$A/B=(\pi_2-\alpha)/(\beta-\pi_2) \qquad (23)$$

Comparing (21 i) and (23) it can be expected that the values of A/B in flash experiments are smaller than those in steady excitation by a factor near α/β, while the values of α and β must not change, since the rate constants n_e, n_u, n_q' etc. are only dependent on the sample.

Now, the decay curves were taken for the same sample, using a mercury lamp on one hand and replacing it by a photo-flash valve on the other. The result was that the two decay curves markedly differ with each other. Three parameters, A/B, α and β for the same sample are shown in Table II for flash and mercury lamps. In both excitations, α and β have the same or approximately the same values (within experimental accuracy) while A/B differs about two or three times.

TABLE II

0.5 μmol./g. AT 25°C

Sample	Exciting Light	α	β	A/B	$A/B\times\alpha/\beta$
a	Hg-lamp	1.74	5.67	0.78	0.24
	Flash	1.74	6.25	0.31	—
b	Hg-lamp	2.18	7.45	0.91	0.27
	Flash	2.18	7.08	0.24	—

The values in column 3 and 4 conform with the above requirements quite well. The agreement between A/B in flash excitation and $A/B\times\alpha/\beta$ in steady excitation is better than expected*.

Thus it can be concluded that the present mechanism not only explains the experimental results of various kinds qualitatively, but it is quite satisfactory from a quantitative standpoint.

Summary

Decay curves of the trypaflavine-silica gel phosphor were measured accurately by means of an oscillograph and a marked deviation from linearity was found at the initial stage. From the spectroscopic studies of fluorescence and phosphorescence, and the effect of light intensity on the shape of the decay curve, it was concluded that Lewis' scheme must be modified in such a way that another state with a life time of the same order as that of T state directly couples with T state.

The quantitative analysis was performed successfully and some of the transition constants between the states involved were partially evaluated.

Institute of Polytechnics
Osaka City University, Osaka

* It is to be noted, however, that scheme (a) and (b) can interpret the result of a flash experiment equally well. Hence the above success cannot be considered as a strong support for the scheme(c).

Studies on the Organic Phosphorescence. III. Quenching by Some Gases and Vapors

By Shunji KATO

(Received August 18, 1956)

Introduction

The preceding investigation[1] on the phosphorescence of trypaflavine-silicagel phosphor has led to a plausible conclusion that there exists a metastable state (M state), which is directly coupled with a triplet state, and it has been proposed that Lewis' scheme must be replaced by the one shown schematically in Fig. 1.

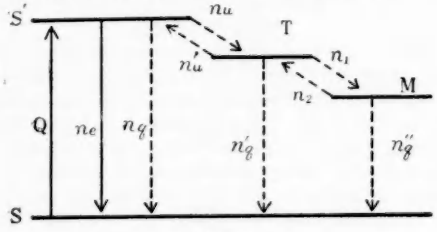

Fig. 1.

On the basis of this mechanism, decay curves are represented by the following equation,

$$I_P = A\exp(-\alpha t) + B\exp(-\beta t) \qquad (1)$$

and putting

$$\pi_1 = n_u'(1 - n_u/\pi) + n_1 + n_q'$$
$$\pi_2 = n_2 + n_q''$$
$$\pi = n_e + n_q + n_u,$$

$\pi_1, \pi_2, n_1 n_2$ and $u_u n_u'/\pi$ are calculated from four parameters ($\alpha, \beta, A/B$ and I_L/I_{P0}) which are obtained from the measurement of I_L (the intensity of luminescence during excitation), I_{P0} (the initial intensity of the phosphorescence) and the decay curve of phosphorescence.

Now, although the existence of another metastable state other than Lewis' triplet state has been established in the preceding paper, nothing as yet is known about its nature.

As a first step to study about it, the author has investigated the influence of the addition of a third substance upon the steady state emission and upon the decay curve of phosphorescence.

1) S. Kato and M. Koizumi, This Bulletin. **30**, 27 (1957).

Such an investigation is expected, in addition, to refer to our first plan mentioned in the first paper[2] of this series, i. e. the problem whether a third substance (quencher) affects S' or T state, because the analysis of the decay curve makes it possible to evaluate some of the transition probabilities between the states involved in the phosphorescence.

In this paper the influence of some gases and vapors upon the phosphorescence of trypaflavine-silica gel phosphor will be reported. It is well known that such a phosphorescence is effectively quenched by certain gases and especially, a remarkable quenching action of oxygen has been studied from various view points[3], but the precise investigation about the variation of the decay curve caused by the addition of these gases including oxygen, has not yet been undertaken.

Experimental

Materials.—*Trypaflavine-silica gel phosphors* were prepared in the same way as described in the previous paper.

Oxygen and hydrogen were prepared by the electrolysis of baryta water and were first passed over platinized asbestos, then through a dry ice trap.

Nitrogen, argon and methane: The gas from a cylinder was stored for several days, to remove oxygen, in an ampoule the inner surface of which was covered by an evaporated film of metallic sodium.

Nitric oxide was prepared by the reaction between potassium nitrate and ferrous sulfate in the acidified aqueous solution, and then purified by a standard method*.

Other quenchers (*n*-hexane, propylene, benzene, acetone, methanol, SO_2, I_2, ether, dioxane, cyclohexene, 2-ethyl-1-hexene, styrene and methylmethacrylate), after ordinary purification, were distilled or sublimed five times in high vacuum to remove oxygen.

Procedure and Measurement.—A known amount of a gas or a vapor to be investigated was taken in a space between two taps and then

2) S. Kato and M. Koizumi, This Bulletin, **27**, 189 (1954).

3) J. Franck and P. Pringsheim, *J. Chem. Phys.*, **11**, 21 (1943).

* "Inorganic Synthesis", (1939), 11, P. 126.

was introduced into the ampoule containing the phosphor. If there was any fear of even a slight reaction between a gas and tap-grease, the taps were replaced by a mercury cut and a break-seal.

The apparatus used was the same one described in the preceding paper and the phosphorescence of a sample was recorded, before and after introduction of a quencher at 25°C.

In every experiment the greatest caution was paid to eliminate any trace of oxygen and to avoid contamination of a sample with it throughout all procedures. In fact, the disturbance from oxygen is so strong that a noticeable fall of the phosphorescence is observed if the connection tube of the ampoule is carelessly sealed off by fusion.

Results and Discussion

a) General Remarks. — Among the materials examined, argon (38×10^{-5} mol.), nitrogen (43×10^{-5}), hydrogen (32×10^{-5}), methane (42×10^{-5}), *n*-hexane (6.6×10^{-5}), propylene (3.3×10^{-5}), benzene (1.0×10^{-5}), acetone (42×10^{-5}), methanol (3.2×10^{-5}) and water (3.5×10^{-5}) had no effects on a 4 g. phosphor (contained in an ampoule of 20 ml.) of which the dye concentration is 5×10^{-7} mol./g. silica gel; the intensity of the steady state emission and the shape of the decay curve were not affected at all by the introduction of these gases.

When more than 10^{-3} mol. of methanol or water is introduced, the life of the phosphorescence is somewhat shortened and its initial intensity decreases, though only very little. In view of a rather large quantity of a quencher in these cases, it is more plausible to attribute these effects to the variation in the property of gel, hence these cases will be omitted from the discussion given below.

The substances which show more or less positive effects are O_2, NO, SO_2, I_2, ether, dioxane, cyclohexene, 2-ethyl-1-hexene, styrene and methyl methacrylate.

When a suitable amount of a quencher listed above, is introduced, the phosphorescence intensity, the decay constant as well as the intensity of the steady state emission show measurable changes. Decay curves are still represented by equation (1) unless the quantity of a quencher is not too large. When it exceeds a certain value, equation (1) must be replaced by a more general one

$$I_P=\sum a_i \exp(-\alpha_i t) \qquad (2)$$

in order to represent the decay curve satisfactorily. But even in these cases, the decay curves are exactly the same in shape for different intensities of the exciting light, so it is certain that no process of higher kinetic order is involved in the phosphorescence phenomenon.

TABLE I

Sample Dye conc.		Quencher mol.	I_L	I_L/I_{P0}	$I_L^0/(I_L^0-I_L^q)$
0.43 μmol./g.	4 g.	None	100	2.88	2.86
		O_2 : 1.26×10^{-5}	65	—	
0.5 μmol./g.	4.2 g.	None	100	2.59	2.63
		Styrene : 2.63×10^{-5}	62	—	

TABLE II

Phosphor: 0.5 μmol./g., 4 g.; 25°C. Time unit is second.

No.	Quencher mol.	α	β	A/B	I_L/I_{P0}	π_1	π_2	n_1n_2	n_1n_1'/π
1	None	2.02	5.6	0.79	2.77	4.8	2.8	2.2	5.2
	O_2 : 1.5×10^{-10}	4.35	12.3	0.54	4.3	11.0	5.6	8.3	4.1
2	None	1.60	5.2	0.62	2.59	4.8	2.2	1.8	2.4
	O_3 : 7.5×10^{-10}	4.49	30	0.32	8.72	29	5.7	28	3.0
3	None	1.77	6.2	0.74	2.66	5.4	2.5	2.8	2.6
	NO : 1.2×10^{-9}	4.42	19	0.45	13.2	18	5.8	18	1.2
4	None	1.68	6.2	0.57	2.60	5.5	2.3	2.4	2.8
	Styrene : 1.2×10^{-6}	3.54	12.7	0.49	7.53	12	4.7	9.2	1.5
5	None	1.58	5.3	0.74	2.94	4.6	2.2	1.9	1.9
	Ether : 6.9×10^{-6}	2.82	8.0	0.51	3.67	7.2	3.6	4.4	1.8
6	None	1.42	5.0	0.68	2.92	4.4	2.0	1.7	1.9
	Dioxane : 3.0×10^{-5}	3.46	16	0.36	6.32	15	4.4	11.0	2.3
7	None	2.52	8.0	0.88	2.57	6.8	2.7	5.0	3.5
	SO_2 : 2.6×10^{-6}	6.27	16	1.31	3.94	13	9.6	21	3.6

b) Effect of Quenchers on I_L. — When a suitable amount of gas depending on its quenching efficiency is introduced, the phosphorescence is completely quenched and an interesting relation in the form of (3) is found to hold. Thus, rewriting I_L before and after the addition of a quencher as I_L^0 and I_L^q respectively and denoting the initial phosphorescence intensity as I_{P0}^0 and I_{P0}^q respectively for the corresponding case*,

$$I_L^0/(I_L^0-I_L^q)=I_L^0/I_{P0}^0. \tag{3}$$

From (3)

$$I_L^0-I_L^q=I_{P0}^0$$

or

$$I_L^q=I_L^0-I_{P0}^0=I_F^0. \tag{4}$$

Since

$$I_{P0}^q=0,\quad I_F^q=I_F^0. \tag{5}$$

Equation (5) shows that in such a favorable condition, phosphorescence is completely quenched and yet a pure fluorescence is not affected at all.

I_F is the luminescence emitted by molecules which after having been excited to S′ state, drop to the ground state directly without going to T or M state. Therefore, it can be concluded that in such a case S′ state is not affected at all by a quenching gas. A few examples are shown in Table I.

For other quenchers the same relation holds, hence it is quite certain in general, that under the situation that the phosphorescence is partially quenched, the quencher does never affect S′ state and the intensity of pure fluorescence remains constant.

c) Analysis of Decay Curves. — Decay curves were taken for the same sample with and without a quencher; usually when a quenching gas was removed by evacuation the sample regained exactly the same decay curve as that of the original one. Results of the analysis are shown in Table II, where the data for a quenched sample is paired with them for a reference. The data for each reference sample do not always coincide, probably because of some difference in the pretreatment of the sample or in the source of silica gel.

Here it is to be noted that although the values of α and I_L/I_{P0} are rather accurately obtained, those for β, and A/B are not so accurate; probable errors for the latter two quantities would usually be ±10% or so. Hence accuracy for π_1, π_2, n_1n_2, n_un_u'/π is much worse than this.

It is seen from the table that π_1, π_2 and n_1n_2 are increased much by the introduction of a quenching gas, while n_un_u'/π in most cases are not affected beyond probable error. From the latter result, it can be concluded that n_u', the transition probability from T to S′ is not affected by a quencher, because, as already established in the preceding section, π and n_u must remain constant in the present conditions.

This result may perhaps support the view that the transition from the lower state to the higher state is in general not promoted by such a perturbation as is due to spin orbital interaction.

It is noteworthy that the quenching gases not only induce the emissionless transitions from T to S and perhaps M to S, but they also increase the transition probability between T and M.

Judging from the relation

$$\frac{I_F}{I_{F0}}=\frac{I_L-I_{P0}}{I_{P0}}=\frac{\pi\alpha\beta}{n_un_u'\pi_2}=\frac{\pi}{n_un_u'}\left(\pi_1-\frac{n_1n_2}{\pi_2}\right),$$

the decrease in the initial intensity of phosphorescence is mainly due to the increase of π_1 value, since this is usually much greater than that of n_1n_2/π_2. Thus broadly speaking, quenching action of the gaseous substances comes from their attack on T state.

Next it is worthy to note that the quantities of quenchers are, in some cases, exceedingly small compared with that of the dye. For example, the quantity of oxygen or nitric oxide which is required to cause a measurable quenching is of the order of 10^{-10} mol. as against 2×10^{-6} mol. of dye. Consequently it is clear that one oxygen or nitric oxide molecule acts as an effective quencher towards more than one thousand molecules of dye. Hence it may safely be concluded that the quenching action of these substances is not of static type but of kinetic or collisional one.

In other quenchers, styrene etc., the quantities are comparable to that of the dye. In spite of such great differences in quantity, the general features of quenching are similar at least qualitatively, no specificity being observed in most quenchers. It seems, however, that SO_2 is an exception, since the increase of n_1n_2 and π_2 is abnormally high compared with other cases. The problem would be worthy of further study.

d) Effect of Oxygen on the Pure

* Throughout this paper analogous notations will be used for all the other constants. For example, π_1, which will still be used in general case, will be replaced by π_1^0 and π_1^q when the distinction is necessary.

Fluorescence.—As described above, only phosphorescence is quenched by a very small amount of oxygen, but a much larger quantity of it quenches the fluorescence too to some extent. Some examples are shown in Table III.

TABLE III

O_2 press. in mmHg	<0.1	10	30	100	720
I_L	100	87	74	50	2

In the experiment at <0.1 mm O_2 press., fluorescence keeps its full intensity while phosphorescence is completely quenched, so that I_L in this case is equal to the intensity of pure fluorescence I_F when the quencher is absent. Other data for I_L, accordingly, are the values of I^0_F. Now the volume of the ampoule, used for the quenching experiment of phosphorescence is about 20 ml., therefore, 10^{-10} mol. of oxygen corresponds to 10^{-4} mmHg under the assumption that oxygen is not adsorbed on silica gel at all. Thus the quenching constant for the phosphorescence is estimated to be roughly of the order more than 10^6 times greater than that for fluorescence. The lifetime of S′ state, on the other hand, being of the order 10^{-7}–10^{-9} sec., is 10^5–10^8 times shorter than that of T or M state. Thus it appears that the great difference in the behavior of T state against S′ state when oxygen is introduced, is mainly due to its long lifetime and not due to its intrinsic reactivity.

e) Another Evidence for the Present Scheme of Phosphorescence. — Although the present scheme of phosphorescence has been supported to some extent in the preceding paper, here another evidence will be added which can be derived from the above quenching experiments.

As already described[2], if phosphorescence obeys Lewis' mechanism and a quencher only acts on T state, promoting only the emissionless transition to the ground state, then the initial intensity of phosphorescence must be exactly proportional to the lifetime.

Now, according to the present investigation, S′ state is not affected at all when the phosphorescence is partially quenched. Therefore, if the phosphorescence consisted of two independent ones, the product of the decay constant and the initial intensity should be unchanged for each independent process when a quenching gas is introduced. In other words, $A\alpha$ and $B\beta$ should be constant and accordingly the product $A/B\times\alpha/\beta$ should also be unaffected. This conflicts with the data given in Table II.

Some examples are shown in the following Table.

TABLE IV

	Quencher	$A/B\times\alpha/\beta$
No. 1	None	0.28
	O_2 1.5×10^{-10} mol.	0.19
No. 2	None	0.19
	O_2 7.5×10^{-10} mol.	0.05
No. 3	None	0.2
	NO 1.2×10^{-9} mol.	0.1

Thus the existence of any two independent phosphorescence processes is not compatible with the above results, unless the transition probability from T to S′ is notably increased by a quenching molecule; this increase appears to be very improbable.

Summary

The quenching action of some gases and vapors upon the phosphorescence of silica gel-trypaflavine phosphor was investigated. The gases which have more or less quenching effects are O_2>NO>SO_2, styrene> ether, dioxane, cyclohexene, 2-ethyl-1-hexene, methyl methacrylate, and the gases with no effects (when the quantities are not too large) are N_2, Ar, H_2, methane, *n*-hexane, propyrene, benzene, acetone, methanol and water.

The influence of quenching gases on the decay curve of phosphorescence were accurately examined and by analysing them on the basis of the scheme proposed in the preceding paper, it was established that in general S′ is not affected while both T and M state are appreciably affected. Furthermore, it was found that T→S′ transition is not promoted in general.

The quenching actions of O_2 and NO were interpreted to be of kinetic type.

Institute of Polytechnics
Osaka City University, Osaka

Studies on the Organic Phosphorescence. IV. Quenching by Inorganic Salts

By Shunji KATO, Ko KIMURA and Masao KOIZUMI

(Received August 18, 1956)

Introduction

As a continuation of the preceding investigation, the present paper will chiefly deal with the effects of some inorganic salts upon the phosphorescence of trypaflavine-silica gel phosphor. Although the effects of some gases upon the trypaflavine-filter paper phosphor have also been investigated, they will be reported rather briefly since they are generally very small and cannot be discussed quantitatively.

Experimental

Sample.—*Trypaflavine-silica gel phosphor*—The phosphor prepared by the same method as described in part II was soaked in the aqueous solution of a salt (usually chloride) in vacuum and after standing for many hours (sometimes the sample was kept in a bath of 100°C to make the state of adsorption as uniform as possible), water was distilled off in vacuum. The sample then was once more evacuated at 200°C under as similar condition as that for a reference sample.

Salts employed are chloride of Fe^{3+}, Co^{3+}, Fe^{2+}, Cr^{3+}, Cu^{2+}, Cu^{+}, Ag^{+}, Ni^{2+}, Mn^{2+}, Co^{2+}, Pb^{2+} and Cd^{2+}.

Among these, cobaltic- and chromic- chloride were used in the form of ammine complex and silver- and cuprous-chloride were dissolved in the ammoniacal solution; in these cases ammonia could be expelled from the sample by the above treatment. The dye concentration was usually 0.4 μmol./g. and that of a salt was chosen in most cases to be more than several times larger.

Trypaflavine-filter paper phosphor.—Filter paper was dyed by immersing it in the aqueous solution of trypaflavine and was evacuated at 100°C. The concentration of dye was 0.8 μmol./g. (filter paper, ca. 0.5 g.).

Procedures.—The quantities measured were

1) decay curves of the phosphorescence
2) the intensity of the steady state luminescence

$$I_L = I_F + I_{P0}$$

3) absorption spectra (only for the silica gel phosphor).

The methods for measuring (1) and (2) are essentially similar to those reported in the preceding papers.

The absorption spectra were likewise taken by the same method described in Part II. Short path cells (0.1 or 0.2 cm.) for Beckman DU were used and the solvent was a mixture of benzene and *n*-hexane 1 : 0.3 in volume ratio.

Experimental Results and Discussion

(a) Decay Curves.—Decay curves are little or scarcely affected by the adsorption of all the salts tested, except cupric ion, the results of which will be discussed separately. The following data show the upper limit of concentration of each salt examined in the present investigation (expressed in μmol./g.)

Fe^{3+}(2), Co^{3+}(4), Fe^{2+}(4), Cr^{3+}(6),
Cu^{+}(8), Ag^{+}(5), Ni^{2+}(7), Mn^{2+}(11),
Co^{2+}(3), Pb^{2+}(9), Cd^{2+}(12).

Decay curves can be analyzed by the scheme proposed in part II, and the chief results of analysis are shown in Table I. For other salts not included in this table, the decay curve was practically the same as that of the reference.

(b) The Intensity of the Steady State Luminescence I_L.—From I_L, the intensity of pure flurorescence I_F can easily be calculated from the formula $I_F = I_L - I_{P0}$.

As to the relation between I_F and the concentration of a salt, it has been established that Stern-Volmer's equation holds approximately

$$I_F^0/I_F^q = 1 + K_Q C,$$

where I_F^0 is the fluorescence intensity of a reference sample while I_F^q is that of the sample containing a salt adsorbed on silica gel*. The concentration of a salt "*C*" is expressed in μmol./g. silica gel. The results are shown in Fig. 1 (a) and (b) (which includes the one of cupric ion) where I_F^0/I_F^q are plotted against *C*.

* π_1 in the preceding paper is replaced by $\pi' = \pi_1 + n_u n'_u/\pi = n_u' + n_1 + n'_e + n'_q + n'_i$, because the latter is more expedient when the value of $n_u n_u'/\pi$ changes.
π'' is the same as π_2.
n_q, n_q' and n_q'' in the preceding two papers correspond to $n_i + n_q$ etc. in this paper, n_i being the constant for inner quenching.

TABLE I

Dye conc., 0.4 μmol./g.; At 25°C. Time in sec.

Quencher		α	β	A/B	I_L/I_{F0}	π'^*	π''^*	n_1n_2	n_un_u'/π	I_F
Fe^{3+}	Reference	2.55	8.60	1.0	2.74	10.5	3.9	6.6	3.2	26
	0.4 μmol./g.	2.55	8.60	0.8	2.76	10.9	3.7	5.9	3.4	15
Cr^{3+}	Reference	2.61	8.49	1.1	2.81	10.0	4.1	6.5	3.0	36
	6.2 〃	2.91	10.0	1.2	2.91	11.3	4.8	9.8	3.2	18
Cu^{+}	Reference	2.58	9.11	1.2	2.78	10.7	4.2	8.0	3.2	58
	2.5 〃	2.72	9.52	0.9	2.77	11.7	4.1	7.3	3.6	35
Pb^{2+}	Reference	2.34	7.35	0.9	2.84	9.1	3.4	4.2	2.8	43
	9.1 〃	2.43	8.21	0.9	2.48	10.8	3.6	5.2	3.8	40

TABLE II

	Fe^{3+}	Co^{3+}	Cu^{2+}	Fe^{2+}	Cr^{3+}	Cu^{+}	Ag^{+}, Ni^{2+}, Mn^{2+}	Co^{2+}, Pb^{2+}, Cd^{2+}
K_Q	1.54	0.71	0.62	0.59	0.40	0.25	0.1~0.05	0

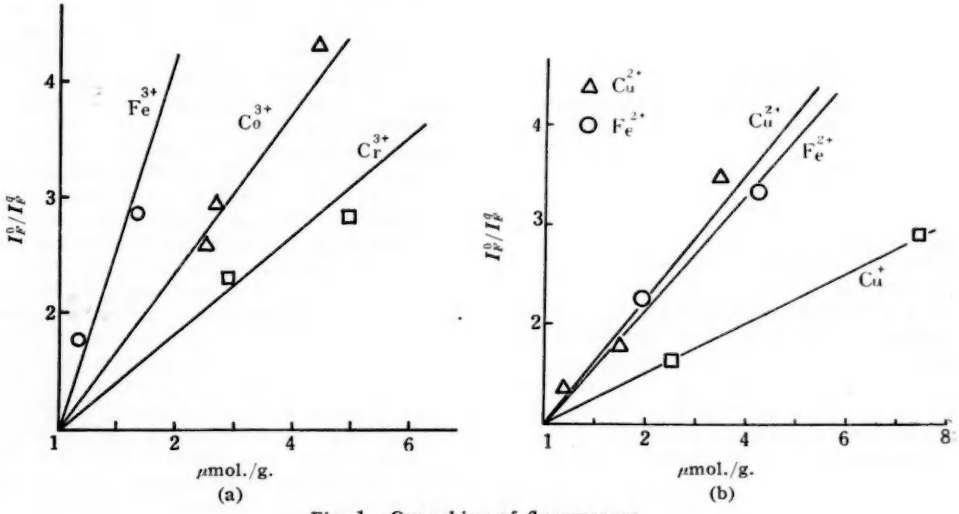

Fig. 1. Quenching of fluorescence.

Quenching constants are evaluated from the inclinations and are tabulated in Table II.

Cobaltous-, lead- and cadmium-ion show no noticeable effects up to concentration ca. 10 μmol./g..

(c) Absorption Spectra.—Except cupric ion, all the salts scarcely affect the features of the original spectra of trypaflavine adsorbed on silica gel. In all cases the extinction declines more or less, but the decrease is not so large, except in the case of cobaltic- and ferrous-ion, that it may be neglected as a first approximation. Some typical examples are shown in Fig. 2. Somewhat large decreases in the cases of cobaltic- and ferrous- ion, however, are most certainly to be attributed to the partial decomposition of dye during the evacuation at elevated temperature. As for cobaltic ion, it is almost certain that it really decomposes, since it is well known that cobaltic chloride is unstable in the solid state and a part of chlorine is eliminated during the above treatment.

In view of the above results, it is true that the quenching constants shown in Table II must be corrected since they have been derived from the total decrease of fluorescence intensity which is due to a genuine quenching action on one hand and to the decomposition of dye on the other. For semiquantitative discussion, however, they may be taken as a measure of a genuine quenching action exclusive of the case of cobaltic- and ferrous-ion.

* Analogous notation will be used in general, when it is necessary to distinguish the quantity referring to the quenching experiment from that of the reference one.

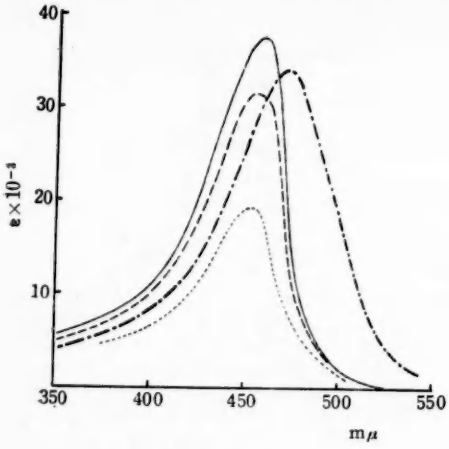

——— Reference
– – – – Fe^{3+} (1.7 μmol./g.),
····· Co^{3+} (3.2 〃),
–·–·– Cu^{2+} (9.3 〃).

Fig. 2. Absorption spectra.

Even in the most extreme case of cobaltic ion, the following data show that the fall of fluorescence intensity cannot be accounted for only by the decomposition of dye.

TABLE III

	εmax.	I_F
Reference	37×10^3	33
with Co^{3+} (3.2 μmol./g.)	20×10^3	10

(d) Discussion. — It can be concluded from the above results that except cupric chloride, the addition of a salt to the phosphor scarcely affects the absorption spectra and yet it reduces remarkably the intensity of pure fluorescence. Values of I_F^0/I_F^q in Fig. 1 are considered to give the ratio π^q/π^0 which changes from ca. 2 to 4 in the case of ferric-, ferrous- and chromic-ion and yet the values of π'^q, π''^q, $n_1{}^q n_2{}^q$ and $n_u^q n'^q_u/\pi^q$ do not differ much from the corresponding values of a reference phosphor.

Taking the data relating to ferric ion 0.4 μmol./g., for example, the following estimation will be helpful to make the situation clear. From the 9th column of Table I,

$$n_u^0 n'^0_u/\pi^0 = 3.2/3.4\times n_u^q n'^q_u/\pi^q$$

If one assumes, as is probable, that

$n'^q_u \simeq n'^0_u$

then, $\quad n_u^0/\pi^0 = 3.2/3.4\times n_u^q/\pi^q$

From the data of fluorescence, on the other hand,

$$\pi^q/\pi^0 = 1.7 \qquad (1)$$

Hence $\quad n_u^q = 1.8\times n_u^0 \qquad (2)$

Combining (1) and (2) with the relations

$\pi^0 = n_l + n_e + n_u^0$, $\pi^q = n_l + n_e + n_u^q + n_q$,

one gets $\quad n_q = 0.7(n_l+n_e) - 0.1\times n_u^0$

Thus it can safely be concluded that the addition of a salt quenches S′-state not only in a genuine sense, but it also promotes S′→T transition to some extent.

Here it is to be noted, however, that there is another possibility which must be taken into account. This is related to the state of adsorption of a salt. Since in general, inorganic salts are not capable of adsorbing very easily on silica gel and in view of the method of preparation of samples, it is rather likely that the state of adsorption is not uniform. There may exist on silica gel surface such a situation as that instead of a uniform distribution of positive and negative ions, a group of many ions coalesces into a tiny crystalline grain, which is located at random from place to place. If it be the case, it may occur that the dye molecule which happens to lie close to this tiny grain of a salt cannot make any contribution to the emission phenomenon and only an isolated dye molecule participates in fluorescence and phosphorescence. It is evident that in such a situation fluorescence intensity remarkably decreases and yet the decay curve remains almost unaltered. The real situation may perhaps be a superposition of the above two cases. At any rate, there is no doubt that these quenchers chiefly affect S′-state but scarcely affect T- and M-state.

(e) Anomalous Behaviours of Cupric Ion.—The results obtained when cupric ion was employed as a quencher are very interesting from various viewpoints. The absorption spectra of trypaflavine in this case are shown in Fig. 2. As seen from it, the maximum displaces about 15 mμ towards a longer wavelength (which corresponds to about 1.7 kcal./mol.) showing that a cupric ion affects the electronic state of dye.

From the fact that pure fluorescence is markedly quenched by cupric ion (the

TABLE IV

Quencher	α	β	A/B	I_L/I_{P0}	π'	π''	n_1n_2	n_un_u'/π	I_F
Reference	2.53	8.47	1.1	2.66	10	4.0	6.5	3.3	28
1.5 μmol./g.	2.69	10.0	0.8	2.61	13	4.0	7.9	4.2	17
3.6 〃	3.92	20.0	0.4	1.94	35	5.1	18	16	8

quenching constant is 0.6 as listed in Table II), it is evident that S'-state is remarkably affected. But, in contrast to other salts, the change in the decay curve is rather large. The analysis is possible, at least approximately, on the basis of our scheme, and the results obtained from the analysis of the decay curves at 25°C are shown in Table IV.

A notable result in Table IV is that the value of n_un_u'/π is increased by the addition of cupric ion. In all the other cases so far investigated including gaseous molecules, this quantity is almost constant. π'' remains practically unaltered, while π', n_1n_2 and n_un_u'/π increase remarkably. Hence it can be said that M-state is not affected and the increase of n_1n_2 can be attributed mainly to n_1.

If one assumes that the adsorption of cupric chloride is uniform, the reduction of pure fluorescence must be attributed to the increase of π. For example in the case of 3.6 μmol./g. cupric chloride,

$$\pi^q=3.5\times\pi^0$$

from the data in Fig. 1.

Combining with the data in Table IV, $n_u^qn_u'^q=18\times n_u^0n_u'^0$. Thus it is certain that the transitions between S'- and T-state are enormously promoted. If one assumes, as it seems probable, that the main part of the increase in $n_u^qn_u'^q$ is due to that of n_u^q, then the great value of π'^q must partially be attributed to the participation of a genuine quenching process.

Thus it is plausible that the cupric ion not only influences S'-state but also T-state pretty markedly while it scarcely affects M-state.

The temperature effect on various constants in the range from 0°C to 50°C, throughout which β-phosphorescence is practically negligible, is shown in Table V.

In this table, apparent activation energy obtained from the Arrhenius' plot for π', π'', n_un_u'/π and n_1n_2 respectively, is also included.

The activation energy for π', π'' and n_un_u'/π does not change beyond probable error but it seems quite definite that the activation energy for $n_1^qn_2^q$ is about half that for $n_1^0n_2^0$. Since n_2 is approximately independent of the existence of cupric ion and moreover π'' has practically the same temperature dependence, the above result is mainly due to the difference in the temperature dependence of n_1^0 and n_1^q.

Thus it seems plausible to consider that T→M transition is a process accompanied with an activation energy the magnitude of which, however, is much less than that for T→S' transition; the promotion of the transition T→M by the cupric ion at least partially, is attributed to the decrease of this activation energy.

Finally the decrease of I_L/I_{P0} by the addition of a cupric ion and its temperature dependence will be discussed briefly.

From the relation

$$I_F/I_{P0}=I_L/I_{P0}-1=\frac{\pi_1-(n_1n_2/\pi_2)}{n_un_u'/\pi}$$

it is evident that I_F/I_{P0} decreases when n_un_u'/π and n_1n_2/π_2 increases while it increases when π_1 increases. In the present case π_2 and n_2 are scarcely affected by a cupric ion and the increase of π_1 and n_1 partially cancels, so that the variation of the numerator on the right side becomes much less than that of n_un_u'/π. Thus the main factor which reduces I_F/I_{P0} is n_un_u'/π, which in the present case is remarkably increased by the addition of cupric ion.

The result that the value of I_F/I_{P0} decreases with rise of temperature, irrespective of the addition of cupric ion, is due to the fact that the temperature coefficient of n_un_u'/π is larger than that of π_1, π_2 and n_1n_2 (see Table V).

(f) Trypaflavine-filter Paper Phosphor. —As already reported in part II, deviation from linearity in decay curves is much smaller than that of silica gel phosphor. Moreover the effect of addition of a third substance is also much smaller than that in the case of silica gel, so that the analysis on the basis of the scheme involving M-state cannot be done very accurately. Here only a few examples will be shown and the results will be discussed only qualitatively.

The Table VI shows the results of analysis of the decay curve when oxygen or water vapor is added to the phosphor.

In the case of oxygen π' and π'' remain constant while n_1n_2 seems to be somewhat

TABLE V

Dye conc., 0.4 μmol./g.; $CuCl_2$, 3.6 μmol./g.; Time in sec.

$1/T$	α	β	A/B	I_L/I_{F0}	π'	π''	n_1n_2	n_un_u'/π
3.65×10^{-3}	2.08	15.4	0.48	2.53	22	2.9	10	7.2
3.51	2.65	16.6	0.48	2.38	24	3.7	12	8.7
3.36	3.92	20.0	0.40	1.94	35	5.1	17	16
3.24	4.58	23.6	0.29	1.87	44	5.6	19	22
3.12	6.5	27.1	0.24	1.73	58	7.6	22	32
Apparent activation energy (kcal./mol.)					1.7	1.6	1.2	2.6
				Reference Sample				
3.65	1.43	4.58	1.4	3.73	4.59	2.4	2.2	0.99
3.53	1.84	6.28	1.3	3.12	6.9	3.0	3·9	1.8
3.36	2.53	8.47	1.1	2.66	10.3	4.0	3.3	6.3
3.24	3.04	10.35	0.77	2.53	13.7	4.4	7.8	4.7
3.12	4.51	14.85	0.75	2.42	21.7	5.8	12	8.1
Apparent activation energy (kcal./mol.)					2.3	1.3	3.2	2.4

TABLE VI

Dye conc., 0.8 μmol./g. (filter paper, ca. 0.5 g). At 25°C. Time in sec.

	α	β	A/B	I_L/I_{F0}	π'	π''	n_1n_2	n_un_u'/π	I_F
Reference	2.15	6.43	1.5	4.59	6.0	3.6	4.2	1.1	76
O_2, 2.4 *m*.mol. (190 mmHg)	2.08	5.79	0.7	5.95	6.0	2.8	2.2	0.9	65
O_2, 3.6 *m*.mol. (290 mmHg)	2.32	6.30	0.5	8.31	6.3	3.0	2.2	0.7	60
Reference	2.28	7.11	1.4	4.74	6.7	3.8	5.0	1.1	80
H_2O, 40 μmol. (1/4 mmHg)	2.35	6.85	1.4	5.04	6.3	3.9	4.3	1.0	55
H_2O, 320 μmol. (2 mmHg)	2.52	6.52	1.9	7.69	5.4	4.2	3.7	0.6	21

diminished. But since the results are not so certain and moreover data are rather few, it will not be suitable to discuss further about this point. There is however no doubt that the decrease of I_F is closely connected with that of n_un_u'/π. Hence broadly speeking, it can be said that only S'-state is affected and only fluorescence is quenched.

This result is in sharp contrast with that obtained for the case of trypaflavine-silica gel phosphor. It is to be noted, however, that in the present case the quantity of oxygen is very large compared with that in the case of silica gel.

The situation is quite similar for the quenching caused by water vapor; thus only S'-state is affected and the intensity of pure fluorescence decreases without any noticeable effect on the decay curve.

The influence of the addition of some organic vapors such as acrylonitrile (the quantity is 1700 times that of dye), styrene (about equal to that of dye), etc. was also tested but none of them showed any effects beyond experimental error.

General Features of the Quenching Phenomena as Revealed from the Results so far Obtained

The main features of the quenching phenomena so far established can be summarized in Table VII.

TABLE VII

Carrier	Quencher	S'	T	M
Silica gel	Gases	$\times \overset{\times}{\leftarrow}$	$\bigcirc \overset{\circ}{\rightarrow}$	$\circ$
	SO_2	$\times \overset{\times}{\leftarrow}$	$\bigcirc \overset{\circ}{\rightarrow}$	$\bigcirc$
	Salts	$\bigcirc$	$\times$	$\times$
	$CuCl_2$	$\bigcirc$	$\bigcirc \overset{\circ}{\rightarrow}$	$\times$
Filter-paper	O_2, H_2O	$\bigcirc$	$\times$	$\times$
	Self-quenching	$\bigcirc$	$\times$	$\times$

In this Table $\bigcirc$ and $\times$ under S'-, T- and M-state represent respectively that the state in question is affected or not by a quencher. A small circle means that the action is somewhat small. Very little can be said whether each transition is influenced or not by a quencher, but the

results written in this Table are reliable.

The informations summarized in the above Table are still very scanty, yet some suggestive arguments will be based upon them.

From the survey of the above Table it seems permissible to classify the quenching effects into two groups; collisional quenching which attacks chiefly T- and M-state, and a static one attacking S′-state. Let us consider the results from this point of view.

That the quenching action of oxygen toward silica gel phosphor is of collisional nature has been argued already in part III. Hence it is considered that oxygen on silica gel phosphor is so weakly adsorbed that it is quite free to move.

On the contrary, filter paper is less porous than silica gel and oxygen adsorbed on it is supposed to be fixed at a definite position. The adsorbed oxygen in this case is thus remote from the adsorbed dye molecule and this is perhaps the reason why it falls into the class of a static type. There may be no question that salts act as static quenchers since they are adsorbed on fixed positions. Self quenching in the case of filter paper is also undoubtedly of static type. Thus all the results conform well with the above classification.

Now, this classification becomes more plausible and more instructive if one assumes the following molecular model of adsorbed dye. From the observations made when polyvinyl alcohol was used as a carrier (Part II), it seems probable that molecules of trypaflavine are fixed on a carrier at the positions of two amino-groups. It is very natural then, to suppose that if the two amino-groups attached on a carrier are subject to some perturbation, then T- or M-state will be affected appreciably. Such a reasoning conforms well with the general view that molecular rigidity is one of the essential conditions for the phosphorescence to be observed. Thus it is comprehended that only when a quencher molecule approaches closely to an amino-group can it affect T- or M-state. This may be the reason why only collisional quenching affects T- and M-state. In the case of a cupric ion which is a sole exception in static quenching, the field may be so intense that it is able to affect amino-groups to some extent.

To sum up, the behavior of T- and M-state probably depends on the interaction of amino and polar group of a carrier and is supposed to be perturbed only by extremely short range force.

The physical or chemical property of M-state is not yet known, but the fact that cupric chloride only affects T-state while oxygen and other gases attack both T- and M-state seems to be due to a specific nature of this state.

In order to reveal the nature of M-state, it will be most helpful to study about various combinations of dye and carrier.

Summary

The effects of the addition of inorganic salts upon trypaflavine-silica gel phosphor were studied, and it was found that decay curves are not affected much by any of the metallic ions except cupric ion. On the contrary, the intensity of pure fluorescence ($I_L - I_{P0}$) was reduced more or less by many metallic ions. From these results, it was concluded that many metallic ions chiefly affect S′-state but not T- and M-state.

The result for cupric chloride was somewhat anomalous on the point that a cupric ion affects both S′- and T-state.

A general survey on the quenching action of various substances upon adsorbed trypaflavine phosphor was given.

The cost of the present research has been partly defrayed from the Scientific Research Grant from the Ministry of Education.

Institute of Polytechnics
Osaka City University, Osaka

Microcolorimetric Determination of Sulfate by Reduction to Hydrogen Sulfide with Tin(II)—Strong Phosphoric Acid

By Toshiyasu KIBA and Ikuko KISHI*

(Received August 27, 1956)

In a previous paper[1] from the authors' laboratory it was shown that both soluble and insoluble sulfates could be quantitatively reduced to hydrogen sulfide by heating with tin(II)-strong phosphoric acid, a new powerful and stable reducing agent first described by the authors. The discovery of this reagent led the authors to the development of a new rapid and simple method for the determination of semimicro quantities of sulfate sulfur. The established method[1] consists of the following three succesive steps: (a) reduction of sulfate to hydrogen sulfide by tin(II)-strong phosphoric acid, (b) absorption of the hydrogen sulfide by zinc acetate solution, (c) iodometric titration of the resulting zinc sulfide by ordinary procedures.

The present report concerns a later investigation in which the above method has been extended to the microgram scale by adopting the sensitive methylene blue method for sulfides[2]. The rapidity and simplicity of the original method are still retained in this new colorimetric procedure, by which 1 to 35 micrograms of sulfate sulfur can be estimated.

Apparatus

Reduction and Absorption Apparatus.—The apparatus for the reduction of the sulfate and the absorption of the hydrogen sulfide evolved is shown in Fig. 1. The reaction vessel (A) is of fused silica. Unexpectedly high values of sulfur were occasionally obtained when glass vessels were used, probably owing to minute amounts of sulfur in the glass. A bent glass tube (F) is attached to the outlet arm of the reaction vessel with a short piece of rubber tubing (G). A detachable delivery tube (D) is connected with another rubber tubing to the bent tube (F) and inserted into the absorbing vessel (C). Since zinc sulfide adheres to that part of the tube immersed in the solution, it must be disconnected and allowed to remain in the absorbing vessel during the development of the methylene blue color. A Kipp's apparatus is employed for the production of carbon dioxide, which is purified by six-washing bottles (not shown in Fig. 1.) and introduced into the reaction vessel through the inlet arm. Solutions used for the purification of carbon dioxide are described below.

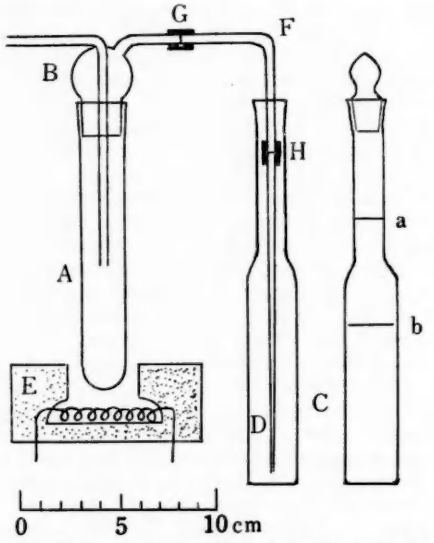

Fig. 1. Apparatus for reduction and absorption.
A: Reaction vessel of fused silica
B: Glass cap fitted to the reaction vessel
C: Absorbing vessel a: the mark of 50 ml.
b: the mark of 35 ml.
D: Detachable delivery tube (4 mm. in outside diameter)
E: Electric heater
F: Gas leading tube
G, H: Short pieces of rubber tubing

Photoelectric Colorimeter.—A "Hirama" photoelectric colorimeter with 1 cm. cells and a filter 655 mμ were used throughout this work.

Reagents

Tin(II)-Strong Phosphoric Acid.—Prepare from 250 g. of strong phosphoric acid and 50 g. of tin(II) chloride dihydrate of extra pure grade as described in the previous paper[1].

Carbon Dioxide.—Purify carbon dioxide produced in the Kipp's apparatus by passing through five gas-washing bottles containing respectively

* Her present name is Mrs. Ikuko AKAZA.

1) T. Kiba et al., This Bulletin, **28**, 641 (1955).

2) J. F. Fogo and M. Popowsky, *Anal. Chem.*, **21**, 732 (1949).

3) S. Nakayama, *J. Chem. Soc. Japan*, **47**, 197 (1926).

water, 1% potassium permanganate in 10% sodium carbonate solution, vanadium (II) sulfate in sulfuric acid, 5% barium chloride, and zinc acetate absorbing solution. Place a sixth, empty bottle to equalize the flow of the gas and to intercept mist. The vanadium (II) sulfate solution is employed to remove oxygen completely from the carbon dioxide. To prepare it, dissolve 2 g. of ammonium vanadate in 200 ml. of water, add 20 ml. of 6 N sulfuric acid, and shake vigorously with 3% zinc amalgam in an atmosphere of carbon dioxide until the violet color of vanadium (II) appears. Transfer the solution quickly into a gas-washing bottle containing a small amount of the amalgam.

Zinc Acetate Absorbing Solution.— Dissolve 20 g. of zinc acetate dihydrate of extra pure grade in 1 l. of redistilled water. If necessary, add two or three drops of glacial acetic acid to clarify the solution, but the pH of the solution should not be below 5. The redistilled water is prepared by distilling ordinary distilled water with a small amount of sodium hydroxide in an all-glass still.

***p*-Amino Dimethyl Aniline Solution.**—Dissolve 1.4 g. of *p*-amino dimethyl aniline sulfate crystals of pure grade in 200 ml. of 1:1 sulfuric acid.

Ferric Chloride Solution.—Dissolve 10 g. of ferric chloride hexahydrate in 100 ml. of distilled water.

Standard Sulfate Solution.—Dissolve 4.4299 g. of anhydrous sodium sulfate of extra pure grade in 1 l. of sulfur-free water. Take 20 ml. of this solution with a pipet and dilute it to 1 l., so that the final solution contains 20 micrograms of sulfur in 1 ml. Pipet accurately required amounts of this stock solution for the analysis.

Barium Chloride Solution. — Dissolve 1 g. of barium chloride dihydrate in 100 ml. of sulfur-free water, and use 0.5 ml. of this solution in each test.

Procedure

When the sample is a solution, pipet accurately an aliquot containing 1 to 35 micrograms of sulfur. When it is a solid, take an accurately weighed quantity containing the same range of sulfur. Put the measured sample into the reaction vessel (A) (Fig. 1.), add 0.5 ml. of the barium chloride solution to fix the sulfate as barium sulfate, and evaporate the content to dryness at the bottom of the vessel. Pour 5 ml. of tin (II)-strong phosphoric acid over the dried residue from a pipet. Fill the absorbing vessel up to the 35 ml. mark with the zinc acetate solution. Connect all the apparatus as shown in Fig. 1. Pass carbon dioxide very rapidly through the apparatus for five minutes. The passage of the gas should be rapid enough to cause strong agitation of the surface of the liquid in the absorbing vessel, and the end of the gas delivery tube should reach to the bottom of the vessel. After five minutes, reduce the flow of the gas to a rate of one bubble per second. Heat the bottom of the reaction vessel on a small etectric heater, which is regulated by a variable transformer, until white fumes of phosphoric acid appear. Continue the heating for about fifteen minutes. It is unnecessary to keep the reaction temperature strictly constant, but it should be high enough to ensure that the mixture exhibits a white turbidity near the end of the reaction. Stop the heating and continue to pass carbon dioxide for about five minutes.

Remove the absorbing vessel, leaving the gas delivery tube in it. Stopper the vessel and place it in a thermostat kept at 24°C for several minutes. Add quickly 1.5 ml. of *p*-amino dimethyl aniline solution using a rapid delivery pipet, stopper the vessel, shake it vigorously, and then quickly add 0.5 ml. of the ferric chloride solution. Stopper and shake the vessel again. After keeping the vessel in the thermostat at 24°C for fifteen minutes, add more distilled water till the liquid reaches the 50 ml. mark, while the delivery tube is hung up from the solution with washing. Stopper and shake the vessel so as to make the solution homogeneous. Read the absorbancy of the solution in the colorimeter at 655mμ within thirty minutes.

Results and Discussion

Standard Sulfate Calibration Curve.— As shown in Fig. 2, the linear relationship

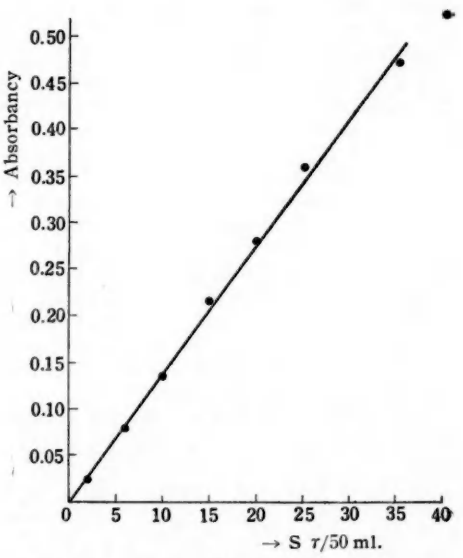

Fig. 2. Standard sulfate calibration curve.

was obtained between the amount of sulfate and the absorbancy of the resulting methylene blue solutions in the range 1 to 35 micrograms of sulfur. Measurements were made in 1-cm. cells at 655 mμ, using

a mixture of the absorbing solution and the reagent of the same amounts as reference. For more than 40 micrograms of sulfur the linearity is not held, because of mutual interaction of the light-absorbing molecules or of spectral purity of the instrument. According to the authors' experience, the main sources of error in this method seemed to be imperfect removal of oxygen from the carbon dioxide and careless delay in adding the reagents, viz., *p*-amino dimethyl aniline and ferric chloride.

A comparison of the standard curve with that drawn for sodium sulfide by direct coloration with *p*-amino dimethyl aniline, indicated that the two curves coincided with each other satisfactorily. Both curves could be expressed by the equation, $x=a+by$, where x is the absorbancy measured and y the amount of sulfur in micrograms. The average values of a and b computed from the sulfate curves were 0.00614 and 0.01084, respectively, whereas those obtained from the sulfide curves were 0.00245 and 0.01087, respectively. These numerical values were calculated by the method of the least square. It may be concluded from this fact that the sulfate was completely reduced to hydrogen sulfide under the given condition.

Interferences and their Elimination.— The effect of chloride was examined by the addition of various amounts of sodium chloride to sodium sulfate solutions, containing 1 to 35 micrograms of sulfur through the standard procedure. It was found that, when the amount of the sulfate sulfur was less than 20 micrograms, the presence of as much as 36.9 mg. of the chloride ion does not interfere with the determination. When the amount of coexisting chloride ions was decreased to 12 mg., the linearity of the curve was recovered for a wider range of sulfur, i. e., from 1 to 35 micrograms.

The presence of nitrate in the sample, on the other hand, was found to result in apparently low values for sulfate sulfur.

As the sulfate ion is customarily separated from other anions with barium chloride, the effect of the barium ion was examined. By the addition of 1 ml. of 1% barium chloride solution to sodium sulfate solutions containing 1 to 40 micrograms of sulfur, the determination of sulfate sulfur was carried out. Although in this case a large excess of the barium ion was always present, it did not bring about any deviation from the linear relationship as shown in the standard sulfate sulfur curve. The experiment conclusively showed that the barium ion does not affect the accuracy of the method.

The collector action of ferric hydroxide may have great importance in analytical procedures, particularly in a micro analysis. Minute amounts of the sulfate ion, coexisting with other interfering soluble ions, may also be separated by centrifugation or filtration as barium sulfate, which is occluded in the ferric hydroxide precipitate. So the effect of the ferric ion was examined as follows. To sodium sulfate solution containing 1 to 40 micrograms of sulfur were added 0.5 ml. of 1% solution of barium chloride and 3.35, 5.58, and 11.17 mg. of ferric ion as iron(III) chloride, respectively. After the drying of the mixed solutions in the reaction vessels, the entire procedure was carried out and the absorbancy of the resulting methylene blue solution was measured. As illustrated in Fig. 3, the solution containing 11.17 mg. of the ferric ion showed lower

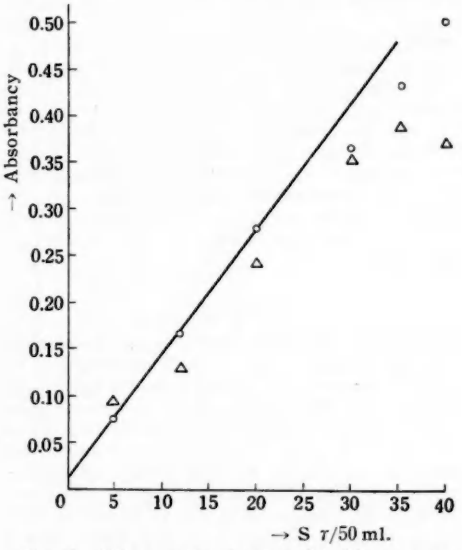

Fig. 3. Effect of ferric and chloride ions on the sulfate calibration curve.
○: 5.5_5 mg. Fe and 12.2 mg. Cl
△: 11.1_7 mg. Fe and 22.9_5 mg. Cl

sulfur values. Moreover, even by the use of 5.58 mg. of ferric ions, the linearity of the curve could not be preserved for more than 20 micrograms of sulfur content. As it might be considered that the effect was caused by both ferric and chloride

ions, the following experiments were carried out to eliminate their interference. To the sulfate solution taken in the reaction vessels were added 11.2 mg. of ferric ion as ferric chloride, 0.5 ml. of 1% barium chloride solution, and 0.5 ml. of aqueous ammonia (d=0.88). The mixture was evaporated to dryness, and heated in an electric oven to 500°C. By this treatment all acidic components but sulfate would be decomposed, unless too large amounts of alkali or alkaline earth metal ions were present. The ferric chloride was eventually converted into ferric oxide. Then the reduction of the sulfate to hydrogen sulfide was carried out according to the procedure without further addition of barium chloride. The linear relationship between the amount of the sulfate and the absorbancy of the resulting methylene blue solution was obtained. So it was found that the elimination of the effects of ferric and chloride ions could be completed by this treatment.

Determination of Sulfur in Commercial Ferric Chloride Reagent.—The method described above can be readily applied to the determination of sulfate in various substances. For example, weigh accurately about 27 g. of ferric chloride hexahydrate, and dissolve it in 500 ml. of distilled water.

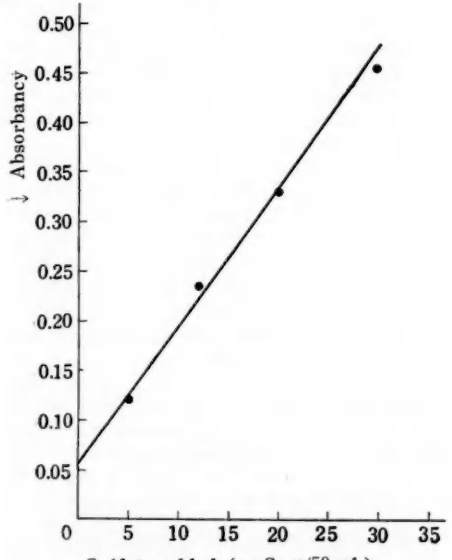

Fig. 4. Sulfate calibration curve after treatment with ammonia, in the presence of 54 mg. of ferric chloride hexahydrate.

Pipet 1 ml. of the solution into a reaction vessel, and after the treatment described above, the analysis is similarly carried out. In the course of the treatment some ferric chloride volatilizes, but barium sulfate is stable at as high as 900°C[3] and most of the ferric chloride is converted into ferric oxide at 500°C[4]. The experimental data of the analysis are given in Fig. 4 showing satisfactory recovery of the sulfate added. The absorbancy measured in the absence of sulfate was 0.052, which is the sum of the absorbancy of 0.039 for the blank of ammonia and that of 0.019 for sulfur in the ferric chloride tested. So the amount of sulfur in 54 mg. of ferric chloride hexahydrate is estimated to be as small as 1 microgram and that contained in 0.5 ml. of aqueous ammonia 2.4 micrograms.

Determination of Sulfur in Japanese Acid Clay.—A 0.1 to 0.5 g. portion of air-dried clay was weighed directry in a reaction vessel. The analysis was similarly carried out without any preliminary treatment. As shown in Table I, a linear relationship was obtained between the amount of the clay and that of sulfur found. Moreover, it was verified that as little as 4 micrograms of sulfur in 0.1 g. of the clay could be estimated accurately and rapidly with satisfactory reproducibility.

TABLE I

DETERMINATION OF SULFUR IN JAPANESE ACID CLAY

Acid Clay Taken g.	Absorbancy	Sulfur Found μg.	Sulfur Content %
0.1000	0.056	3.8	0.0038
0.2175	0.119	8.6	0.0039
0.3825	0.195	14.3	0.0037

Summary

A new reagent, "Tin(II)-strong phosphoric acid" has been prepared to permit a rapid and simple determination of sulfate sulfur by reduction to hydrogen sulfide. The procedure for the determination of semi-micro quantities of sulfate sulfur, previously devised by the authors, has been extended to the microgram scale by adopting the sensitive methylene blue colorimetric method. The rapidity and simplicity of the original method are still retained in this new colorimetric method,

4) L. Marvin, *Ind. Eng. Chem. Anal. Ed*, **17**, 554 (1945).

by which 1 to 35 micrograms of sulfate sulfur can be estimated. The apparatus is very simple, a test-tube of fused silica being employed as the reaction vessel. The standard calibration curve for colorimetric determination of sulfate sulfur by this method coincides well with that drawn for sodium sulfide by direct coloration with *p*-amino dimethyl aniline and ferric chloride. Interference of other anions can be kept out of consideration, because the sulfate ion is easily separated by addition of barium chloride solution and coprecipitation with ferric hydroxide. Large amounts of ferric hydroxide do not affect the method. Some examples of the determination of sulfate sulfur in ferric chloride reagent and Japanese acid clay are described.

A part of the expenses for this study was defrayed from a grant given by the Ministry of Education, to which the authors' thanks are due.

Department of Chemistry
Faculty of Science
Kanazawa University
Kanazawa

Studies on Amino-hexoses. IV. N-Deacylation with Hydrazine and Deamination with Nitrous Acid, a Clue to the Structure of Aminopolysaccharides[1]

By Yoshio MATSUSHIMA and Noriko FUJII

(Received August 30, 1956)

Considerable confusion is observed in the older literature concerning the nitrous deamination products of glucosamine. However, the formation of chitose, a 2, 5-anhydro-hexose[2], from glucosamine is understood in terms of intramolecular rearrangement[3,4] which accompanies the deamination, and a few years ago one of present authors demonstrated experimentally that the same mechanism operated in the nitrous deamination both of glucosaminol and 2-amino-erythro-pentitols which form 2-deoxy-glucose[3] and 2-deoxy-ribose[5] respectively.

The nitrous deamination of chitosan (deacetylated chitin or polyglucosamine) has also resulted in conflicting conclusions[6], but it is noteworthy that every worker reports the rupture of glucosaminidic linkage and the formation of highly reducing saccharides. More recently, it was reported[7] that ψ-heparin (the desulfated heparin) also produced reducing saccharides with nitrous acid. In these instances, it is not conceivable that the hydrolytic cleavage of amino-glycosidic linkages preceede the deamination, since it is known[8] that glucosaminidic linkage strongly resists to acid hydrolysis (see Fig. 1) and nitrous acid is so weak an acid. Therefore, some special mechanism must operate.

It may be expected that the cleavage of glucosaminidic linkage (or probably 2-amino-glycosidic linkages in general) with nitrous acid will provide a clue to the structure of amino-polysaccharides. However, it seems desirable to obtain more experimental evidences and to establish the theory according to which the 2-amino-glycosidic linkage cleaves.

The authors have isolated from the deamination mixture of chitosan a diphenylhydrazone which is identical with the long known diphenylhydrazone[9] which was obtained from the deamination mixture of glucosamine. Although, as we

1) A Part of this article was delivered at the 9th annual meeting of the Chemical Society of Japan, April 1956.
2) E.Fischer and F.Tiemann, *Ber.*, **27**, 138 (1894); E.Fischer and F. Andreae, ibid., **36**, 2587 (1903); W. N.Haworth, E.L.Hirst and V.S.Nicholson, *J. Chem. Soc.*, **1927**, 1513.
3) Y.Matsushima, *Bull. Chem. Soc. Japan*, **24**, 144 (1951).
4) A.B.Foster, *Chem. and Ind.*, **1955**, 627.
5) Y.Matsushima and Y.Imanaga, This Bulletin, **26**, 506 (1953).
6) W.Armbrecht, *Biochem. Z.*, **95**, 108 (1919); P. Karrer and S.M.White, *Helv. Chim. Acta*, **13**, 1105 (1930); K.H.Meyer and H.Wehrli, *Helv. Chim. Acta* **20**, 353 (1937).
7) A.B.Foster, E.F.Martlew and M.Stacey, *Chem. and Ind.* **1953**, 825.
8) J.C.Irvine and A.Hynd, *J. Chem. Soc.*, **101**, 1128 (1912).
9) P.Schorigin, and N. N. Makarowa-Semljanskaya, *Ber.* **68**, 965 (1935).

lacked the structural proof, the diphenylhydrazone was not necessarily thought to be the diphenylhydrazone of chitose until recently, a report[10] proving the 2,5-anhydromannose structure of the diphenylhydrazone has appeared. Therefore, the isolation

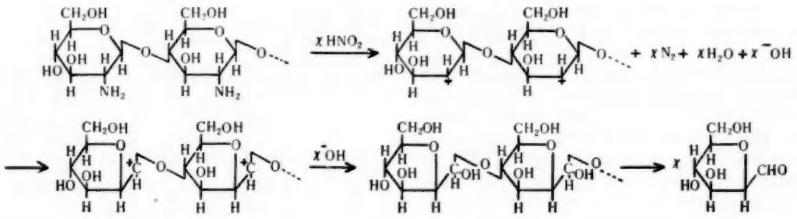

of the diphenylhydrazone provides a proof of the existence of chitose in the deamination products of chitosan. How chitose is produced may be seen in the following scheme:

Here also the mechanism of intramolecular rearrangement operates and the formation of the intermediate half-acetal which may be highly labile explains the result. This theory has its counterparts in the anomerism of free sugars[11] and in the ease of hydrolysis of fructofuranosidic linkage[11,12]. The ease of hydrolysis of fructofuranosidic linkages, e. g. of sucrose, was attributed to the foregoing hydrolysis of the furanoid ring of fructose moiety, thus forming an intermediate half-acetal structure.

Unfortunately, since the amino residue of natural amino-polysaccharides is acylated without exception, nitrous acid can not attack it as such. Common deacylating agents, strong acid or alkali, may cause too far reaching degradation with two known exceptions of chitin and heparin. Therefore, the authors adopted the method of hydrazinolysis which was successfully introduced[13] into the protein chemistry. With anhydrous hydrazine, the amide linkage, or ester linkage if present, in polysaccharides may be cleaved, liberating free amino residue and the glycosidic or other linkages may remain intact.

To begin with, the authors applied the hydrazinolysis method to chondroitin sulfate. The ratio of amino to total nitrogen reaches about 0.9 when barium chondroitin sulfate is treated with anhydrous hydrazine for 10 hours at 100°. The hydrazine-treated specimen, only after treatment with nitrous acid, gives several spots on paper chromatograms, thus indicating the cleavage of galactosaminidic linkage with nitrous acid (see Fig. 2). Though no quantitative conclusion about the structure of chondroitin sulfate can be drawn so far, this method seems to be promising for the structural study of amino-polysaccharides. The work will be continued.

Experimental Part

Appearance of Reducing Power when Chitosan is treated with Nitrous Acid.—500 mg. of chitosan was dissolved in 25 cc. of acetic acid (ca. 15%) and a solution of 230 mg. of sodium nitrite in 25 cc. of water was added. 5 cc. aliquots were pipetted off and the reducing power was determined by Bertrand's method. A comparison run with hydrochloric acid was carried out similarly.

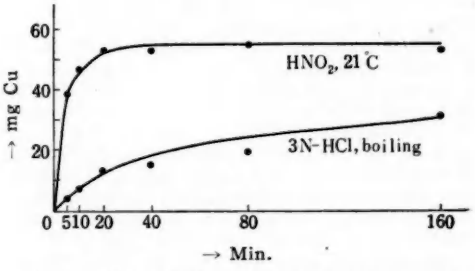

Fig. 1. The velocity of the appearance of reducing power in nitrous deamination and acid hydrolysis respectively of chitosan.
Ordinate: Reducing power in mg. Cu.
Abscissa: Time in minutes.

Isolation of Chitose Diphenylhydrazone from the Nitrous Deamination Mixture of Chitosan.—To the highly viscous solution which was prepared by dissolving 2 g. of chitosan into a mixture of 1N hydrochloric acid (13.2 cc.) and water (20 cc.), 4.6 g. of silver nitrite was added at room temperature. The evolution of gas and

10) S.Akiya and T.Osawa, *J. Pharm. Soc. Japan*, **74**, 1259 (1954).
11) S. Akabori and K.Uehara, "Discussion on Enzymes," Tokyo, (1942).
12) S.Matsumoto, *J. Chem. Soc. Japan*, **61**, 387, 395 (1940).
13) S.Akabori, K,Ohno and K.Narita, This Bulletin, **25**, 214 (1952).

the diminution of viscosity was observed immediately. After two days standing at room temperature, the silver chloride formed and the residual silver nitrite was filtered off, and the silver ion in the solution was removed by hydrochloric acid. A small amount of urea could exclude residual nitrous acid. To the solution the pH of which was adjusted to 4, were added 1.5 g. of diphenylhydrazine and a necessary amount of ethanol to obtain a clear solution. After heating at 80° for one hour the solution was concentrated in vacuo and the residue was agitated with a small amount of benzene and seed crystals. White needles began to crystallize in an hour. The crystals were washed thoroughly with water and benzene. The crude crystals thus obtained melted at 140–141° and weighed 0.97 g. Recrystallization was carried out as follows: the crude crystals were dissolved in 10 cc. of ethanol, and 40 cc. of water was added. Fine crystals came out immediately and the mixture was agitated thoroughly with a small amount of benzene-petroleum ether (1 : 1) in order to make free from coloring matter, filtered and washed with ethanol-water (1 : 4) and benzene. The recrystallized specimen weighed 0.67 g. and melted at 143.4–144.0° alone or at 145–145.5° with an authentic specimen of chitose diphenylhydrazone melting at 145.8–146.2°.

Anal. Found: C, 65.39; H, 6.05; N, 8.28. Calcd. for $C_{18}H_{20}O_4N_2$: C, 65.85; H, 6.09; N, 8.54%.

Hydrazinolysis of Barium Chondroitin Sulfate.—4.57 g. of barium chondroitin sulfate (N, 2.7%) was heated with 11.1 g of anhydrous hydrazine at 100° for ten hours. The excess hydrazine was evaporated off in vacuo and the residue was dissolved in 20 cc. of water and dialysed to running water of nineteen hours using collodion membrane. The inorganic precipitate was discarded and the solution was dried up in vacuo yielding 0.5 g. of a faintly yellow substance.

Anal. Found: N, 3.02 (Kjeldahl method); 2.65 % (van Slyke method).

Deamination of the Hydrazine-treated Specimen with Nitrous Acid.—0.4 g. of the specimen was dissolved in 4.6 cc. of water and to this solution 0.87 g. of silver nitrite and 3.4 cc. of 1N hydrochloric acid was added. A gas evolved immediately. After standing for one day at room temperature, the silver chloride formed and the residual silver nitrite was filtered off and the silver ion was removed with 1N hydrochloric acid. A small amount of urea was added in order to decompose the residual nitrous acid, and after the pH was adjusted to 5.8 the solution was concentrated in vacuo. The residue was paper-chromatographed. It is to be noted that color develops with such ketose reagents as resorcinol-hydrochloric acid or urea-hydrochloric acid[14]. These facts suggest that every spot in chromatograms contains 2,5-anhydro-hexose (Hydrofurfural) structure.

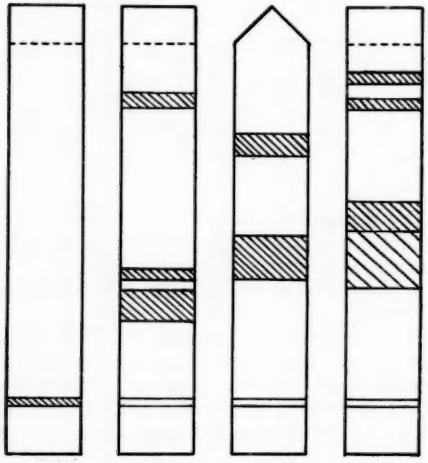

Fig. 2. Diagrammatic representation of the paper chromatograms.
I: The specimen without the treatment with nitrous acid. II: Urea-HCl development. III: Long run chromatography with urea-HCl development. IV: Resorcinol-HCl development. The moving solvent is butanol-ethanol-water-acetic acid (35 : 35 : 30 : 10) in all the run.

The authors wish to record their thanks to Professor S. Akabori of the Osaka University, for his stimulating discussions and encouragement.

Department of Science,
Nara Women's University, Nara

14) A.I. Oparin, *J. Japanese Chem.* **10**, 506 (1956).

Bromometric Oxidation of Red Phosphorus by Bromide Bromate Mixtures

By M. VENUGOPALAN and K. J. GEORGE

(Received June 12, 1956)

In a previous communication, Venugopalan and George[1] suggested the utility of the instantaneous and complete reaction

$$5Br^- + BrO_3^- + 6H^+ = 3Br_2 + 3H_2O \quad \text{(i)}$$

for a quantitative oxidation of red phosphorus to phosphoric acid bromometrically. Various substances react quantitatively with an excess of bromine, and acid solutions of bromine of exactly known concentration can readily be obtained from a standard potassium bromate solution by adding acid and an excess of bromide. In this reaction one mole of bromate yields six atoms of bromine and hence the equivalent weight is identical with that of potassium bromate alone. Bromine is very volatile and hence the experiments are carried out at as low a temperature as possible and in Erlenmeyer flasks provided with ground glass stoppers. The excess of bromine is determined iodometrically and from the reacted bromine the amount of phosphorus can be calculated.

Earlier workers[2] have shown that bromine reacts with red phosphorus at a very rapid rate at the ordinary temperature; but the reaction could proceed with a measurable speed at low temperatures and hence, it was of interest to undertake a kinetic study of the oxidation process.

Experimental

Solutions of bromide and bromate were prepared in the proportions given in equation (i) so that when mixed together in presence of an acid (H_2SO_4) both bromide and bromate react together instantaneously and completely to give a known amount of bromine.

Pure dry red phosphorus was weighed into a ground-glss stoppered Erlenmeyer flask. Equal volumes (40 cc.) of bromide and bromate solutions were added, followed by 20 ml. of 1 N sulphuric acid so that the overall normality of the system was maintained at or about 0.2 N H_2SO_4. The phosphorus dissolved in the evolved bromine in solution, thereby indicating that the initial reaction is very rapid and almost instantaneous. The system was maintained at a desired constant temperature for a few minutes prior to the addition of the oxidant and also during the course of subsequent observations in an ice-cooled water bath provided with an accurate thermometer. The contents of the flask were swirled from time to time and an aliquot portion (5 ml.) of the clear solution was pippetted out carefully at different time intervals and titrated iodometrically with standard thiosulphate[3]. Experiments were carried out at different temperatures, viz., 5, 10, 15, 20°C using the same concentration and by varying the concentration of the oxidant.

Results and Discussion

The order of the reaction was calculated by the integration method from the initial titre value of bromide bromide-bromate mixture and that obtained at various time intervals during the course of the oxidation, applying the equation

$$K = \frac{2.303}{tC_\infty} \log_{10} \frac{C_t(C_o - C_\infty)}{C_o(C_t - C_\infty)}$$

where C_o—initial concentration of bromide-bromate mixture
C_t—concentration at time t
C_∞—concentration at time ∞
and t—time in minutes

A representative group of results is shown in Table I. These results therefore show

TABLE I

Temperature: 20°C
Reaction Mixture: 5 ml.
Weight of P: 0.02 g.
Strength of KBr—$KBrO_3$ Mixture: N/35 solution

Time in Minutes	N/40 Thio ml.	$\frac{C_t(C_o - C_\infty)}{C_o(C_t - C_\infty)}$	$K \times 10^3$
0	3.40	—	—
15	3.05	0.0363	3.98
30	2.80	0.0706	3.87
45	2.60	0.1053	3.85
60	2.45	0.1375	3.86
90	2.20	0.2088	3.82
∞	1.40	—	—

Mean $K = 3.87 \times 10_3$

1) M. Venugopalan and K. J. George, *Bull. Chem. Soc. Japan*, **29** (3), 350-353, (1956).
2) J. W. Mellor, "A comprehensive Treatise on Inorganic and Theoretical Chemistry", Vol. VIII, Longmans Green & Co. (1928). p. 785.
3) A. I. Vogel, "Text Book of Quantitative Inorganic Analysis", Longmans Green & Co., London (1953). p. 369.

that the oxidation of red phosphorus by bromide-bromate mixture is an overall bimolecular reaction.

The influence of temperature on the velocity constant K, when the concentrations of the reactant are kept constant are given in Table II. The above results show

TABLE II

Weight of P Taken: 0.02 g.
Strength of Bromide-bromate Mixture: N/35
Normality of Thiosulphate: N/40

Temperature (t) °C	Mean $K\times10^3$
5	2.0
10	2.4
15	3.1
20	3.87

that the velocity constant K increases with a rise in temperature; the values of $\log_{10}\frac{C_t(C_o-C_\infty)}{C_o(C_t-C_\infty)}$ plotted against time t for different temperatures, at which the reaction has been studied are represented graphically in Fig. 2.

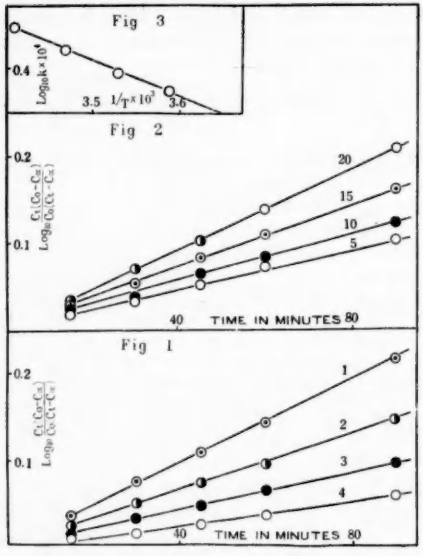

Fig. 1. Variation of $\log_{10}\frac{C_t(C_o-C_\infty)}{C_o(C_t-C_\infty)}$ with time t for different initial concentrations of bromide-bromate mixture at the same temperature.

Fig. 2. Variation of $\log_{10}\frac{C_t(C_o-C_\infty)}{C_o(C_t-C_\infty)}$ with time t for different temperatures.

Fig. 3. Variation of $\log_{10}K$ with $1/T$.

Variation of the velocity constant K for different initial concentrations of the reactants has been studied by varying the concentration of bromide-bromate mixture and keeping the weight of phosphorus constant in all the experiments.

TABLE III

Temperature: 5°C
Weight of Phosphorus Taken: 0.02 g.
Normality of Thiosulphate: N/30

Expt. No.	Concentration of KBr—$KBrO_3$ Mixture	Mean $K\times10^3$
1	N/35	4.0
2	N/40	2.9
3	N/45	2.1
4	N/50	1.2

Fig. 1 represents graphically the variation of $\log_{10}\frac{C_t(C_o-C_\infty)}{C_o(C_t-C_\infty)}$ with time for different concentrations of the oxidant (bromide-bromate mixture) at the same temperature.

The temperature coefficient and energy of activation were calculated from the values obtained for K at different temperatures T_1 and T_2 and are given below:

TABLE IV

Temp. T_1—T_2	K_1	K_2	Temp. Coeff. K_2/K_1	Energy of Activation/g. kcal.
278-288	2.0	3.1	1.56	7.00
283-293	2.4	3.87	1.60	7.78

The variation of $\log_{10}K$ with $1/T$ is shown in Table V; the results are plotted in Fig. 3.

TABLE V

Temperature Absolute $T°$	$1/T\times10^3$	$K\times10^3$	$\log_{10}K\times10^3$
278	3.59	2.0	0.3010
283	3.53	2.4	0.3802
288	3.47	3.1	0.4914
293	3.41	3.87	0.5877

The linear relationship between $\log_{10}K$ and $1/T$ (Fig. 3) is in accord with the Arrhenius equation[4] which expresses the influence of temperature on reaction velocity.

Bromometric Determination of Red Phosphorus

A series of experiments was carried out in which the difference in the quantity of bromide-bromate mixture added initially

4) S. Arrhenius, *Z. Phys. Chem.* **4**, 226 (1889); *Trans. Farad Soc.*, **33**, 72 (1937).

to a given weight of phosphorus and that left over after its complete disappearance i.e. the titre value at infinite time served as a measure of the quantity of bromide-bromate mixture required for the oxidation reaction. Hence a knowledge of the quantity of bromide-bromate mixture utilized in the reaction is useful for the direct determination of red phosphorus bromometrically. A typical set of results of such determinations are given in Table VI.

TABLE VI

Wt. of P Taken g.	Wt. of P Calculated* g.	Difference in g.
0.018	0.01788	−0.00012
0.015	0.01488	−0.00012
0.028	0.02772	−0.00028
0.017	0.01693	−0.00003
0.029	0.02909	+0.00009
0.018	0.01788	−0.00012
0.032	0.03208	+0.00008
0.023	0.02272	−0.00028
0.020	0.01983	−0.00013

* Weight of P calculated from reacted bromine according to the equations:

$$5Br^- + BrO_3^- + 6H^+ = 3Br_2 3H_2O$$

and $$2P + 5Br_2 + 8H_2O = 12H^+ + 10Br^- + 2H_2PO_4^-$$

Mechanism of the Reaction

Since the interaction of bromide-bromate mixture is instantaneous and complete

$$5Br^- + BrO_3^- + 6H^+ = 3Br_2 + 3H_2O$$

bromine is quantitatively liberated. This bromine oxidizes phosphorus to phosphoric acid according as

$$2P + 3Br_2 + 6H_2O = 6H^+ + 6Br^- + 2H_3PO_3$$

$$H_3PO_3 + Br_2 + H_2O = 3H^+ + 2Br^- + H_2PO_4^-$$

The former reaction is quite rapid, whereas the tatter one is slow and depends on the H^+ ion concentration. It appears that the oxidation of phosphorus acid by bromine (obtained from acid bromide-bromate mixture) determines the rate of reaction as a whole.

Summary

Bromometric oxidation of red phosphorus using an acid solution of bromide-bromate mixture has been studied and applied in the volumetric determination of red phosphorus. The kinetics of the oxidation process show that the reaction is of the second order. The influence of temperature and concentration of the reactants, have been investigated and the energy of activation calculated. Further the applicability of this procedure for a bromometric determination of red phosphorus is emphasized and such determinations can be carried out over a period of three to four hours.

The grateful thanks of the authors are due to Prof. S. S. Joshi for facilities and for his kind interest in the work.

Department of Chemistry, Banaras Hindu University, India

Interaction between Surface Active Agents and Proteins. IV. Heat of Interaction of Sodium Dodecyl Sulfate and Egg Albumin

By Koichiro AOKI* and Yasushi SUZUKI

(Received January 11, 1956)

Introduction

As previously described[1], we studied electrophoretically the sodium dodecyl sulfate (SDS) and egg albumin system at points of higher pH's than that of the isoelectric point of egg albumin. In that study it was concluded that SDS-egg albumin complexes were formed in the following way at pH 6.8: When the weight mixing ratio albumin/SDS was between 100/0 and 80/20 the composition of the complex was AD_n (n=40), and when the mixing ratio albumin/SDS was between 80/20 and 35/65 the composition of the complex changed continuously from AD_n to the completion of AD_{8n}.

In the present study we measured the temperature change occurring when SDS

* Present temporary address: Department of Chemistry, Purdue University, Lafayette, Indiana, U. S. A.

1) K. Aoki, This bulletin **29**, 369 (1956).

and egg albumin solutions were mixed at the same condition as in the above electrophoretic study and calculated the heat of interaction.

Experimental

The apparatus is shown in Fig. 1[2]. Experiments were carried out in a thermostat at 25± 0.001°C. Because very slight temperature changes accompanied the reaction, 10-junction of copper-constantan thermocouple and a galvanometer of high sensitivity were used to trace the temperature change[3,4]. We found that the sensitivity of the apparatus we assembled was such that a 1 mm movement of the needle on the lamp scale corresponded to 0.0006°C. The reaction vessel was unsilvered Dewar flask, the volume of which was about 120 cc. and the water equivalent 93.0 cal.*

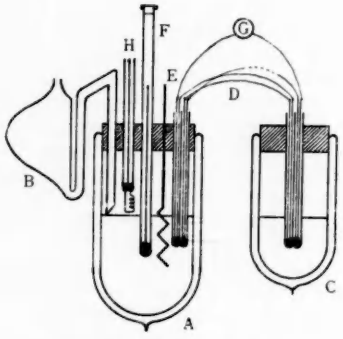

Fig. 1. Apparatus.

A. Reaction vessel.
B. Vessel for warming SDS solution.
C. Vessel for holding one end of thermocouple.
D. 10-junction of copper-constantan thermocouple.
E. Stirrer.
F. Beckmann thermometer.
G. Galvanometer.
H. Platinum wire.

The buffer solution used was pH 6.8 and ionic strength 0.10. Into a reaction vessel A, 50 cc. of 1.00% buffered albumin solution was put. Fifty cc. of buffered SDS solution varying in concentration were put into another vessel B. Then we let these two solutions stand in the thermostat for about ten hours to make them aquire the temperature of the thermostat. After that they were mixed, and at the same time we began to measure the temperature change which accompanied the reaction.

In addition, we measured the heat of dilution of albumin and of SDS. We put 50 cc. of buffered albumin solution or buffered SDS solution into reaction vessel A and put the same amount of buffer solution into vessel B. We measured the temperature change occurring when albumin or SDS solution was diluted to twice the original volume by pouring the solution in vessel B into vessel A.

Results

Heat was generated when SDS or albumin solution was diluted with the buffer. Fig. 2 shows a typical run of the temperature change occurring when albumin and SDS solutions were diluted. Considering the maximum value of this curve to be the amount of heat generated, the following values were obtained for the heats of dilution:

SDS	1.2 cal./g.
egg albumin	0.8 cal./g.

These are the values obtained when the solutions, the concentrations of which were less than 1.00%, were diluted to twice their original volumes.

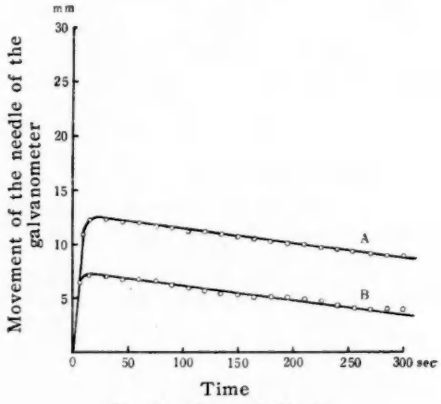

Fig. 2. Heat of dilution.

A: Heat generated when 1.00% buffered SDS solution was diluted to twice its original volume.
B: Heat generated when 1.00% buffered albumin solution was diluted to twice its original volume.

Hutchinson et. al.[5] measured accurately the heats of dissolution of sodium alkyl sulfates. Using their data, we can calculate the heat produced when 0.050M (1.30%) aqueous sodium decyl sulfate solution is diluted to 0.025 M (0.65 %) at 25.00°C. The value is found to be 1.0 cal./g. Our values of the heat of dilution are considered reasonable when compared with this value.

Heat was instantly generated when SDS and egg albumin solutions were mixed. Fig. 3 shows

2) E. Suito, *Rev. Phys. Chem. Japan*, **13**, 74 (1939).
3) N. H. Ray. *Trans. Faraday Soc.*, **48**, 809 (1952).
4) J. Osugi and K. Hiromi, *Rev. Phys. Chem. Japan.* **22**, 76 (1952).
* The experimental procedure to find this value was the same as used by E. Suito[2].

5) E. Hutchinson, K. E. Manchester and L. Winslow, *J. Phys Chem.*, **58**, 1124 (1954).

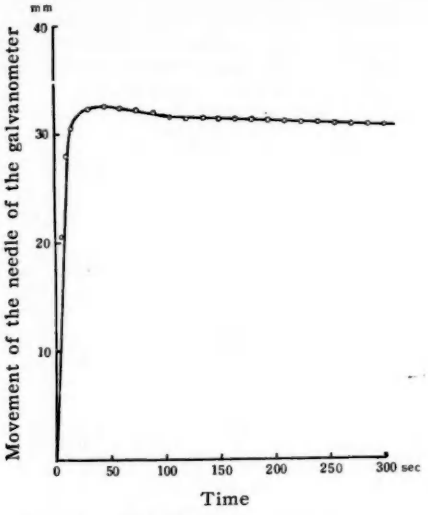

Fig. 3. Heat of reaction.
Heat produced when 1.00% SDS solution and 1.00% albumin solution were mixed.

one tracing of the temperature change with time. Taking the maximum value of this curve as the total heat produced, we deducted from this maximum value the heat of dilution of egg albumin and that of SDS, to obtain the value of the heat of the reaction itself. As the amount of SDS used was different in each experiment, the value of the heat of dilution of SDS to be deducted was calculated proportionally using the value of 1.2 cal./g.

In this study the concentration of egg albumin was kept constant at 1.00%. Each of the SDS solutions varying in concentration from 0.05% to 1.00% was mixed with this egg albumin solution. Thus we obtained the relation between the mixing ratio albumin/SDS and the heat evolved. The results are shown in Fig. 4. In these experiments any error in measuring the heat produced is within ±0.2 cal.

Discussion

It was concluded from the electrophoretic experiment that SDS and egg albumin did not combine in the same way above and below the mixing ratio albumin/SDS=80/20, that is, the composition of the complex was constant when the mixing ratio albumin/SDS was between 100/0 and 80/20, while it changed continuously in the region from 80/20 to 35/65[5]. Referring to the result, we assume that the curve *abc* in Fig. 4 consists of two straight lines *ab* and *bc*, which change the slope near the point albumin/SDS=80/20.

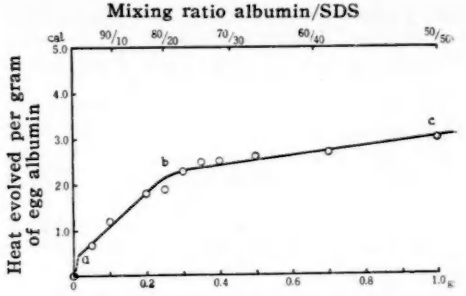

Fig. 4. Relation between mixing ratio albumin/SDS and heat of reaction.

Recently, Hill[6] observed by equilibrium dialysis that after one mole of anionic detergent* combined with one mole of egg albumin, another kind of interaction took place. Considering his results SDS and egg albumin may combine in a different way also above and below the mixing ratio albumin/SDS=99.4/0.6. Here the molecular weight of egg albumin and of SDS was assumed to be 46,000 and 288, respectively. When *ba* in Fig. 4 is extended to the left, it does not pass the origin. This may be fact which corresponds to the above Hill's observation.

In the region where the mixing ratio albumin/SDS is between 100/0, or more precisely 99.4/0.6, and 80/20, 40 molecules of SDS are bound to one egg albumin molecule. Using the molecular weights cited above, the following equation is obtained from the slope of the straight line *ab*.

$$\text{Egg albumin} + 40\,\text{SDS} = \text{Complex} + 92.1\,\text{kcal.}$$

or

$$-\Delta H = 92.1\,\text{kcal./mol. albumin} = 2.3\,\text{kcal./mol. SDS}$$

If we assume that one NH_3^+ radical on the egg albumin molecule reacts with one OSO_3^- radical of SDS within this mixing ratio, we can rewrite the above equation as

$$\cdots NH_3^+ + \cdots OSO_3^- = \text{Complex} + 2.3\,\text{kcal.}$$

This value of heat of reaction is far smaller than that of the heat of neutralization between strong acid and strong base, 13.7 kcal./mol. (at about 30°C).

In the range where the mixing ratio albumin/SDS is between 80/20 and 35/65,

6) R. M. Hill, Ph. D. Thesis, University of Minnesota, 1955.

* He used sodium-*n*-octylbenzene-*p*-sulfonate.

the following equation is obtained from the slope of the straight line *bc*.

$$\text{Complex}+\text{SDS}=\text{Complex}'+0.3\,\text{kcal}.$$

The values of the heat of interaction obtained in this study are of the same order as those found by Goddard and Pethica[7] in the bovine serum-albumin-SDS system.

The CMC (critical micelle concentration) of SDS is 0.04% (0.0013 mol./l.) in a buffer solution of ionic strength 0.10[8]. Thus when 1.00% albumin solution and 0.05% SDS solution are mixed, the concentration of SDS is above the CMC before mixing and below it after mixing. When they are mixed, there should be an adsorption of heat owing to the decomposition of the micelle. Goddard and Benson[9] calculated the heat of micelle formation of SDS to be ca. 0.1 kcal./mol. SDS at 25°C, using their data and the assumption of Hutchinson et. al.[5] The amount of SDS used at this mixing ratio was so small, 0.05 g. (0.002 mol.), that such a small quantity of heat could not be measured.

7) E. D. Goddard and B. A. Pethica, *J. Chem. Soc.*, **1951**, 2659.
8) K. Aoki and J. Hori, This bulletin, **29**. 104 (1956).
9) E. D. Goddard and G. C. Benson, *Trans. Faraday Soc.*, **52**, 409 (1956).

Summary

We measured the heat evolved when egg albumin and SDS solutions were mixed at pH 6.8 and at 25.00°C, and calculated the heat of interaction.

The authors wish to express their sincere thanks to Prof. R. Goto of Kyoto University for his kind encouragement throughout this work, and to Prof. J. F. Foster of Purdue University for information about Dr. Hill's thesis. The cost of this work has been partially covered by a Research Grant from the Ministry of Education.

Chemistry Laboratory, Nagoya City University, Nagoya

*Studies on Azeotropic Mixtures. II. Constancy of Molecular Interchange Energies in Homologous Azeotropic Series and Calculation of Azeotrope-forming Range**

By Toshio YOSHIMOTO and Yo-ichiro MASHIKO

(Received September 25, 1956)

Introduction

Reflecting the importance of azeotrope formation in the distillation process, a great number of experimental data have been accumulated in recent times[1]. Also, several independent correlation rules of azeotropic data have been proposed on the practical side[2]. They are, however, all empirical and it appears difficult to find out the physical basis from any of them or to derive the one from the other without any additional assumptions. The following is an attempt to correlate binarily azeotropic data by a method with explicit representation of interaction energies of component molecules.

Recently Prigogine[3] has presented a similar method of correlating azeotropic

* Partly Presented at the 9th Annual Meeting of the Chemical Society of Japan held in Kyoto, April, 1956.

1) L. H. Horsley, "Azeotropic Data", American Chemical Society (1952); F. D. Rossini, B. J. Mair and A. J. Streiff, "Hydrocarbons from Petroleum", Reinhold (1952), p. 88; L.H. Horsley, *Anal. Chem.*, **19**, 508 (1947); **21** 831 (1949); Lange, "Handbook of Chemistry", 5th ed., Handbook Publishers (1944); Ewell, Harrison and Berg, *Petroleum Engr.*, **16** 219, 255, 259 (1944); "Chemical Engineers' Handbook" 2nd ed., McGraw-Hill (1941); "International Critical Tables" Vol.3 McGraw-Hill (1928); M. Lecat, "La tension de vapeur des mélanges des liquides. L'Azéotropisme", Lamertin, Brussels (1918).

2) M. Lecat, *Z. anorg. u. allgem. Chem.*, **186**, 123 (1930); H. Skolnik, *Ind. Eng. Chem.*, **40**, 442 (1948); H. P. Meissner and S. H. Greenfeld, ibid., **40**, 438 (1948); R. L. Denyer, F. A. Fidler and R. A. Lowry, ibid., **41**, 2727 (1949); D. H. Desty and F. A. Fidler, ibid., **43**, 905 (1951); L. H. Horsley, *Anal. Chem.*, **19**, 603 (1947).

3) I. Prigogine and R. Defay, "Chemical Thermodynamics", (Translated by D. H. Everett), Longmans (1954), Chapt. XXVIII.

data that is very satisfactory also from our standpoint. As has been mentioned in part I[4], our standpoint is, however, a little different from that of Prigogine in that we are always considering the phenomenon from the molecular point of view, i. e., using the explicit form of the molecular interchange energy.

Graphical Method of Correlating Azeotropic Data

It has been shown in part I[4] that the azeotrope-forming power of many binary solutions could be estimated by molecular interchange energies w which were calculated from

$$\Delta_v S_1^0(T_1^0 - T^a) = Nwx_2^2 \quad (1)$$

and

$$\Delta_v S_2^0(T_2^0 - T^a) = Nwx_1^2, \quad (2)$$

where T^a is the azeotropic point (for $p=1$ atm.), N the Avogadro number and $\Delta_v S_i^0$ the molar entropy of vaporization at boiling point (for $p=1$ atm.) of ith pure component. ($i=1$ and 2).

Here, w is expressed, based on the quasi-crystalline model of the solution, as

$$w = \frac{z}{2}(\varepsilon_{11} + \varepsilon_{22} - 2\varepsilon_{12}),$$

where z is the average coordination number of the quasi-lattice and ε's are all the absolute average potential energies of molecular pairs. Equations (1) and (2) have only one unknown parameter w, all others being known from experiment.

Trouton proposed the celebrated rule that the entropy of vaporization is the same for all liquids[5]. A glance at the entropies of vaporization (for $p=1$ atm.) given in literature[6] shows, however, that the rule applies only roughly, and departs seriously from the truth if the liquids are "abnormal". Nevertheless, the rule appears to stand, to some degree, for members of homologous series if the liquids are not so highly associated. This condition will accordingly make it possible to apply invariably the equations (1) and (2) to the azeotropes formed by a fixed azeotropic reagent (or azeotrope former) with a series of homologues, if w_s are nearly the same for the series of azeotropes. Thus, if these allowances are made, we can expect straight-line relationships between $T_i^0 - T^a$ and x_i^2 for the series.

In the following, we have examined the relationship on a number of series by taking the known values of the thermodynamic quantities appearing in equations (1) and (2). In most cases, however, because of lack of data, an appropriate value of $\Delta_v S_1^0$ for the series is assumed from the known values for a few members of the series.

In each case two kinds of plots, that is, first $T_2^0 - T^a$ against x_1^2 and second $T_1^0 - T^a$ against x_2^2 are presented. For each case the second component 2 is a fixed azeotropic reagent and the first components 1 are homologous members. Examples taken are arranged into four classes according to the different types of intermolecular forces as in part I.

(a) Dispersion Force Solutions

Examples taken are azeotropes of toluene with paraffinic and naphthenic hydrocarbons. They form always minimum type azeotropes[4] (A, Fig. 1).

(b) Solutions Involving Addition Compounds

Examples taken are azeotropes of bromodichloromethane with "donor type" liquids such as ketones and esters. They form always maximum type azeotropes[4] (B, Fig. 2).

(c) Solutions Involving Associations in Non-polar Solvents

This class involves most of the useful azeotropes, since they have the largest azeotrope-forming powers among four classes. The following nine series are taken as examples.

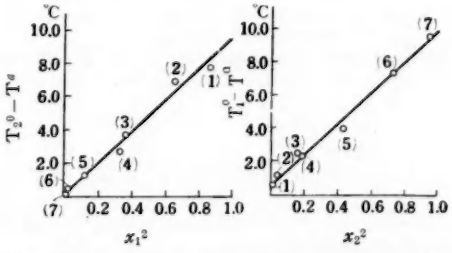

Fig. 1. The plots of toluene azeotropes with aliphatic hydrocarbons.
Aliphatic hydrocarbons (A): (1), ethylcyclopentane; (2), 1,1,3-trimethylcyclopentane; (3), 2,5-dimethylhexane; (4), *cis-trans-cis*-1,2,4-trimethylcyclopentane; (5), 2,3,4-trimethylpentane; (6), 2-methylheptane; (7), *cis*-1,3-dimethylcyclohexane.

4) T. Yoshimoto and Y. Mashiko, This Bulletin, **29**, 990 (1956).
5) F. Trouton, *Phil. Mag.* (5), **18**, 54 (1884).
6) "International Critical Table", Vol. V (1929).

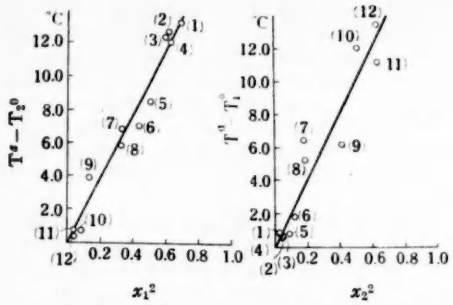

Fig. 2. The plots of bromodichloromethane azeotropes with " donor type liquids ".
Donor liquids (B): (1), methyl butyrate; (2), 2-pentanone; (3), 3-pentanone; (4), propyl acetate; (5), isobutyl formate; (6), 3-methyl-2-butanone; (7), *n*-propyl ether; (8), isopropyl acetate; (9), diethoxymethane; (10), propyl formate; (11), 2-butanone; (12), ethyl acetate.

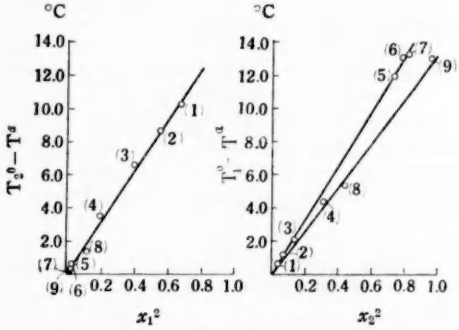

Fig. 3. The plots of 1-propanethiol azeotropes with paraffinic and naphthenic hydrocarbons.
Paraffinic hydrocarbons (C): (1), 2,3-dimethylbutane; (2), 2-methylpentane; (3), 3-methylpentane; (4), *n*-hexane; (5), 2,2-dimethylpentane; (6), 2,4-dimethylpentane; (7), 2,2,3-trimethylbutane.
Naphthenic hydrocarbons(D): (8), methylcyclopentane; (9), cyclohexane.

1-Propanethiol
—Paraffinic Hydrocarbons (C, Fig. 3)
1-Propanethiol
—Naphthenic Hydrocarbons (D, Fig. 3)
1-Butanethiol
—Paraffinic Hydrocarbons (E, Fig. 4)
1-Butanethiol
—Naphthenic Hydrocarbons (F, Fig. 4)
1,2-Benzenediol
—Aromatic Hydrocarbons (G, Fig. 5)
1,3-Benzenediol
—Aromatic Hydrocarbons (H, Fig. 6)

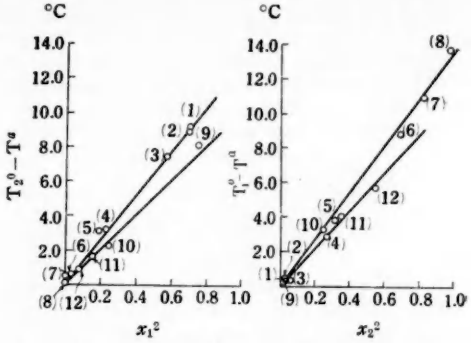

Fig. 4. The plots of 1-butanethiol azeotropes with paraffinic and naphthenic hydrocarbons.
Paraffinic hydrocarbons (E): (1), 2,3-dimethylpentane; (2), 2-methylhexane; (3), 3-methylhexane; (4), *n*-heptane; (5), 2,2,4-trimethylpentane; (6), 2,2-dimethylhexane; (7), 2,5-dimethylhexane; (8), 3,3-dimethylhexane.
Naphthenic hydrocarbones (F): (9), *trans*-1,3-dimethylcyclopentane; (10), *cis*-1,2-dimethylcyclopentane; (11), methylcyclohexane; (12), ethylcyclopentane.

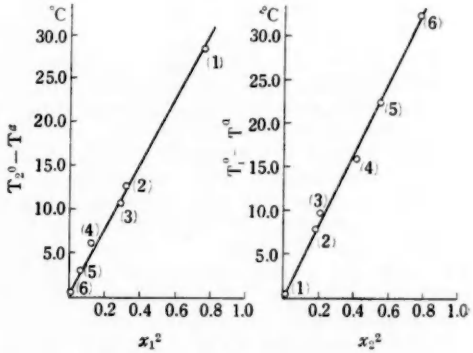

Fig. 5. The plots of 1,2-benzenediol azeotropes with aromatic hydrocarbons.
Aromatic hydrocarbons (G): (1), naphthalene; (2), 2-methylnaphthalene; (3), 1-methylnaphthalene; (4), biphenyl; (5), diphenyl methane, (6), acenaphthene.

Nitromethane
—Aliphatic Hydrocarbons (I, Fig. 7)
Nitromethane
—Aromatic Hydrocarbons (J, Fig. 7)
Methanol
—Paraffinic Hydrocarbons (K, Fig. 8)

The last involves highly associated liquid that is apparently not to be regarded as a component of regular solutions even at azeotropic points[4].

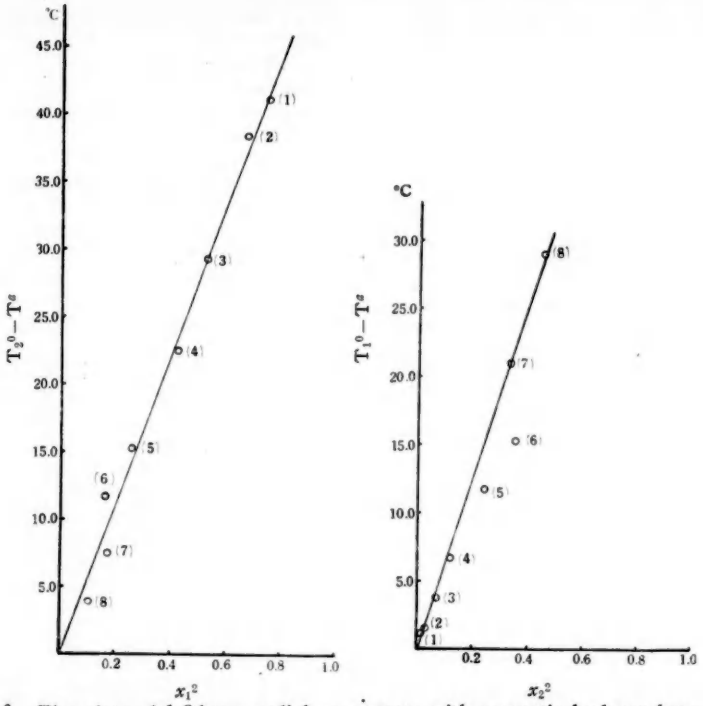

Fig. 6. The plots of 1,3-benzenediol azeotropes with aromatic hydrocarbons.
Aromatic hydrocarbons (H): (1), 2-methylnaphthalene; (2), 1-methylnaphthalene; (3), biphenyl; (4), diphenyl methane; (5), acenaphthene; (6), 1,2-diphenylethane; (7), fluorene; (8), *trans*-stilbene.

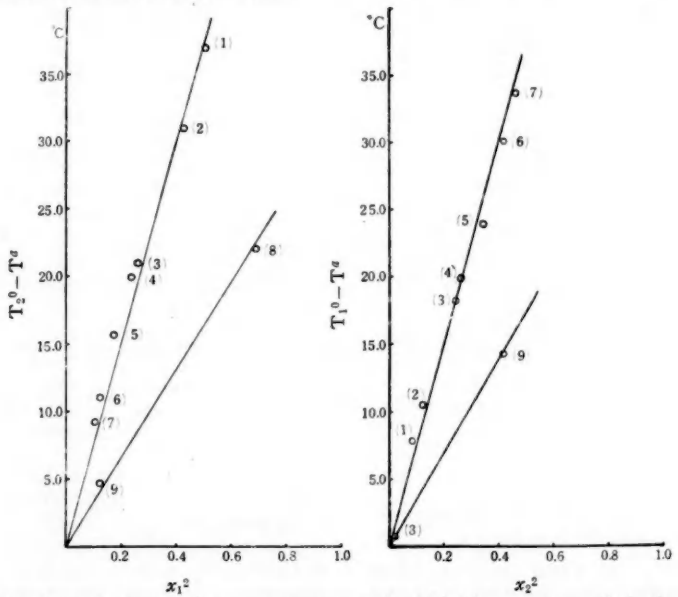

Fig. 7. The plots of nitromethane azeotropes with aliphatic and aromatic hydrocarbons.
Aliphatic hydrocarbons (I): (1), methylcyclopentane; (2), cyclohexane; (3), *n*-heptane; (4), methylcyclohexane; (5), 2,5-dimethylhexane; (6), 1,3-dimethylcyclohexane; (7), *n*-octane. Aromatic hydrocarbons (J): (8), benzene; (9), toluene.

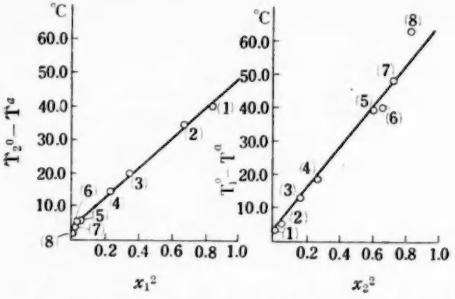

Fig. 8. The plots of methanol azeotropes with paraffinic hydrocarbons.
Paraffinic hydrocarbons (K): (1), isopentane; (2), *n*-pentane; (3), 2,3-dimethylbutane; (4), *n*-hexane; (5), *n*-heptane; (6), 2,2,4-trimethylpentane; (7), 2,5-dimethylhexane; (8), *n*-octane.

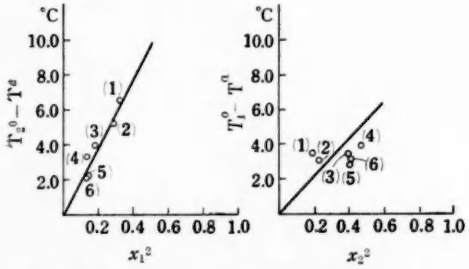

Fig. 9. The plots of nitromethane azeotropes with ketones and esters.
Ketones and esters (L): (1), butyl formate; (2), ethyl propionate; (3), propyl acetate; (4), methyl butyrate; (5), 3-pentanone; (6), 2-pentanone.

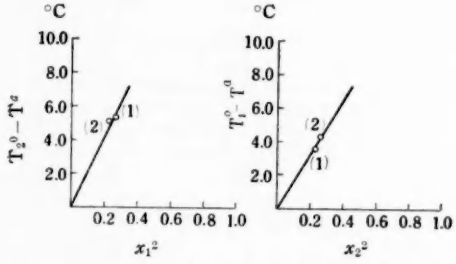

Fig. 10. The plots of acetonitrile azeotropes with esters.
Esters (M): (1), methyl propionate; (2), propyl formate.

(d) Solutions Involving Associations in Polar Solvents

Azeotropes in this class have smaller azeotrope-forming powers and involve more complicated interaction of component molecules than those in class (c).

Examples taken are as follows.
Nitromethane
—Ketones and Esters (L, Fig. 9)
Acetonitrile—Esters (M, Fig. 10)

In general the straight-line relationship is observed satisfactorily in every plot except the series which involves special molecular interactions such as in class (b) and (d). Furthermore, as shown in Table I, the slopes of two independent plots that involve $T_1^0 - T^a$ and x_2^2 on the one hand, and $T_2^0 - T^a$ and x_1^2 on the other are approximately equal when devided by $\Delta_v S_1^0$ and $\Delta_v S_2^0$ respectively. This leads to a conclusion from equations (1) and (2) that the molecular interchange energy w of azeotropes, which are formed between a fixed azeotropic reagent and members of a homologous series, is characteristic of the series in many cases and therefore regarded as azeotrope-forming power of a series of azeotropic mixtures. The new correlation thus introduced from equations (1) and (2) is considered to be essential to compare azeotrope-forming powers of a number of solutions.

TABLE I

MOLECULAR INTERCHANGE ENERGIES CALCULATED FROM THE SLOPES OF TWO KINDS OF PLOTS

Azeotropic[a] Series	$N\omega_1$ (kcal./M)	$N\omega_2$ (kcal./M)	$\Delta_v S_1^0$[b] (cal./M°C)	$\Delta_v S_2^0$[b] (cal./M°C)
A	190	200	(20.3)	20.8
B	−450	−430	(22.0)	21.0
C	340	340	(20.3)	(22.0)
D	270	—	(20.4)	—
E	280	280	(20.3)	(22.0)
F	230	230	(20.3)	(22.0)
G	850	850	(20.3)	(22.5)
H	1300	1300	(20.3)	(23.5)
I	1560	1630	(20.3)	22.1
J	710	730	20.8	22.1
K	1170	1140	(20.3)	25.0
L	Diffuse	420	—	22.1
M	360	420	(22.0)	20.2

a) Azeotropic data are all taken from Horsley's "Azeotropic Data"[1].
b) Values taken from "International Critical Table" Vol. V (1929). Values enclosed in parentheses are assumed ones.

Here, it should be mentioned from the view-point of our approximation[4] that as x_2 approaches to 0 in $(T_1^0 - T^a) - x_2^2$ plots and x_1 to 0 in $(T_2^0 - T^a) - x_1^2$ plots, the error of the above approximation will be considerable. In fact, the error in the plots of methanol-paraffins series is remarkable as shown in Fig. 8, while it is con-

sidered to be small in other series according to the results so far obtained. The $(T_1^0-T^a)-x_2^2$ plots in toluene-hydrocarbons series does not pass through the origin (Fig. 1). The cause of this abnormality is uncertain and will be left to the further study.

Azeotrope-forming Range

From equations (1) and (2) we obtain maximum boiling point $T_1^{0\max}$ and minimum boiling point $T_1^{0\min}$ of pure component 1 that can form azeotropes with component 2 as follows.

If $w>0$, we have

$$T_1^{0\max}=T_2^0+\frac{Nw}{\Delta_v S_1^0} \tag{3}$$

and

$$T_1^{0\min}=T_2^0-\frac{Nw}{\Delta_v S_2^0}. \tag{4}$$

If $w<0$, we have

$$T_1^{0\max}=T_2^0+\frac{Nw}{\Delta_v S_2^0} \tag{5}$$

and

$$T_1^{0\min}=T_2^0-\frac{Nw}{\Delta_v S_1^0}. \tag{6}$$

Graphically the intercepts of the lines with the ordinate at $x_2^2=1$ in $(T_1^0-T^a)-x_2^2$ plots and at $x_1^2=1$ in $(T_2^0-T^a)-x_1^2$ plots give respectively $T_1^{0\max}$ and $T_1^{0\min}$ (see Figs. 1–10). The difference between maximum and minimum boiling points give therefore the boiling point range, over which azeotrope formation is allowable for the series. Denyer et al.[7] and Swietoslawsky[8] regarded azeotrope-forming range, $T_1^{0\max}-T_1^{0\min}$, as a measure of the azeotrope forming powers of a given azeotropic series. We have for this range, with explicit representation of w, from (3) and (4) or (5) and (6),

$$T_1^{0\max}-T_1^{0\min}=Nw\left(\frac{1}{\Delta_v S_1^0}+\frac{1}{\Delta_v S_2^0}\right). \tag{7}$$

$T_1^{0\max}$ and $T_1^{0\min}$ are calculated from w's which are obtained from the slopes of plots in Figs. 3 and 4, and are presented in Table II along with those obtained from Denyer's and Skolnik's[9] plots. The agreement is excellent. Denyer's and Skolnik's azeotropic ranges are considered to be slightly different in their physical meaning, though the difference will be trivial whenever w is small as will be shown later.

TABLE II

COMPARISON OF T_1^{0} max AND T_1^{0} min CALCULATED BY THREE METHODS

Azeotropic Series	This work		Denyer's		Skolnik's
	T_1^{0} max (°C)	T_1^{0} min (°C)	T_1^{0} max (°C)	T_1^{0} min (°C)	T_1^{0} max (°C)
C	85	52	84	52	83.5
E	112	86	112	85	112

Conclusion

Applying Trouton's rule to a homologous series, the constancy of molecular interchange energy w for azeotropes composed of a fixed component and the series is exemplified in a number of cases. The fundamental equations derived in part I is thus proved to be useful in correlating azeotropic data. Also maximum and minimum boiling points of components in a homologous azeotropic series are derived and values calculated are compared with those obtained by other methods.

Government Chemical Industrial Research Institute, Tokyo

7) R. L. Denyer, F. A. Fidler and R. A. Lowry, *Ind Eng. Chem.*, **41**, 2727 (1949); D. H. Desty and F. A. Fidler, ibid., **43**, 905 (1951).

8) W. Swietoslawsky, *Prezemyl. Chem.*, **1**, 363 (1951).

9) H. Skolnik, *Ind. Eng. Chem.*, **40**, 442(1948).

A Refinement of the Crystal Structure of Tropolone Hydrochloride

By Yoshio SASADA and Isamu NITTA

(Received September 27, 1956)

Introduction

Previously we have reported the crystal structure of tropolone hydrochloride as an example of successful application of the inequality method[1]. Owing to the following two reasons we had for a time to abandon further refinements of the structure: (i) The crystals are considerably hygroscopic and unstable. Even the specimens sealed in the borosilicate capillaries were decomposed in summertime, giving Debye-Scherrer patterns together with single crystal reflexions of this compound. (ii) Crystals with suitable form were rather few and much of them were twinned. Therefore it was impossible to obtain reliable data for the general (*hkl*) reflexions except for (0*kl*). Thus we had to be contented with the approximate crystal structure described in the previous paper.

On the other hand, we have investigated the crystal structure of sodium tropolonate by means of (F_o-F_c) and three-dimensional Fourier techniques and obtained very accurate molecular dimensions together with approximate positions of hydrogen atoms and some knowledge of anisotropic thermal vibrations[2].

As emphasized in the previous papers[1,2], the comparative determinations of accurate structures of tropolone, its anion and cation are very interesting problems of the structural chemistry of tropolone derivatives. Moreover it will be significant in the case of cation to determine, if possible, directly the positions of hydrogen atoms attached to oxygen, which were supposed to be somewhere between O and Cl atoms. Such situations made us hope to re-investigate the crystal structure of hydrochloride. Fortunately, at this time Nozoe and his collaborators brought us suitable specimens of this compound and we have been able to find non-twinned crystals among them. This account will describe the refinement of the structure based on new sets of three-dimensional data obtained from integrated Weissenberg photographs with multiple-film technique, the main features of the structure, of course, being unchanged.

Crystal Data and Intensity Measurement

Crystals were obtained from ethanol-ether solution saturated with hydrogen chloride gas as white needles[3], elongated in the *a* axis direction.

Crystallographic and physical data obtained are:

Tropolone hydrochloride $C_7H_7O_2Cl$: m. p. 125–130°C, monoclinic,

$$a=4.71\pm0.02\,\text{Å},\quad b=18.01\pm0.03\,\text{Å},$$
$$c=8.56\pm0.03\,\text{Å},\quad \beta=98.2°\pm0.5°.$$

Absent spectra: (*h*0*l*) when *l* is odd, (0*k*0) when *k* is odd. Space group $P2_1/c$. Four formula units per cell. Volume of unit cell=718 Å^3.

Density (by floatation)=1.43,

Density (calc.)=1.47 g.cm^{-3}.

Linear absorption coefficient for Cu K_α radiation, $\mu=42.0\,\text{cm}^{-1}$. Total number of electrons per unit cell, $F(000)=328$.

These cell dimensions slightly differ from those reported in the previous paper[1]. The differences are mainly due to low accuracy of previous value of β.

In order to refine the atomic coordinates and to reveal the positions of hydrogen atoms by (F_o-F_c) syntheses, it is necessary to use considerably accurate intensity data. Two complete sets of relative intensities for (0*kl*), (1*kl*), (2*kl*) and (3*kl*) were obtained by the integrated Weissenberg procedures. The specimens used have the following maximum and minimum dimensions at right angle to the axis of rotation:

Crystal 1: 0.04×0.02; Crystal 2: 0.03×0.02cm.

Intensities were estimated by visual comparison with the calibrated scale. The multiple-film technique was used to correlate strong and weak reflexions, ranging in relative intensities from 6000 to 1 for (0*kl*) zone. The corrections for absorption were made in the usual way only for (0*kl*). The values of structure factors used in the following analysis are the weighted means of the values in the above-mentioned two sets. Reflexions from 150 planes were observed out of 186 possible (0*kl*)'s and 458 out of 995 (*hkl*)'s.

Refinement of Atomic Coordinates and Location of the Hydrogen Atoms.

Starting from the approximate structure

1) Y. Sasada, K. Osaki and I. Nitta, *Acta Cryst.* **7**, 113, (1954).

2) Y. Sasada and I. Nitta, ibid., **9**, 205 (1956).

3) T. Nozoe, S. Seto, T. Mukai. K. Yamane and A. Matsukuma, *Proc. Japan Acad.*, **27**, 224 (1951).

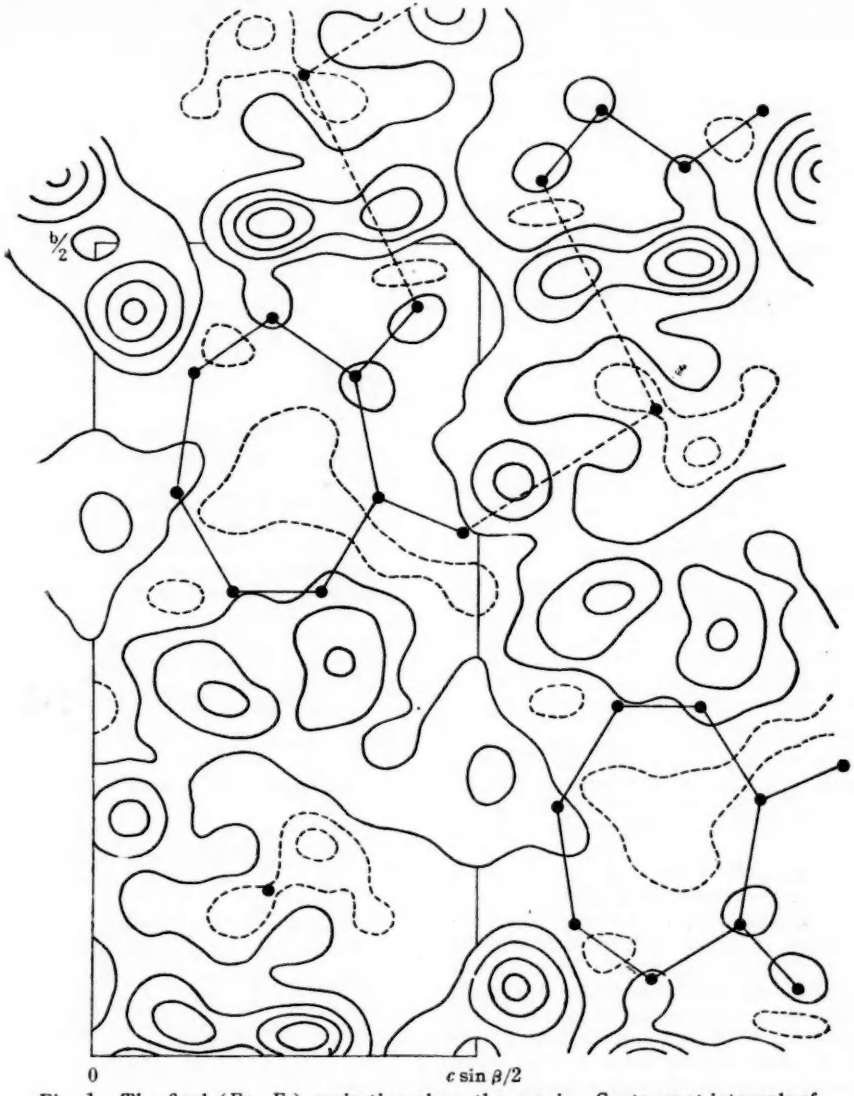

Fig. 1. The final ($Fo-Fc$) projection along the a axis. Contours at intervals of 0.2 eÅ^{-2} with the lowest solid contour at ±0.2 eÅ^{-2}.

projected along the a axis mentioned in the previous paper[3], (at this stage the value of $R=\Sigma||F_o|-|F_c||/\Sigma|F_o|$ was 0.168, unobserved reflexions being omitted), successive refinements by (F_o-F_c) syntheses were made[4]. In the structure-factor calculation, the atomic scattering factors were taken from McWeeny[5], using for oxygen $\bar{f}_0=\frac{1}{3}(f^{\parallel}+2f^{\perp})$, and for carbon the values for 'valence states'.

It was observed from the ($\rho_o-\rho_c$) maps that the thermal vibration of chlorine ion was considerably anisotropic. Consequently scattering factor of form, $f=f_0\exp[-\{\alpha+\beta\sin^2(\varphi-\psi_c)\}(\sin\theta/\lambda)^2]$ were employed[4,6] for this atom, where α and β

4) W. Cochran, *Acta Cryst.*, **4**, 81 (1951).
5) R. McWeeny, ibid., **4**, 513 (1951).
6) E. W. Hughes, *J. Am. Chem. Soc.*, **63**, 1737 (1941).

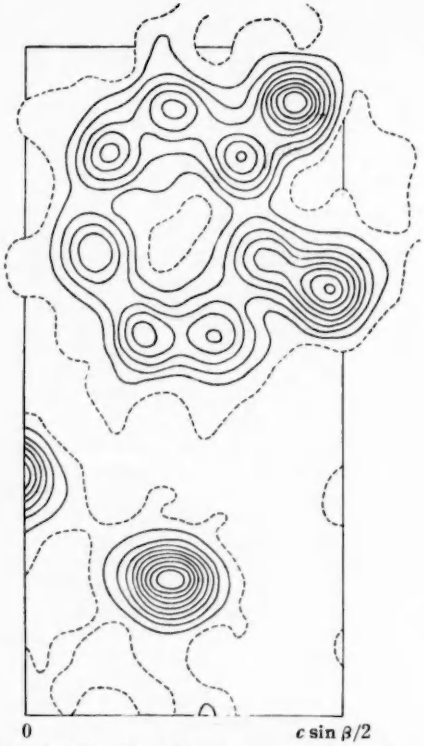

Fig. 2. The final Fourier projection of the electron density along the a axis.
Contours at intervals of 2Å^{-2} for chlorine and those at intervals of $1\,\text{eÅ}^{-2}$ for the other atoms. Contour at $1\,\text{eÅ}^{-2}$ is broken.

are constants, ψ_c is the angle between the direction of maximum vibration and the c axis, and $(2\sin\theta, \varphi)$ are the polar coordinates of a point in the $(0kl)$ section of the reciprocal lattice, measured from the b^* axis. In the projection it should be noted that only two chlorine ions are equivalent in relation to anisotropic vibrations. As thermal motions of the other atoms were not significantly anisotropic, ordinary B factors were applied. The assignments of these thermal constants proceeded simultaneously with the refinement of atomic coordinates. (The detailed procedures will be shown elswhere[7].) The best thermal factors deduced from the seventh $(\rho_o-\rho_c)$ map were:

B=5.55 for oxygen, 5.15 for C_1 and C_2, 5.95 for $C_3\cdots\cdots C_7$, 5.75 for H and $\{3.75+4.0\sin^2(\varphi-25°)\}$ for chlorine.

The R index for $(0kl)$ was 0.071 including the contributions from hydrogen atoms.

7) Y. Sasada and I. Nitta, Unpublished.

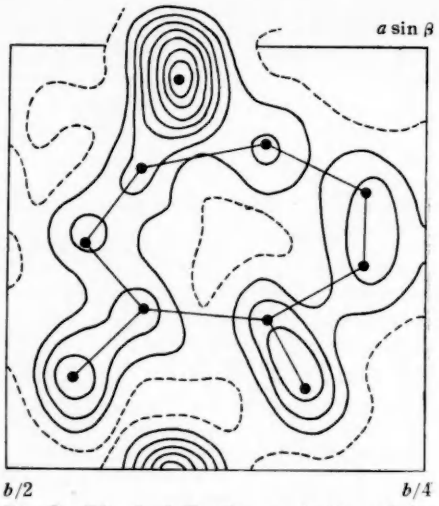

Fig. 3. The final Fourier projection of the electron density along the c axis.
Contours at intervals of $2\,\text{eÅ}^{-2}$, that at $2\,\text{eÅ}^{-2}$ being broken. Black circles show the final atomic positions.

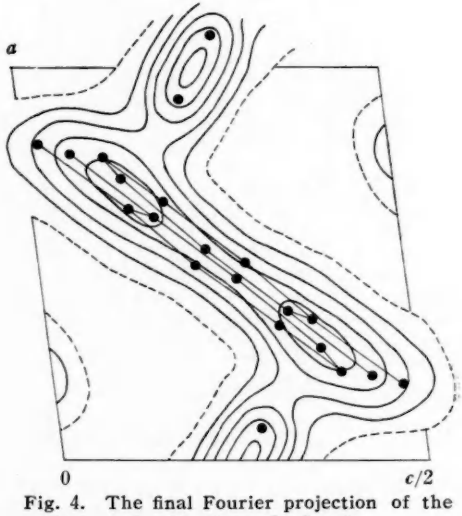

Fig. 4. The final Fourier projection of the electron density along the b axis.
Contours at intervals of $4\,\text{eÅ}^{-2}$, that at $4\,\text{eÅ}^{-2}$ being broken. Black circles show the final atomic positions.

The final $(\rho_o-\rho_c)$ map (the eighth) is shown in Fig. 1. The significant peaks are evidently due to the hydrogen atoms. It should be emphasized that the positions of some hydrogen atoms, especially one attached to O_2, are revealed after the full correction was made for anisotropic motion of chlorine.

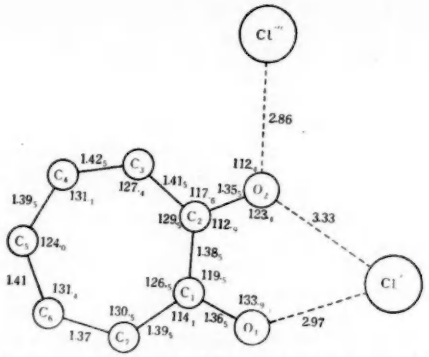

Fig. 5. Bond lengths (Å) and bond angles (°).

As the projections along the b and c axes were unsuitable for refinement owing to considerable overlapping, the x-coordinates of the carbon, oxygen and chlorine atoms were determined by successive three-dimensional line syntheses through atomic centres. Series termination errors were corrected by means of the back-shifts[8]. In the structure-factor calculation for (hkl), the mean value of B, 4.8, was used and the contributions from the hydrogen atoms were omitted. That the B for (hkl) came out smaller than those for $(0kl)$ was mainly due to the omission of correction for absorption. The R index was 0.227 for (hkl), (0.127 unobserved reflexions being omitted).

The final electron density projections along three principal axes are shown in Figs. 2, 3 and 4.

Coordinates, Molecular Dimensions and Estimation of Accuracy

The final values of the coordinates of carbon, oxygen and chlorine atoms are shown in Table I. The coordinates x, y and z are referred to the monoclinic axes, and X', Y and Z' referred to orthogonal axes a, b and c', c' being taken perpendicular to the a and b crystal axes.

TABLE I

ATOMIC COORDINATES

Atom	y/b	z/c	x/a	Y(Å)	Z'(Å)	X'(Å)
Cl	0.1015	0.2268	−0.075	1.828	1.921	−0.630
O_1	0.3205	0.4785	0.191	5.772	4.053	0.316
O_2	0.4610	0.4200	0.217	8.303	3.557	0.509
C_1	0.3430	0.3680	0.355	6.177	3.117	1.223
C_2	0.4180	0.3350	0.375	7.528	2.837	1.357
C_3	0.4540	0.2280	0.533	8.177	1.931	2.232
C_4	0.4200	0.1280	0.713	7.564	1.084	3.202
C_5	0.3455	0.1030	0.773	6.222	0.872	3.515
C_6	0.2860	0.1795	0.655	5.151	1.520	2.866
C_7	0.2850	0.2960	0.483	5.133	2.507	1.914

The bond lengths and valency angles in the tropolone ring are shown in Fig. 5.

The standard deviations of the atomic coordinates, $\sigma(x)$, etc., were estimated using

$$\sigma(x)=\frac{1}{V}\frac{2\pi}{a}\{\sum h^2\sigma^2(F)\}^{\frac{1}{2}}\Big/\left|\frac{\partial^2\rho_3}{\partial x^2}\right|,$$

$$\sigma(y)=\frac{1}{A}\frac{2\pi}{b}\{\sum k^2\sigma^2(F)\}^{\frac{1}{2}}\Big/\left|\frac{\partial^2\rho_2}{\partial y^2}\right|$$

and the corresponding expression for $\sigma(z)$[9,10], where A is the area of the cell projection, V the volume of the cell, $\sigma(F)$ the standard deviation of F values, $\frac{\partial^2\rho_3}{\partial x^2}$ the curvature of the three-dimensional electronic density at the atomic centre, and $\frac{\partial^2\rho_2}{\partial y^2}$ the curvature of two-dimensional density. In evaluating these expressions, we have taken $\sigma(F)=||F_o|-|F_c||$. The curvature was estimated by assuming that the electron density within 0.4 Å from the atomic centre can be represented by the Gaussian distribution, so that $\partial^2\rho/\partial x^2=-2p\rho(0)$. The constant p was evaluated by graphical plots of $\log\rho$ against r^2 from the final F_0 synthesis.

The coordinate standard deviations obtained by these methods were:

$\sigma(y)=\sigma(z)=0.003$, $\sigma(x)=0.004$ Å for chlorine,
$\sigma(y)=\sigma(z)=0.008$, $\sigma(x)=0.010$ Å for oxygen,
$\sigma(y)=\sigma(z)=0.015$, $\sigma(x)=0.017$ Å for carbon.

From these results the standard deviation of a C–C bond comes out to be about 0.023 Å and that of a C–O bond about 0.018 Å. The average standard deviation of bond angles computed by the equation given by Ahmed and Cruickshank[11] was found to be 1.4°. The standard deviation of electron density, given by

$$\sigma(\rho)=\frac{1}{A}\{\sum(|F_o|-|F_c|)^2\}^{\frac{1}{2}},$$

was found to be 0.17 eÅ^{-2} for the projection along the a axis.

Discussion

Planarity of Tropolone Ring.—First it

8) A. D. Booth, *Proc. Roy. Soc.*, (London), **A188**, 77 (1946).

9) D. W. J. Cruickshank, *Acta Cryst.*, **2**, 65 (1949).
10) D. W. J. Cruickshank, ibid., **7**. 519 (1954).
11) F. R. Ahmed and D. W. J. Cruickshank, ibid., **6**, 385 (1953).

will be examined more in detail whether all atoms in tropolone ring lie on one plane or not. By least squares the best plane through seven carbon atoms was determined to be

$$X' = -0.0786\,Y - 1.0257\,Z' + 4.8786. \quad (1)$$

The perpendicular displacements of the carbon atoms from this plane are listed in Table II. From the standard deviations of atomic coordinates only the displacement of C_6 is possibly significant. However, it will be noticed that there is a systematic variation in the displacements. In order to confirm this the χ^2 test was applied[12]. The value of χ^2 is 8.92 and $n=4$, then $P=0.06$; that is seven-membered carbon ring is not truly planar.

If O_1 and O_2 were included in the calculation, the mean plane was

$$X' = -0.0907\,Y - 1.0246\,Z' + 4.9546, \quad (2)$$

and perpendicular displacements are also listed in Table II. In this case, the displacements of O_1, O_2, C_4 and C_6 seem to be possibly significant. But χ^2 test shows that $P=0.0001$; that is, the deviation from this plane is highly significant.

TABLE II

PERPENDICULAR DISPLACEMENTS OF ATOMS FROM POSSIBLE MOLECULAR PLANES (Å)

Atom	Plane (1)	Plane (2)
O_1	$+0.03_2$	$+0.02_6$
O_2	-0.04_8	-0.03_3
C_1	$+0.01_7$	$+0.01_7$
C_2	-0.01_4	-0.00_5
C_3	-0.01_7	-0.00_1
C_4	$+0.02_1$	$+0.03_1$
C_5	$+0.01_3$	$+0.01_3$
C_6	-0.03_4	-0.04_4
C_7	$+0.00_6$	-0.00_5
Cl'	$+0.52_9$	
Cl''	-1.13_9	
O_2'	-0.56_2	

Thus we may say only that the tropolone ring deviates slightly from a strictly planar form. It seems to be likely from the molecular packing and somewhat shorter intermolecular distances between particular atoms that such deviations may be due to some effects of crystalline field or others.

Intramolecular Distances.—The C–O distances are 1.355 and 1.365 Å as shown in Fig. 5. From the significant test, the two C–O bonds are of the same nature. The identical character of the two C–O bonds, which have been observed in the case of sodium tropolonate[2] (mean C–O length; 1.285 Å), is an essentially different feature from the case of neutral tropolone, in which C–O lengths are 1.26 and 1.34 Å[13]. As previously mentioned, these three compounds are isoelectronic with respect to the π-electron system. It is noted that the mean values of two C–O distances become larger when the number of added protons increases.

The mean C–O length, 1.360 Å in the present case, is in good agreement with those in the structures of resorcinol[14,15] and 1–4 dimethoxy benzene[16].

The canonical formulae of the Kekulé type with formal charges are shown in Fig. 6. In terms of the resonance theory, the bond lengths observed will imply that, in the actual ground state, the contributions from the structures of the type (B), including III–IX, should be considered to be more appreciable than those of the type (A). It agreed with the famous conclusion[17] that the seven-membered carbon ring prefers to lose one electron to form the stable 6π electron system, and with also more recent molecular orbital calculation of tropolone[18]. It can further account for the measurement of dipole moment[19] and some chemical evidences[20].

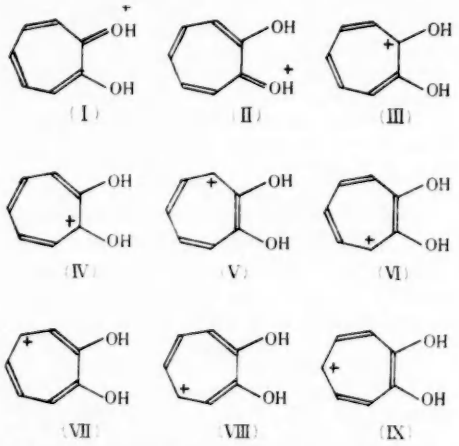

Fig. 6. Canonical formulae of tropolonium cation.

12) P. J. Wheatley, *Acta Cryst.*, **6**, 369 (1953).

13) M. Kimura and M. Kubo, This Bulletin, **26**, 250 (1953).

14) J. M. Robertson, *Proc. Roy. Soc.* (*London*)., **A 157**, 79 (1936).

15) J. M. Robertson, ibid., **A167**, 122 (1938).

16) T. H. Goodwin, M. Przybylska and J. M. Robertson. *Acta Cryst.*, **3**, 279 (1950).

17) E. Hückel, *Z. Physik*, **70**, 204 (1931).

18) Y. Kurita and M. Kubo, This Bulletin, **24**, 13 (1951).

19) Y. Kurita, T. Nozoe and M. Kubo, ibid., **24**, 10 (1951).

20) T. Nozoe, *Proc. Japan Acad.*, **26**, 30 (1950).

As the standard deviations of the C–C bonds are about 0.023 Å, the bond C_6–C_7 is shorter than the bonds C_2–C_3 and C_3–C_4 significantly, while the other fluctuations among the bonds can not be discussed seriously. The significant fluctuations among the seven C–C bonds show evidently that the contributions from the component structures of the type B are not equal. As complete interpretation of this fact is not yet given, we will only present some qualitative considerations. The first reason will be the non-equivalent orientations of the two O–H bonds with respect to the line through C_5 and the mid-point of C_1–C_2. In 1–4 dimethoxy benzene[16] the C–C bond in the cis-position to the methyl group is greater than that in the trans-position significantly (1.44 and 1.36 Å). The same situation is observed in the molecule of hydroquinone in the quinhydron crystal (1.42 and 1.34 Å[21]). However, it is not the case for the structure of resorcinol, although the accuracy of the analysis is rather low[14,15]. For a quantitative discussion, it will be desirable to make complete structure analysis of catechol[22,23].

The second reason is the rather closer approaches of chlorine ions to some ring atoms; that is, C_3, C_5 and C_6 as shown in Fig. 8. These values are smaller than those in similar cases, that is, 3.85 Å in aniline hydrochloride[24], 3.63 Å in *m*-toluidine dihydrochloride[25], 3.71 Å in adenine hydrochloride[4], 3.56 Å in guanine hydrochloride[26]. At twin boundary in the crystal of *m*-toluidine dihydrochloride[25] the nearest approaches between carbon and chlorine are 3.52 Å, but this value seems to be less significant. It will be natural to consider that these carbon atoms close to chlorine ions become more positively charged than the others. If we use the terms of the resonance theory, it corresponds to the increased contributions of the components, V, VIII and IX.

The best agreement between measured and calculated bond lengths was obtained taking the following contributions:

I–II, each 11%, III and VII–IX, each 10%, IV and VI, each 4%, V, 30%, the relation $R=R_1-(R_1-R_2)3x/(2x+1)$[27], where x is double bond character, being used with $R_1=1.54$ (C–C), $R_2=1.34$ (C=C), $R_1=1.42$ (C–O) and $R_2=1.20$ Å (C=O). The calculated values are shown in Fig. 7(b), together with observed values in the present crystal (a) and in sodium tropolonate(c).

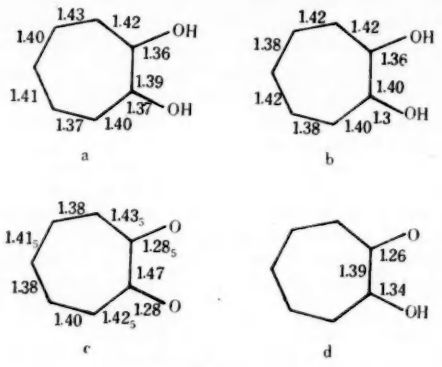

Fig. 7. (a) Observed bond lengths.
(b) Bond lengths calculated, using Pauling's relation.
(c) Bond lengths in tropolonate anion.
(d) Bond lengths in neutral tropolone.

Hydrogen Bonding and Molecular Arrangement.—The refined values for O···Cl are 2.97 and 2.86 Å, and are slightly shorter than those in chloral hydrate[28](3.05kX),

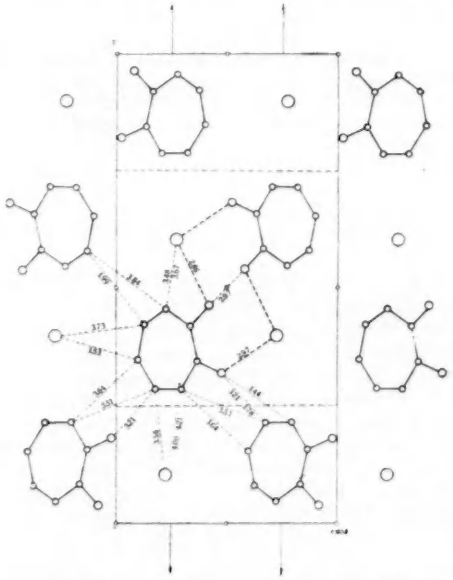

Fig. 8. Arrangement of molecules projected along the *a* axis.

21) I. Nitta, K. Osaki and H. Matsuda, To be published.
22) W. A. Caspari, *J. Chem. Soc.*, **1926**, 573.
23) A. N. Sarker, *Phil. Mag.*, **2**. 1153 (1926).
24) C. J. Brown, *Acta Cryst.*, **2**,228 (1949).
25) F. Fowweather and A. Hargreaves, ibid., **3**, 81 (1950).
26) J. M. Broomhead, ibid., **4**, 92 (1951).
27) L. Pauling, "The nature of the chemical bond" (1948).
28) S. Kondo and I. Nitta, *X-ray*, **6**, 53, (1950).

hydroxyl ammonium chloride[29] (2.99 Å), guanine hydrochloride[26] (3.16 Å), adenine hydrochloride[4] (C–H=0.95 and H···Cl=2.17 Å), ephedrine hydrochloride[30] (3.06 Å) and D(−) isoleucine hydrochloride[31] (3.05, 3.07 and 3.24 Å). Although it seems to be not quite reasonable to claim the hydrogen bonding only from these distances, the angles C–O–Cl, 133.9° and 112.4°, are favourable to hydrogen bond formation. Further this conclusion is supported evidently by the direct determination of the positions of hydrogen atoms, as seen in Fig. 1. If the hydrogen bonds are operative in this crystal, the dimer formation linked by them may be concluded and it seems interesting in respect to the relation with the cystal structure of neutral tropolone, in which the presence of dimer was supposed[32]. Moreover, it is observed from the difference map that the anisotropic thermal motions of each atom seem to originate from the oscillation of the dimer, as a whole, about its centre.

Finally will be described an outline of the crystal structure ignoring, for the present, the dimer formation. Each tropolone ring was surrounded by six chlorine ions and each chlorine ion has six tropolone rings as first neighbours. The packing is closely related to ionic crystals of the NaCl type. This arrangement of chlorine ions and centres of gravities of tropolone rings also supports the above argument that the net positive charges distribute over the whole ring of the latter.

The authors wish to express their thanks to Professor T. Nozoe and his collaborators for supplying the specimens and also for continued encouragement. We are also indebted to the members of the group who have been making the cooperative physico-chemical investigations of "tropolone chemistry" for their helpful discussions. This research was supported by a grant from the Ministry of Education.

Department of Chemistry
Osaka University, Osaka

29) B. Jerslev, *Acta Cryst.* **1**, 21, (1948).
30) D. C. Phillips, ibid., **7**, 159, (1954).
31) J. Trommel and J. M. Bijvoet, ibid., **7**, 703, (1954).
32) K. Osaki and I. Nitta, Unpublished.

Studies on the Chemical Constitution of Agar-agar. XIX[1]*. Pyruvic Acid as a Constituent of Agar-agar (Part 1). Identification and Estimation of Pyruvic Acid in the Hydrolysate of Agar*

By Susumu HIRASE

(Received October 8, 1956)

Agar is composed mainly of D-galactose and 3,6-anhydro-L-galactose. Partial depolymerization by means of acid hydrolysis[2], mercaptolysis[3] and methanolysis[4] gave rise to agarobiose(4-O-β-D-galactopyranosyl-3,6-anhydro-L-galactose)and its derivatives. Enzymatic hydrolysis[1] led to the isolation of neoagarobiose (3-O-3,6-anhydro-α-L-galactopyranosyl-D-galactose). From this and other evidences, Araki[5] recently suggested that 1,3-linked β-D-galactopyranose and 1,4-linked 3,6-anhydro-α-L-galactopyranose are alternately repeated to build up the chain of agarose, a principal polysaccharide of agar. Through further investigation, however, it has become probable that agar contains a small amount of pyruvic acid as a constituent.

A preliminary experiment involving the use of paper chromatography has indicated that pyruvic acid is produced in the hydrolysate of agar. For confirmation, agar was hydrolysed with very dilute hydrochloric acid, which caused little formation of degradation products of sugar components. Pyruvic acid liberated was easily isolated as its 2,4-dinitrophenylhydrazone though in a slight yield. The fact that pyruvic acid is set free with very dilute acid suggests that it would not

1) Part XVIII : C. Araki, and K. Arai, This Bulletin, **29**, 339 (1956).
2) C. Araki, *J. Chem. Soc. Japan.* **65**, 533, 627 (1944).
3) S. Hirase and C. Araki, This Bulletin, **27**, 105 (1954).
4) C. Araki and S. Hirase, ibid., **27**, 109 (1954).
5) C. Araki, ibid., **29**, 543 (1956).

be a secondary by-product, but an inherent constituent of agar, and also that, in the latter instance, it is engaged in the linkage susceptible to hydrolysis.

In order to examine the content of pyruvic acid, agar was subjected to hydrolysis with N-sulfuric acid. Pyruvic acid produced was completely extracted with ether, and the ether was then removed by distillation. Pyruvic acid obtained was contaminated by a large amount of formic acid, levulinic acid and hydroxymethylfurfural[6], the contaminants arising chiefly from 3,6-anhydro-L-galactose[7], and hence the 2,4-dinitrophenylhydrazine method could not be applied for the estimation of pyruvic acid. The method successfully employed in this study involves the oxidation with sodium metaperiodate at 65° followed by gravimetric determination of carbon dioxide liberated thereby:

$$CH_3COCOOH \xrightarrow{NaIO_4} CH_3COOH + CO_2$$

The content of pyruvic acid found by this method was 1.06% of agar by weight, or one residue for every fifty one hexose residues.

Since it has never been reported that pyruvic acid is present in a polysaccharide, further experiment has been made to examine any distribution of pyruvic acid in several polysaccharides other than agar. But it was detected in none of hydrolysates of mucilages of *Chondrus ocellatus Holmes* and *Gloiopeltis furcata*, gum arabic, apple pectin, konjak mannan and starch. Pyruvic acid seems to be a component peculiar to agar.

It may be of interest from the view point of biochemistry that agar contains pyruvic acid, because agar constitutes the chief cell wall structural material in several red sea weeds and pyruvic acid represents an important intermediate in the metabolism of carbohydrate, fat and protein.

Experimental

Isolation of Pyruvic Acid from Agar.—Commercial agar powder (10.0 g., moisture 17.31%) was hydrolysed with 0.1N-hydrochloric acid (100 cc.) in a boiling water bath for four hours. The solution was decolorized with active carbon, and 2,4-dinitrophenylhydrazine (1 g.) dissolved in warm 4N-hydrochloric acid (150 cc.) was added, when no precipitation occurred. After being kept overnight at room temperature, the solution was extracted four times with 50 cc. portion of ethyl acetate. The extracts were combined, washed once with water, and then treated five times with 10 cc. portion of 5% sodium carbonate solution. The carbonate extracts were combined, and ethyl acetate dissolved in it was removed by evaporation under reduced pressure at 40°. Acidification with concentrated hydrochloric acid under ice cooling afforded fine yellow crystals of pyruvic acid 2,4-dinitrophenylhydrazone, which was then collected on a glass filter, washed with dilute hydrochloric acid and water, and dried at 100° until a constant weight was reached. Yields in duplicate runs were 0.157 g. and 0.162 g., which were equivalent, respectively, to 0.0514 g. and 0.0532 g. of free pyruvic acid. The crystals obtained were nearly pure as indicated by m. p. 214°. Recrystallization from ethanol-ethyl acetate gave a pure specimen melting at 218°. The m. p. was not depressed on admixture with an authentic sample (m. p. 218°).

Anal. Found: C, 40.43; H, 3.34; N, 20.68. Calcd. for $C_9H_9O_6N_4$: C, 40.30; H, 3.01; N, 20.89 %.

Examination of Polysaccharides other than Agar.—Each 10 g. of mucilages of *Chondrus ocellatus Holmes* and *Gloiopeltis furcata*, gum arabic and apple pectin was hydrolysed with 0.1N-hydrochloric acid (100 cc.) in a boiling water bath for four hours. Konjak mannan and starch (each 10 g.) was hydrolysed with N-hydrochloric acid (100 cc.) for five hours. Each hydrolysate was treated with 2,4-dinitrophenylhydrazine exactly in the same manner as that described for agar. None of them afforded 2,4-dinitrophenylhydrazone of pyruvic acid.

Quantitative Determination of Pyruvic Acid.—*Apparatus and Procedure.*—The quantitative determination of carbon dioxide evolved from pyruvic acid during the periodate oxidation was carried out by passing a slow current of carbon dioxide-free air through the reaction flask to sweep the evolved gas into an adsorption vessel through a train assembled as follows: (1) a washing bottle containing a 30% potassium hydroxide solution, and an U-tube filled with soda-lime, (2) the reaction flask (an 100 cc. Erlenmeyer flask) with two-holed rubber stopper carrying the inlet and outlet tubes, (3) a trap kept at −10° for the removal of most of moisture, (4) an adsorption vessel charged with concentrated sulfuric acid for the prevention of any moisture and volatile organic material from getting into the next adsorption vessel, and (5) a weighed adsorption vessel charged with a 30% potassium hydroxide solution for the quantitative determination of carbon dioxide.

A sample containing 0.05–0.3 g. of pyruvic acid was dissolved in water (20 cc.) in the reaction flask. Crystals of sodium metaperiodate (1.0 g.) were added, and the flask was immediately connected to the remainder of the apparatus. The mixture was then heated at 65°, while a slow stream of air was bubbled through the apparatus. The increase in weight of the carbon dioxide adsorption vessel was measured after two

6) C. Araki, *J. Chem. Soc. Japan*, **58**, 1214 (1937).
7) C. Araki and K. Arai, ibid., **63**, 1720 (1942).

hours, and the amount of pyruvic acid was calculated from the weight of carbon dioxide found.

Control Analysis. — Pyruvic acid alone and contaminated by arbitrary amounts of a mixture of formic acid, levulinic acid and hydroxymethylfurfural was analysed by the above method. These contaminants exhibited no harmful influence upon the results. Some typical results are given in Table I.

TABLE I

QUANTITATIVE DETERMINATION OF PYRUVIC ACID IN THE PRESENCE OF CONTAMINANTS

PA, g. taken	FA, LA and HMF, g. added	PA, g. found	Error, g.
0.1119	—	0.1123	+0.0004
0.1116	—	0.1105	−0.0011
0.3387	—	0.3377	−0.0010
0.1211	each 0.5	0.1215	+0.0004
0.1100	each 1.5	0.1145	+0.0045
0.1048	each 3.0	0.1065	+0.0017

PA: Pyruvic acid. FA: Formic acid.
LA: Levulinic acid. HMF: Hydroxymethylfurfural.

Quantitative Determination of Pyruvic Acid in the Hydrolysate of Agar.—Each 10 g. of agar powder (moisture 17.31%) was hydrolysed with N-sulfuric acid (100 cc.) in a boiling water bath for two, four and six hours, respectively. Humus substances formed were removed by filtration through a charcoal bed, and the filtrate was extracted with ether for thirty hours in a Soxhlet's apparatus. A control experiment indicated that the extraction was complete. Water (10 cc.) was added to the extract, and ether was then removed by careful distillation. The residual solution was quantitatively transferred to the reaction flask for analysis, and the pyruvic acid present in the solution (20 cc.) was determined by the method above described. The results obtained were 0.0777 g. in a two hours hydrolysate, 0.0853 g. and 0.0877 g. in a four hours hydrolysate, and 0.0885 g. and 0.0873 g. in a six hours hydrolysate, respectively. The average value excluding the result of two hours hydrolysis is 0.0872 g. or 1.06% of moisture-free agar by weight. This figure indicates the presence of one residue of pyruvic acid for every fifty one residues of hexose.

Summary

1. Pyruvic acid has been isolated as its 2,4-dinitrophenylhydrazone from the hydrolysate of agar for the first time.

2. Quantitative determination has indicated that the content of pyruvic acid is 1.06% of agar or one residue for every fifty one hexose residues.

3. It has been suggested that pyruvic acid would be an intrinsic constituent of agar.

4. Several polysaccharides other than agar have been examined, but none of them produced pyruvic acid on hydrolysis.

The writer wishes to express his hearty thanks to Professor S. Tanaka, Department of Science, Kyoto University, and Professor C. Araki, this University, for their great interest and discussion. Thanks are also due to Mr. K. Arai for microanalysis and to Mr. T. Ito for assistance.

Institute of Chemistry, Faculty of Industrial Arts, Kyoto Technical University
Matsugasaki, Kyoto

Studies on the Chemical Constitution of Agar-agar. XIX. Pyruvic Acid as a Constituent of Agar-agar (Part 2)[1]*. Isolation of a Pyruvic Acid-linking Disaccharide Derivative from the Methanolysis Products of Agar*

By Susumu HIRASE

(Received October 8, 1956)

In the previous communication[1], it was suggested that pyruvic acid, produced in 1.06% yield by the hydrolysis of agar, would not be secondary by-product, but an intrinsic constituent. This suggestion has been substantiated herein by the isolation of a crystalline disaccharide derivative carrying a pyruvic acid residue in the molecule from the partial methanolysis products of agar.

The partial methanolysis of agar has been carried out by heating it in 0.5%

1) Part XIX-1 : S. Hirase, This Bulletin, **30**, 68 (1957).

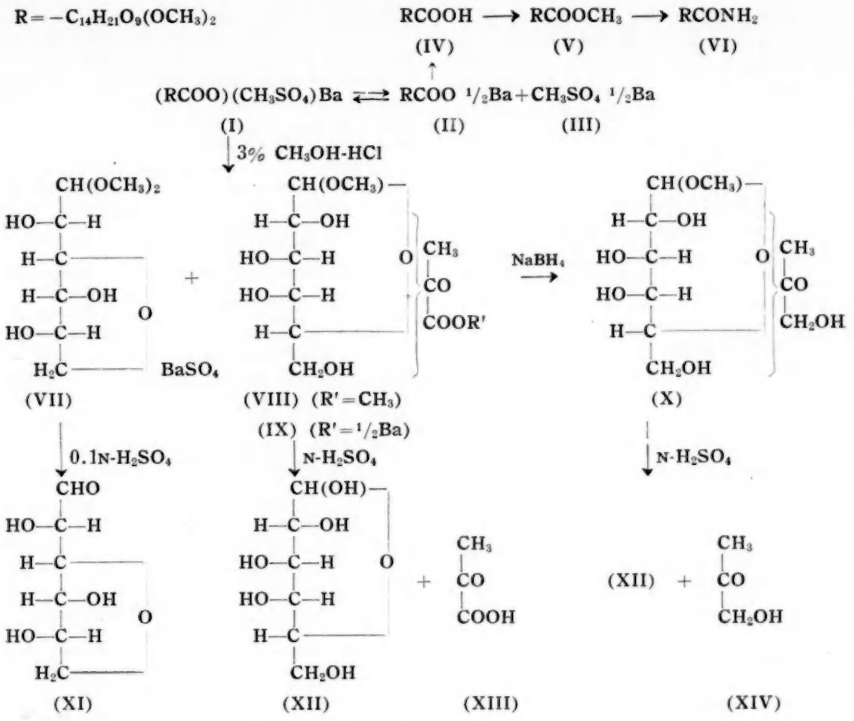

methanolic hydrogen chloride for two hours according to the method of Araki and the present writer[2]. The product was treated with barium hydroxide solution and passed through columns of cation and anion resins in succession. Acidic compounds, which were retained by the anion resin, were eluted by displacement with excess sulfuric acid. Neutralization with barium hydroxide followed by evaporation afforded a mixture of barium salts, from which a crystalline salt was isolated in 6.3% yield by weight.

The crystalline barium salt obtained has been proved to be monohydrates of a double salt (I) consisting of barium methylsulfate (III) and a barium salt of an organic acid (II). This follows from the fact that the double salt was separated into its two component salts II and III by means of an anion exchange resin. When II and III were separately dissolved in methanol and the solutions were mixed, the double salt was immediately regenerated. Methylsulfuric acid constituting a part of the double salt may have arisen from the sulfuric acid residues present in agar.

2) C. Araki and S. Hirase. ibid., **27**, 109 (1954).

From the barium salt (II), there has been obtained a free acid (IV) having the formula $C_{14}H_{21}O_9(OCH_3)_2COOH$ as its crystalline monohydrates. The acid was converted into the methyl ester (V) by reaction with diazomethane, and the ester was further converted into the amide (VI) by reaction with ammonia. Both derivatives were obtained in a crystalline condition.

In order to examine the components of the acid (IV), the original double salt (I) was subjected to methanolysis. There were produced barium sulfate, 3,6-anhydro-L-galactose dimethylacetal (VII) and a methyl ester methyl glycoside (VIII), the last one being separated from the second through its barium salt (IX). 3,6-Anhydro-L-galactose dimethylacetal (VII) was hydrolysed to give a free sugar (XI), which was identified as its crystalline diphenylhydrazone. The barium salt methyl glycoside (IX) yielded upon hydrolysis D-galactose (XII) and pyruvic acid (XIII). D-Galactose was isolated as crystals, and pyruvic acid was identified as its semicarbazone, phenylhydrazone and *p*-nitrophenylhydrazone. This result indicates that the acid (IV) is a disaccharide derivative composed of 3,6-anhydro-L-

galactose and D-galactose, the latter component carrying a pyruvic acid residue.

On the other hand, the ester group of VIII was reduced to a hydroxyl group with sodium borohydride. Hydrolysis of the resulting product (X) yielded D-galactose (XII) and hydroxyacetone (XIV), the latter product being identified as its semicarbazone. This result demonstrates that the pyruvic acid residue is linked through its carbonyl group with the D-galactose residue.

The isolation of the compound (IV) verifies the view that pyruvic acid is a constituent of agar, because the mild treatment in its isolation completely excludes the possibility that pyruvic acid might be a secondary product derived from some unidentified compound. For instance, oxalacetic acid would be decarboxylated to give pyruvic acid on being heated in an aqueous medium, but it undergoes no decarboxylation on being treated with methanolic hydrogen chloride.

The compound (IV) represents the first example of a carbohydrate with which pyruvic acid is linked through its carbonyl group. The structure will b elater reported.

Experimental

Unless otherwise stated, concentration and evaporation were carried out under reduced pressure below 40°. Melting points are uncorrected.

Partial Methanolysis of Agar.—Commercial agar powder (50 g., dry weight 41.9 g.) was suspended in 0.5% methanolic hydrogen chloride (500 cc.) and heated under reflux for two hours. The undissolved agar (5.5 g.) was removed by filtration, and the filtrate was neutralized with silver carbonate, refiltered and concentrated to a sirup (40.7 g.). It was then saponified by heating in a 0.2N-barium hydroxide solution (500 cc.) at 60° for two hours. Excess barium hydroxide was removed by neutralization with carbon dioxide and filtration, and the filtrate was passed through a column of Amberlite IR-120 (2.8×20 cm.) to remove cations, and then through a column of Amberlite IR-4B (2.8×25 cm.), where anions of acidic compounds were adsorbed. The columns were thoroughly washed with water (5 l.), and the neutral effluent was concentrated to a sirup (32.1 g.); $[\alpha]_D^{26}$-17.7° (water, *c* 1.64). This was a mixture of neutral sugar derivatives, which were not investigated in this communication.

Isolation of the Double Salt (I).—The above IR-4B resin, by which acidic compounds were retained, was stirred with N-sulfuric acid (300 cc.) under ice cooling for ten minutes, poured into a glass tube (2.8 cm. diameter), and drained. The column was washed with additional 100 cc. of N-sulfuric acid and then with water (2 l.). The effluent and washings were immediately neutralized with a saturated barium hydroxide solution as soon as they percolated, barium sulfate removed by filtration, and the filtrate was concentrated to a sirup. Dissolution in boiling methanol (50 cc.) followed by cooling afforded crystals of the double salt (I), which were filtered, washed with methanol and dried; yield 2.3 g. (6.3% of the agar concerned in methanolysis); $[\alpha]_D^{26}$-29.0° (water, *c* 1.0). The filtrate and washings were concentrated to a sirup (3.0 g.), $[\alpha]_D^{26}$-2.3° (water, *c* 1.75).

The crude crystals above obtained were purified by recrystallization from aqueous methanol until no more change in specific rotation and in barium content was recognized. The pure double salt forms elongated prisms, having $[\alpha]_D^{14}$-30.1° (water, *c* 1.56) and slowly decomposing over 200°C. It is soluble in water and insoluble in organic solvents.

Anal. Found: Ba, 19.42; SO_4, 13.55; OCH_3, 13.09; Ash, 33.01. Calcd. for $(C_{17}H_{27}O_{13})(CH_3SO_4)Ba \cdot H_2O$: Ba, 19.48; SO_4, 13.61; OCH_3, 13.20; Ash (as $BaSO_4$), 33.09%.

Separation of the Double Salt (I) into its Component Salts.—The double salt (I) (6.0 g.) in water (30 cc.) was passed through a column of Amberlite IR-120 (2.8×10 cm.) to remove barium ion, and the column was washed with water (100 cc.). The acidic effluent and washings were combined and immediately passed through a column of Amberlite IR-4B (sulfate form) (2.8×20 cm.), which had been prepared by the reaction of the resin (hydroxide form) with excess N-sulfuric acid and had been washed with large volumes of water (20 l.). The column was then washed with water (400 cc.). In this process, methylsulfuric acid was retained by the resin, while the carboxylic acid (IV) was passed through.

(a) **Barium Salt (II).**—The effluent from the above anion resin was immediately neutralized with a barium hydroxide solution and concentrated to dryness. The residue was dissolved in a small volume of methanol, filtered and poured into dry acetone, giving a white powder of the barium salt (II), which was collected on a glass filter, washed with acetone and dried in vacuo; yield 4.0 g. (93%); $[\alpha]_D^{20}$-40.3° (water, *c* 1.54).

Anal. Found: OCH_3, 11.95; Ba, 13.34; SO_4, nil. Calcd. for $(C_{17}H_{27}O_{13})_2Ba$: OCH_3, 12.20; Ba, 13.52%.

(b) **Barium Methyl sulfate (III).**—Methylsulfuric acid, which had been adsorbed by the IR-4B resin, was eluted from the column with N-sulfuric acid (50 cc.) and then with water (300 cc.). Effluents were immediately neutralized with a hot saturated barium hydroxide solution, filtered and evaporated to dryness. The residue was crystallized from aqueous ethanol, giving barium methylsulfate dihydrates; yield 1.4 g. (82%).

Anal. Found: Ba, 34.66; SO_4, 48.39; OCH_3,

15.81. Calcd. for $(CH_3SO_4)_2Ba \cdot 2H_2O$: Ba, 34.73; SO_4, 48.58; OCH_3, 15.67%.

Regeneration of I from II and III.—The barium salt (II) (0.51 g.) and barium methylsulfate dihydrate (III) (0.20 g.) were separately dissolved in methanol. When the solutions were combined, the double salt (I) was immediately crystallized; yield 0.71 g. (100%); $[\alpha]_D^{15}$-30.6° (water, *c* 1.21).

Anal. Found: Ba, 19.33; SO_4, 13.40; OCH_3, 13.31. Calcd. for $(C_{17}H_{27}O_{13})(CH_3SO_4)Ba \cdot H_2O$: Ba, 19.48; SO_4, 13.61; OCH_3, 13.20%.

Free Acid (IV).—The barium salt (II) (2.0g.) in water (20 cc.) was passed through a column of Amberlite IR-120 (2.8×10 cm.) to remove barium ion, and the column was washed with water (80 cc.). The acidic effluent was partly neutralized with 1 cc. of 0.1N-barium hydroxide solution and concentrated below 30° to a sirup, which was freed from a barium compound by dissolution in dry acetone and filtration. The filtrate was concentrated to a sirup (1.7 g.), which was redissolved in ethyl acetate and kept overnight in a refrigerator. Crystals deposited were filtered, washed with ethyl acetate and dried; yield 1.4 g (78%). Recrystallization twice from ethyl acetate afforded a pure specimen of the acid (IV) in a monohydrate form melting at 118–120° and foaming at 122°; $[\alpha]_D^{20}$-46.7° (water, *c* 1.05) and -51.6° (methanol, *c* 1.24). It is soluble in water, methanol, ethanol and acetone, and hardly soluble in cold ethyl acetate and ether. Seliwanoff's ketose reaction was strongly positive.

Anal. Found: C, 44.39; H, 6.83; OCH_3, 13.31%; Neutralization equivalent, 457. Calcd. for $C_{17}H_{28}O_{13} \cdot H_2O$: C, 44.55; H, 6.59; OCH_3, 13.53; Neutr. equiv., 458.

Methyl Ester (V).—To a solution of the acid (IV) (0.5 g.) in methanol (5 cc.) was added dropwise an ethereal solution of diazomethane, evolution of nitrogen being observed. After being kept for one hour, it was concentrated to a sirup (0.5 g.), which was then dissolved in ethyl acetate, and a small amount of ether was added to form a slight cloudiness. The solution was left in a refrigerator, when the methyl ester (V) was slowly crystallized; yield 0.32 g. An additional crop (0.10 g.) was obtained from the mother liquor. Crude crystals were purified by recrystallization twice from ethyl acetate-ether, giving prisms; m. p. 153–154°; $[\alpha]_D^{15}$-44.4° (water, *c* 1.04), and -52.9° (methanol, *c* 1.04). It is soluble in water, methanol, ethanol and acetone, hardly soluble in cold ethyl acetate, and insoluble in ether.

Anal. H, Found: C, 47.51; 6.75; OCH_3, 20.69%; Saponification equivalent, 452. Calcd. for $C_{18}H_{30}O_{13}$: C, 47.57; H, 6.65; OCH_3, 20.47%; Sapon. equiv., 454.

Amide (VI).—A methanolic solution (5 cc.) of the methyl ester (V) (0.15 g.) was saturated with dry ammonia under ice cooling, and left overnight at room temperature. Evaporation gave a sirup, which solidified on standing. Recrystallization was carried out by dissolving it in acetone and adding ether, the amide (VI) being obtained as monohydrates; yield 0.08 g.; m. p. 102–105°; $[\alpha]_D^{25}$-43.2° (water, *c* 0.51).

Anal. Found: C, 44.66; H, 6.95; N, 3.11. Calcd. for $C_{17}H_{29}O_{12}N \cdot H_2O$: C, 44.64; H, 6.82; N, 3.06%.

Methanolysis of the Double Salt (I).—The double salt (I) (4.0g.) in 3% methanolic hydrogen chloride (150 cc.) was heated under reflux for twenty hours. Barium sulfate precipitated was removed by filtration, and the filtrate was neutralized with silver carbonate, filtered and concentrated to a colorless sirup (2.5 g.); $[\alpha]_D^{13}$ +35.1° (water, *c* 0.74). This was proved to be a mixture of VII and VIII, the separation being effected by saponification as described below.

(a) Barium Salt Methyl Glycoside (IX).—The above sirup was heated in 0.3N-barium hydroxide solution (150 cc.) at 60° for two hours. The solution was neutralized with carbon dioxide, filtered and concentrated to a sirup (3.1 g.). It was then dissolved in a small volume of methanol and poured into dry acetone with stirring, the barium salt methyl glycoside (IX) being precipitated as a white powder, which was collected on a glass filter, washed with acetone and dried in vacuo; yield 2.3 g.; $[\alpha]_D^{14}$+56.2° (water, *c* 0.89).

Anal. Found: OCH_3, 9.05; Ba, 20.66. Calcd. for $(C_{10}H_{15}O_8)_2Ba$: OCH_3, 9.34; Ba, 20.70%.

(b) 3,6-Anhydro-L-galactose Dimethylacetal (VII).—The filtrate and washings, separated from the above salt (IX), were combined and evaporated to dryness, when VII was obtained as a colorless sirup[3]; yield 0.7 g.; $[\alpha]_D^{13}$-27.0° (water, *c* 0.74); OCH_3, found: 26.32% (calcd. for $C_8H_{16}O_6$: 29.81%). It migrated on a paper chromatogram at the same rate as an authentic sample (R_f 0.67[2]), *n*-butanol-ethanol-water (4:1:2) being used as a solvent and *o*-aminophenol reagent[4] being sprayed.

3,6-Anhydro-L-galactose Diphenylhydrazone.—The dimethylacetal (0.15 g.) above obtained was hydrolysed with 0.1N-sulfuric acid at 95° for two hours in the usual manner, giving 3,6-anhydro-L-galactose (XI) (0.12 g.). It was then converted into its diphenylhydrazone in the usual manner[3]; m. p. 153–155°, not depressed on admixture with an authentic sample; $[\alpha]_D^{13}$ −34.4° → −21.5° (methanol, *c* 0.93).

Methyl Ester Methyl Glycoside (VIII).—The barium salt methyl glycoside (IX) (2.6 g.) above obtained was esterified by heating in 4% methanolic hydrogen chloride (100 cc.) for four hours. The solution was neutralized with silver carbonate, filtered and concentrated to a sirup, which was purified by extraction with hot acetone and evaporation. The methyl ester methyl glycoside

3) C. Araki, *J. Chem. Soc. Japan*, **65**, 725, (1944).
4) S. Hirase, C. Araki and S. Nakanishi, This Bulletin, **26**, 183 (1953).

(VIII) was obtained as a pale yellow viscous sirup; yield 1.7 g.; $[\alpha]_D^{13}$ +74.8° (water, *c* 1.27) and +69.0° (methanol, *c* 1.26).

Anal. Found: OCH_3, 21.80%; Saponification equivalent, 278. Calcd. for $C_{11}H_{18}O_8$: OCH_3, 22.29 %; Sapon. equiv., 278.

Hydrolysis of IX.—The barium salt methyl glycoside (IX) (0.8 g.) was dissolved in a small amount of water and N-sulfuric acid (15 cc.) was added with stirring. Barium sulfate precipitated was removed by filtration, and the filtrate was heated in a boiling water bath until the optical rotation of the solution reached a constant value after five hours ($[\alpha]_D$ +52° → +28°). The solution was placed in a Soxhlet's apparatus and treated with ether for seven hours to extract pyruvic acid. The residual solution was used for isolation of D-galactose.

(a) D-Galactose (XII).—The residual solution just mentioned was neutralized with barium carbonate, filtered and concentrated to a sirup, which gave D-galactose on dissolution in hot methanol and cooling; yield 0.30 g.; m. p. 166–168°, not depressed on admixture with an authentic sample; $[\alpha]_D^{14}$ +80.6° (after twentyfour hours, water, *c* 1.08).

(b) Pyruvic Acid (XIII).—The ether extract above described was distilled under atmospheric pressure to remove ether, and the residue was dissolved in water (9 cc.). The solution was used to prepare the following derivatives of pyruvic acid in the usual manner.

Phenylhydrazone.—Needles; m. p. and mixed m. p. 192°.

p-Nitrophenylhydrazone.—Yellow fine crystals; m. p. and mixed m. p. 226°.

Semicarbazone.—Prisms; m. p. and mixed m. p. 212°.

Reduction of VIII and Hydrolysis.—Sodium borohydride (0.3 g.) was added to a solution of VIII (0.9 g.) in water (10 cc.). The reaction solution was left aside with occasional shaking for five days at room temperature. Then it was neutralized with dilute sulfuric acid, deionized by passing through columns of Amberlite IR-120 and IR-4B in succession, and concentrated to a sirup, which was purified by dissolution in absolute methanol and filtration. Evaporation afforded a viscous sirup of the reduction product (X); yield 0.8 g.; $[\alpha]_D^{24}$ +74.5° (water, *c* 0.50); OCH_3, found: 12.15% (calcd. for $C_{10}H_{18}O_7$: 12.40%).

The product (X) (0.40 g.) obtained was heated in N-sulfuric acid (10 cc.) until the optical rotation of the solution reached a constant value after four and a half hours ($[\alpha]_D$ +74°→+40°). The solution was neutralized with barium carbonate and filtered. The filtrate, diluted with water up to 40 cc., was distilled under atmospheric pressure, the same volume of water as that of the distillate being supplied as the distillation progressed. Forty cc. of the distillate was collected to identify hydroxyacetone therein, while the residual solution was used for the isolation of D-galactose.

(a) D-Galactose (XII).—The residual solution of the distillation was concentrated to dryness, giving D-galactose; m. p. and mixed m. p. 166–167°; $[\alpha]_D^{25}$ +80.5° (after twentyfour hours, water, *c* 1.15).

(b) Hydroxyacetone (XIV).—To the distillate above obtained, semicarbazide hydrochloride (0.5 g.) and sodium acetate trihydrate (0.8 g.) were added. After being left overnight at room temperature, the solution was concentrated to a small volume, when hydroxyacetone semicarbazone was crystallized; yield 0.06 g.; m. p. 195–196°, not depressed on admixture with an authentic sample.

Decarboxylation of Oxalacetic Acid.—Oxalacetic acid (0.3064 g.) in water (25 cc.) was heated in a boiling water bath, the evolved gas being swept by a slow current of carbon dioxide-free air into an adsorption vessel charged with a 30% potassium hydroxide solution. Carbon dioxide found was 0.1013 g. (99.3% of theory). From the reaction solution, pyruvic acid was obtained as its phenylhydrazone melting at 192°. When oxalacetic acid (0.3106 g.) was heated under reflux in 0.5% methanolic hydrogen chloride (25 cc.), which was used for the isolation of I from agar, carbon dioxide evolved was only 0.0042 g. (4.06% of theory). From the reaction solution, methyl oxalacetate was obtained as its phenylhydrazone, melting at 116–118°.

Summary

1. Partial methanolysis of agar has led to isolation of a crystalline double barium salt, which is separable into its components, barium methylsulfate and a barium salt of an organic acid.

2. From the last salt above mentioned, there has been obtained a free acid having the formula $C_{14}H_{21}O_9(OCH_3)_2COOH$ as its crystalline monohydrates. Its methyl ester and amide have also been prepared in a crystalline condition.

3. The acid obtained, a new compound, has been proved to be a disaccharide derivative composed of 3,6-anhydro-L-galactose, D-galactose and pyruvic acid.

4. It has also been proved that the pyruvic acid residue is linked through its carbonyl group with the D-galactose residue.

5. The isolation of the pyruvic acid-linking disaccharide derivative substantiates the view that pyruvic acid is an intrinsic constituent of agar.

The writer wishes to express his hearty thanks to Professor S. Tanaka, Department of Science, Kyoto University, and

Professor C. Araki, this University, for their great interest and discussion. Thanks are also due to Mr. K. Arai for microanalysis and to Mr. T. Ito for assistance.

Institute of Chemistry, Faculty of Industrial Arts, Kyoto Technical University
Matsugasaki, Kyoto

Studies on the Chemical Constitution of Agar-agar. XIX. Pyruvic Acid as a Constituent of Agar-agar (Part 3)[1]. Structure of the Pyruvic Acid-linking Disaccharide Derivative Isolated from the Methanolysis Products of Agar

By Susumu HIRASE

(Received Octover 8, 1956)

In the previous work[1], a crystalline acid having the formula $C_{14}H_{21}O_9(OCH_3)_2$–COOH was isolated from the partial methanolysis products of agar. The compound was shown to be a disaccharide derivative consisting of 3,6-anhydro-L-galactose, D-galactose and pyruvic acid, the pyruvic acid residue being linked through its carbonyl group with the D-galactose residue. The structure of the compound has been further investigated, and has been proved to be 4-O-4′,6′-O-1″-carboxyethylidene-β-D-galactopyranosyl-3,6-anhydro-L-galactose dimethylacetal (I).

First, the manner in which the pyruvic acid is linked with the D-galactose residue has been studied by methylation of the methyl ester methyl galactoside (III), obtained by methanolysis of I in the previous work. The methylation was carried out by the use of Purdie's reagents to give a methylated methyl ester (VI), a viscous liquid purified by distillation in high vacuum. On hydrolysis it afforded pyruvic acid (X) and 2,3-di-O-methyl-D-galactose (XI). Pyruvic acid was identified as its crystalline phenylhydrazones. 2,3-Di-O-methyl-D-galactose, which had been synthetically known, was identified as follows. (1) Treatment with aniline gave a crystalline anilide, which was in good agreement with a synthetic sample. (2) Treatment with phenylhydrazine and acetic acid resulted in the formation of 3-O-methyl-D-galactosazone, a methoxyl group on the carbon atom C_2 being lost meanwhile. The osazone was identical with a synthetic sample. And, (3) according to the procedure of Luckett and Smith[2], the sugar was oxidized with nitric acid to give 2,3-di-O-methyl-D-galactaric acid, which was then converted to a crystalline bisamide. The identity was again established by comparison with a synthetic sample. The identification of pyruvic acid and 2,3-di-O-methyl-D-galactose as cleavage fragments of VI indicates that the pyruvic acid residue is connected through acetal linkages either with carbon atoms C_4 and C_6 of the D-galactopyranose residue or with C_5 and C_6 of the D-galactofuranose residue. The former structure, namely, methyl 4,6-O-1′-carbomethoxyethylidene-D-galactopyranoside, has been assigned to the methyl ester methyl galactoside (III), because the compound shows a positive value of optical rotation, which is in agreement only with the pyranoside structure.

On the other hand, the ester group of VI was reduced to a hydroxyl group with lithium aluminium hydride and the newly formed hydroxyl group was methylated with Purdie's reagents. The resulting product on hydrolysis yielded methoxyacetone (IX) and again 2,3-di-O-methyl-D-galactose (XI), the former product being identified as its *p*-nitrophenylhydrazone. This fact brings the same conclusion as that already brought as to the linkage between pyruvic acid and D-galactose residues.

Next, in order to study the mode of the linkage between 3,6-anhydro-L-galactose and 4,6-O-1′-carboxyethylidene-D-galactose residues, the methyl ester (II), prepared

1) Part XIX-2 : S. Hirase, This Bulletin, **30**, 70 (1957).

2) S. Luckett and F. Smith, *J. Chem. Soc.*, **1940**, 1106.

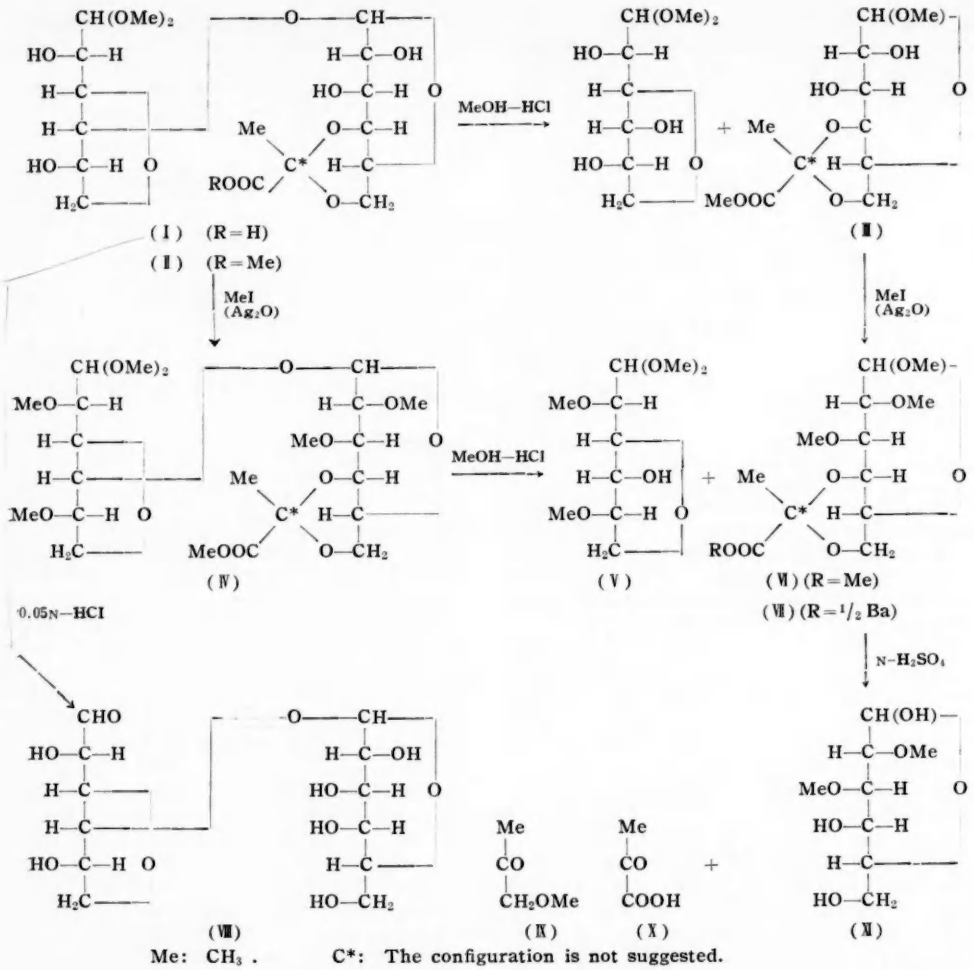

(I) (R=H)
(II) (R=Me)
(III)
(IV)
(V)
(VI) (R=Me)
(VII) (R=1/2 Ba)
(VIII)
(IX)
(X)
(XI)

in the previous work, was methylated with Purdie's reagents. The resulting methylated compound (IV) was obtained as crystals. On methanolysis it afforded a mixture of 2,5-di-O-methyl-3,6-anhydro-L-galactose dimethylacetal (V) and methyl 2,3-di-O-methyl-4,6-O-1′-carbomethoxyethylidene-D-galactoside (VI). The latter, separated from the former through its barium salt (VII), was further hydrolysed to give pyruvic acid (X) and 2,3-di-O-methyl-D-galactose (XI) in the same manner as that already described. 2,5-Di-O-methyl-3,6-anhydro-L-galactose dimethylacetal (V) was hydrolysed to the corresponding reducing sugar, which was then oxidized with bromine water to give crystalline 2,5-di-O-methyl-3,6-anhydro-L-galactonic acid. The amide of the last compound was also prepared in a crystalline condition. These two crystalline derivatives were exactly identical with the corresponding authentic samples. The identification of V and VI as cleavage fragment of IV points to the conclusion that the D-galactopyranose residue is glycosidically joined with the carbon atom C_4 of the 3,6-anhydro-L-galactose residue. Furthermore, on the basis that the compound (I) and its derivatives have negative values of optical rotation, the galactoside linkage has been suggested to be of the β-configuration. Thus, it becomes now possible to assign the structure 4-O-4′, 6′-O-1″-carboxyethylidene-β-D-galactopyranosyl-3,6-anhydro-L-galactose dimethylacetal (I) to the compound under problem.

Further support for the structure is

derived by the fact that careful hydrolysis of I resulted in the formation of pyruvic acid (X) and agarobiose (4-O-β-D-galactopyranosyl-3, 6-anhydro-L-galactose) (VIII). Moreover, the compound (I) rapidly consumed one mole of periodate in the presence of a sodium bicarbonate buffer, indicating that the presence of a pair of adjacent hydroxyl groups. In conclusion, all the experimental results are compatible with only one structure (I) for the compound isolated from the methanolysis products of agar. However, no information has been made available as to the configuration of the carbon atom C_1 (starred) of the ethylidene group.

It is of interest to note that biochemically important pyruvic acid is connected with an agarobiose unit, which is a repeating unit of agarose, a principal polysaccharide of agar[3]. Moreover, it seems probable that the carboxyl group of the pyruvic acid residue may make some contribution to a gel-forming behavior of agar. But further work is needed to solve the problem whether or not pyruvic acid is connected in the same manner of the linkage in the polysaccharide molecule as that in the compound (I) isolated.

Experimental

Unless otherwise stated evaporation and concentration were carried out under reduced pressure below 40°. All the melting points are uncorrected.

Methyl 2,3-Di-O-methyl-4,6-O-1'-carbomethoxyethylidene-D-galactoside (VI).— Methyl 4, 6-O-1'-carbomethoxyethylidene-D-galactoside (III) (2.0 g.), designated as a methyl ester methyl glycoside (VIII) in the previous paper[1], was directly dissolved in methyl iodide (20 g.) and methylated with silver oxide (7 g.) in the usual manner. The methylation was repeated four times, and the final product was purified by high vacuum distillation, VI being obtained as a colorless viscous liquid boiling at 110–115°/0.027 mm Hg; yield 1.7 g.; n_D^{20} 1.4711; $[\alpha]_D^{10}$ +97.1° (water, *c* 1.02) and +98.5° (chloroform, *c* 0.65).

Anal. Found: C, 50.65; H, 7.32; OCH_3, 40.76%; Saponification equivalent, 300. Calcd. for $C_{13}H_{22}O_8$: C, 50.97; H, 7.24; OCH_3, 40.48%; Sapon. equiv., 306.

Hydrolysis of VI.—The methylated compound (VI) (1.25 g.) above obtained was dissolved in N-sulfuric acid (50 cc.) and heated in a boiling water bath until the optical rotation of the solution reached a constant value after five hours ($[\alpha]_D$ +96°→+54°). The solution was treated with ether in a Soxhlet's apparatus for seven hours. The ether extract was used for the identification of pyruvic acid, while the residual solution was used for the isolation of 2,3-di-O-methyl-D-galactose.

(a) Pyruvic Acid (X).—The ether extract was evaporated under atmospheric pressure to remove ether. The residue, which revealed no spot of a sugar derivative on a paper chromatogram, was treated in the same manner as described in the previous paper[1]. Phenylhydrazone and *p*-nitrophenylhydrazone of pyruvic acid were prepared, the identity being established by mixed m.p. determination.

(b) 2, 3-Di-O-methyl-D-galactose (XI).—The residual solution, separated from pyruvic acid, was neutralized with barium carbonate, filtered and concentrated to a sirup, which was redissolved in acetone, filtered and again evaporated to dryness. The sugar (XI) was obtained as a colorless sirup; yield 0.70 g.; $[\alpha]_D^{11}$ +61.5° (an initial value)→+84.6° (an equilibrium value, water, *c* 0.78); OCH_3, found: 30.23% (calcd. for $C_8H_{16}O_6$: 29.81%). It migrated on a paper chromatogram to the same position as that of a synthetic sample[4,5], *n*-butanol-ethanol-water (4 : 1 : 2) being used as a mobile phase.

Anilide.—The sugar (0.16 g.) above obtained and aniline (0.07 g.) in ethanol (3 cc.) were heated under reflux for three hours. The anilide was crystallized from acetone-petroleum ether; m.p. 152–154°; $[\alpha]_D^{13}$ −61.9° (an initial value)→+12.9° (an equilibrium value, ethanol, *c* 0.63). Reported values[5] are m.p. 154–155° and $[\alpha]_D$ −56.8°→+12.1° (ethanol). The melting point was not depressed on admixture with an synthetic sample melting at 153–154°.

Anal. Found: C, 59.23; H, 7.46; N, 5.37. Calcd. for $C_{14}H_{21}O_5N$: C, 59.35; H, 7.24; N, 4.95%.

3-O-Methyl-D-galactosazone.—A mixture of 2, 3-di-O-methyl-D-galactose (0.15 g.), phenylhydrazine (0.25 g.) and 50% aqueous acetic acid (0.5 cc.) in water (2 cc.) was heated in a boiling water bath for two hours. Reddish precipitates formed were filtered, washed with water and dried. The precipitates were chromatographed on a column of active alumina, ethyl acetate being used as a developing solvent. The fresh yellow zone at the top of the column was eluted by methanol containing pyridine, and the eluate was concentrated to a small volume. Addition of water precipitated the osazone, which was further purified by dissolution in ethyl acetate and precipitation with petroleum ether; yield 0.05 g.; yellow powder; m. p. 188–191°; $[\alpha]_D^{13}$ −13.3° (ethanol, *c* 0.30). Various values are reported: m. p. 176–179°[4], 178–194°[6] and about 200°[6]. The synthetic sample, prepared and purified exactly in the same manner as above mentioned, melted at 188–191°. Mixed m.p. determination showed no depression.

Anal. Found: N, 15.31; OCH_3, 8.52. Calcd. for $C_{19}H_{24}O_4N_4$: N, 15.05; OCH_3, 8.38%.

2,3-Di-O-methyl-D-galactaric Acid Bisamide.—

3) C. Araki, This Bulletin, **29**, 543 (1956).

4) G. J. Robertson and R. A. Lamb, *J. Chem. Soc.*, **1934**, 1321.

5) D. J. Bell and G. D. Greville, ibid., **1955**, 1136.

6) F. Rebber and T. Reichstein, *Helv. Chim. Acta*, **28**, 1164 (1945).

2,3-Di-*O*-methyl-D-galactose (0.15 g.) obtained was treated by the procedure of Luckett and Smith[2], 2,3-di-*O*-methyl-D-galactaric acid bisamide was obtained as prisms; m.p. 226–228°, not depressed on admixture with a synthetic sample (m.p. 226–228°).

Anal. Found: C, 40.50; H, 6.90. Calcd. for $C_8H_{16}O_6N_2$: C, 40.67; H, 6.83%.

Reduction of VI.—A solution of VI (1.3 g.) in dry ether (20 cc.) was added dropwise to a solution of lithium aluminium hydride (0.5 g.) in dry ether (30 cc.) with stirring. After thirty minutes, an excess of water was added to the reaction mixture, which was then filtered, and the residue was washed thoroughly. Evaporation of the filtrate and washings gave a sirup, which was purified by dissolution in ether and filtration. Evaporation gave methyl 2,3-di-O-methyl-4,6-O-hydroxyisopropylidene-D-galactoside, a colorless sirup; yield 1.2 g.; n_D^{20} 1.4780; $[\alpha]_D^{25}$ +101.3° (water, *c* 0.78); OCH_3, found: 32.50% (calcd. for $C_{12}H_{22}O_7$: 33.42%).

Methyl 2,3-Di-O-methyl-4,6-O-methoxyisopropylidene-D-galactoside and its Hydrolysis.—The reduction product (1.1 g.) above obtained was twice methylated with methyl iodide and silver oxide in the usual manner. Methyl 2,3-di-O-methyl-4, 6-O-methoxyisopropylidene-D-galactoside was obtained as a colorless sirup; yield 1.0 g.; n_D^{20} 1.4681; $[\alpha]_D^{24}$ +108.1° (water, *c* 0.74); OCH_3, found: 41.77% (calcd. for $C_{13}H_{24}O_7$: 42.42%).

The sirup (0.9 g.) above obtained was dissolved in N-sulfuric acid (20 cc.) and heated in a boiling water bath for four and a half hours, at which time the optical rotation of the solution reached a constant value ($[\alpha]_D$ +107°→+66°). Methoxyacetone liberated in the hydrolysate was distilled in steam under atmospheric pressure, 60 cc. of the distillate being collected. The residual solution was used for the isolation of 2,3-di-O-methyl-D-galactose.

(a) Methoxyacetone (IX).—To the above distillate was added a methanolic solution of *p*-nitrophenylhydrazine, which caused an immediate precipitation of methoxyacetone *p*-nitrophenylhydrazone; golden needles; yield 0.35 g.; m.p. 112–113°, not depressed on admixture with an authentic sample (m.p. 112–113°).

(b) 2, 3-Di-O-methyl-D-galactose (XI).—The distillation residue was neutralized, filtered and evaporated to dryness, giving 2,3-di-O-methyl-D-galactose, a colorless sirup; yield 0.55 g.; $[\alpha]_D^{24}$ +55.6° (an initial value)→+82.8° (an equilibrium value, water, *c* 0.70); OCH_3, found: 29.62% (calcd. for $C_5H_{16}O_6$: 29.81%). It migrated to the same position on a paper chromatogram as that of a synthetic sample. Identification was carried out by its conversion into the anilide, 3-O-methyl-D-galactosazone and 2,3-di-O-methyl-D-galactaric acid bisamide exactly in the same manner as that already described.

4-O-2′,3′-Di-O-methyl-4′,6′-O-1″-carbomethoxyethylidene-β-D-galactopyranosyl-2,5-di-O-methyl-3,6-anhydro-L-galactose Dimethylacetal (IV).—The methyl ester (II) (1.0 g.), prepared in the previous paper[1], was directly dissolved in methyl iodide (35 g.), and was methylated by occasional additions of silver oxide (10 g.) in the usual manner. The methylation was repeated five times. The final product, isolated by extraction with ether and evaporation, was a colorless sirup (1.0 g.), which solidified on standing for a few months. It was recrystallized by dissolving in a small amount of absolute ether, adding petroleum ether (b.p.34–45°) and keeping the solution in a refrigerator for a few weeks. Pure IV was obtained as brilliant prisms; yield 0.78 g., m. p. 78–80°; $[\alpha]_D^{20}$ −31.6° (water, *c* 1.33) and −20.9° (chloroform, *c* 1.15).

Anal. Found: C, 51.96; H, 7.39; OCH_3, 42.50%; Saponification equivalent, 508; m.w. (Rast), 510. Calcd. for $C_{22}H_{38}O_{13}$: C, 51.75; H, 7.50; OCH_3, 42.55%; Sapon. equiv. and m.w., 511.

Methanolysis of IV.—The methylated compound (IV) (2.7 g.) in 3% methanolic hydrogen chloride (30 cc.) was heated under reflux for twentyfive hours. It was neutralized with silver carbonate, filtered and concentrated to a sirup (2.7 g.), which was proved to be a mixture of V and VI. The separation was effected by saponification as described below.

(a) Barium Salt of Methyl 2,3-Di-O-methyl-4,6-O-1′-carboxyethylidene-D-galactoside (VII).—The above mixture (2.7 g.) was heated in a 0.3 N-barium hydroxide solution (50 cc.) at 60° for two hours. The solution was neutralized with carbon dioxide, filtered and concentrated to a sirup (3.0 g.). It was then dissolved in methanol (10 cc.) and ether (100 cc.) was added with shaking, the barium salt (VII) being precipitated as a fine powder; yield 2.1 g.; $[\alpha]_D^{19}$ +48.8° (water, *c* 1.33). The filtrate was kept aside for the isolation of V.

Anal. Found: OCH_3, 25.32; Ba, 19.11. Calcd. for $(C_{12}H_{19}O_8)_2$ Ba: OCH_3, 25.84; Ba, 19.08%.

Methyl Ester (VI).—The above barium salt (2.2 g.) was converted to the methyl ester by heating in 3% methanolic hydrogen chloride (20 cc.) for five hours. The product, isolated in the usual manner, was purified by distillation in high vacuum, yielding VI as a colorless viscous liquid; yield 1.2 g.; b. p. 110–115°/0.030 mmHg; $[\alpha]_D^{21}$ +67.7° (water, *c* 0.93) and +72.4° (chloroform, *c* 1.16); n_D^{20} 1.4685.

Anal. Found: C, 50.78; H, 7.26; OCH_3, 40.42%; Saponification equivalent, 304. Calcd. for $C_{13}H_{22}O_8$: C, 50.97; H, 7.24; OCH_3, 40.48%; Sapon. equiv.; 306.

Hydrolysis.—The methyl ester (VI) above obtained was hydrolysed with N-sulfuric acid (30 cc.) for five hours. Pyruvic acid (X) and 2,3-di-*O*-methyl-D-galactose (XI) produced were identified in the same manner as that already described.

(b) 2, 5-Di-O-methyl-3, 6-anhydro-L-galactose Dimethylacetal (V).—The filtrate, separated from the barium salt (VII), was evaporated to dryness, V being obtained as a colorless sirup; yield 0.50 g.; $[\alpha]_D^{19}$ −6.67° (water, *c* 0.90); n_D^{20} 1.4563; OCH_3, found: 52.15% (calcd. for $C_{10}H_{20}O_6$: 52.48%).

2,5-Di-O-methyl-3,6-anhydro-L-galactonic Acid.

—The above dimethylacetal (0.35 g.) was hydrolysed with 0.1N-sulfuric acid (5 cc.) in a boiling water bath for two hours, neutralized with barium carbonate, filtered and concentrated to dryness. 2,5-Di-O-methyl-3,6-anhydro-L-galactose was obtained as a slightly colored sirup; yield 0.25 g.; $[\alpha]_D^{2°}$ −13.3° (water, *c* 0.75); OCH_3, found: 32.02% (calcd. for $C_8H_{14}O_5$: 32.60%).

The sugar (0.20 g.) obtained was oxidized by bromine water in the usual manner[7]. The product was crystallized from ethyl acetate. 2,5-Di-O-methyl-3,6-anhydro-L-galactonic acid was obtained as colorless prisms; yield 0.12 g.; m.p. 159–161°, not depressed on admixture with an authentic sample[7]; $[\alpha]_D^{21}$ −61.9° (water, *c* 0.42).

The mother liquor from the above crystals was concentrated to a sirup (0.08 g.), which was esterified by diazomethane in ether. The methyl ester obtained was converted to the amide by reaction with ammonia in the usual manner[7]; m.p. 171–172°, not depressed on admixture with an authentic sample[7]; $[\alpha]_D^{22}$ −71.7° (water, *c* 0.46).

Partial Hydrolysis of I.—The crystalline acid (I) (0.50 g.) in 0.05N-hydrochloric acid (10 cc.) was heated in a boiling water bath until the optical rotation of the solution reached a constant value: $[\alpha]_D$ −46.7° (initial), −30.0° (0.5 hour), −22.0° (1 hour), −18.6° (1.5 hours), −14.6° (2.0 and 2.5 hours). The solution was neutralized with silver carbonate, filtered and concentrated to a sirup. Extraction with absolute methanol separated agarobiose from insoluble silver pyruvate.

(a) Pyruvic Acid.—The silver pyruvate (0.20 g.) obtained was dissolved in water (2 cc.), N-hydrochloric acid (2 cc.) was added, and precipitates of silver chloride were removed by filtration. When phenylhydrazine (0.10 g.) was added to the filtrate, pyruvic acid phenylhydrazone was crystallized; yield 0.12 g.; m.p. and mixed m.p. 190–191°.

(b) Agarobiose (VIII).—The methanol extract, separated from silver pyruvate, gave on evaporation agarobiose as a colorless sirup, which reduced Fehling's solution at room temperature; yield 0.33 g.; $[\alpha]_D^{14}$ −13.8° (water, *c* 0.80). It was identified by conversion into its dimethylacetal.

Agarobiose Dimethylacetal.—The above sirup (0.30 g.) was dissolved in 0.5% methanolic hydrogen chloride (3 cc.) and heated under reflux for two hours. The solution was neutralized with silver carbonate, filtered and concentrated to a sirup (0.30 g.), which was then chromatographed on a cellulose powder column, *n*-butanol-water (6 : 1) being used as a mobile phase. Agarobiose dimethylacetal was obtained as crystals, which were further purified by recrystallization from ethanol-acetone (1 : 2); yield 0.20 g.; m.p. 163–164°, not depressed on admixture with an authentic sample[5]; $[\alpha]_D^{14}$ −29.5° (water, *c* 0.98); OCH_3, found; 16.39% (calcd. for $C_{14}H_{26}O_{11}$: 16.76%).

Periodate Oxidation of I.—The compound (I) (0.1615 g.) was dissolved in water (10 cc.), and 0.215M-solution of sodium metaperiodate (10.0 cc.) was added. The solution was immediately neutralized with sodium bicarbonate until it became slightly alkaline to a methyl redi ndicator, and then was diluted exactly to 50.0 cc. Aliquotes were withdrawn periodically for the determination of the residual oxidant in the usual manner. The sample consumed 0.63, 1.02 and 1.05 mole of the oxidant, respectively, after six, twenty-four and forty-eight hours. On standing for a longer period, up to two moles of the oxidant were consumed on account of the gradual hydrolysis of the pyruvic acid residue.

Summary

1. The structure of the acidic compound, isolated from the partial methanolysis products of agar in the previous work, has been investigated.

2. Methylation data have indicated that the structure of the compound is 4-O-4′, 6′-O-1″-carboxyethylidene-β-D-galactopyranosyl-3,6-anhydro-L-galactose dimethylacetal, the β-linkage being suggested on the basis of the optical rotatory behavior.

3. The structure assigned is also supported by the result of partial hydrolysis and periodate oxidation of the compound.

4. No information has been obtained as to the configuration of the carbon atom C_1 of the ethylidene group in the molecule.

The writer wishes to express his hearty thanks to Professor S. Tanaka, Department of Science, Kyoto University, and Professor C. Araki, this University, for their great interest and discussion. Thanks are also due to Mr. K. Arai for microanalysis and to Mr. T. Ito for assistance.

Institute of Chemistry, Faculty of Industrial Arts, Kyoto Technical University, Matsugasaki, Kyoto

7) C. Araki, *J. Chem. Soc. Japan*, **65**, 627 (1944).

Studies on the Organic Reagents for the Inorganic Analysis. I. Phenylfluorone as Sensitive Reagent for Colorimetric Determination of Zirconium

By Kenjiro KIMURA and Hirotoshi SANO

(Received September 25, 1956)

Although many reagents and procedures are available for the determination of macro amounts of zirconium, the situation is far from satisfactory with respect to the determination of microgram amounts. Alizarin (or Alizarin Reds)[1-5] is the most general reagent for the colorimetric determination of zirconium, but its reaction is not too sensitive. The procedures using *p*-dimethylaminoazophenylarsonic acid[6,7] and the method using phosphomolybdic acid[8] are both indirect. Only quercetin has been recently reported as the sensitive reagent for the colorimetric determination of zirconium[9].

The purpose of this investigation was to find a colorimetric reagent sensitive to small concentrations of zirconium. The studies on the reaction between ortho diphenol derivatives and zirconium or other metals show that the ortho diphenol derivatives, having the mesomeric group at its para position, combine with metals and cause remarkable color change, which is larger in the case of zirconium than the other metals[10]. On the other hand the phenylfluorone (abbreviation of 2,3,7-trihydroxy-9-phenylfluorone), which is one of the ortho diphenol derivatives concerned, has been recently employed as the sensitive reagent for germanium[11]. These facts lead us to the expect that this reagent might be one of the most sensitive reagents for the colorimetric determination of zirconium.

1) H. A. Liebhafsky and E. H. Winslow, *J. Am. Chem. Soc.*, **60**, 1776 (1938).
2) J. F. Flagg, H. A. Liebhafsky and E. H. Winslow, ibid., **71**, 3630 (1949).
3) D. E. Green, *Anal. Chem.*, **20**, 370 (1948).
4) G. B. Wengert, ibid., **24**, 1449 (1952).
5) A. Mayer and G. Bradshaw, *Analyst*, **77**, 476 (1952).
6) V. A. Nazarenko, *Zhur, Priklad, Khim*, **10**, 1696 (1937).
7) W. G. Hayes and E. W. Jones, *Ind. Eng. Chem., Anal. Ed.*, **13**, 603 (1941).
8) E. W. Kiefer and D. F. Boltz, *Anal. Chem.*, **24**, 542 (1952).
9) F. S. Grimaldi and C. E. White, ibid., **25**, 1886 (1953).
10) F. Ihmura, H. Sano and M. Asada, Symposium on complex Chemistry, Osaka City Univ., Nov. 1955 : To be published shortly.

Experimental

Apparatus and Reagents.—The absorbancy measurements were made with a Beckman Model DU spectrophotometer and 1 cm. glass cell. The reference cell contained distilled water for all the measurements.

The alcoholic solution of phenylfluorone (1 ml. contain 0.6 mg. of phenylfluorone) was made up in the following way: 0.6 g. phenylfluorone, which was synthesized from hydroxyhydroquinone triacetate and benzaldehyde according to Cluley's prescription[11], was dissolved into 800 ml. of ethyl alcohol and 5 ml. of 0.1N hydrochloric acid and was diluted to 1 l. with ethyl alcohol.

Zirconyl chloride stock solution was prepared from reagent grade zirconium dioxide contained less than 0.2 per cent hafnium dioxide by spectrographic tests, and standardized gravimetrically using distilled ammonium hydroxide. The working zirconium chloride solution was prepared by dilution from the stock solution every time of experiment.

Distilled hydrochloric acid was used for all work.

Ethyl alcohol: Reagent grade 100 percent ethyl-alcohol.

Cyclohexanol: Reagent grade.

Fundamental Reaction.—The treatment of slightly acidic solution of zirconyl ions with an excess of a standard phenylfluorone solution results in the color change from yellow to red, and then the precipitation after being allowed to stand. This precipitation has the composition of four phenylfluorone to a zirconium atom quantitiatively. This shows, therefore, also the possibility of micro gravimetric analysis of zirconium. Various organic solvents, such as benzene, toluene, cyclohexanol, ethyl ether, isopropyl ether, acetone, ethyl isopropyl ketone, dioxane, methyl alcohol, ethyl alcohol, isopropyl alcohol, *n*-butyl alcohol, isobutyl alcohol, *n*-amyl alcohol, acetic acid, acetic anhydride, ethyl acetate, carbon tetrachloride, chloroform, petroleum ether, quinoline, carbon disulfide, etc., were tried to dissolve the red colored complex, but it was difficult. Then, it was alternatively tried to keep the complex in the colloidal solution with the addition of a suitable stabilizer. Among gum arabic, gelatin, soluble starch, cylohexanol, etc., tested, cyclohexanol was found as the most favorable stabilizer. In the experiments all the

11) H. J. Clueley, *Analyst*, **76**, 523 (1951).

solutions were made to a total volume of 50 ml. The order of addition of the reagents was always the same. The zirconium solution was added first; and acid, alcohol, cyclohexanol, and alcoholic solution of phenylfluorone were added in this order.

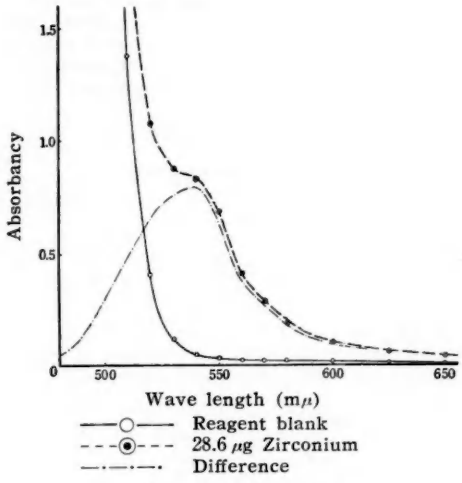

Fig. 1. Absorption spectra.

Spectral absorbancy data for the reagent blank and 28.6 μg. of zirconium (following the standard procedure mentioned later) are given in Fig. 1. The optimum wave length was taken as 530-550 mμ because at this range the absorption given by the blank is small and that by zirconium sufficiently large.

Effect of Alcohol and Cylohexanol Concentration.—A precipitate of zirconium phenylfluoronate is obtained after a while from solutions containing no cyclohexanol and less than 10ml. of alcohol. Although the colored solution becomes stable with increase in the amount of cyclohexanol added, cyclohexanol layer separates from alcoholic water layer in above a certain amount of cyclohexanol to the amount of alcohol added. The solution shows no differece in its absorbancy with the variation of the amount of alcohol or cyclohexanol added. From these results 5 ml. of cyclohexanol, 10 ml. alcohol and 10ml. alcoholic solution of phenylfluorone was taken as optimum.

Effect of Acidity and Digestion Time.— The effect of acid concentration and digestion time on the absorbancy given by 17.2 μg. of zirconium and 3 mg. phenylfluorone is illustrated in Table I. A precipitate of zirconium phenylfluoronate is obtained after it is allowed to stand for a day, but the stable suspension is able to regenerate with short shaking by hand. The absorbancy given by this procedure was shown as the data after a day. The absorbancy in 0.05 N hydrochloric acid solution is nearly constant but that in 0.10 N hydrochloric acid solution increases slowly by time. These data show that the increase of acidity causes the decrease of its absorbancy and that it means the decrease of the velocity to reach its equilibrium.

From these results it would be expected that the increase of the amount of phenylfluorone is available for obtaining the stable absorbancy in higher acidity, because the reaction should be the competition of hydrogen ion concentration with reagent concentration. The data given by 17.2 μg. of zirconium and 6 mg. of phenylfluorone are shown in Table I, too.

The stability in this condition is more favorable particularly in 0.10 N HCl, than the case of 3 mg. reagent. The reagent blank shows no variation in absorbancy at 540 mμ or more, for increasing its acidity, though the decrease in absorbancy occurs at below 530 mμ.

The stability of absorbancy for the time in the acid concentrations above 0.15 N is not so suitable as below 0.10 N for the practical procedure, probably because of its slow velocity to reach the equilibrium.

Standard Procedure.—The following was recommended as the optimum procedure from the results above mentined.

Transfer the sample solution (less than 20ml.) to a 50 ml. volumetric flask. If the sample is known to contain more than 40 to 50 μg. zirconium, an aliquot portion of the sample solution containing the desired amount of zirconium in a final volume is pipetted into a 50 ml. volumetric flask. Additional acid will then be required to bring the acidity up to 0.10 N hydrochloric acid used in the determination of zirconium with phenylfluorone. Adjust the volume to about 20 ml. with distilled water. Add 10 ml. of alcohol, 5 ml. of cyclohexanol, and 10 ml. of alcoholic solution containing 6 mg. of phenylfluorone in this order using pipettes. Make the solution to the mark, mix with shaking by hand, allow to stand for about two hours, and obtain the absorbancy of the solution in the spectrophotometer

TABLE I

ABSORBANCY IN DIGESTION TIME (min.)

Amount of Phenylfluorone	30	50	75	90	120	180	240	1500	Concn. of HCl
3 mg.	0.410	0.450	0.448	0.448	0.447	0.445	0.444	0.443	0.05N
	0.226	0.260	0.295	0.317	0.349	0.389	0.418	0.432	0.10N
6 mg.	0.507	0.520	0.528	0.535	0.542	0.557	0.565	0.574	0.05N
	0.442	0.470	0.486	0.496	0.510	0.523	0.530	0.540	0.10N
	0.359	0.400	0.430	0.445	0.463	0.492	0.501	0.518	0.15N

at 540 mμ using a 1 cm. glass cells and distilled water as a control solution. Determine the amount of zirconium by reference to a standard working curve.

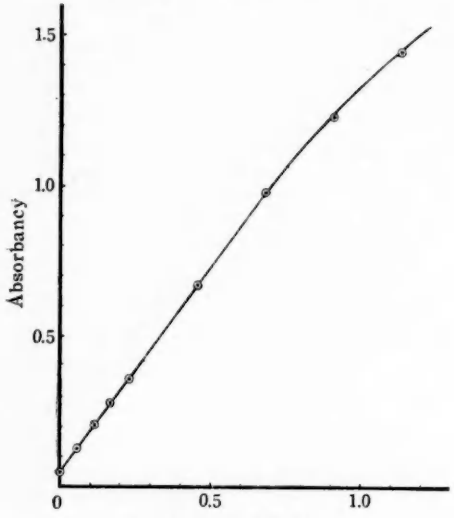

Fig. 2. Working curve

Working Curve.—Data for the working curve are given in Fig. 2. These data were obtained following the standard procedure. The solution was 0.10 N in hydrochloric acid and contained 10 ml. of alcohol, 5 ml. of cyclohexanol, and 10 ml. alcoholic solution of phenylfluorone in a total volume of 50 ml. The absorbancy was measured after allowing it to stand for about two hours. A straight line relationship between absorbancy and micrograms of zirconium is shown up to 0.7 p. p. m. Solutions containing from 0.7 to 1.0 p. p. m. deviate from the Beer's law but their absorbancies are reproducible.

The sensitivity of this method, given by the inclination of the working curve, is about forty or fifty times for Alizaline Red S method, and several times for quercetin method reported as the sensitive method for the determination of zirconium.

Effect of Diverse Ions.—The effect of various ions was studied using 0.3 p. p. m. of zirconium. The standard procedure was employed, with the exception that the desired amount of the diverse ion was added prior to the zirconium solution. In present of iron (III) or titanium (IV) a precipitation occurs, so the solution was allowed to stand for about two hours in a cell and the absorbancy was measured after they precipitated. The concentration of zirconium and diverse ion are expressed on the basis of the final volume 50 ml. The change in absorbancy was then measured at 540 mμ. Errors of less than 2 per cent of the zirconium present were considered negligible. A negligible error was obtained with the following maximum about:

2000 p. p. m. of: sodium, potassium, ammonium, magnesium, calcium, barium, strontium, zinc, cadmium, mercurous and mercuric.

500 p. p. m. of: lanthanum, neodymium, cerrous, silver and lead.

100 p. p. m. of: aluminium, thorium and uranyl. Chloride, bromide, nitrate, acetate (2000 p. p. m.) and sulfate (1000 p. p. m.) ions do not interfere.

Some elements interfere by decreasing the color intensity given by zirconium. Some elements produce colors with phenylfluorone. Table II lists the interfering ions and their effect.

TABLE II
INTERFERING DIVERS IONS

Ion	Amount added p. p. m.	Error, %	Permissible Amount, p. p. m.
Fe^{3+}	1.5	10	0.3
Ti^{4+}	0.5	20	0.05
Ge^{4+}	0.1	10	0.02
Sn^{4+}	0.1	10	0.02
As^{3+}	10	2	10
Sb^{3+}	1	5	0.4
F^-	2	25	0.1
$C_2O_4^{2-}$	55	20	0.5
HPO_4^{2-}	5	10	1

Serious interference is given by the following ions: oxalate, fluoride, phosphate, titanium, germanium, tin, iron (III) and antimony tested.

Some additional observations are to be noted. Phenylfluorone is useful as a colorimetric reagent for fluorine (by quenching of the zirconium phenylfluoronate color)[12] and may prove effective for tin (IV) or hafnium. These color reactions are being investigated.

Summary and Discussion

Methods reported in the literature for the determination of zirconium are generally designed for relatively large amounts of this element, in spite of the fact that a procedure using colorimetric reagent for the determination of trace amounts is desirable. The systematic studies on the organic reagents for the spectrophotometric determination of several metals led us the phenylfluorone as one of the most sensitive reagents for the colorimetric determination of zirconium. The phenylflurone method recommended here, which is carried out in 0.1 N hydrochloric acid solution, shows the about forty or fifty times sensitivity of Alizarine Red S method and the several times of Quercetin method reported later as a sensitive reagent for zirconium. The solution becomes stable enough to carry on the colorimetric determination by adding some cyclohexanol and

12) H. Sano, *Japan Analyst*, **5**, 289 (1956).

ethyl alcohol, although it is not true solution but colloidal.

On the other hand the investigation to find a phenylfluorone derivative to make a soluble complex with metals has succeeded recently[13]. The new reagent, 2,3,7-trihydroxyl-9-(4-dimethylaminophenyl)-fluorone, synthesized by the authors and Miss M. Asada give a soluble colored complex with germanium and make colorimetric procedure very convenient. This new reagent also forms a soluble intense colored complex with zirconium. This detailed investigation will be published before long.

The authors are indebted to Dr. Nobufusa Saito, Assistant Professor in this laboratory, for his encouragement to carry on this study.

Department of Chemistry
Faculty of Science
The University of Tokyo
Tokyo

13) K. Kimura, H. Sano, and M. Asada, *Bull. Chem. Soc. Japan*, **29**, 640 (1956).

Mikroanalyse mit Hilfe von Ionenaustauschharzen. IX. Über den Nachweis geringer Menge des Wismutes mit Thioharnstoffe[1]

Von Masatoshi FUJIMOTO

(Eingegangen am 25. Juni, 1956)

Einleitung

Es ist wohl bekannt, dass eine intensiv orange bzw. orangegelbe Färbung, die der Thioharnstoff mit wässeriger Lösung der Wismutsalze gibt, wegen ihrer bemerkenswerten Empfindlichkeit für den Nachweis[2] oder die Bestimmung geringer Menge des Wismutes und für die komplexometrische Titration des Wismutes häufig angewandt worden ist.

Kürzlich hat der Verfasser gefunden, dass die genannte sich färbende Verbindung in die Kationenaustauschharzphase stark adsorbiert wird und infolgedessen auf diese Phase eine gelbe bzw. orange Färbung, welche ausserordentlich stärker als die der Aussenlösung ist, liefert.

Im folgenden werden die Ergebnisse verschiedenartiger Versuche, die, um die Optimalbedingungen von einer neuen Nachweismethode für Wismut festzustellen, durchgeführt wurden, eingehend beschrieben.

Die in der vorliegenden Untersuchung benutzten Kationenaustauschharze

Es wurden die beinahe farblosen sowie starksauren Kationenaustauschharze[3], „1proz. DVB," „2.5proz. DVB," Dowex 50 W-X8 und -X12 angewandt und zwar alle diese als NaR- oder HR- Form.

Versuchsanordnung

Auf eine weisse Tüpfelplatte bringt man einige Körnchen der starksauren sowie farblosen Kationenaustauschharze und einen Tropfen der Probelösung, rührt sie mit einem Glasstäbchen völlig um, und lässt sie zehn Minuten lang stehen. Dann fügt man dazu einen Tropfen der wässerigen Lösung des Thioharnstoffes, und nach einigen Minuten beobachtet man mit einer Lupe eine orange bzw. orangegelbe Färbung, die in der Harzphase entsteht.

Bestimmung der Experimentalbedingungen höchster Empfindlichkeit[4]

(1) Massflüssigkeit.—Man stellte eine Stammlösung der Massflüssigkeiten des Wismutes her, indem man das Wismutnitrat in die verdünnte Salpetersäure eintrug. 1 ccm dieser Lösung enthielt genau 100.0 mg von Wismut[5].

(2) Einfluss des Vernetzungsgrades von starksauren Harzen.—Zu diesem Zwecke wurden die obigen vier Arten der starksauren Kationenaustauschharze von verschiedenem Vernetzungs-

1) Die achte Mitteilung: M. Fujimoto, Dieses Bulletin **29**, 833 (1956).
2) Z. B., vgl. I. Mellan, „Organic Reagents in Inorganic Analysis," 1. Aufl., Philadelphia (1941), S. 278.
3) M. Fujimoto, Dieses Bulletin, **29**, 600 (1956).
4) In bezug auf die halbquantitative Darstellungsweise der scheinbaren Durchschnittsintensität der Färbung der Harzphase, vergleiche die dritte Mitteilung: M. Fujimoto, Dieses Bulletin, **29**, 567 (1956).
5) Der Wismutgehalt von der genannten Massflüssigkeit wurde durch komplexometrische Titration mit 0.01 M Massflüssigkeit des Äthylendiamintetraessigsauren Natriums und 0.1prozentiger wässeriger Lösung des Brenzkatechinsulfophthaleins als Metallindikator genau bestimmt.

grade, d. h., die Harze, in denen 1-, 2.5-, 8- und 12-prozentiges Divinylbenzol enthalten sind, angewandt. Die Resultate der mit gesättigter wässeriger Lösung des Thioharnstoffes durchgeführten Untersuchung stehen gesamt in Abb. 1.

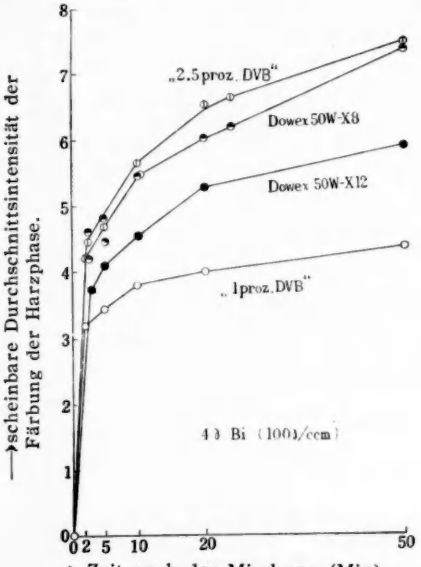

Abb. 1. Einfluss der Differenz des Vernetzungsgrades von den benutzten Harzproben (HR-Form).

Wie in dieser Abbildung zu ersehen ist, nimmt die scheinbare Intensität der Färbung von der Harzphase nach folgender Reihenfolge ab:

„2.5 proz. DVB" > Dowex 50 W-X8 > Dowex 50 W-X12 > „1 proz. DVB."

Daher wurde im folgenden lediglich „2.5proz. DVB" zur Gegenüberstellung der Experimentalbedingungen angewandt.

(3) Einfluss der anfänglich benutzten Form von „2.5 proz. DVB."—Die Gegenüberstellung von Abb. 2 stellt den Einfluss der HR- oder NaR-Form des Harzes, „2.5 proz. DVB," auf die scheinbare Intensität der Färbung von der Harzphase dar. Hier wurde auch die gesättigte Lösung des Thioharnstoffes angewandt. In Betracht des Verlaufes beider Kurven scheint es, dass das Harz von HR-Form dem von NaR-Form etwas überlegen ist.

(4) Einfluss der Zeitdauer des Eintauchens der Harzkörnchen in die Probelösung.—Abb. 3 stellt den Einfluss der Differenz von der Zeitdauer, in der die Harzkörnchen in die Probelösung eingetaucht waren, auf die Färbungsintensität der Harzphase dar; nämlich, bei der Kurve „A" wurden die Harzkörnchen zehn Minuten lang, vor dem Zusatze von Reagenslösung, in die Probelösung eingetaucht, und bei „B" wurde die Reagenslösung sofort nach dem Eintauchen der Harzkörnchen in die Probelösung hinzugefügt. Wie klar zu ersehen ist, ist es sehr wirksam, Harzkörnchen eine Weile in der Probelösung stehen zu lassen. Dies führt darauf zurück, dass die Menge des in die Harzphase adsorbierten Wismutes während etwa zehn Minuten, wegen seiner hohen Austauschaffinität

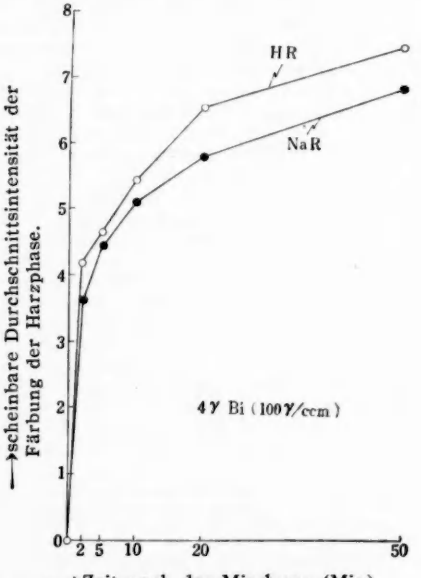

Abb. 2. Einfluss der Differenz von der Form des Harzes, „2.5 proz. DVB", auf die scheinbare Färbungsintensität.

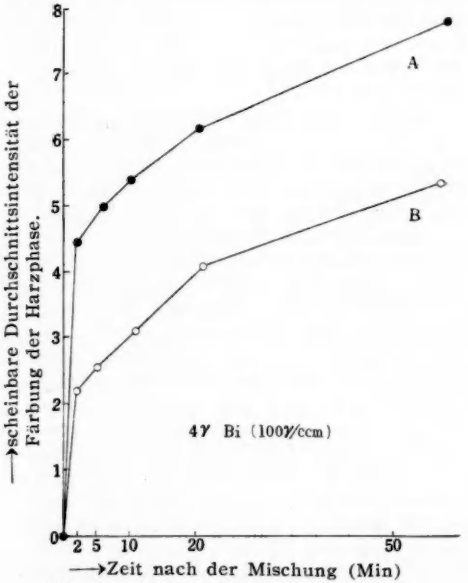

Abb. 3. Einfluss der Differenz von der Zeitdauer, in der man die Harzkörnchen in der Probelösung stehen lässt.

sowie seiner etwas kleineren Austauschgeschwindigkeit, merklich zunimmt.

(5) Einfluss der Konzentration der Reagenslösung.—Um die genannte Orangefärbung vollkommen zu entwickeln, sei es notwendig, hohe Konzentration an der Thioharnstofflösung anzuwenden, wie es in der genannten Literatur Mellans darauf hingewiesen wird, dass es bei der Anwendung betreffender Reaktion zur gewöhnlichen Tüpfelmethode empfehlenswert sei, einige Kristallchen des Thioharnstoffes hinzuzufügen[2]. Abb. 4 stellt die Abhängigkeit der

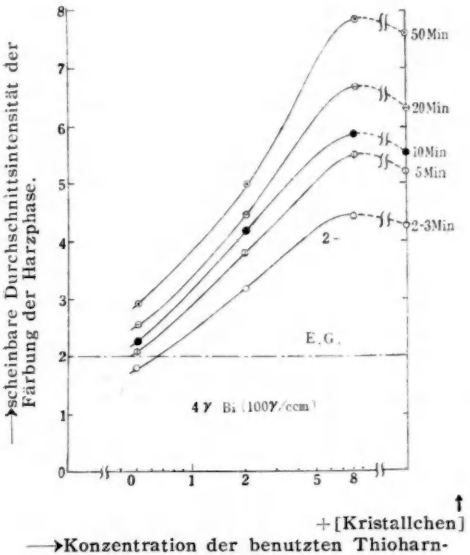

Abb. 4. Beziehung der Konzentration der benutzten Thioharnstofflösung auf die scheinbare Intensität der Färbung der Harzphase.

scheinbaren Intensität der an der Harzphase entstandenen Färbung von der Konzentration der hinzugefügten Thioharnstofflösung dar. Wie aus dem Verlauf dieser Kurvengruppe zu ersehen ist, hat die Intensität der auf die Harzphase gelieferten Färbung beim Zusatze von etwa achtprozentiger Lösung des Thioharnstoffes, d.h., von gesättigter Reagenslösung, einen Optimalwert. Zusatz von überschüssigen Kristallchen des Thioharnstoffes wirkt vielmehr nachteilig auf die Farbenentwicklung an der Harzphase ein. Über diese Tatsache könnte man aus blosser Rücksicht des später diskutierten Einflusses von der Neutralsalzkonzentration etwas erwarten.

(6) Einfluss der Salzkonzentration.—Abb. 5 stellt den Einfluss der Neutralsalzkonzentration an der Probelösung auf die scheinbare Intensität der Färbung der Harzphase dar. Ammoniumnitrat wurde dabei als ein Vertreter solcher

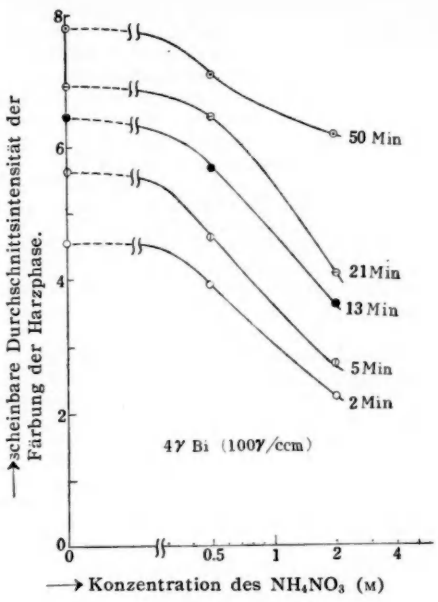

Abb. 5. Einfluss von der Neutralsalzkonzentration an der Probelösung auf die scheinbare Intensität der Färbung der Harzphase.

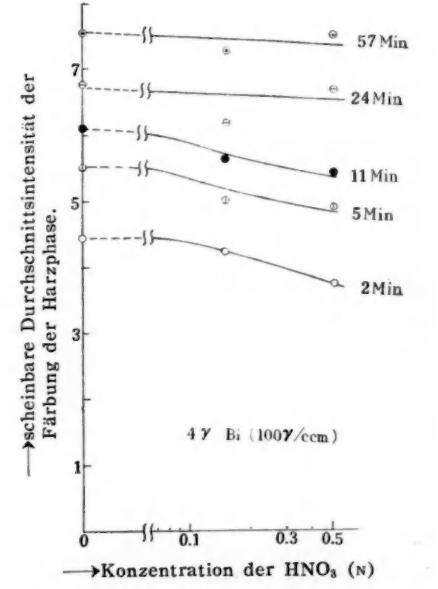

Abb. 6. Einfluss von der Säurekonzentration an der Probelösung auf die scheinbare Intensität der Färbung der Harzphase.

Neutralsalze ausgewählt. Diese Kurven zeigen, dass die in der Probelösung vorhandenen Neutralsalze bis zu etwa 0.5 M an ihrer Konzentration kaum die Färbung der Harzphase schwächen.

(7) Einfluss der Säurekonzentration.—Wie Abb. 5 und 6 zeigen, übt die Anwesenheit der Salpetersäure, deren Konzentration niedriger als 0.5 N liegt, auf die Färbungsintensität der Harzphase keinen Einfluss mehr als die der letzterwähnten Neutralsalzkonzentration aus.

(8) Experimentalbedingungen höchster Empfindlichkeit. — Aus Rücksicht aller obenerwähnten Fa ktoren wurde das folgende Verfahren als das empfindlichste ausgewählt:

„Man bringt auf eine weisse Tüpfelplatte einige Körnchen starksauren Kationenaustauschharzes, dessen Divinylbenzolgehalt etwa 2.5 prozentig ist, einen Tropfen der Probelösung, für welche man vorher die Neutralsalzkonzentration niedriger als 0.5 N reguliert, rührt dieses Gemisch mit einem Glasstäbchen völlig um und lässt es länger als zehn Minuten stehen. Dann fügt man einen Tropfen gesättigter wässeriger Lösung des Thioharnstoffes dazu, und nach etwa zehn Minuten beobachtet man eine in der Harzphase entstandene Orange- bzw. Gelborangefärbung gewöhnlicherweise mit einer Lupe von zwanzigfacher Vergrösserung."

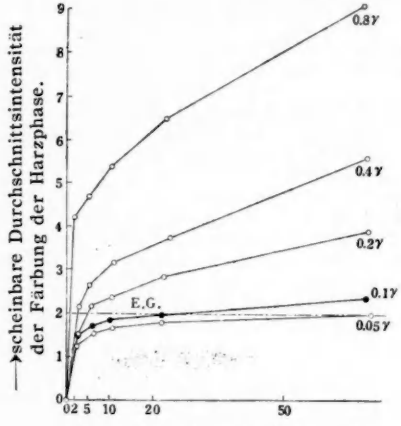

Abb. 7. Bestimmung der Erfassungsgrenze.

TABELLE I

EINFLÜSSE DER BEGLEITSTOFFE

Begleitstoffe	benutzter Verbindungstypus	Färbung der Harzphase*	Menge der Begleitstoffe	nachweisbare Wismutmenge	Grenzverhältnis	Bemerkungen**
Ti(IV)	$TiOSO_4$	farblos	110 γ	0.1 γ	$1:1.1\times10^3$	—
V(V)	NH_4VO_3	himmelblau	40 γ	0.4 γ	$1:1\times10^2$	*a*, V≦0.2 proz.
Cr(III)	$KCr(SO_4)_2$	dunkelgrau-violettblau	400 γ	0.4 γ	$1:1\times10^3$	*a*
Mn(II)	$MnSO_4$	farblos	1600 γ	0.1 γ	$1:1.6\times10^4$	—
Fe(III)	$Fe(NO_3)_3$	hellviolett	200 γ	0.1 γ	$1:2\times10^3$	—
Fe(II)	Mohrsches Salz	farblos	510 γ	0.1 γ	$1:5.1\times10^3$	—
Co(II)	$CoSO_4$	hellblau	320 γ	0.16 γ	$1:2\times10^3$	*a*
Ni(II)	$Ni(NO_3)_2$	hellblaugrün	360 γ	0.1 γ	$1:3.6\times10^3$	*a*
Cu(II)	$CuSO_4$	himmelblau	160 γ	0.16 γ	$1:1\times10^3$	*a*, Cu≦0.4 proz.
Zn(II)	$ZnSO_4$	farblos	360 γ	0.1 γ	$1:3.6\times10^3$	—
Cd(II)	$CdSO_4$	farblos	1800 γ	0.1 γ	$1:1.8\times10^4$	—
Hg(II)	$Hg(NO_3)_2$	dunkelgelb bzw. schwarz	115 γ	0.34 γ	$1:3.4\times10^2$	Hg≦0.3 proz.
Cr(VI)	$K_2Cr_2O_7$	grasgrün	20 γ	0.4 γ	$1:5\times10$	Cr(VI)≦0.1 proz.
Mo(VI)	$(NH_4)_2MoO_4$	farblos	410 γ	0.1 γ	$1:4.1\times10^3$	—
W(VI)	Na_2WO_4	farblos	450 γ	0.4 γ	$1:1.1\times10^3$	—
U(VI)	$UO_2(CH_3COO)_2$	sehr hell gelb	36 γ	0.1 γ	$1:3.6\times10^2$	*a*, U≦0.1 proz.
Pb(II)	$Pb(NO_3)_2$	blassgelb	2200 γ	0.1 γ	$1:2.2\times10^4$	*a*
Ge(IV)	GeO_2	farblos	26 γ	0.1 γ	$1:2.6\times10^2$	—
Al(III)	$Al(NO_3)_3$	sehr hell gelb	1600 γ	0.16 γ	$1:1\times10^4$	—
Ag(I)	$AgNO_3$	farblos	180 γ	0.1 γ	$1:1.8\times10^3$	—
F^-	KF	farblos	660 γ	0.16 γ	$1:4.1\times10^3$	—
HPO_4^{2-}	Na_2HPO_4	farblos	190 γ	0.4 γ	$1:4.8\times10^2$	—
NO_2^-	$NaNO_2$	farblos	350 γ	0.1 γ	$1:3.5\times10^3$	—

* Dies bedeutet die Färbung der Harzphase in dem Falle, wo nur der Begleitstoffe in der Versuchslösung vorhanden ist.

** *a*: Nur dann ist das gegebene Grenzverhältnis nutzbar, wenn der Nachweis mit einem Blindversuche miteinander ausgeführt wird.

Bestimmung der Erfassungsgrenze

Die Resultate der für verschiedene Wismutmengen durch das obigerweise bestimmte beste Verfahren durchgeführten Untersuchung werden in Abb. 7 zusammengestellt, woraus man als Erfassungsgrenze für Wismut 0.1 γ einfach bestimmen kann. Die Grenzkonzentration des in der Probelösung vorhandenen Wismutes beträgt $1 : 4 \times 10^5$.

Einflüsse der Begleitstoffe

Die Resultate dafür stehen gesamt in Tabelle I.

Wie aus der genannten Tabelle zu ersehen ist, übt die grössere Menge von allen fremden Stoffen ausser Vanadate, Chromate und Uranylsalze kaum einen Einfluss auf die Nachweisreaktion aus, d. h., die vorliegende Nachweismethode ist von hoher Selektivität.

Zusammenfassung

1. Die Anwendung der niedriger vernetzten, farblosen und starksauren Kationenaustauschharze zur Farbenreaktion zwischen Wismutsalzen und Thioharnstoffen ist für den Nachweis des Wismutes entschieden wirksam und dadurch kann man geringe Menge des Wismutes sehr scharf und auch spezifisch nachweisen.

2. Das beste Verfahren wird durch ausführlichste Untersuchung über verschiedenartige Experimentalbedingungen vollkommen bestimmt (vgl. den Abschnitt „Bestimmung der Experimentalbedingungen"), und die Einflüsse von zahlreichen Begleitstoffen werden genau untersucht.

Zum Schluss möchte der Verfasser Herrn Prof. Dr. E. Minami für seine zahlreichen wertvollen Ratschläge bei der vorliegenden Untersuchung seinen herzlichsten Dank aussprechen.

Für die Harzproben, „1 proz. DVB" und „2.5 proz. DVB", ist der Verfasser Herrn Prof. Dr. A. Kawamura an der Landwirtschaftlichen und Technischen Universität zu Tokyo zu grossem Dank verpflichtet.

Die hier benutzte komplexometrische Titration für die Wismutmassflüssigkeit wurde von Herrn K. Mizumachi freundlich angeleitet, wofür der Verfasser ihm seinen verbindlichsten Dank sagt.

Laboratorium der analytischen Chemie,
Chemisches Institut der
wissenschaftlichen Fakultät,
Tokyo Universität, Tokyo

Mikroanalyse mit Hilfe von Ionenaustauschharzen. X. Über den Nachweis geringer Menge des Kupfers mit p-Phenylendiamin und Ammoniumrhodanid[1]

Von Masatoshi Fujimoto

(Eingegangen am 28. Juni, 1956)

Einleitung

Wenn eine ammoniakalische Lösung der Kupfersalze mit *p*-Phenylendiamin und Kalium- oder Ammoniumrhodanid reagiert, so fällt ein schwarzer Niederschlag, sogenanntes „Kupferrhodanid-*p*-phenylendiamin," aus. Dieser Niederschlag ist zum Nachweis geringer Menge des Kupfers anwendbar, obgleich dessen Zusammensetzung gegenwärtig nicht genau bekannt ist[2]. Bei der vorliegenden Arbeit wurden die farblosen sowie starksauren Kationenaustauschharze zur genannten Niederschlagbildungsreaktion angewandt, und eine empfindliche sowie spezifische Nachweismethode für Kupfer wurde neu festgestellt[3].

Die in der vorliegenden Untersuchung benutzten Ionenaustauschharze

Zum gegenwärtigen Zwecke wurden hauptsächlich beinahe farblose sowie starksaure Kationenaustauschharze[4] von verschiedenem Vernetzungsgrad, „1proz. DVB," „2.5proz. DVB," Dowex 50W-X8 und „20proz. DVB,"

1) Die neunte Mitteilung: M. Fujimoto, Dieses Bulletin **30**, 83 (1957).

2) Es ist empirisch schon bekannt, dass der genannte schwarze Niederschlag 25.08prozentiges Kupfer enthält: vgl. I. Mellan, „Organic Reagents in Inorganic Analysis" 1. Aufl., Philadelphia (1941), S. 356.

3) Hinsichtlich der mikroanalytischen Anwendbarkeit der Ionenaustauschharze zur Niederschlagbildungsreaktionen, vergleiche M. Fujimoto, Dieses Bulletin **29**, 646 (1956).

angewandt. Überdies wurde ein käufliches aus Methacrylsäure und Divinylbenzol dargestelltes schwachsaures und weisses Harz von Carbonsäuretypus angewandt.

Alle diese wurden vor dem Gebrauch in gewöhnlicher Weise durch zweimaliges Durchlaufen der 2N Salzäure sowie des „entionisierten Wassers"[5] in die HR-Form völlig übergeführt.

Versuchsanordnung

Zuerst bringt man auf eine weisse Tüpfelplatte einige Körnchen des farblosen, starksauren Kationenaustauschharzes von HR-Form und einen Tropfen verdünnter wässeriger Lösung des *p*-Phenylendiamins, rührt sie mit einem Glasstäbchen völlig um und lässt sie etwa fünf Minuten stehen. Dann fügt man nacheinander je einen Tropfen der Probelösung, verdünnten Ammoniakwassers und verdünnter wässeriger Lösung des Ammoniumrhodanids dazu. Nach etwa zehn Minuten beobachtet man mit einer Lupe eine Dunkelviolettbraun- bzw. Violettgraufärbung, die in der Harzphase entsteht.

Massflüssigkeit und Reagenzien

(1) Massflüssigkeit.—Man stellte eine Stammlösung der Massflüssigkeiten des Kupfers her, indem man umkristallisiertes Kupfersulfat in 0.1N Schwefelsäure eintrug. 1 ccm dieser Stammlösung enthielt genau 1.000 mg von Kupfer[6].

(2) Reagenzien

(1) Entionisiertes Wasser.—Um die Verunreinigung der Spurmenge des Kupfers, welches in dem mit einem Messingapparat destillierten Wasser häufig enthalten ist, gründlich zu beseitigen, wurde bei dieser Arbeit ausserordentlich reines Wasser, das aus gewöhnlichem destilliertem Wasser durch eine Mischharzsäule (Durchmesser von 4.5 cm und Länge von 5 cm), welche aus Äquivalentmenge des Kationenaustauschharz von HR-Form sowie des Anionenaustauschharz von ROH-Form besteht, d. h., sogenanntes „Monobed," dargestellt wurde, folgerichtig angewandt[7]. Nunmehr wird dieses Wasser kurz als „entionisiertes Wasser" bezeichnet.

(2) Einprozentige Lösung des *p*-Phenylendiamins.—Als Stammlösung des *p*-Phenylendiamins wurde 1prozentige wässerige Reagenslösung hergestellt. Diese Stammlösung wird, wenn es nötig ist, mit entionisiertem Wasser beliebig verdünnt. Da die wässerige Lösung des *p*-Phenylendiamins nicht länger als ein paar Tage vorhält, ist es wünschenswert, dass man diese gerade vor dem Gebrauch frisch herstellt.

(3) Zwanzigprozentige wässerige Lösung des Ammoniumrhodanids.—Aus extrareinem Ammoniumrhodanid und entionisiertem Wasser wurde diese Stammlösung hergestellt.

(4) Ammoniakwasser.—Käufliches extrareines Ammoniakwasser wurde vorbereitet.

Bestimmung der Bedingungen höchster Empfindlichkeit[8]

(1) Vergleichung verschiedenartiger Verfahren.—Abb. 1 zeigt den Färbungsverlauf der Harzphase an, worin die Resultate der durch verschiedenartige Verfahren durchgeführten Untersuchungen gegenübergestellt werden. In diesem Falle wurde lediglich „1proz. DVB" von HR-Form und 6N Ammoniakwasser benutzt. Wie aus dieser Vergleichung zu erwarten ist, wurde hiernach das Verfahren „I_c" als das beste Verfahren verwandt.

(2) Einfluss der Konzentration benutzter

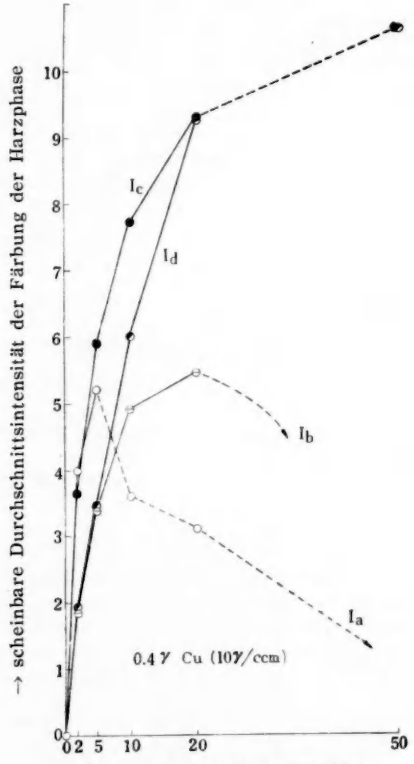

Abb. 1. Vergleichung verschiedener Verfahren

4) In bezug auf die abgekürzte Schreibweise wie „1proz. DVB" usw., vergleiche die sechste Mitteilung: M. Fujimoto, Dieses Bulletin, **29**, 630 (1956).

5) Dieses „entionisierte Wasser" wurde von Herrn Y. Sateau in solcher weise, wie in den Abschnitt „Massflüssigkeit und Reagenzien" genau erwähnt, dargestellt.

6) Die Menge des in der obengenannten Stammlösung vorhandenen Kupfers wurde aus der Menge des anfänglich benutzten umkristallisierten Kupfersulfates, $CuSO_4 \cdot 5H_2O$, rückgängig berechnet.

7) Herr Y. Sateau hat kürzlich die Reinheit dieses Wassers mit Dithizon geprüft und er hat es bewiesen, dass das betreffende Wasser überhaupt kein Kupfer enthielt.

8) In bezug auf die halbquantitative Darstellungsweise der scheinbaren Durchschnittsintensität der Färbung der Harzphase, vergleiche die dritte Mitteilung: M. Fujimoto, Dieses Bulletin, **29**, 567 (1956).

TABELLE I

VERSCHIEDENE EXPERIMENTALBEDINGUNGEN VON ABB. 1

Nr. des Expts.	Zeichen der Kurve	Ordnung der Versetzung von Harze, Reagenzien u. Probelsg. 1.	2.	3.	4.	5.	Bemerkungen*
Ia	---○---	HR**	6N Ammoniakwasser	20proz. Lsg. des Ammoniumrhodanids	Probelsg.***	1proz. Lsg. des *p*-Phenylendiamins	*a*
Ib	---⊖---	HR	6N Ammoniakwasser	20proz. Lsg. des Ammoniumrhodanids	Probelsg.	0.1proz. Lsg. des *p*-Phenylendiamins	*b*
Ic	——●——	HR	0.1proz. Lsg. des *p*-Phenylendiamins—(5 Min)****	→Probelsg.	6N Ammoniakwasser	1proz. Lsg. des Ammoniumrhodanids	*c*
Id	——◐——	HR	Probelsg.—(5 Min)	→6N Ammoniakwasser	1proz. Lsg. des Ammoniumrhodanids	0.1proz. Lsg. des *p*-Phenylendiamins	*c*

* *a*: Da die Harzkörnchen sich selbst dann schwarz bzw. grauschwarz färben, wenn kein Kupfer in der Probelösung enthalten ist, ist der Nachweis geringer Menge des Kupfers kaum ausführbar.
b: Die Harzkörnchen färben sich etwas schwächer violettbraun.
c: Die Harzkörnchen färben sich bedeutend stark braunschwarz. Enthält die Probelösung kein Kupfer, so färbt sich die Harzphase nur sehr hell bläulich grau.

** An dieser Tabelle bedeutet HR „1 proz. DVB" von HR-Form.

*** Die hier angewandte Probelösung enthielt 0.4 γ Kupfer (10 γ/ccm).

**** Zeitdauer nach dem Eintauchen der Harzkörnchen in die betreffende Lösung.

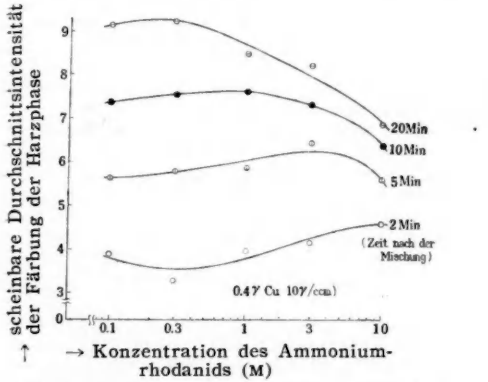

Abb. 2. Einfluss der Konzentration des Ammoniumrhodanids auf die scheinbare Intensität der Färbung.

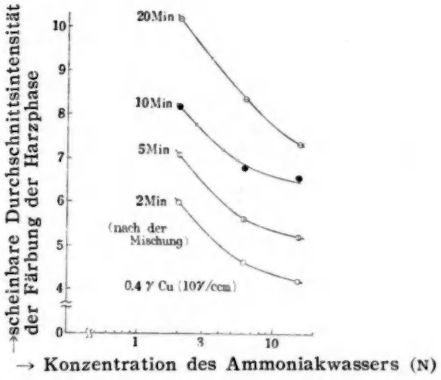

Abb. 3. Einfluss der Konzentration des Ammoniakwassers auf die scheinbare Intensität der Färbung

Ammoniumrhodanidlösung.—Wie in Abb. 2 zu ersehen ist, übt die Konzentration der benutzten Ammoniumrhodanidlösung auf die Färbungsintensität der Harzphase nur geringfügigen Einfluss aus. Jedoch wurde im folgenden 0.3prozentige Lösung des Ammoniumrhodanids deshalb besser angewandt, weil bei dieser Konzentration die Färbung der Harzphase später als etwa 15 Min nach der Mischung merklicher als bei den Fällen der anderen Konzentrationen zunimmt.

(3) Einfluss der Konzentration des Ammoniakwassers. — Die Anwendung konzentrierten Ammoniakwassers beeinflusst die Färbung der Harzphase nachteilig. Abb. 3 zeigt die Abhängigkeit der Färbungsintensität der Harzphase von der Ammoniakwasserkonzentration. Aus der Vergleichung von 2,6 und 15N Ammoniakwasser, wurde 2N Ammoniakwasser als das geeignetste ausgewählt.

(4) Einfluss der Konzentration der Reagenslösung.—Mit dem Harze, „1proz. DVB", von HR-Form, 0.3prozentiger Lösung des Ammoniumrhodanids, 2N Ammoniakwasser und 1-, 0.1- und 0.01-prozentiger Lösung des *p*-Phenylendiamins wurde der Einfluss der Konzentration der *p*-Phenylendiaminlösung auf die Färbungsintensität der Harzphase gegenübergestellt. Die Resultate stehen in Abb. 4. Mit 0.01prozentiger Lösung war die Färbung sehr schwach, mit 1prozentiger Lösung färbte sich die Harzphase selbst dann stark violettbraun, auch wenn die Probelösung kein Kupfer enthielt. Daher ist hierbei die Anwendung 1prozentiger wässeriger Lösung des *p*-Phenylendiamins wünschenswert.

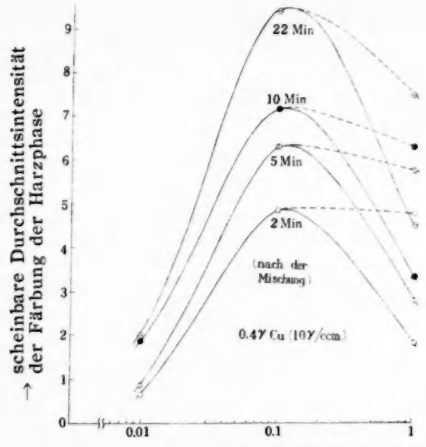

→ Konzentration der Reagenslösung (proz.)

Abb. 4. Einfluss der Konzentration benutzter Reagenslösung
--- Bruttofärbungsintensität der Harzphase
—— Nettofärbungsintensität der Harzphase verglichen mit dem Blindversuche.

(5) Einfluss der Harzart.—Schliesslich wurde der Einfluss verschiedenartiger Harzproben von HR-Form auf die Färbungsintensität untersucht. Abb. 5 zeigt die Resultate solcher Versuche an, wonach die scheinbare Intensität der Färbung von der Harzphase nach folgender Reihenfolge abnimmt:

„1proz. DVB" > „2.5proz. DVB" > Dowex 50 W-X8 > Amberlite IRC-50 > „20proz. DVB."

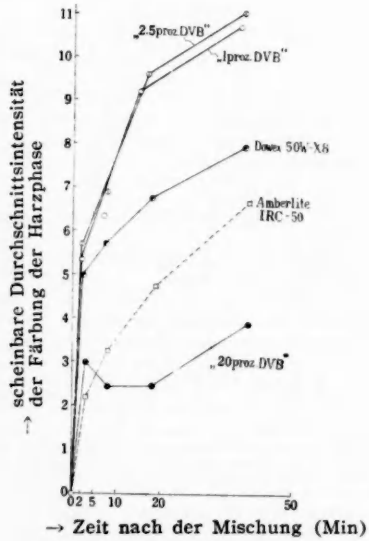

→ Zeit nach der Mischung (Min)

Abb. 5. Einfluss der Harzart

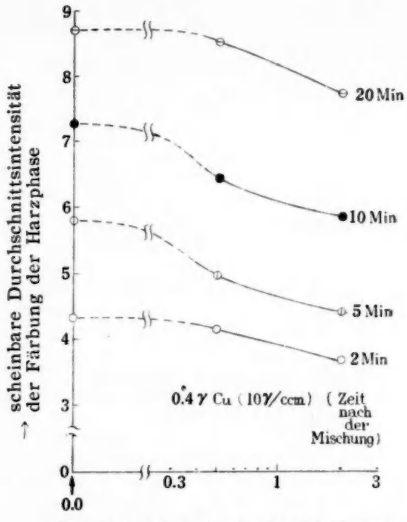

→ Konzentration des in der Probelösung vorhandenen Natriumchlorids (N)

Abb. 6. Einfluss der Neutralsalzkonzentration auf die Färbungsintensität der Harzphase

Mit Rücksicht auf die Färbung des Blindversuches, wurde im folgenden „1proz. DVB" schlechthin angewandt.

(6) Einfluss der Neutralsalzkonzentration.—Wie aus dem Verlaufe in Abb. 6 beschriebenen Kurven zu ersehen ist, beeinflusst die Salzkonzentration der Probelösung die scheinbare Färbungsintensität der Harzphase sehr wenig, d. h., wenn man nur die Neutralsalzkonzentration an der Probelösung niedriger als 3N hält, so wird die Violettbraunfärbung der Harzphase kaum geschwächt.

(7) Bedingungen höchster Empfindlichkeit.—Alles Obenerwähnte zusammengenommen, wird das beste Verfahren wie folgt genau festgestellt:—

„Man bringt auf eine weisse Tüpfelplatte einige Körnchen des starksauren und niedrig vernetzten farblosen Kationenaustauschharzes, „1proz. DVB," von HR-Form und einen Tropfen frisch hergestellter 0.1prozentiger wässeriger Lösung des *p*-Phenylendiamins, rührt sie mit einem Glasstäbchen sorgfältig um, und lässt sie etwa fünf Minuten stehen. Dann fügt man dazu nacheinander je einen Tropfen der Probelösung, des 2N Ammoniakwassers, und 0.3prozentiger Lösung des Ammoniumrhodanids, und lässt dieses Gemisch noch etwa zehn Minuten stehen. Schliesslich beobachtet man eine in der Harzphase entstandene Dunkelviolettbraun- bzw. Violettgraufärbung unter Beleuchtung einer Tischlampe mit einer Lupe von zwanzigfacher Vergrösserung."

Bestimmung der Erfassungsgrenze

Die Resultate der mit dem letztgenannten besten Verfahren durchgeführten Experimente,

TABELLE II

EINFLÜSSE DER BEGLEITSTOFFE

Begleitstoffe	benutzter Verbindungstypus	Färbung der Harzphase*	Menge der Begleitstoffe	nachweisbare Kupfermenge	Grenzverhältnis	Bemerkungen**
Cr(III)	$KCr(SO_4)_2$	hellgraugrün	32 γ	0.04 γ	$1:8\times10^2$	*a*, Cr(III) ≤0.1proz.
Mn(II)	$MnSO_4$	farblos	360 γ	0.04 γ	$1:9\times10^3$	—
Fe(III)	**$FeCl_3$**	**dunkelgelbbraun**	**3.2 γ**	**0.08 γ**	**$1:4\times10$**	**Fe(III) ≤0.01proz.**
〃	〃	grau	32 γ	0.08 γ	$1:4\times10^2$	*a*, *b*, Fe(III) ≤0.1proz.
Fe(II)	Mohrsches Salz	dunkelgrün	46 γ	0.08 γ	$1:5.7\times10^2$	*a*, Fe(II) ≤0.15proz.
Co(II)	**$CoCl_2$**	**olivengrün (?)**	**2.8 γ**	**0.16 γ**	**$1:1.8\times10$**	**Co(II) ≤0.01proz.**
Ni(II)	$Ni(NO_3)_2$	dunkelgrün	1000 γ	0.2 γ	$1:5\times10^3$	—
Zn(II)	$ZnSO_4$	hellviolettbraun	320 γ	0.08 γ	$1:4\times10^3$	*a*
Cd(II)	$CdSO_4$	dunkelgrün	1200 γ	0.06 γ	$1:2\times10^4$	—
Hg(II)	$Hg(NO_3)_2$	hellviolettgrau	72 γ	0.04 γ	$1:1.8\times10^3$	*a*
Ag(I)	**$AgNO_3$**	**bläulich hellgrau**	**3.2 γ**	**0.04 γ**	**$1:8\times10$**	**Ag ≤0.01proz.**
〃	〃	〃 〃	270 γ	0.13 γ	$1:2\times10^3$	*c*
Pb(II)	$Pb(NO_3)_2$	grauviolettbraun	2300 γ	0.02 γ	$1:1.1\times10^5$	*a*
Bi(III)	$Bi(NO_3)_3$	hellgrünbraun	3200 γ	0.08 γ	$1:4\times10^4$	—
Cr(VI)	**$K_2Cr_2O_7$**	**bläulich grauviolett**	**3.6 γ**	**0.02 γ**	**$1:1.8\times10^2$**	***a*, Cr(VI) ≤0.01proz.**
Mo(VI)	$(NH_4)_2MoO_4$	sehr hell violettbraun	36 γ	0.02 γ	$1:1.8\times10^3$	Mo(VI) ≤0.2proz.
〃	〃	grauviolett	440 γ	0.04 γ	$1:1.1\times10^4$	*a*, *b*
W(VI)	Na_2WO_4	dunkelviolett	330 γ	0.08 γ	$1:4.1\times10^3$	*a*
U(VI)	$UO_2(CH_3COO)_2$	grau	72 γ	0.02 γ	$1:3.6\times10^3$	U(VI) ≤0.2proz.
Al(III)	$Al(NO_3)_3$	hellgraublauviolett	160 γ	0.08 γ	$1:2\times10^3$	*a*, Al ≤0.5proz.
NO_2^-	**$NaNO_2$**	**hell violettlich grau**	**7 γ**	**0.04 γ**	**$1:1.8\times10^2$**	***a*, NO_2^- ≤0.02proz.**
〃	〃	hell violettlich braun	350 γ	0.04 γ	$1:8.8\times10^3$	*d*
$C_2O_4^{2-}$	Oxalsaures Ammonium	hellgrauviolett	890 γ	0.04 γ	$1:2.2\times10^4$	—
$C_4H_4O_6^{2-}$	Seignettesalz	bläulich hellgrau	950 γ	0.04 γ	$1:2.4\times10^4$	—
$C_6H_5O_7^{3-}$	Zitronensaures Ammonium	bläulich grau	1340 γ	0.04 γ	$1:3.6\times10^4$	—

* Dies zeigt den Ton der Färbung, die in der Harzphase dann entsteht, wenn die genannte Probelösung nur den Begleitstoff enthält.

** *a*: Nur dann ist das obige Grenzverhältnis nutzbar, wenn der Nachweis mit einem Blindversuche miteinander ausgeführt wird.

b: Nach dem Zusatze eines Tropfens 5prozentiger Lösung des Ammoniumzitrates wurde der Nachweis ausgeführt.

c: Hier fallen alle Silberionen durch Zusatz eines Tropfens der 0.5N Lösung von Natriumchlorid als Silberchlorid aus. Danach wurde der Nachweis mit einem Tropfen von dessen Lösungsphase ausgeführt.

d: Nach dem Zusatze eines Tropfens der 6N Salzsäure und von etwa 5 mg festen Harnstoffes wurde der Nachweis ausgeführt.

bei denen die verschiedene Menge des Kupfers enthaltenden Probelösung angewandt wurden, stehen zusammen in Abb. 7:

Die Erfassungsgrenze von 0.02 γ Kupfer unter Grenzkonzentration $1:2\times10^6$ wurde so eindeutig bestimmt.

Einflüsse der Begleitstoffe

Tabelle II schildert die Einflüsse fremder Stoffe auf die vorliegende Nachweismethode. Eisen(III)-, Kobalt(II)- und Silbersalze, Chromate, Bichromate und Nitrite stören den Nachweis beträchtlich. Diese werden an der genannten Tabelle mit fetten Schriften beschrieben.

Beobachtung des an der Grenzfläche zweier Phasen sich bildenden Niederschlags

Abb. 8 stellt das vergrösserte Bild des mit einer Sicherheitsrasierklinge abgeschnittenen Querschnitts von einem der Harzkörnchen dar, „1 proz. DVB", welche sich nach dem Verfahren „I_c" von Abb. 1 etwa eine Stunde nach der Mischung stark färben. Dabei ist es sehr interessant, dass, wie Abb. 8c klar zeigt, nur die

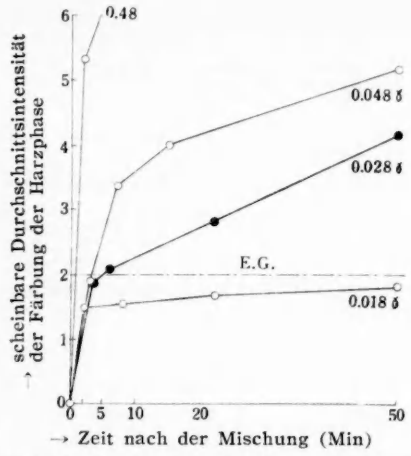

Abb. 7. Bestimmung der Erfassungsgrenze.

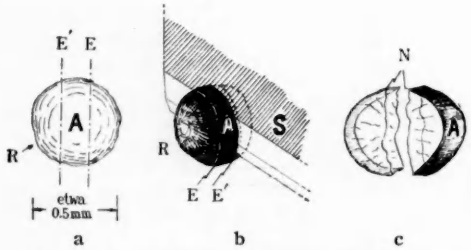

Abb. 8. Vergrössertes Bild des mit Rasierklinge abgeschnittenen Harzkörnchens

R: Harzkörnchen,
A: Abschnitt des Harzkörnchens,
E, E': Einschnitt,
S: Sicherheitsrasierklinge,
N: Niederschlagschale des Kupferrhodanid-*p*-Phenylendiamins, und
c: vergrössertes Bild vom Abschnitt des Harzkörnchens, das sich in die zwei Bruchstücke abspaltet.

Oberfläche des Harzkörnchens wie die Apfelschale sich entschieden stark färbt, während gerade die Innenseite der Oberfläche des Harzkörnchens genau wie dessen Kern sich gar nicht färbt.

Aus dieser Beobachtung wird es klar, dass die hier gewonnene ausserordentliche Erhöhung der Empfindlichkeit von der gegenwärtigen Nachweisreaktion gerade auf dem Niederschlag beruht, der sich an der dünnsten Grenzfläche zweier Phasen bildet[3].

Zusammenfassung

1. Durch mikroanalytische Anwendung farbloser starksaurer sowie niedrig vernetzterKationenaustauschharze zurNiederschlagbildungsreaktion zwischen den Kupfersalzen und dem *p*-Phenylendiamin sowie dem Ammoniumrhodanid steigt die Empfindlichkeit genannter Reaktion ausserordentlich an, und dadurch wird eine empfindliche Nachweismethode für die geringe Menge des Kupfers neu festgestellt.

2. Das empfindlichste Nachweisverfahren wird durch genaue Vergleichung verschiedener Experimentalfaktoren, wie Ordnung der Versetzung, Konzentration des Ammoniakwassers, der Ammoniumrhodanid- oder der *p*-Phenylendiaminlösung, Harzart, Neutralsalzkonzentration der Probelösung, usw., einwandfrei genau bestimmt.

3. Die Einflüsse verschiedenartiger Begleitstoffe werden, wie in Tabelle II zu ersehen ist, ausführlich untersucht.

4. Aus der einfachen Beobachtung des mit einer Rasierklinge abgeschnittenen Querschnitts des Harzkörnchens, wird die auf die dünnste Grenzfläche zwischen Harz- und Lösungsphase eingeschränkte Niederschlagbildung deutlich gezeigt.

Herrn Prof. Dr. E. Minami sowie den jüngeren Fachgenossen an seinem Laboratorium möchte der Verfasser für ihre zahlreichen freundlichen Anregungen bei dieser Untersuchung seinen herzlichsten Dank aussprechen.

Für die Harzproben, „1 proz. DVB", „2.5 proz. DVB" und „20 proz. DVB" ist der Verfasser Herrn Prof. Dr. A. Kawamura an der Landwirtschaftlichen und Technischen Universität zu Tokyo zu verbindlichstem Dank verpflichtet.

Laboratorium der analytischen Chemie,
Chemisches Institut der
wissenschaftlichen Fakultät,
Tokyo Universität, Tokyo

Mikroanalyse mit Hilfe von Ionenaustauscherharzen.[*1] *XI. Über den Nachweis kleinster Menge des Nickels mit Dimethylglyoxim und Bromwasser*[1]

Von Masatoshi FUJIMOTO

(Eingegangen am 31. August, 1956)

Einleitung

Es wurde hier eine Rosa- bzw. Braunfärbung, die die ammoniakalische wässerige Lösung der Nickelsalze bei Anwesenheit von verschiedenartigen Oxydationsmitteln unter Einwirkung von Dimethylglyoxim gibt[2], zur Mikroanalyse mit Ionenaustauscherharzen angewandt. Nach F. Feigl wurde vermutet, dass die genannte Färbung auf der Bildung von einer wasserlöslichen Chelatverbindung vierwertigen Nickels wie

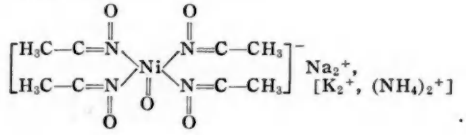

beruht[3],[*2].

Lässt man in diese sich stark färbende Lösung einige Körnchen farblosen starkbasischen Anionenaustauscherharzes eintauchen, so werden derartigeChelatanionen in die Harzphase stark adsorbiert. Die Harzkörnchen werden infolgedessen entschieden stärker als die Aussenlösung gefärbt.

Bei dieser Arbeit wurde die obengenannte Ionenaustauschreaktion zum Nachweis geringer Menge des Nickels angewandt, und durch ausführliche Untersuchung über die Experimentalbedingungen wurde eine neue verbesserte Nachweismethode für Nickel festgestellt.

Die in der gegenwärtigen Untersuchung benutzten Anionenaustauscherharze

Die wohlbekannten beinahe farblosen käuflichen Anionenaustauscherharze, Dowex 1-X1, -X2, -X4, -X8; Dowex 2-X2; Amberlite XE-114 und Amberlite IR-45, wurden alle in Chloridform angewandt[5].

Versuchsanordnung

Auf einer weissen Tüpfelplatte versetzt man je einen Tropfen von Probelösung, Ammoniakwasser und Bromwasser miteinander, und lässt sie etwa fünf Minuten stehen. Dann fügt man dazu einen Tropfen verdünnter alkoholischer Lösung des Dimethylglyoxims und einige Körnchen starkbasischen sowie farblosen Anionenaustauscherharzes, und danach rührt man dieses Gemisch mit einem Glasstäbchen gründlich um. Einige Minuten nach der Mischung beobachtet man mit einer Lupe eine Orangerosa- bzw. Orangebraunfärbung in der Harzphase.

Massflüssigkeit und Reagenzien

1. Massflüssigkeit. — Man stellt hier eine Stammlösung der Nickelmassflüssigkeit her, indem man kobalt- und eisenfreies Nickel(II)-chlorid („Scherring-Kahlbaum A. G." zur Analyse) in 0.01N Salzsäure eintrug. 1 ccm dieser Stammlösung enthielt genau 44.02 mg von Nickel[*3]. Alle folgende Untersuchungen über die beste Experimentalbedingungen werden mit einer 0.01N-salzsauren Lösung ausgeführt, deren 1 ccm 4.40 γ von Nickel enthielt.

2. Reagenzien.—**(1) Bromwasser.**—Etwa 0.3-prozentige wässerige Bromlösung wurde durch Verdünnung gesättigter Bromwasser mit etwa zweifacher Menge destillierten Wassers hergestellt.

(2) Ammoniakwasser.—Käufliches extrareines 15N Ammoniakwasser wurde vorbereitet.

(3) Alkoholische Lösung des Dimethylglyoxims[*4].—Einprozentige alkoholische Lösung des extrareinen Dimethylglyoxims („Wako" zur Analyse) wurde vorbereitet.

---

*1 Von nun an wird die in den vorhergehenden Mitteilungen angewandte Terminologie „Ionenaustauscherharz" durch „Ionenaustauscherharz" ersetzt, da diese gegenwärtig üblicher als jene im Gebrauch ist.

1) Die zehnte Mitteilung: M. Fujimoto, Dieses Bulletin, **30**, 87 (1957).

2) F. Feigl, *Ber.*, **57**, 758 (1924).

3) F. Feigl, „Chemistry of Specific, Selective and Sensitive Reactions," übersetzt von R. E. Oesper, 1. Aufl., New York (1949), S. 278.

*2 Es wurde kürzlich von K. Yamasaki und Ch. Matsumoto vermutet, dass in alkalischer Lösung ein Komplexanion, $[Ni^{IV}D_3]^{2-}$ sich bildet (DH_2 bedeutet Dimethylglyoximmolekül)[4].

4) K. Yamasaki und Ch. Matsumoto, *J. Chem. Soc. Japan* (*Pure Chem. Sect.*) **77**, 1111 (1956).

5) Vgl. die siebente Mitteilung: M. Fujimoto, Dieses Bulletin **29**, 776 (1956).

*3 Der Nickelgehalt von der obigen Massflüssigkeit wurde durch komplexometrische Titration mit 0.01 M Massflüssigkeit des Äthylendiamintetraessigsauren Natriums und Murexide als Metallindikator genau bestimmt.

*4 Eine Dimethylglyoximlösung in Aceton wurde auch angewandt, und dabei wurden gleicherweise befriedigende Ergebnisse erhalten.

Bestimmung der Bedingungen höchster Empfindlichkeit*5

1. Abhängigkeit der Färbungsintensität der Harzphase von der Menge des Dimethylglyoxims.—Mit 6N Ammoniakwasser und Dowex 1-X1 wurde der nachfolgende Versuch ausgeführt. Wie aus Abb. 1 klar zu ersehen ist, übt die Menge des angewandten Dimethylglyoxims auf die Färbungsintensität der Harzphase beträchtlichen Einfluss aus. Bei allzu niedriger Konzentration des Dimethylglyoxims färbt sich die Harzphase ungenügend. Die Färbung dieser Phase verstärkt sich allmählich mit steigender Reagenskonzentration und bei etwa Einprozent zeigt sie den höchsten Wert. Die Anwendung mehrerer Tropfen dieser einprozentigen Reagenslösung wirkt auf die Farbenentwicklung der Harzphase nachteilig ein. Diese Tatsachen zusammengenommen, empfiehlt es sich, nur einen Tropfen (=0.015 ccm) der einprozentigen alkoholischen Dimethylglyoximlösung anzuwenden.

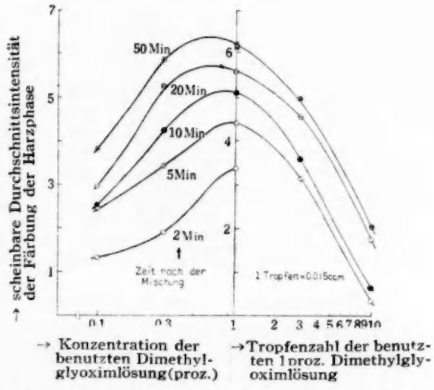

Abb. 1. Abhängigkeit der Färbungsintensität von der benutzten Dimethylglyoximmenge

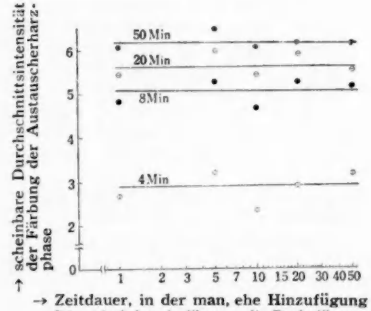
→ scheinbare Durchschnittsintensität der Färbung der Austauscherharzphase
50 Min
20 Min
8 Min
4 Min
→ Zeitdauer, in der man, ehe Hinzufügung der Dimethylglyoximlösung, die Probelösung und die Harzkörnchen im Bromwasser stehen lässt. (Min)

Abb. 2. Einfluss der Berührungsdauer der Probelösung mit Bromwasser.

*5 In bezug auf die halbquantitative Darstellungsweise von der scheinbaren Durchschnittsintensität der Färbung, vergleiche die dritte Mitteilung: M. Fujimoto, Dieses Bulletin, **29**, 567 (1956).

2. Einfluss der Berührungsdauer der Probelösung mit Bromwasser.—Abb. 2 zeigt den Einfluss der Zeitdauer, die nach der Versetzung der Probelösung und Ammoniakwasser mit Bromwasser verläuft. Aus dieser Abbildung ist es klar, dass die Nickel(II)salze in ammoniakalischer Lösung durch Einwirkung des Broms zu Nickel-(IV)salze schon nach 1 Minute fast vollkommen oxydiert werden.

3. Einfluss der Ammoiakwasserkonzentration.—Abb. 3 stellt den Einfluss der Konzentration des Ammoniakwassers auf die Färbungsintensität der Harzphase dar. Wie man darin klar ersieht, übt der Überschuss freien Broms auf den Färbungsverlauf höchst schädlichen Einfluss aus. So ist es nötig, das Ammoniakwasser in solch einem grösseren Überschusse anzuwenden, dass die Bromfarbe von der Versuchslösung völlig verschwindet.

Wie es in dem Verlauf genannter Kurven deutlich zu ersehen ist, nimmt die Färbungsintensität der Harzphase mit steigender Konzentration des Ammoniakwassers allmählich ab (vgl. den Paragraph, „5. Einfluss der Salzkonzentration"). Im folgenden wurde lediglich 1N Ammoniakwasser angewandt.

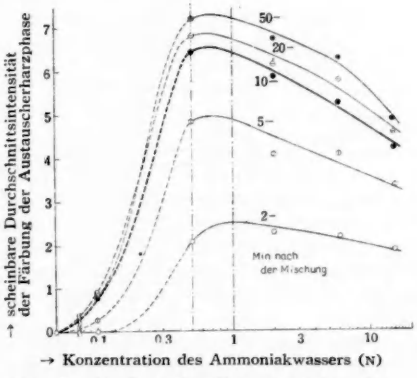

Abb. 3. Einfluss der Konzentration des benutzten Ammoniakwassers auf die scheinbare Färbungsintensität der Harzphase.

4. Einfluss der Sorte sowie des Vernetzungsgrades der Harze.—Aus dem in Abb. 4 dargestellten Färbungsverlauf wurde Dowex 1-X4 als das am besten geeignete Harz ausgewählt.

Dowex 2-X2 sowie Dowex 1-X2 färben sich etwas schwächer, und Dowex 1-X1 sowie -X8 beträchtlich schwächer. Schwachbasische Harze, Amberlite IR-45 sowie XE-114, waren dabei nicht zweckmässig.

5. Einfluss der Salzkonzentration.—Mit steigender Salzkonzentration der Probelösung wird die Rosafärbung der Harzphase bedeutend geschwächt. Wie in den Kurven in Abb. 5 klar gezeigt wird, nimmt die scheinbare Färbungsintensität der Harzphase dann rasch ab, wenn die Salzkonzentration der Probelösung höher als

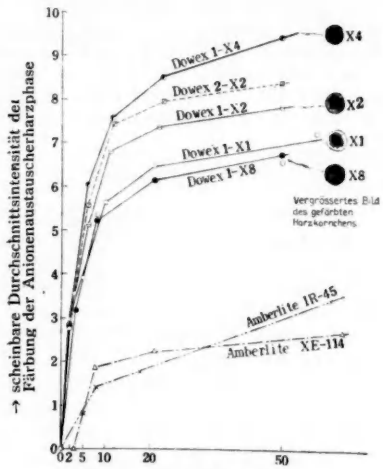

Abb. 4. Abhängigkeit der Färbungsintensität von Sorten der Harze (RCl-Form)

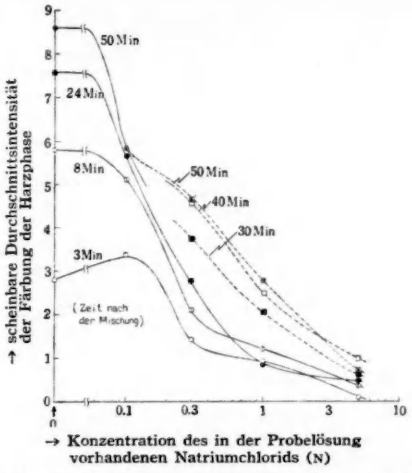

Abb. 5. Einfluss der Konzentration des in der Probelösung vorhandenen Neutralsalzes auf die scheinbare Färbungsintensität der Harzphase.

TABELLE I

EINFLÜSSE DER BEGLEITSTOFFE

Begleitstoffe	benutzter Verbindungstypus	Farbton der Harzphase*	Menge der Begleitstoffe	nachweisbare Nickelmenge	Grenzverhältnis	Bemerkungen**
V(V)	NH_4VO_3	farblos	18 γ	0.018 γ	$1:1\times10^3$	*a*, V≦0.05proz.
Cr(III)	$KCr(SO_4)_2$	grau	64 γ	0.035 γ	$1:1.8\times10^3$	*b*
Mn(II)	$MnSO_4$	farblos	32 γ	0.021 γ	$1:1.5\times10^3$	Mn≦0.1proz.
Fe(III)	**$FeCl_3$**	**farblos**	**13 γ**	**0.12 γ**	**$1:1.1\times10^2$**	—
Fe(II)	**Mohrsches Salz**	**farblos**	**8 γ**	**0.14 γ**	**$1:5.7\times10$**	*c*
Co(II)	$Co(NO_3)_2$	farblos	118 γ	0.053 γ	$1:2.3\times10^3$	*a*
Cu(II)	$CuSO_4$	sehr hell braun	36 γ	0.018 γ	$1:2\times10^3$	Cu≦0.1proz.
Zn(II)	$ZnSO_4$	farblos	270 γ	0.035 γ	$1:7.7\times10^3$	*a*
Cd(II)	$CdSO_4$	farblos	18 γ	0.021 γ	$1:8.5\times10^2$	Cd≦0.1proz.
Hg(II)	$Hg(NO_3)_2$	beinahe farblos	34 γ	0.016 γ	$1:2.2\times10^3$	*a*
Cr(VI)	$K_2Cr_2O_7$	zitronengelb	32 γ	0.035 γ	$1:9\times10^2$	*d*, Cr≦0.1proz.
Mo(VI)	$(NH_4)_2MoO_4$	farblos	330 γ	0.062 γ	$1:5.3\times10^3$	—
W(VI)	Na_2WO_4	farblos	330 γ	0.035 γ	$1:9.4\times10^3$	—
U(VI)	$UO_2(CH_3COO)_2$	lebhaft gelb	270 γ	0.062 γ	$1:4.4\times10^3$	*b*
Pb(II)	$Pb(NO_3)_2$	farblos	170 γ	0.035 γ	$1:4.8\times10^3$	—
Al(III)	**$Al(NO_3)_3$**	**farblos**	**70 γ**	**0.12 γ**	**$1:5.7\times10^2$**	*a*
F^-	KF	farblos	170 γ	0.021 γ	$1:8\times10^3$	—
$C_6H_5O_7^{3-}$	Zitronensaures Ammonium	farblos	430 γ	0.13 γ	$1:3.3\times10^3$	—
$C_4H_4O_6^{2-}$	Seignettesalz	farblos	770 γ	0.028 γ	$1:2.7\times10^4$	—
$C_2O_4^{2-}$	Oxalsaures Ammonium	farblos	495 γ	0.09 γ	$1:5.7\times10^3$	—

* Der Farbton hervorgerufen durch nur die Begleitstoffe:

** *a*: 6N Ammoniakwasser (1 Tropfen) wurde angewandt.
b: 15N Ammoniakwasser (1 Tropfen) wurde angewandt.
c: Hierbei wurde überschüssiges Bromwasser angewandt, um alle gebildete Eisen(II)-hydroxyd zum Eisen(III)hydroxyd völlig zu oxydieren.
d: Neben Blindversuche wurde der Nachweis durchgeführt.

0.1N ist. Diese Tatsache ist der einzige Fehler vorliegender Nachweismethode. Jedoch, durch Verdünnung der Probelösung mit etwa 1 ccm destillierten Wassers, ist dieser Nachteil bis zu einem gewissen Grade zu vermeiden, wie die gestrichelten Kurven der genannten Abbildung zeigen. Auf alle Fälle empfiehlt es sich, die Salzkonzentration der Versuchslösung niedriger als 0.3N zu halten.

6. Bedingungen höchster Empfindlichkeit.— So wurde das beste Verfahren wie folgt vollkommen festgestellt:

„Auf einer weissen Tüpfelplatte versetzt man je einen Tropfen von Probelösung, 1N Ammoniakwasser und 0.3prozentigem Bromwasser miteinander. Wenn die Salzkonzentration der Probelösung höher als 0.3N liegt, so empfiehlt es sich, noch etwa 1 ccm destillierten Wassers zuzugeben. Nach zwei bis fünf Minuten langem Stehen fügt man dazu einen Tropfen (etwa 0.015 ccm mit Kapillarpipette) einprozentiger alkoholischer Dimethylglyoximlösung und einige Körnchen starkbasischen sowie farblosen Anionenaustauscherharzes, Dowex 1-X4 (RCl-Form), und danach rührt man dieses Gemisch mit einem Glasstäbchen gründlich um. Etwa zwanzig Minuten nach der Mischung beobachtet man, mit einer Lupe, eine in der Harzphase entstandene Orangerosa- bzw. Orangebraunrosafärbung."

Bestimmung der Erfassungsgrenze

Aus dem Verlauf der Kurven in Abb. 6 wurde die Erfassungsgrenze vorliegender Nachweisreaktion als 0.011 γ Nickel(II) unter Grenzkonzentration $1 : 3.8 \times 10^6$ eindeutig bestimmt.

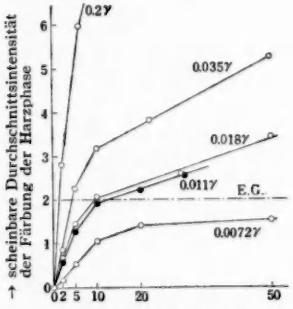

Abb. 6. Bestimmung der Erfassungsgrenze.

Einflüsse der Begleitstoffe

Tabelle I stellt die Einflüsse verschiedenartiger fremder Ionen auf die vorliegende Nachweisreaktion zusammenfassend dar. Wie es klar zu ersehen ist, stört nur Eisen(III)- und Eisen(II)-salze beträchtlich den genannten Nachweis*6.

Zusammenfassung

1. Durch einfache Anwendung der farblosen starkbasischen Anionenaustauscherharze zur Farbenreaktion zwischen Nickelsalzen und Dimethylglyoxim bei Anwesenheit des Bromwassers steigt die Empfindlichkeit der genannten Reaktion beträchtlich an.

2. Die besten Experimentalbedingungen werden durch gründliche Untersuchung der verschiedenen Faktoren, wie Konzentration der Reagenzien, Harzart, Salzkonzentration der Probelösung, usw., vollkommen festgestellt. Der etwas grössere Einfluss der Neutralsalzkonzentration der Probelösung zur Reaktionsempfindlichkeit ist der einzige Nachteil von der hier vorgeschlagenen Nachweismethode.

3. Die Einflüsse der verschiedenartigen Begleitstoffe werden auch ausführlich untersucht. Eisen(III)- und Eisen(II)salze stören den Nachweis.

Zum Schluss möchte der Verfasser Herrn Prof. Dr. E. Minami für seine freundlichen Anregungen zur vorliegenden Untersuchung seinen herzlichsten Dank aussprechen.

Laboratorium der analytischen Chemie,
Chemisches Institut der
wissenschaftlichen Fakultät,
Tokyo Universität, Tokyo

*6 Über das raffinierte mikrochemische Verfahren zur Trennung verschiedenartiger Übergangselemente mit einer Mikrosäule des Anionenaustauscherharzes, wird der Verfasser später in der nächsten Mitteilung genau diskutieren.

Electrochemical Study of Ethylene Glycol-Acetic Acid System

By V. K. Venkatesan and C. V. Suryanarayana

(Received April 21, 1956)

Introduction

The well known effect of certain hydroxy bearing compounds in increasing the acidity of aqueous solutions of boric acid pointed to a further exploration into the possibility of such and other similar effects of ethylene glycol on anhydrous acetic acid. Hence a systematic investigation of electrical conductance, volume contraction, viscosity, dielectric constant, and refractometric measurements has been made and reported herein.

Experimental Procedure

Purest Eastman Kodak ethylene glycol was dried over anhydrous sodium sulphate, decanted and fractionally distilled under reduced pressure and the middle fraction collected. Dielectric constant determinations showed the same value both for the original material and for the purified one. So further requirements of ethylene glycol were drawn from the Eastman Kodak supply. Purest Kahlbaum glacial acetic acid was used. Ethylene glycol and acetic acid were kept at 30°C in a thermostat for several hours and by pipetting out the required volumes of the two compounds totalling 50 cc. into 250 cc. glass stoppered pyrex bottles, different compositions of the mixtures differing by 10 per cent were made ranging from 10 to 90 per cent. Weight per cent or mole per cent composition could be computed by considering the density of the glycol (1.10800) and that of acetic acid (1.03777) and their respective molecular weights.

For measuring the dielectric constant "Dekameter type DKO3" of Wissenschaftlich-Technische Werkstatten was used at a fixed frequency of 1.8 MC/S controlling the temperature of the cell with Hoppler's ultra thermostat.

A platinized vertical cell with a cell constant value of 0.1845 was used for measuring conductance. Resistance of the solutions was measured with conductivity bridge type LBR of Wissenschaftlich-Technische Werkstatten, at 50 cycles per second (due to high resistance of the solutions). Temperature was controlled at 30±0.05°C using Townson and Mercer's thermostat, S427. The same thermostat, provided with glass panels with suitable arrangements, was used for viscometric measurements, with an Ostwald viscometer. Hilger's Abbe refractometer with Hoppler's utlra thermostat was used for making refractometric measurements. pH measurements were attempted with a Cambridge pH meter using a glass electrode. But no steady reproducible pH values could be recorded. Also with quinhydrone electrode irreproducible values were obtained. Results are reported below.

The resistance of ethylene glycol could not be measured with the above set-up due to its very high value. Hence in reporting equivalent conductivity values no solvent correction could be applied.

Discussion

Acetic acid is known, from surface tension measurements[1,2], to exist as $(C_2H_4O_2)_2$ throughout the temperature range from 15 to 150°C. From the variation of the Ramsay-Shield's constants with temperature[3] and the dispersion and absorption of polyhydric alcohols in the Hertzian region[4] molecular associations are known to exist in ethylene glycol.

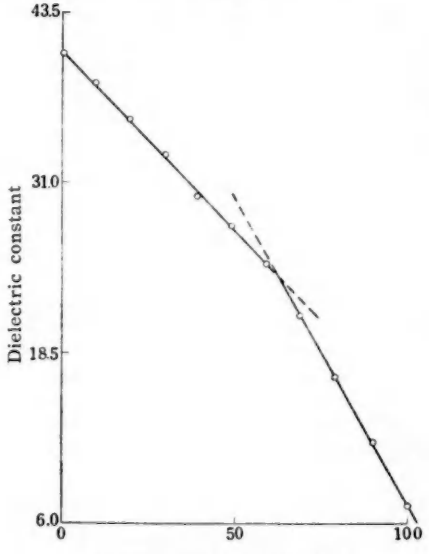

Fig. 1. Dielectric constant of ethylene-glycol-acetic acid system.

1) G. M. Bennet, *J. Chem. Soc.*, 351-360, 107 (1915).
2) Emile Band, *Bull. Soc. Chim.*, 435-438, 13 (IV) (1913).
3) G. G. Eliseef and W. A. Kurbastoff, *J. Russ. Phys. Chem. Soc.*, 1426-1427, 41 (1909).
4) Pierre Girand and P. Abadie, *Compt. rend*, 1995-1997, 196 (1933)

TABLE I

ETHYLENE GLYCOL-ACETIC ACID SYSTEM

Vol. Percent of Acetic Acid	Mole Percent of Acetic Acid	Density	Volume Contraction in c.c.	Viscosity in Poises	Dielectric Constant	Molar Polarization	Specific Conductivity	Equivalent Conductivity	Refractive Index	Molar Refraction
(1)	(2)	(3)	(4)	(5)	(6)	(7)	(8)	(9)	(10)	(11)
0	0	1.10800		0.1346	40.500	52.08			1.4270	14.38
10	9.712	1.10494	0.49	0.1188	38.250	51.83	6.151×10^{-6}	3.548×10^{-3}	1.4243	14.29
20	19.480	1.10086	0.67	0.1013	35.625	51.57	5.741×10^{-6}	1.651×10^{-3}	1.4198	14.18
30	29.350	1.09722	0.77	0.08750	33.000	51.23	6.331×10^{-6}	1.210×10^{-3}	1.4148	14.03
40	39.220	1.09224	0.71	0.07350	30.500	50.94	6.963×10^{-6}	0.9963×10^{-3}	1.4118	13.97
50	49.180	1.08798	0.71	0.06127	27.750	50.35	6.474×10^{-6}	0.7387×10^{-3}	1.4070	13.81
60	59.210	1.08130	0.56	0.04976	24.875	50.05	6.625×10^{-6}	0.6301×10^{-3}	1.4020	13.71
70	69.330	1.07477	0·48	0.03829	21.250	49.17	7.236×10^{-6}	0.5891×10^{-3}	1.3968	13.61
80	79.490	1.06583	0.32	0.02775	16.610	47.58	6.933×10^{-6}	0.4948×10^{-3}	1.3905	13.48
90	89.710	1.05539	0.17	0.01819	12.075	44.94	4.500×10^{-6}	0.2865×10^{-3}	1.3820	13.29
100	100.000	1.03777		0.01040	6.400	37.20			1.3700	13.09

A plot of dielectric constant values (column 6 of the Table) against mole per cent of acetic acid (Fig. 1) is made up of two straight lines intersecting at a composition of 62 mol. per cent of acetic acid. From 62 mol. per cent of acetic acid onwards the rate of fall of " D " is greater. All the mixtures have in each case a value for dielectric constant greater than to be expected if the variation is linear and at 62 mole per cent the deviation is a maximum. Likewise the plot of molar polarization against mole per cent of acetic acid (Fig. 2) is almost linear varying slightly with composition up to about 60 mole per cent of acetic acid, beyond which the fall is very rapid. All the mixtures have for each a value of molar polarization greater than to be expected if the variation is linear. The equation for molar polarization of a mixture

$$P_{1,2} = \frac{D-1}{D+2} \cdot \frac{M_1x_1+M_2x_2}{\rho_{1,2}}$$

is expected to hold[5] only for solutions of non-associated liquids. But some workers[6] applied it with success to mixtures of associated liquids. It is known[7] that the effect of association on the dielectric constant depends on the sizes and shape of the participating dipoles. As a result of a greater electrostatic moment of a polymerised molecule[8] than the simple one the dielectric constant of the solvent will be greater in its associated state. De-association in some solutions is indicated by the lowering of the dielectric constant of that component in solution. Conversely when dipole-dipole interaction occurs the forces holding the electric charge will be weakened as a result of a probable increase of the electrostatic moment of the molecule and the dielectric constant of a component becomes greater in solutions than in pure state. It has been shown[9] that when liquids are mixed there are at least two simultaneous reactions taking place, a de-association of the liquids and a combination between the two liquids. These

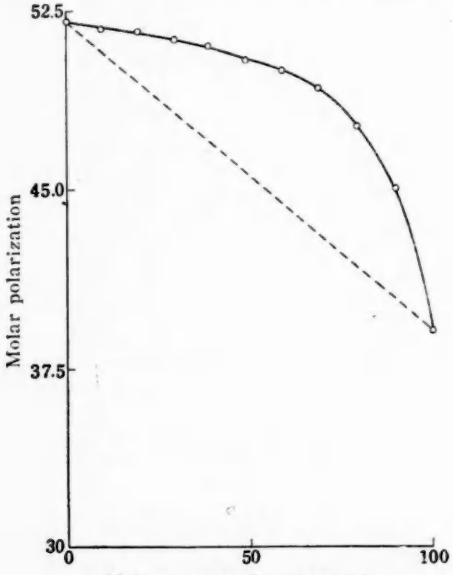

Fig. 2. Molar polarization of ethylene-glycol-acetic acid system.

5) G. Åkerlöf, *J. Am Chem. Soc.*, 4125, 54 (1932).
6) W Graffunder and Erich Heymann, *Z. Physik. Chem.*, 744, 72 (1931).
7) R. N. Kerr, *J. Chem. Soc.*, 2756-2804, 128 (1926).
8) J. W. Williams and I. J. Krchma, *J. Am. Chem. Soc.*, 1886, 48 (1926).
9) J. W. Williams and F. Daniels, ibid., 1490, 47 (1925).

factors should lead to opposing tendencies in any physical property. The only obvious conclusion is that starting from zero per cent ethylene glycol and proceeding towards per cent of it, the positive deviation of either the dielectric constant or the molecular polarization from linearity increases to a maximum at about 60 mole per cent of acetic acid and decreases from there onwards. It is probable that from zero to about 40 mole per cent of ethylene glycol dipole-dipole interaction predominates attaining its maximum at 40 mole per cent of ethylene glycol from where further increase of mole per cent of ethyleneglycol results in setting off a de-association of one or both of the components.

A plot of equivalent conductivity against mole per cent of acetic acid (Fig. 3) shows a rapid fall from 10 to 30 mole per cent of acetic acid, then a gradual fall up to about 60 mole percent round about which an inflexion occurs in the curve followed by a rapid fall towards the end. An electrochemical study of water-glycerol and water-ethylene glycol mixtures[10] showed that while it is possible to assume with ethanol the production of $EtOH_2^+$ ions, in the case of glycol or glycerol, ions of this type are formed to such a slight degree that the electrode potential remains practically unchanged. Since the equivalent conductivity, though slight, rises rapidly from 30 mole per cent of acetic acid downwards, it may be probable that in this region acetic acid starts slightly dissociating. From 60 mole per cent to 30 mole per cent the equivalent conductivity rises more rapidly than from 90 to 60 mole per cent of acetic acid, the overall increase in the former region being about double that in the latter. Hence it is probable that to anhydrous acetic acid, as more and more ethylene glycol is added, dipole-dipole interactions should occur up to about 60 mole per cent of acetic acid from where it starts de-association up to 30 mole per cent of acetic acid from where it must start slightly dissociating.

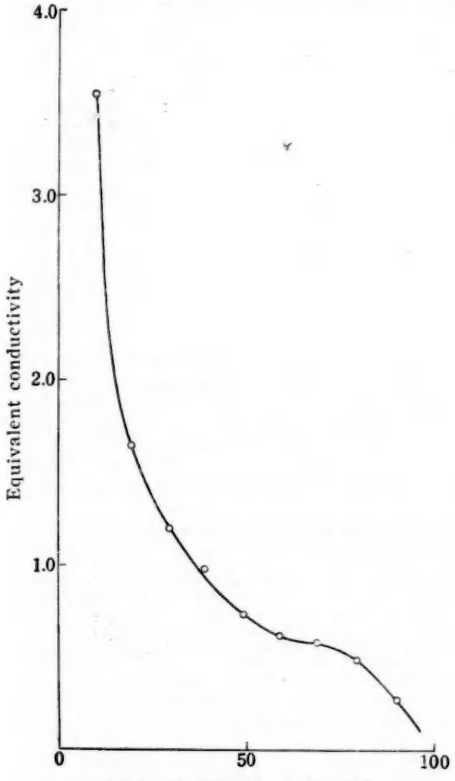

Fig. 3. Equivalent conductivity of ethylene-glycol-acetic acid system.

A plot of viscosity (column 5 of the Table) against percentage compositions (not shown) shows a gradual fall as mole per cent of acetic acid increases deviating from linearity with a convexity towards the axes.

Plots of refractive index and molar refractions (column 10 and 11) against mole per cent composition (not shown) show a gradual fall with increase in the mole per cent of acetic acid with a slight dip at 30 mole per cent of it.

A plot of volume contraction in c.c. against mole per cent composition (not given) shows an unsymmetrical parabola with a maximum at 30 mole per cent of acetic acid with a stationary value between 40 and 50 mole per cent of it.

Comparison of the behaviour of ethylene glycol-acetic acid system with those of aqueous boric acid and some polyhydric alcohols brings out a great dissimilarity. Perhaps the presence of water as an additional component and the basicity of the acid used may be among other contributing factors for the above dissimilarity.

Summary

Equivalent conductivity, volume contraction, viscosity, dielectric constant and

10) I. I. Zhukov and I. F. Karpova, *J. Gen. Chem. (U.S.S.R.)*, 161-166, 6 (1936).

refractometric measurements of mixtures of ethylene glycol and acetic acid at different percentage compositions have been made. Probably a predominating dipole-dipole interaction occurs when ethylene glycol is added to anhydrous acetic acid up to about 60 mole per cent of the latter from where up to 30 mole per cent of acetic acid de-association seems to occur and from 30 mole per cent of acetic acid downwards slight dissociation is evidenced. This system is dissimilar in behaviour to those of aqueous boric acid and some polyhydric alcohols.

Physico-Chemical Laboratory
Annamalai University
South India

Electron Diffraction Investigation on the Molecular Structures of Some Organosilicon Compounds. I

By Masatoki YOKOI*

(Received September 19, 1956)

Introduction

Those organosilicon polymers, which have bonds between silicon and organic radicals, possess various properties of practical importance, i. e., low boiling points, small temperature coefficients of viscosity, high thermal stability, etc. These characteristic properties are closely related to their molecular structures. The knowledge of bond lengths and valence angles of low-molecular compounds provides the basis for consideration of the structures of polymers. The present study deals with the electron diffraction experiments on the vapors of several low-molecular organosilicon compounds. Organosilicon compounds which have so far been investigated by electron diffraction are mainly the derivatives of silane containing methyl groups and halogen atoms as substituents. In the present study, hexamethyldisiloxane, tetra-(trimethylsiloxy)-silane, octamethylcyclotetrasiloxane, and the two lowest members of dimethylcyclopolysilazanes and dimethylcyclopolysilthianes were investigated in order to determine the bond lengths of Si-O, Si-N and Si-S as well as the valence angles of O, N, S and Si atoms. In addition to the results on these compounds, data are also presented on several methyl, ethyl and phenyl derivatives of silane and halogenosilane.

Experimental

Method and Apparatus.—The electron diffraction apparatus used in this study has been described by Kimura[1]. The photographs taken were studied visually. The radial distribution curves and the theoretical intensity curves were calculated accorcing to the approximate formula used by Spurr and Schomaker[2]. In the temperature factors, $\exp(-b_{ij}q^2)$, for the theoretical intensity curves, b_{ij} was assumed to be equal to zero for all bonded distances, 0.0001 or 0.0002 for the atom pairs $\overset{Si}{O}\cdots C$, $\overset{Si}{C}\cdots C$, $\overset{Si}{Cl}\cdots Cl$, $\overset{O}{Si}\cdots Si$, etc., and 0.0004 or larger values for other non-bonded long distances. As the compounds used in this study constained relatively large numbers of parameters concerning their molecular structures, it was very difficult to derive unique conclusions from the observed intensity data unless some reasonable assumptions were made. Therefore the C-H distance and the valence angle of carbon in aliphatic organic radicals were assumed to be 1.09 Å and 109.5°, respectively. For particularly complicated compounds such as $((CH_3)_2SiS)_3$ and $((CH_3)_2SiO)_4$, the bond lengths well resolved in the radial distribution curves were used to evaluate the valence angles. The results thus obtained gave one of the models which could reproduce the observed intensity data, but other possibilities could not entirely be ruled out.

Compounds Studied.—(1) *Methylbromosilanes.*—Monomethyltribromosilane and dimethyldibromosilane were prepared by passing methyl bromide over heated silicon containing copper at 350°[3]. The product was fractionated. The boiling point of $(CH_3)SiBr_3$ was 130-134° and that of $(CH_3)_2SiBr_2$ was 112-113°. Trimethylmonobromosilane was prepared by passing the mixture of methyl bromide and dimethyldibromosilane over aluminum heated at 350°[4]. It boiled at 80°.

* Present address : Faculty of Textile and Sericulture, Shinshu University, Ueda, Nagano Prefecture.

1) M. Kimura, *Chem. Researches (Japan)*, **9**. 53 (1951).
2) R.A.Spurr and V.Schomaker, *J. Am. Chem. Soc.*, **64**, 2693 (1942).
3) E.G.Rochow, *J. Am. Chem. Soc.*,, **67**, 963 (1945).
4) D.T. Hurd, ibid., **67**, 1545 (1945).

TABLE I

Compounds	Si-Br (Å)	Si-C (Å)	∠Br-Si-Br	∠C-Si-C
$(CH_3)SiBr_3$	2.17±0.03	1.93 (assumed)	109.5±2°	—
$(CH_3)_2SiBr_2$	2.21±0.03	1.92±0.06	109.5±2°	109.5° (assumed)
$(CH_3)_3SiBr$	2.21±0.03	1.86±0.05	—	114±4°

(2) *Tetramethylorthosilicate.*—This compound was prepared by the reaction of silicon tetrachloride with methanol[5]. Its boiling point and melting point were 118–120° and 1–2°, respectively.

(3) *Hexachlorodisiloxane.* — This compound was prepared by passing the mixture of oxygen and chlorine over heated silicon[6] and fractionating the product. Its boiling point was 136–138°.

(4) *Hexamethylcyclotrisilazane and Octamethylcyclotetrasilazane.*—These compounds were prepared after Brewer and Haber[7]. The solution of dimethyldichlorosilane in benzene was treated with ammonia. After ammonium chloride was separated by filtration the filtrate was subjected to fractional distillation. The boiling point of the trimer was 185–187° and that of the tetramer was 223–225°.

(5) *Tetramethylcyclodisilthiane and Hexamethylcyclotrisilthiane.*—The trimer was prepared by the method of Champetier et al. who prepared its ethyl homologue[9]. The dimer was prepared by the thermal rearrangement of the trimer at 200° in a stream of hydrogen sulfide[8]. The boiling point of the dimer was 172–173°, and that of the trimer was 151.5–153.5°/38 mmHg.

(6) *Ethyltrichlorosilane, α- and β-chloroethyltrichlorosilane, tetraphenylsilane, phenyltrichlorosilane, octamethylcyclotetrasiloxane and tetra-(trimethylsiloxy)-silane* were furnished by Mr. M. Murata of the Osaka Municipal Technical Research Institute. Hexachlorodisilmethylene and hexamethyldisiloxane were given to the present writer by Dr. M. Kumata of Osaka City University and Mr. I. Hizawa of Sumitomo Chemical Co., respectively.

Results

(1) Methylbromosilanes[10].—The molecular structures of these compounds as revealed by electron diffraction experiments at 20–30° are shown in Table I. Calculations were based on the following: 1) C-H distance equal to 1.09 Å, 2) ∠H-C-Si equal to 109.5°, and 3) staggered relative positions of Br and H in a CH_3 radical with respect to a Si-C bond.

(2) Ethyltrichlorosilane ($(C_2H_5)SiCl_3$), α-Chloroethyltrichlorosilane ($CH_3 \cdot CHCl \cdot SiCl_3$), β-Chloroethyltrichlorosilane ($ClCH_2 \cdot CH_2 \cdot SiCl_3$) and Hexachlorodisilmethylene ($Cl_3Si \cdot CH_2 \cdot SiCl_3$) These compounds were studied to obtain data on the structure of $SiCl_3$ radical as well as on rotation about Si-C bond. The structure of $SiCl_3$ remains unchanged throughout these compounds, that is Si-Cl=2.00±0.02 Å, and ∠Cl-Si-Cl=109.5±2°. Ethyl, chloroethyl, and disilmethylene radicals contribute little to intensity curves and therefore it was necessary to assume the structure of these radicals, i. e., C-C 1.54 Å, C-Cl 1.76 Å, Si-C 1.88 Å, and the valence angles of carbon 109.5°. Under these assumptions, the value of about 3 kcal./mol. was deduced for the potential barrier of the hindered rotation about Si-C bond in α-chloroethyltrichlorosilane. For hexachlorodisilmethylene, almost free rotation about Si-C bond was found to exist.

(3) Tetraphenylsilane and Phenyltrichlorosilane[12].—Two compounds, $Si(C_6H_5)_4$ and $(C_6H_5)SiCl_3$, were studied to determine the bond lengths between silicon and aromatic carbon and to get some information on the rotation about the Si-C bond. For tetraphenylsilane, the interatomic distance Si-C=1.87±0.03Å was obtained. Rotation about the bond between the silicon atom and the phenyl group was found to be restricted. The equilibrium position of four phenyl groups was the same as that of four nitro groups of tetranitromethane studied by stosick[13]. Model B in Fig. 1 is a sketch of the equilibrium configuration of the molecule in which all groups are rotated through the same angle 30° about Si-C bond from the positions of A in Fig. 1. In phenyltrichlorosilane, the contribution of phenyl group to the total scattering curve was so small that no data could be obtained except the following structure of the $SiCl_3$ radical; Si-Cl=2.00 ±0.02 Å, ∠Cl-Si-Cl=109.5±2°.

5) E.G.Rochow, ibid., **70**, 2170 (1945).
6) L. Troost and P. Hautefeuille, *Bull. Soc. Chim. France*, **13**, 213 (1870), ibid., **35**, 360 (1881).
7) S.D.Brewer and C.P.Haber, *J. Am., Chem. Soc.*, **70**, 3888 (1948).
8) T.Nomura, M.Yokoi, and K.Yamasaki, *Proc. Japan Acad.*, **29**, 342 (1953).
9) T.Nomura. *J. Chem. Soc. Japan*, (*Pure Chem. Sect.*), **74**, 513 (1953).
10) K.Yamasaki, A.Kotera, M.Yokoi and M.Iwasaki, *J. Chem. Soc. Japan*, (*Pure Chem. Sect.*), **71**, 349 (1950); *J. Chem. Phys.*, **17**, 1355 (1949).
11) C.Iida, M Yokoi, and K.Yamasaki, *J. Chem. Soc. Japan*, (*Pure Chem.Sect.*), **73**, 882 (1952).
12) M.Yokoi, *J. Chem. Soc Japan*, (*pure Chem. Sect.*), **73**, 822 (1952).
13) A.J. Stosick, *J. Am. Chem. Soc.*, **61**, 1127 (1937).

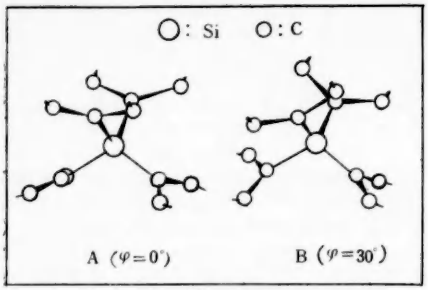

Fig. 1

(4) Tetramethylorthosilicate Si $(OCH_3)_4$[14].—The bond lengths and valence angles obtained were Si–O=1.64±0.03 Å, C–O=1.42±0.04 Å, and ∠Si–O–C=113±2°. A carbon atom in a methoxy group had a staggered configuration relative to the oxygen atoms in the other groups.

(5) Hexamethyltrisilazane $((CH_3)_2SiNH)_3$ and Octamethylcyclotetrasilazane $((CH_3)_2SiNH)_4$[15]. — Trimeric and tetrameric cyclic dimethylpolysilazane were studied for the purpose of evaluating the Si–N bond length and the Si–N–Si valence angle. For the trimer, the following data were obtained assuming ∠C–Si–C to be 110°; Si–N=1.78±0.03 Å, Si–C=1.87±0.05 Å, ∠N–Si–N=111±5° and ∠Si–N–Si=117±4°. For the tetramer, by assuming the values of Si–N, Si–C, ∠N–Si–N and ∠C–Si–C to be the same as those in the trimer, the valence angle of nitrogen was found to be 123±4°. The rings of these two compounds are puckered, although detailed shapes of the rings could not be determined.

(6) Tetramethylcyclodisilthiane and Hexamethylcyclotrisilthiane[16]. — Two compounds, $((CH_3)_2SiS)_2$ and $((CH_3)_2SiS)_3$, were studied to determine the Si–S bond length and the Si–S–Si valence angle. The Si–S bond length was found to be 2.18± 0.03 Å in the former compound and 2.15± 0.03 Å in the latter. Assuming ∠C–Si–C to be 110°, estimated bond agles were ∠Si–S–Si=75° and ∠S–Si–S=105° for the disilthiane, and ∠Si–S–Si=110° and ∠S–Si–S= 115° for the trisilthiane.

(7) Hexamethyldisiloxane $(CH_3)_3SiOSi(CH_3)_3$.—The visual curve (V) and the radial distribution curve (R) are shown in Fig. 2. In (R), two maxima at 1.63 and 1.88 Å correspond to Si–O and Si–C bond lengths. The maxima at 2.84 and 3.12 Å are supposed to correspond to Si···C and Si···C respectively. As the values 2.84 and 3.10 Å are obtained to Si···C and Si···C respectively by assuming Si–O 1.63 Å, Si–C 1.88 Å and ∠O–Si–C 108°, this choice seems to be adequate. The distance Si···Si seems to be masked by these two maxima. If this distance overlaps on the maximum at 3.12 or 2.84 Å, the corresponding valence angle of oxygen would be about 150 or 120°.

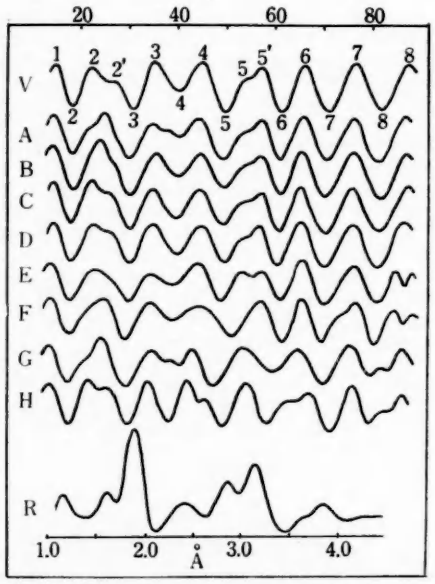

Fig. 2. Visual infensity, theoretical intensity and radial distribution curves of hexamethyldisiloxane.

To estimate Si–O–Si angle and to determine the accuracy of values of Si–O and Si–C bond lengths and O–Si–C angle, the theoretical intensity curves of several models, the bond lengths and the valence angles of which are listed in Table II, were compared with the visual curve in Fig. 2. The configuration of two trimethylsilyl groups was assumed to be the one as illustrated in Fig. 3 throughout these models. Since the relative contribution of long atomic distances to the total intensity was small, and moreover large temperature factors were adopted for the long

14) K.Yamasaki, A.Kotera, M.Yokoi and Y.Ueda. *J. Chem. Soc. Japan (Pure Chem. Sect.)*, **72**, 544 (1951); *J. Chem. Phys.*, **18**, 1414 (1950).
15) M.Yokoi and K.Yamasaki, *J. Am. Chem. Soc.*, **75**, 4139 (1953).
16) M.Yokoi, T.Nomura, and K.Yamasaki, *J. Am. Chem. Soc.*, **77**, 4484 (1955).

distances, a change in the configuration gave little change in the theoretical intensity curves. The shapes and the q-values

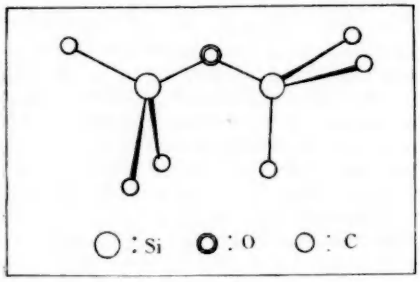

Fig. 3

TABLE II

Model	Si–O (Å)	Si–C (Å)	∠Si–O–Si	∠O–Si–C
A	1.63	1.88	114°	108°
B	1.63	1.88	120	108
C	1.63	1.88	130	108
D	1.63	1.88	140	108
E	1.59	1.92	130	108
F	1.69	1.86	130	108
G	1.63	1.88	130	102
H	1.63	1.88	130	112

of 2nd and 2nd′ maxima of the theoretical intensity curves vary with the change of Si–O–Si angle. The best qualitative fit was obtained by curve C, the Si–O–Si angle of the model being equal to 130°. In the range of q larger than 40, theoretical curves A–D are consistent with the visual curve. The deviations of O–Si–C angle from 108° gave the change of the q-values of 4th and 5th maxima (G and H), while the change of Si–O/Si–C caused the disagreement in the shapes and the q-values of 5th and 5th′ maxima (E and F). The observed and the calculated q-values of curve C are compared quantitatively Table IV. The final results obtained are: Si–O=1.63±0.05 Å, Si–C=1.88±0.03 Å, ∠Si–O–Si=130±10° and ∠O–Si–C=108±4°.

(8) Hexachlorodisiloxane ($Cl_3SiOSiCl_3$).—In this compound the change of Si–O–Si angle had little effect on the over-all scattering intensity. Therefore the Si–O–Si angle was assumed to be 130°. Several theoretical curves are compared with the visual curve (V) in Fig. 4. The bond lengths and the valence angle ∠Cl–Si–Cl of each model are listed in Table III.

TABLE III

Model	Si–O (Å)	Si–Cl (Å)	∠Cl–Si–Cl
A	1.64	2.02	109.5°
B	1.64	2.02	109.5
C	1.68	2.01	109.5
D	1.58	2·03	109.5
E	1.64	2.02	112
F	1.64	2.02	107

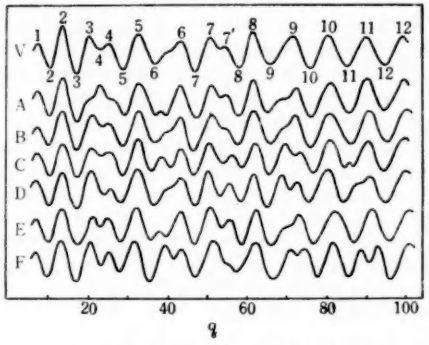

Fig. 4. Visual and theoretical intensity curves of hexachlorodisiloxane.

TABLE IV

Max.	Min.	$((CH_3)_3Si)_2O$ $q_{obs.}$	$((CH_3)_3Si)_2O$ $q_C/q_{obs.}$	$(Cl_3Si)_2O$ $q_{obs.}$	$(Cl_3Si)_2O$ $q_B/q_{obs.}$
1		15.2	0.974	8.0	1.013
	2	18.5	1.030	10.7	0.973
2		21.9	1.072	14.2	0.972
2′		27.1	0.996	—	—
	3	30.5	1.015	17.3	1.000
3		34.9	1.005	20.3	1.024
	4	40.5	0.970	23.1	—
4		45.1	0.980	25.4	1.000
	5	49.5	0.990	28.8	0.993
5		53.8	0.991	32.2	0.991
5′		57.3	1.007	—	—
	6	61.3	1.000	36.5	0.982
6		65.8	1.000	43.2	0.991
	7	70.9	0.994	46.7	1.000
7		76.8	0.994	50.2	1.007
7′		—	—	54.4	1.000
	8	82.3	1.000	57.8	1.011
8		87.4	0.999	61.9	1.001
	9			66.7	0.988
9				71.8	—
	10			76.2	1.012
10				80.9	1.002
	11			86.1	0.994
11				90.1	1.018
Mean			1.001		0.999
Mean deviation			0.015		0.010

When two $SiCl_3$ radicals were fixed in a certain relative position, the interference of long Cl···Cl had some effect on 3rd and 4th maxima as shown in the curve A of Fig. 4. The most satisfactory model (curve B) was the free rotation model. Approximate curves were calculated ignoring the effect of long distances which vary by rotation. Curves C–F were calculated also with the omission of long distances. The change of Cl–Si–Cl angle from tetrahedral angle to 112° gave a small maximum between 5th and 6th maxima, while for ∠Cl–Si–Cl equal to 107°, 7th' maximum disappeared and the shape and the position of 6th maximum were not in accord with those of the visual curve (E and F). The shapes and the q-values of 7th' and 9th maxima of the model, Si–O/Si–Cl in which is 1.58/2.03 or 1.68/2.01, were not in accord with the visual curve (C and D). With these qualitative considerations and the quantitative comparisons given in Table IV, the final results obtained are: Si–Cl=2.02±0.02 Å, Si–O=1.64±0.05 Å and ∠Cl–Si–Cl=109.5±2°.

(9) Tetra-(trimethylsiloxy)-silane ($Si(OSi(CH_3)_3)_4$). — The radial distribution curve calculated from the visual curve is shown in Fig. 5 together with that of octamethylcyclotetrasiloxane. Maxima at 1.63, 1.88 and 3.06 Å appear on both curves. Maxima at 1.63 and 1.88 Å are due to bonded Si–O and Si–C distances, respectively, which are consistent with values determined for hexamethyldisiloxane. In the vicinity of 3 Å in the curves, maxima corresponding to non-bonded Si–O···C and Si···Si distances should appear. If Si–O–Si angle is larger than O–Si–C, and the maximum at 3.06 Å is due to Si···Si, then Si–O–Si angle should be 140°. To clarify this point, comparisons were made of theoretical intensity curves with the visual intensity curve, for models having various valence angles, Si–O and Si–C bond lengths being assumed to be 1.63 and 1.88 Å respectively as obtained from the radial distribution curve. The valence angle of central silicon atom was assumed to be

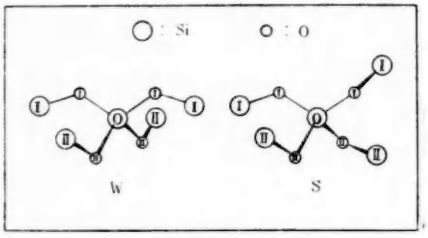

Fig. 6

W: The two Si atoms, the two O atoms designated by I (or II) and the central Si atom are coplanar, forming W-shaped chain.

S: One Si atom at the end of each chain is twisted through 60° about Si–O bond from the position of the W-form.

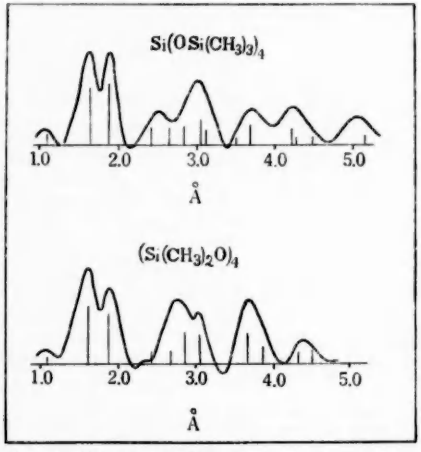

Fig. 5. Radial distribution curves of tetra-(trimethylsiloxy)-silane and octamethylcyclotetrasiloxane.

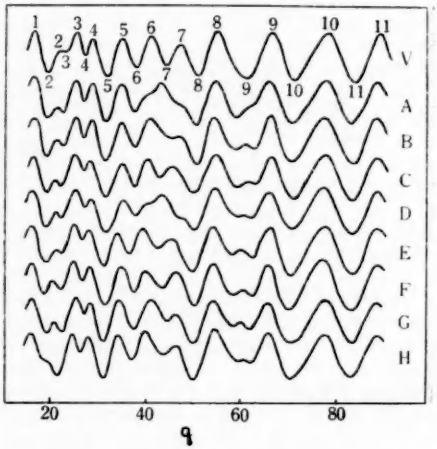

Fig. 7. Visual and theoretical intensity curves of tetra-(trimethylsiloxy)-silane.

tetrahedral. These curves are shown in Fig. 7 with the visual curve (V). The valence angles of each model are listed in Table V. The relative positions of four trimethylsiloxy groups were assumed to take either W- or S-form as shown in Fig. 6. In the theoretical curves of models of W-form (for example, curve H in Fig. 7), the second maximum was near the first maximum and was not consistent with the visual curve. Therefore models having W-form were rejected. For models of S-form (curves A-G), good agreement was obtained for the second maximum. The features of the theoretical intensity curve, which are sensitive to the change of Si-O-Si and O-Si-C angles are the shapes and the q-values of 5th and 6th and 7th maxima. Curve B corresponding to the model in which Si-O-Si and O-Si-C angles are 140° and 107° respectively, well reproduces the features of the visual intensity curve. The variation of Si_0-O and Si_1-O in the vicinity of 1.63 Å gave curve F and G, in which the q-values of 6th maxima are not consitent with the visual curve. From these considerations the values of ∠Si-O-Si and ∠O-Si-C which well reproduce the visual intensity curve, were found to be 140±5° and 107±3° respectively.

(10) Octamethylcyclotetrasiloxane $((CH_3)_2SiO)_4$.—Theoretical intensity curves for models assuming the tetrahedral angle of silicon atom are shown in Fig. 8 together with the visual curve (V). There are several conceivable forms of an eight-membered ring of $(Si-O)_4$ as shown in Fig. 9. The variation of the form caused minor changes in the shapes and the q-values of 2nd and 3rd maxima. This is a natural consequence of large temperaturs factors used for long distances. The

TABLE V

Model	Si_0-O(Å)	Si_1-O(Å)	∠Si-O-Si	∠O-Si-C
A	1.63	1.63	140°	110°
B	1.63	1.63	140	107
C	1.63	1.63	140	104
D	1.63	1.63	135	107
E	1.63	1.63	145	107
F	1.60	1.65	140	107
G	1.65	1.60	140	107
H	1.63	1.63	140	107

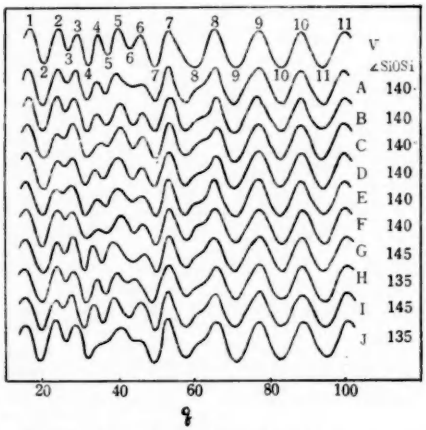

Fig. 8. Visual and theoretical intensity curves of octamethylcyclotetrasiloxane.

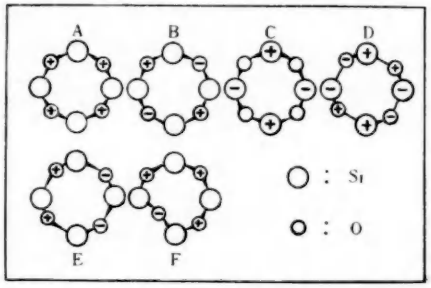

Fig. 9

TABLE VI

Max.	Min.	$Si(OSi(CH_3)_3)_4$ $q_{obs.}$	$q_B/q_{obs.}$	$((CH_3)_2SiO)_4$ $q_{obs.}$	$q_B/q_{obs.}$
1		16.2	(0.950)	16.1	0.975
	2	18.6	1.000	20.1	1.009
2		20.8	0.981	23.4	1.000
	3	22.2	0.972	26.1	0.976
3		24.7	0.979	28.6	0.973
	4	26.4	0.992	31.2	0.987
4		27.9	0.993	33.8	0.994
	5	31.0	1.006	36.5	0.994
5		34.2	1.002	39.1	1.006
	6	37.0	1.011	43.0	0.986
6		40.2	0.997	46.1	0.982
	7	43.2	1.027	49.5	0.988
7		46.4	0.991	52.9	1.012
	8	50.0	0.989	60.4	—
8		54.0	0.989	65.4	1.017
	9	60.7	—	71.2	0.995
9		65.6	1.011	77.3	0.993
	10	69.7	1.012	83.4	0.991
10		77.7	0.998	88.8	1.000
	11	83.4	0.993	95.2	0.990
11		88.4	0.982	100.3	0.998
Mean			0.994		0.994
Mean deviation			0.011		0.009

variation of the Si–O–Si angle of a symmetrical crown form considerably affects the relative positions of 4th, 5th and 6th maxima as indicated by curves G and H. The same is true for a cradle form (cf. curves I and J). In this case, too, the best agreement with the visual curve was obtained with models in which the Si–O–Si angle was 140°. The quantitative comparison of the observed q-values with the calculated ones for the best models of tetra-(trimethylsiloxy)-silane and octamethylcyclotetrasiloxane is shown in Table VI. For the latter compound, the curve of cradle form (B in Fig. 8) was found to be better than those of other forms. The distances appearing in the best curve are shown schematically in Fig. 5. The distances ranging from 2.4 to 2.9 Å in the distribution curve are not consistent with the distances appearing in the best model.

Department of Chemistry
Faculty of Science
Nagoya University, Nagoya

Electron Diffraction Investigation on the Molecular Structures of Some Organosilicon Compounds. II

By Masatoki YOKOI

(Received September 19, 1956)

The results of studies on the molecular structures of several organosilicon compounds as revealed by electron diffraction experiments are described in part I of this report. The results obtained are discussed below.

(1) Silicon-halogen Bond.—A number of compounds containing silicon-halogen bond have been investigated by electron diffraction and by microwave spectroscopy. The data on silicon-halogen bonds which have hitherto been determined are listed in Table 1 together with those of the present study. According to our finding, the distance between silicon and halogen

TABLE I

Compounds	By Electron Diffraction	By Microwave Spectroscopy	Reference
	(Si–F length (Å))		
SiF_4	1.54±0.02		3
$HSiF_3$		1.565±0.005	4
H_3SiF		1.593, 1.595±0.010	5, 4
$(CH_3)_3SiF$	1.57±0.02		6
	(Si–Cl length (Å))		
$SiCl_4$	2.01±0.02		7
$HSiCl_3$	2.01±0.03	2.021±0.002	8, 9
H_2SiCl_2	2.02±0.03		10
H_3SiCl	2.06±0.05	2.0479±0.0007, 2.048	10, 4, 9
$(CH_3)SiCl_3$	2.01±0.02	2.021	11, 9
$(CH_3)_2SiCl_2$	1.99±0.03		11
$(CH_3)_3SiCl$	2.09±0.03	2.03	12, 9
$(CH_3)_2SiClF$	2.03±0.03		6
F_3SiCl	2.01±0.02		10
	(Si–Br length (Å))		
$SiBr_4$	2.15±0.02		1
$HSiBr_3$	2.16±0.03		1
H_3SiBr		2.209±0.001	2
$(CH_3)SiBr_3$	2.17±0.03		Present work
$(CH_3)_2SiBr_2$	2.21±0.03		Present work
$(CH_3)_3SiBr$	2.21±0.03		Present work
F_2SiBr		2.16±0.02	5
F_3SiBr		2.147	5

1) R.Spitzer, W.J.Howell and V.Schomaker, *J. Am. Chem. Soc.*, **64**,62 (1942).
2) A.H.Sharbaugh, J.K. Bragg, J.C. Madison and V. G. Thomas, *Phys. Rev.*, **76**, 1419 (1949).
3) L.Pauling and L.O.Brockway, *J. Am. Chem. Soc.*, **57**, 2684 (1935).
4) B.Bak J,Bruhn and J.Rastrup-Anderson, *Acta Chem. Scand.*, **8**, 367 (1954).
5) J. Sheridan and W.Gordy, *J. Chem. Phys.*, **17**, 965 (1951).
6) C.J.Wilkins and L.E.Sutton, *Trans Faraday Soc.*, **50**, 783 (1954).
7) K. Yamasaki, A. Kotera, M. Iwasaki and N. Tatematsu, *J. Chem. Soc. Japan, (Pure Chem. Sect.)*, **69**, 104 (1953).
8) L.O.Brockway and J.Y.Beach, *J. Am. Chem. Soc.*, **60**, 1836 (1938).
9) R.C.Mockler, Jep H.Bailey and W.Gordy, *J. Chem. Phys.*, **21**, 1710 (1953).
10) L.O.Brockway and I.E.Coop, *Trans. Faraday Soc.*, **34**, 1429 (1938).
11) R.L.Livingston and L.O.Brockway, *J. Am. Chem. Soc.*, **66**, 94 (1944).
12) R.L.Livingston and L.O.Brockway, ibid., **68**, 719 (1946).

is not affected when hydrogen atoms of halogenosilane are replaced by methyl radicals. For example, The Si-Br lengths of $(CH_3)SiBr_3$ and $(CH_3)_3SiBr$ agree with these of $HSiBr_3$[1] and H_3SiBr[2]. On the other hand, these bond lengths vary when the number of halogen atoms attached to silicon is altered.

In general, silion-halogen distance of the derivatives of monohalogenosilane is longer by 0.03–0.06 Å than that of respective tetrahalogenosilane. The sum of Pauling-Huggins atomic radii[13] is longer than the observed lengths, as is also the length calculated from Schomaker-Stevenson's rule[14]. The double bond character of silicon-halogen bond and the change of character with the number of substituents provide an explanation of these facts[13]. A reasonable representation of the ground electronic state of these molecule is a resonance hybrid of the forms a, b and c.

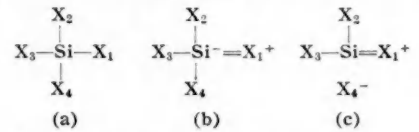

The structure b implies the double bond formation with the use of 3d orbital of silicon. When the number of halogen atoms attached to silicon is more than one, the contribution of the structure c becomes large. This may explain the change of the bond length with the number of substituents.

(2) Silicon-carbon Bond. — Available date on the bond length of Si–C are listed in Table II. These date agree with a value of 1.88 Å within an error of 0.03 Å. Bond and Brockway[15], however, they have recently shown in their electron diffraction investigation using a sector on $Si(CH_3)_nH_{4-n}$ (n=1, 2 and 3) that Si–C length increased by about 0.01 Å with the introduction of each successive methyl radical. The bound length between silicon and aromatic carbon agress with that of

TABLE II

Compounds	Si-C Length (Å)	Reference
$Si(CH_3)_4$	1.888±0.02	16
$Si_2(CH_3)_6$	1.90 ±0.02	17
$HSi(CH_3)_3$	1.873±0.006	15
$H_2Si(CH_3)_2$	1.860±0.004	15
$H_3Si(CH_3)$	1.857±0·007	15
$(CH_3)_3SiF$	1.89 ±0.02	6
$(CH_3)_2SiClF$	1.89 ±0.02	6
$(CH_3)_3SiCl$	1.89 ±0.03, 1.87	12, 9
$(CH_3)SiCl_3$	1.876	9
$(CH_3)_3SiCH_2Cl$	1.88 ±0.04	18
$(CH_3)_3SiBr$	1.86 ±0.05	Present work
$((CH_3)_2SiO)_3$	1.86 ±0.04	19
$((CH_3)_3Si)_2O$	1.88 ±0.03	Present work
$Si(C_6H_5)_4$	1.87 ±0.03	Present work

TABLE III

MOLECULAR STRUCTURES OF SILOXANES

Compounds	Si-O (Å)	Si-C (Å)	∠Si-O-Si	∠O-Si-O	∠C-Si-C	Reference
$((CH_3)_3Si)_2O$	1.63±0.05	1.88±0.03	130±10°	—	114±4°	Present work
$((CH_3)_2SiO)_3$	1.66±0.04	1.86±0.04	125±5	115±5°	112±6	19
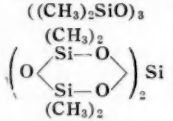	1.64±0.03	1.88±0.03	130±4	109±4	109±4	21*
$((CH_3)_2SiO)_4$	1.63	1.88	140±5	109.5 (assumed)	109.5 (assumed)	Present work
$((CH_3)_2SiO)_4$	1.65	1.92	142.5	109	106	22*
$((CH_3)_3SiO)_4Si$	1.63	1.88	140±5	109.5 (assumed)	112±4	Present work
$(CH_3O)_4Si$	1.64±0.03	—	113±2(∠Si-O-C)			Present work

* Data from X-ray crystal analysis

13) L.Pauling, "The Nature of the Chemical Bond", Cornell Univ. Press, 2nd Ed. (1940).
14) V.Schomaker and D.P.Stevenson, *J. Am. Chem. Soc.*, **63**, 37 (1941).
15) A.C.Bond and L.O.Brockway, *J. Am. Chem. Soc.*, **76**, 3312 (1954).
16) W. F. Sheehan, Jr. and V. Schomaker, *J. Am. Chem. Soc.*, **74**, 3956 (1952).
17) L.O.Brockway and N.R.Davidson, ibid., **63**, 3287 (1941).
18) J. M. Hastings and S.H.Bauer, *J. Chem. Phys.*, **18**, 13 (1950).
19) E.H.Aggarwal and S.H.Bauer, ibid., **18**, 42 (1950).

silicon and carbon in methyl radical within 0.03 Å. The bond angle of C–Si–C of trimethylsilyl group, $-Si(CH_3)_3$, is approximately tetrahedral, and somewhat larger values are obtained in certain compounds such as: $(CH_3)_3SiCl$ (113±2°), $(CH_3)_3SiBr$ (114±4°) and $Si(OSi(CH_3)_3)_4$ (112±4°).

(3) Silicon-oxygen Bond.—Silicon-oxygen bond is an important one which builds up the framework of both inorganic silicates and organosilicon polymers. The nolecular structures of organic compounds containing Si–O bond are summarized in Table 3. The Si–O lengths obtained for organosilicon compounds agree without exception with 1.64 Å. Smith[20] deduced a value of 1.60±0.01 Å for Si–O length by reviewing the obtainable deta on various inorganic silicates and aluminosilicates. Introduction of methyl radical may increase Si–O length somewhat.

The valence angle of the oxygen atom in Si–O–C linkage, 112±3°, obtained for $(CH_3O)_4Si$ is in agreement with that in C–O–C linkage of methyl ether[23]. On the other hand, the angle Si–O–Si has a larger value, 130±10° in $((CH_3)_3Si)_2O$, 125±5° in $((CH_3)_2SiO)_3$, and 140±5° in $((CH_3)_2SiO)_4$ and $((CH_3)_3SiO)_4Si$. Since there may be a strain causing distortion in the ring structure of $((CH_3)_2SiO_3)$, a value of about 140° seems to be normal. The values of Si–O–Si angle reported for α-quartz and for α-cristobalite are 142°[24] and 150°[25] respectively. These values are consistent with those of organic siloxanes. It may be said, therefore, that Si–O–Si chain in organic siloxanes has a geometrical structure similar to that in inorganic silicates.

Smyth and Holland[26] studied the dielectric properties of hexamethyldisiloxane in detail over a wide range of temperature and discussed the properties of Si–O bond. They calculated a dipole moment of 0.66 D in the vapor phase, and of 0.46 D in the pure liquid. The atomic polarization was determined to be 7.9 cc. There were large discrepancies between the values of the group moment of $(CH_3)_3SiO$. Assuming Si–O–Si angle to be 130°, calculation from the observed moment gave 0.54 D (liquid) and 0.78 D (vapor), while a group moment 1.6–2.0 D was obtained from an approximate formula relating ionic character of the bond to electronegativity difference. These data were considered to be consistent with a valence angle of oxygen greater than 130°. However silicon has the ability to expand its 3d orbital and to form a partial double bond with more electronegative elements. Kurita and Kondo[27], assuming Si–O–Si angle to be 130°, showed that there was a fairly good agreement between a bond moment 1.55 D of Si–O calculated from the dipole moment data of hexamethyldisiloxane and a value of 1.1 D obtained by the Pauling's method[28], which permitted us to calculate the degrees of the double bond character and the ionic character of bonds in oxy-acid molecules.

(4) Cyclic Compound Containing Silicon Atoms as Ring Members.—Dimethylcyclopolysiloxane, dimethylcyclopolysilazane and dimethylcyclopolysilthiane can be prepared by treating dimethyldichlorosilane with water, ammonia and hydrogen sulfide respectively.

As regards the trimer of cyclosiloxane, electron diffraction data[19] indicated that the six-membered ring is planar. The trimer can be prepared by the cracking of dimethylpolysiloxanes, while the hydrolysis product of dimethyldichlorosilane contains only a small amount of the trimer[29]. Scott[30] investigated the redistribution equilibrium between dimethylcyclopolysiloxanes and linear polysiloxanes catalyzed by sulfuric acid. He concluded that the ring having the smallest number of members of cyclic polysiloxane, as in the trimer in this case, had a slight strain, while the ring structures of the tetramer or the polymer of larger size were probably free from strain. He attributed this strain to the deformation of normally large Si–O–Si angle in forming a small membered ring. Actually the difference between the molecular structure of the trimer and that of the tetramer exists in the Si–O–Si angle, which is 125° for the trimer and 140° for the tetramer. It is likely that a strain free Si–O–Si angle takes a probable value of about 140° and is easily deformable by intra- and intermolecular forces.

20) J.Smith, *Acta Cryst.*, **7**, 479 (1954).
21) W.L.Roth and D.Harker, ibid., **1**, 34 (1948).
22) H.Steinfink, B.Post and I.Fankuchen, ibid., **5**, 802 (1954).
23) Cited in a paper by P.W.Allen and L. E. Sutton, *Acta Cryst.*, **3**, 46 (1950).
24) F.Machatschki, *Fortschr. Mineral. Krist. Petrog.*, **20**, 45 (1935).
25) W.Niewenkamp, *Z.Krist.*, **96**, 454 (1937).
26) R.S.Holland and C.P.Smyth, *J. Am. Chem. Soc.*, **77**, 268 (1955).
27) U.Kurita and M.Kondo, This Bulletin, **27**, 160 (1954).
28) L.Pauling, *J. Phys. Chem.*, **56**, 361 (1952).
29) W.Patenode and D.Wilcock, *J. Am, Chem. Soc.* **68**, 358 (1946).
30) D.W.Scott, ibid., **69**, 803 (1947).

As regards the silthiane compounds, dimethylsubstituted polymers having a ring larger than that of the trimer have not yet been isolated. When the cyclic trimer is heated at about 200° under atomospheric pressure, the dimer is distilled. In this case, the valence angle of sulfur atom should have been deformed from about 110° in the trimer to about 75° in the dimer. The ring structure of the dimer is similar to that of silicon disulfide, in which successive SiS_4 tetrahedrons are joined with a common edge leading to a fibrous frame extending in one dimension. This structure of silicon disulfide have been interpreted as an ionic packing of Si^{4+} and S^{2-} whose ionic radii ratio has a certain critical value, at which the change in coordination number four to three may be expected to occur. The Si–S bond of tetramethylcyclodisilthiane is supposed to have as large ionic character as that of silicon disulfide.

Brewer and Haber[31] studied the rearrangement equilibrium between linear and cyclic dimethylpolysilazanes at high temperature under high pressure. They found that the tendency of ring formation is greater in the silazane than in the corresponding siloxane systems. The rings of both the trimer and the tetramer of dimethylcyclopolysilazane have puckered structures. The difference between the valence angles of the nitrogen atom in the trimer and the tetramer may be due to the steric repulsion of methyl radicals.

In Table IV, comparison is made of the observed bond lengths of silicon and other electronegative elements with the sums of Pauling-Huggins radii and with the values calculated from Schomaker-Stevenson's rule.

TABLE IV

Bond	Bond Length (Å) Obs.	Calcd. after Pauling-Huggins	Calcd. after Schomaker-Stevenson	Electronegativity Difference
Si-C	1.88	1.94	1.88	0.7
Si-N	1.73[32], 1.78	1.87	1.80	1.2
Si-O	1.63	1.83	1.76	1.7
Si-F	1.54-1.60[3,4]	1.81	1.69	2.2
Si-S	2.15-2.18	2.21	2.15	0.7
Si-Cl	2.00-2.02	2.16	2.15	1.2
Si-Br	2.17-2.21	2.31	2.22	1.0

In general, with increasing electronegativity difference, the difference increases between the calculated bond lengths and observed ones. Among these values, the contraction is remarkable for the most polar Si–O and Si–F bonds. This may indicate the presence of either one or both of the following causes; 1) larger ionic character of the bond than is suggested by the electronegativity difference, 2) partial double bond character arising from resonance. Craig et al.[33] discussed this problem in detail, and were led to the conclusion that presumably $d\pi-p\pi$ bonding is a common one giving rise to a strong bond and that the polar character in σ-bonds can give extra stability by increasing the $d\pi-p\pi$ overlap.

Summary

The vapors of methyl or ethyl substituted silicon compounds containing Si–Cl, Si–Br, Si–O, Si–N and Si–S bonds were studied by electron diffraction method and their molecular structures were determined. Bond lengths obtained are summarized in Table IV. The Si–Br length in methylbromosilane series changes with the number of substitutions of Br, but the length is in accord with the data of corresponding bromosilanes. The valence angles of oxygen in linear and cyclic siloxanes were estimated to be about 140° and this value is nearly the same as that in α-quartz. The valence angles of silicon in cyclic compounds are almost tetrahedral and those of oxygen, nitrogen and sulfur vary with the size of the ring.

The author expresses his sincere gratitude to Drs. K. Yamasaki and M. Kimura for their encouragement and kind discussions throughout this work, and to Mr. H. Murata of the Osaka Municipal Technical Research Institute, Dr. M. Kumata of Osaka City University, and Mr. I. Hizawa of Sumitomo Chemical Co. for furnishing samples.

Department of Chemistry, Faculty of Science, Nagoya University
Nagoya

31) S. D Brewer and C. P. Haber, *J. Am. Chem. Soc.*, **70**, 3888 (1948).
32) K. Hedberg. E. Goldish and M. E. Jones, *J. Am. Chem.* Soc., **77**, 5278 (1955).
33) D. P. Craig, A. Maccoll, R. S. Nyholm and L. E. Sutton, *J. Chem. Soc.*, **1954** 332.

SHORT COMMUNICATIONS

An Improved Synthesis of O-Benzyl-DL-serine

By Kenji OKAWA

(Received September 20, 1956)

In the previous paper*, it was reported that O-benzyl-DL-serine was synthesized from methyl acrylate in 51% yields. The method, however, is not profitable for a large scale preparation. In the present work, ethyl acrylate was used in place of methyl acrylate and the method was improved as follows:

α-Bromo-β-benzyloxy-propionic Acid.—To a solution of 115 g. of ethyl acrylate in 100 cc. of absolute ether was added 57 cc. of dry bromine dropwise at 5°C under stirring, and the mixture was allowed to stand over-night at room temperature (Solution-A).

Twenty six grams of metallic sodium was dissolved in an ether-benzylalcohol mixture (500 cc. of ether-300 cc. of benzylalcohol) under reflux-condenser (Solution-B).

Solution-B was added portionwise into the solution -A under strong stirring at −10°C for one hour, the stirring was continued at the same temperature for thirty minutes after the addition was over.

The precipitated sodium bromide was removed from the ether solution by washing with 200 cc. of water and the extract was acidified with conc. hydrochloric acid. The oily product separated was extracted with ether and both the ether solutions were combined. After removal of the ether, the mixture was shaken with 180 g. of barium hydroxide in 3 l of water for five hours at room temperature. In order to complete the hydrolysis, the residual oil was treated with 100 g. of barium hydroxide in 1.5 l of water under the same conditions. The water layers were collected and acidified with conc. of hydrochloric acid. Then the separated oily product was extracted with ether. After removal of the ether, 370 g. of crude α-bromo-β-benzyloxy-propionic acid was obtained.

O-Benzyl-DL-serine.—The crude product of the α-brom acid was dissolved in 5 l. of aq. ammonia (34%) containning 500 g. of ammonium carbonate and then allowed to stand for 1 week at room temperature. The reaction mixture was concentrated in vacuo until crystals of the amino acid appeared. A small amount of the crystals were obtained from the mother liquor. The fine crystals of O-benzyl-DL-serine (150 g.) were prepared in 67% yields.

Department of Chemistry
Faculty of Science
Osaka University
Osaka

* K. Okawa and H. Tani, *J. Chem. Soc. Japan.*, **75** 1197 (1950).